Alma Mater Studiorum – Università di Bologna

DOTTORATO DI RICERCA IN
Scienze Chimiche

Ciclo XXXI

Settore Concorsuale: 03/C1
Settore Scientifico disciplinare: CHIM/06

NOVEL ASYMMETRIC ORGANOCATALYTIC TRANSFORMATIONS: DEVELOPMENT, OPTIMIZATION AND APPLICATIONS

Presentata da: Giulio Bertuzzi

Coordinatore Dottorato

Prof. Aldo Roda

Supervisore

Prof.ssa Mariafrancesca Fochi

Cosupervisore

Prof. Luca Bernardi

Esame Finale anno 2019

Table of contents

1 Introduction

1.1 Chirality in Nature and everyday life

A molecule is defined as *chiral* if its mirror-image is not superimposable with itself.[1] The majority of chiral compounds can be identified by their lack of a key element of symmetry, namely, an improper axis of rotation. This implies that a chiral molecule cannot display a plan of symmetry or an inversion center. More specifically, the majority of chiral compounds present at least one *asymmetric* carbon atom; however, this is not strictly necessary, as chirality can be generated by a chiral axis or a chiral plane as well. These molecules, called *enantiomers*, are mirror images: identical yet opposite. Indeed, two enantiomers behave exactly the same way in an achiral environment, however, they are different when they interact with other chiral objects. In fact, "pairs" of chiral molecules are *diastereomeric* and, by definition, chemically different between each other.

Beyond this formal definition, the concept of chirality has huge implications for living organisms, demonstrated by the fact that essential biomolecules (proteins, sugars and nucleic-acids) are chiral and occur naturally, most of the times, in only one enantiomeric form. Thus, two enantiomers of the same molecule do not always behave the same in a biological environment, and may have significantly different activity. The following are some examples, from natural compounds to pharmaceuticals, in which chirality is directly involved.

Fragrances

Rose oxide, among the first compounds isolated from rose oil in the early '60s, is a colorless to pale yellow liquid with a distinct rose scent. This compound presents four distinct isomers, of which the (-)-cis isomer is the most desirable for fragrance and flavor use. When produced as a single compound, (-)-cis-rose oxide is a floral green note, with a strong, diffusive rose scent. The odor threshold is 0.5 ppb. Its enantiomer, (+)-cis-rose oxide is herbal, green floral, earthy and heavy. Its odor threshold is 50 ppb. The trans isomers are less rose-like. Diastereomer (+)-trans-rose oxide has a herbal green, fruity, citrus scent with an odor threshold of 80 ppb, while (-)-trans-rose oxide displays, herbal minty notes, with an odor threshold of 160 ppb (Figure 1). The fact that different enantiomers of the same molecule produce different smells, is a direct proof of the presence of homochiral molecules in the human olfactory receptors.

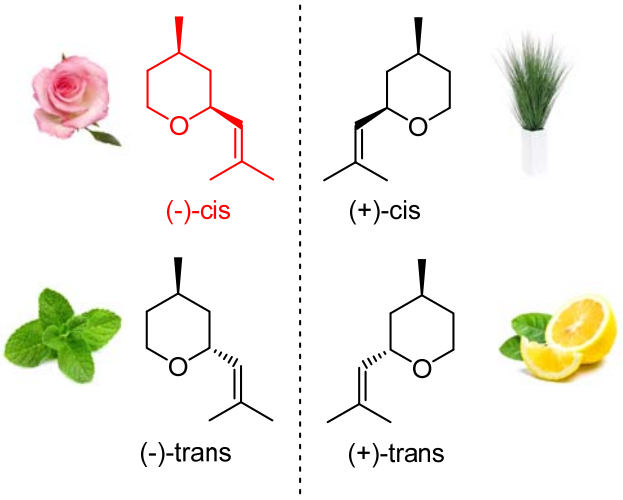

Figure 1. Isomers of rose oxide

Drugs safety and effectiveness

The activity of pharmaceuticals depends on which enantiomer is used. Since a drug must fit into the target receptor, and that being an homochiral molecule, it is often only one enantiomer that is useful. There are many pharmaceuticals that display different activities depending on the enantiomeric form. This is the case of Ibuprofen, one of the most known painkiller drugs. In this case, only the (*S*)-enantiomer is responsible for the beneficial effects, whereas the (*R*)-enantiomer is not effective (Figure 2, top). It is also possible that, while one enantiomer of a pharmaceutical displays the desired activity, the other one is highly toxic and causes severe side-effects. Besides the very well-known case of Thalidomide, another example is Ethambutol. While the (S,S) enantiomer is effective against tuberculosis, the (R,R) form causes blindness (Figure 2, bottom).

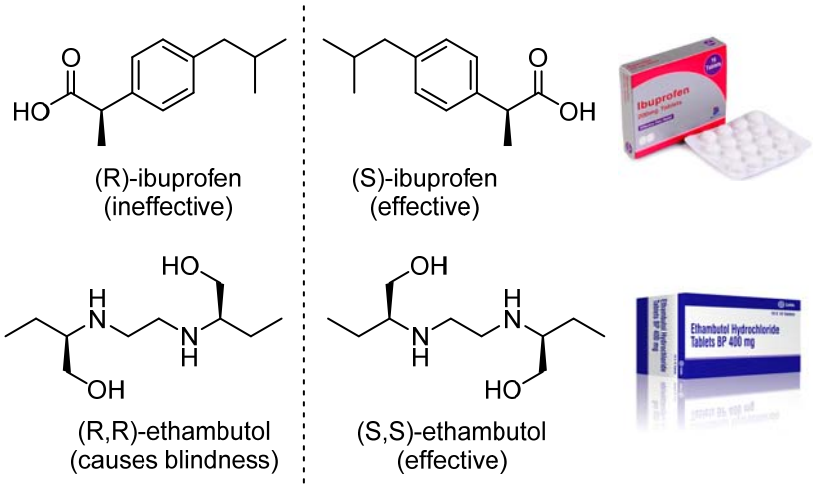

Figure 2. Ibuprofen and Ethambutol

1.2 Asymmetric organocatalysis

The enantioselective synthesis of chiral compounds is a primary issue for organic chemistry researchers. As briefly demonstrated in the previous section,[2] the production of synthetic chiral molecules as single enantiomers is a crucial aspect in organic synthesis and has made asymmetric catalysis a crucial area of research.[3]

Until 1996, enzymes and transition-metals had been considered the only classes of efficient asymmetric catalysts.[4] Biocatalysis, displaying often high enantioinduction and substrate specificity, lie in the use of enzymes as natural catalysts to perform organic transformations.[5] On the other hand, metal-complex catalysts, rendered chiral by homochiral organic ligands, are very effective even at low concentration[6] and are therefore well suited for industrial scale synthesis.[7]

Organocatalysis relies on the use of small chiral organic molecules to catalyze chemical transformations[8] and is inspired by biomimetic concepts,[8b] in order to reproduce the catalytic activity and selectivity of enzymes.[9] The first organocatalytic asymmetric reaction was published in 1970s by two industrial research groups.[10] The authors reported a highly enantioselective aldol reaction, catalyzed by proline. However, it was not until late '90s that some efforts were made, trying to conceptualize a general organocatalytic strategy.

In 1996, reports from Shi,[11] Denmark,[12] Yang,[13] Jacobsen[14] and Corey[15] demonstrated that small organic molecules could be effectively used as powerful tools to promote organic transformations. Then, in 2000, the works from Barbas, List[16] and MacMillan,[17] led to recognize a general mode of action of organocatalysts. This opened the way for a broad and smart applicability of organocatalysis, as it was demonstrated that a stereoselective synthesis could be planned *a priori* employing organocatalysts.[8f]

Organocatalysis, by now, has definitively matured to a recognized methodology, equal to organometallic and enzymatic catalysis and it is viewed as the third pillar of asymmetric synthesis. This is due to undoubted advantages such as the stability of the catalytic system (inert atmosphere or dry/degassed solvents are often not required), its non-toxicity and the possibility of using mild reaction conditions.

1.3 Modes of activation in asymmetric organocatalysis

The decisive success of organocatalysis, suddenly exploded during the past decade, arise from the identification of generic modes of activation, induction and reactivity. Generic mode of activation means that reactive species interacts with the chiral catalyst in a highly organized and predictable manner.

Based on the nature of the interaction between the catalyst and the substrate, the activation modes can be classified in covalent-based and non-covalent based.[8b] As regards to the non-covalent based catalysis, hydrogen-bond donor and Brønsted acid catalysis are based on interactions between the catalyst and the substrate, mimicking the working principles of enzymes.[18] Within the category of covalent-based activation, a prominent position is occupied by aminocatalysis that has emerged as reliable strategy to generate stereocenters at α- and β-position of carbonyl compounds.[19]

The understanding of the activation approaches brought to the development of catalytic strategies in which different modes of activation can be easily combined as in the case of domino/cascade reactions.[20] Furthermore, different organocatalysts can be combined with other catalytic system such as metal-based[21] or photoredox catalysts,[22] reaching an high level of sophistication.

In the following paragraphs, the modes of activation typical of the catalysts encountered in chapters **3**-**7** will be described.

1.3.1 Hydrogen-bond donor catalysis

Hydrogen bond plays a dominant role in biocatalysis and it is frequently exploited by enzymes in order to promote several biochemical processes. The main function is the activation of electrophilic species towards the attack of a nucleophile. This is rendered possible since the H-bond is able to remove electronic density from the acceptor molecule. Thus, H-bond catalysis relies on the stabilization of the transition state of the reaction, induced by dipolar interactions that happen within a confined chiral space. The first examples of the employment of H-bond donors organocatalyst can be found in two reports by Jacobsen[14] and Corey.[15] The authors reported that asymmetric Strecker reactions could be efficiently promoted by hydrogen-bonding catalysts, through the activation of electrophilic imines. Few years later Jacobsen showed that these H-bonding

based catalysts could be used for other reactions,[23] launching *de facto* the generic use of enantioselective H-bonding catalysis.

In general, these catalysts are constituted by a Brønsted basic portion (a tertiary amine), connected through a chiral framework with an acidic portion (mono- double- or multiple hydrogen bond donors such as alcohols, phenols, amides, sulfonamides, thioureas, ureas and squaramides). Importantly, the acidic moieties are considered to be as "neutral" hydrogen bond donors, that means they do not quench the basic amine by quantitative protonation. Most of these catalysts derive from *Cinchona* alkaloids or from *trans*-1,2-cyclohexanediamine.

Cinchona alkaloids are natural occurring compounds extracted from the bark of *Cinchona* tree. The structure of these catalysts consists in two pairs of pseudoenantiomers,[24] namely Quinine (**QN**) – Quinidine (**QD**) and Cinchonidine (**CD**) – Cinchonine (**CN**) (Figure 3).

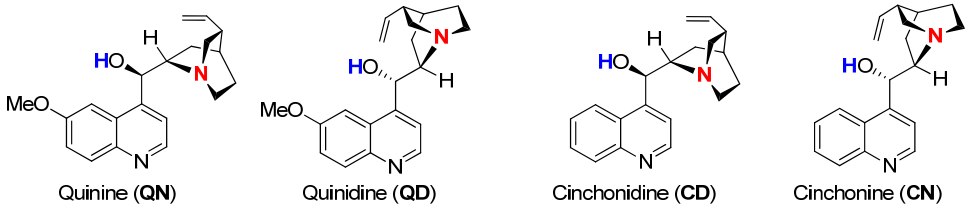

Figure 3. *Cinchona* alkaloids.

The tertiary amine moiety is responsible for the basic/nucleophilic activation, whereas the alcoholic group acts as the hydrogen bond donor. The hydroxyl group can be easily turned into an ester, ether or, by means of a Mitsunobu reaction, into an amine moiety (with inversion of configuration). This, in turn, is a versatile handle for the linkage to other H-bond donors, such as squaramides, ureas or thioureas. The modification of the substituents on their *N*-atoms allows the proper modulation of steric hindrance and electronic proprieties (Figure 4).

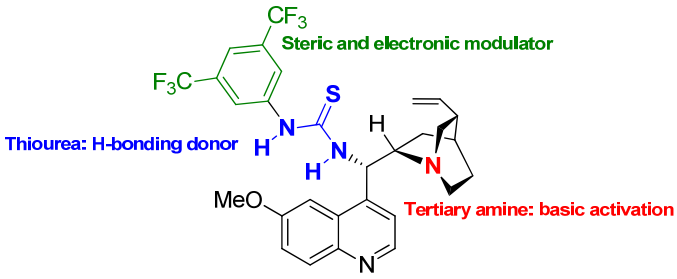

Figure 4. Thiourea-based bifunctional catalyst derived from 9-deoxy-9-amino-*epi* Cinchona alkaloids.

The thiourea is often functionalized with a 3,5-bis(trifluoromethyl)-phenyl group in order to ensure a better catalytic activity.[25] In fact, this electron withdrawing moiety reduces the pK_a of N–H proton, making them more available to the hydrogen-bond donation.

The Michael addition of 1,3-dicarbonyl compounds on nitroolefin mediated by H-bonding based catalysts was developed by Takemoto in 2003.[26] This reaction can be taken in account as a model to understand how these catalysts can promote substrates activation and enantioselective reactions[27] (Scheme 1).

In the first step, the nucleophile is generated by deprotonation of the pronucleophile species, in a soft-enolization process. This anionic species is stabilized, and by so doing strongly anchored to the catalyst chiral scaffold, by multiple H-bonds between the protonated tertiary amine and the acidic N-H moieties of the thiourea. The electrophile is then coordinated to the thiourea protons, generating an ordered tertiary complex. Both the reaction partners are activated and brought together in a chiral environment and can easily form a new C-C bond. The thus formed nitronate is then quenched by protonation through a proton transfer from the tertiary amine moiety (now an ammonium cation), delivering the final product and releasing the free catalyst, ready to deprotonate another molecule of pronucleophile again.

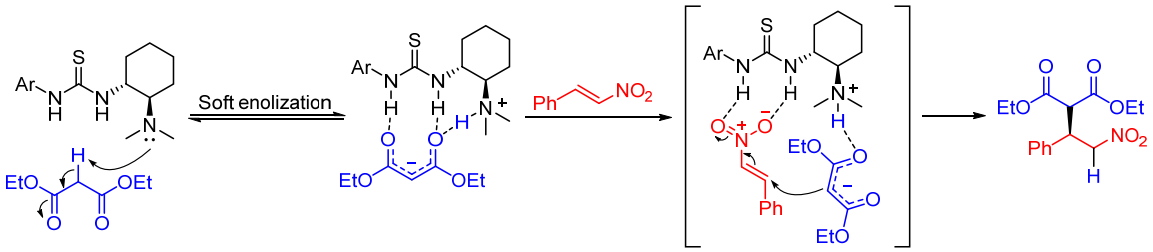

Scheme 1. Reaction model for the catalytic asymmetric addition of malonate to nitroalkene Ar = 3,5-$(CF_3)_2C_6H_3$.

An alternative transition state model was computationally disclosed by Pápai one year later.[28] It consists in the coordination of the malonate to the thiourea, while the activation of the electrophile is provided by the protonated tertiary amine moiety. Summing up, the acidic moiety of the hydrogen bond donors, together with the protonated tertiary amine, play a key role in the stabilization of the transition state of the reaction. The presence of these H-bonds generates a well-defined chiral environment which determines the preferential orientation of the reagents, therefore inducing enantioselectivity.

Another representative example is the famous Morita-Baylis-Hillman reaction. In the racemic version, the reaction is catalyzed by tertiary amines or phosphines, and involves

a Michael acceptor acting as the nucleophilic component, and an aldehyde or other electrophiles as the electrophilic reaction partner. The development of asymmetric versions for this reaction has proven to be particularly challenging, also because even nowadays the real mechanism is not fully clear. Chiral catalysts able to promote this reaction in an enantioselective fashion exist, and very often are related to the bifunctional catalysts described before, bearing a tertiary amine moiety, acting as the Lewis base, and a hydrogen bond donor able to stabilize negatively charged transition states and intermediates. This reaction shows that these catalysts, usually classified into the "non-covalently bonding" class, are instead able to act as nucleophiles as well as bases, generating reactive intermediates activated by covalent bonds to the catalyst (Scheme 2).[29]

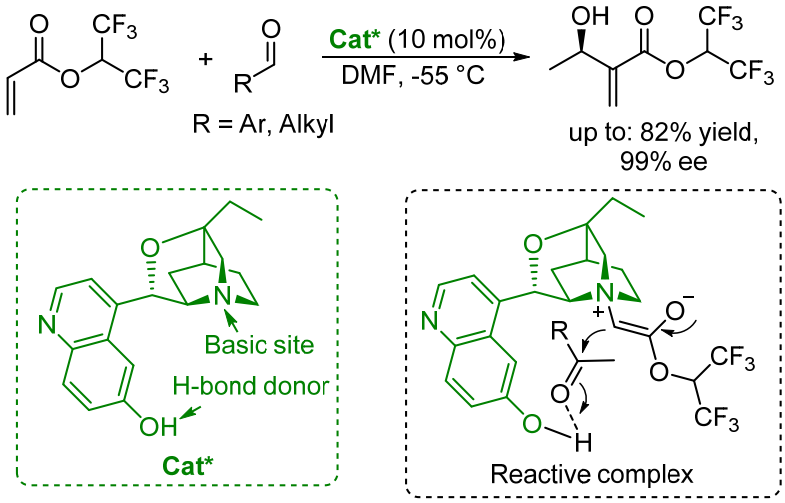

Scheme 2. Asymmetric Morita-Baylis-Hillman reaction, as reported by Hatakeyama.

1.3.2 Aminocatalysis: enamine and iminium ion activation

The use of chiral amines as catalysts for the asymmetric functionalization of carbonyl compounds is called aminocatalysis.[19,30]

Activation modes in aminocatalysis are based on covalent interaction generated upon the condensation of a chiral amine with a carbonyl group. This leads to the production of new activated compounds, undergoing functionalization. The reversible condensation leads to the generation of a positive charged iminium ion intermediate in which the energy of the lowest unoccupied molecular orbital (LUMO) is lowered. In the case of extended conjugated systems, such as enals or enones, the respective iminium ions display increased electrophilicity, thus facilitating conjugated additions of nucleophiles

onto the terminal carbon atom (β-position). This concept can be extended to polyconjugated systems such as dienals or trienals, usually achieving functionalization of the very terminal electrophilic carbon, thus relying on the vinylogy principle (Scheme 3b). On the other hand, in the case of isolated π systems, the generation of an iminium ion increases the α-proton acidity, favoring a rapid deprotonation. This generates a nucleophilic enamine, having a higher energy of the highest occupied molecular orbital (HOMO), compared to the parent enolate. This HOMO-raising activation allowed the α-functionalization of carbonyl compounds with different electrophilic species (Scheme 3a). Propagation of the HOMO-raising activation mode has led do the development of dienamine- and trienamine- based reactions, enabling γ- and ε-functionalizations.[31] The potential generation of both nucleophilic and electrophilic species, along with the possibility to extend the reactivity through conjugated systems, enlightens the broad applicability of aminocatalysis as a powerful tool to achieve a wide range of functionalizations of carbonyl compounds.

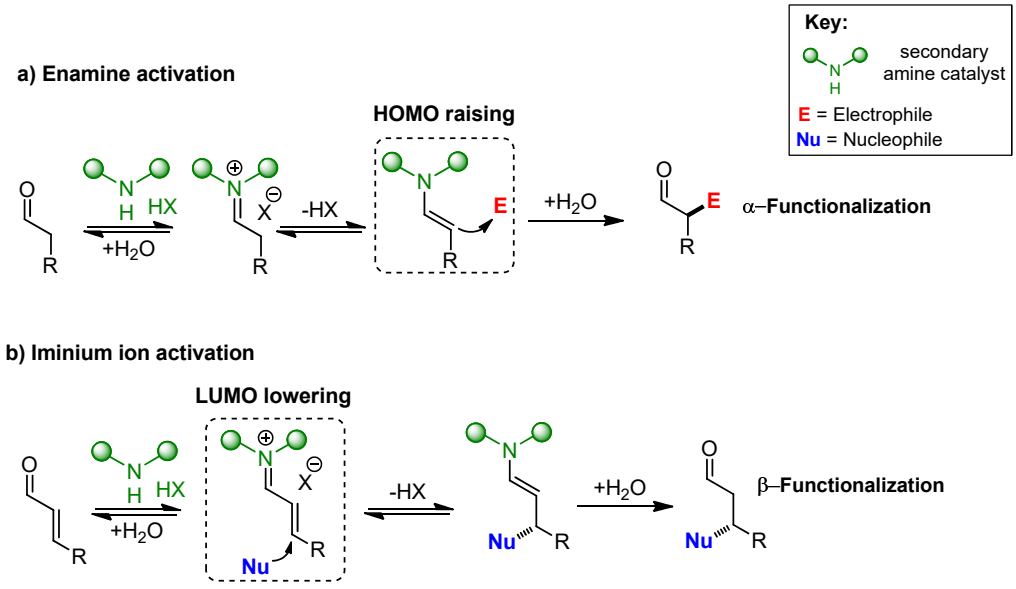

Scheme 3. Activation modes in aminocatalysis.

Diarylprolinol silyl ethers (Figure 5), independently developed by Jørgensen[32] and Hayashi[33] in 2005, are proline-derived catalysts which have proven to be very effective, promoting many kinds functionalization of aldehydes, either proceeding *via* iminium ions or *via* enamines.[30c] The bulky diaryl silyl ether group is the key for the high enantioselectivities generally displayed by this catalyst. In fact, this sterically demanding moiety forces the enamine in the conformation shown (*s-trans* and π-*trans*), and shields one of its two faces very efficiently, thus determining the approach of the electrophile

from the opposite face (Figure 5a). This mode for the enantioinduction is valid for the iminium ion activation as well. Here, the bulky fragment is extended enough to shield effectively the more distant β-position, allowing the nucleophilic attack only from the less hindered face (Figure 5b).

Besides relying on a conceptually different activation mode, these catalysts display some advantages, if compared to simple proline or unprotected prolinol. Indeed, if the first presents solubility issues, requiring most of the times very polar solvents such as DMF or *N*-methylpyrrolidone, protection avoids intramolecular parasite reactions leading to stable unreactive off-cycle intermediates, responsible for the low activity of the latter.

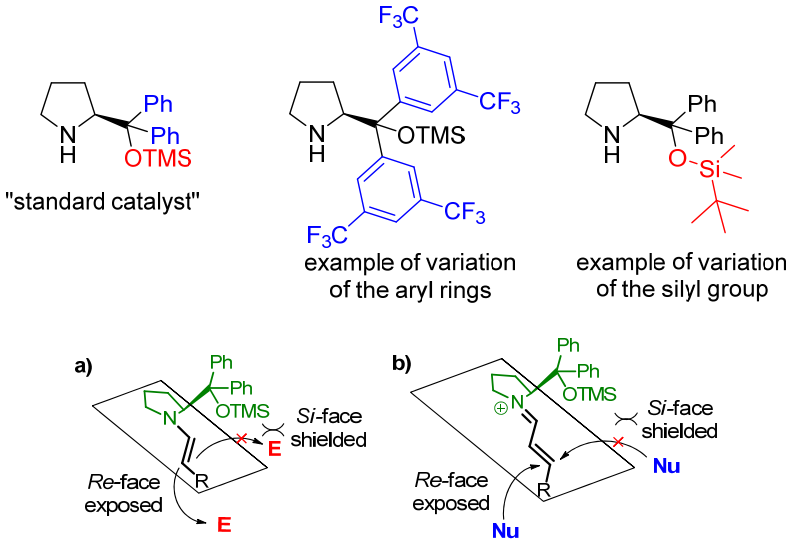

Figure 5. Examples of Jørgensen-Hayashi catalysts and models accounting for the enantioinduction of diphenyl silyl prolinol ethers through enamine activation (a) and iminium ion activation (b).

In both models, the efficiency of *O*-protected diaryl prolinols is related to the size of the substituents on the catalyst. Consequently, a proper modification of the aryl structure, as well as the silyl protecting group, permits a fine tuning of the catalytic stereoinduction.

Recently, Michael addition reaction between enamine-activated aldehydes and nitroalkenes, originally reported by Hayashi,[33] has become a focus of attention. In fact, this reaction has been intensively studied from a mechanistic point of view by several groups.[34] Initial investigations led to conclude that the reaction follows the mechanism outlined in Scheme 4, where a cyclobutane, deriving from a formal [2+2] cycloaddition, and an oxazine *N*-oxide, deriving from a formal hetero-[4+2], are formed as "off-cycle" species (observed by NMR analysis), isomers of the productive intermediate, which is a non-cyclic zwitterion. The rate-determining step was then found to be the protonation of

the zwitterionic intermediate. Therefore, addition of an acidic co-catalyst is important to achieve high reactivity and rapid turnover.

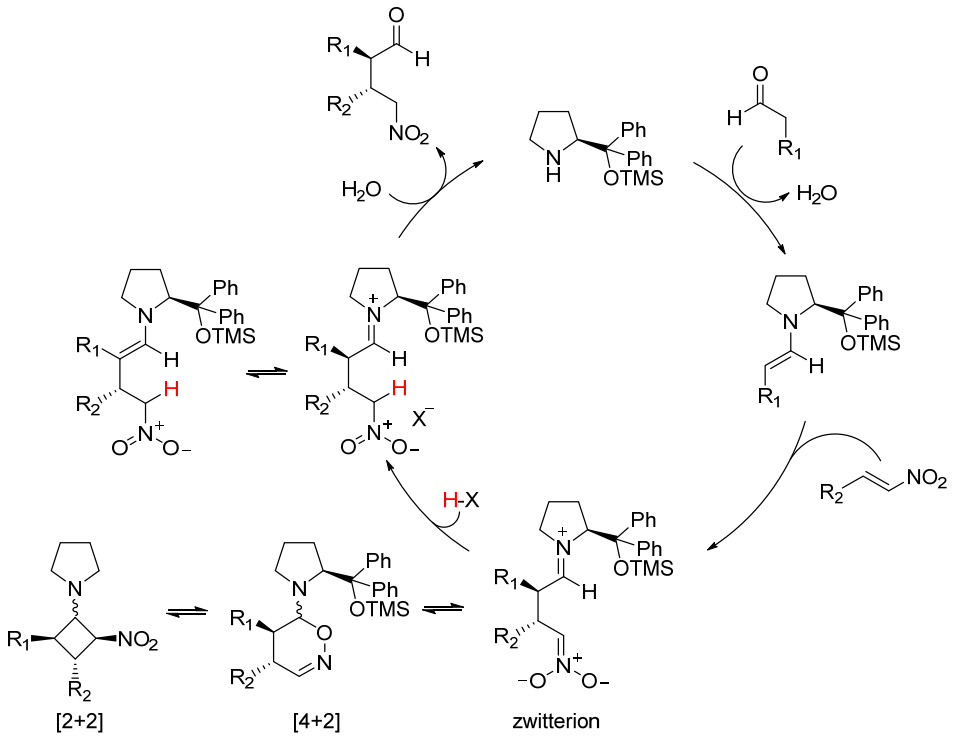

Scheme 4. Mechanism for the enantioselective addition of nitroalkenes to enamines with some experimentally observed intermediates.

These studies, conducted by Seebach and Hayashi, as well as by Blackmond and Pihko, shed light on the mechanism. Although some controversy regarding the reaction route and the role for the observed intermediates still remains, these researches gave a detailed insight into a synthetically important reaction. These studies demonstrate that the mechanisms of these reactions might be much more complex than it is often supposed to be.

2 Aim of the Thesis

The aim of this Doctoral Thesis is to capitalize the versatility of organocatalysis having as target the development of novel asymmetric organocatalytic transformations. With the perspective to expand the frontiers of this field of research in mind, when many robust and reliable organocatalytic protocols have been already developed and successfully applied to a multitude of reactions, the challenge lays in finding new classes of compounds that may act as compatible substrates. By so doing, a type of reactivity that was previously limited to stoichiometric or metal-catalyzed processes becomes accessible under a new type of catalysis, tackling the possibility to impart stereoselection where only racemic protocols had been disclosed.

During the course of my PhD studies, different types of reactions have been devised and developed. This has required to assess different families of organocatalysts. Particular attention has been devoted at the study and optimization of the reaction conditions and catalyst structure, in order to maximize yield and enantiopurity of the products as well as minimizing the catalyst loading and using the mildest conditions. The substrate scope of asymmetric reactions has always been thoroughly investigated to demonstrate the broad applicability of the proposed transformations, as well as the performance of synthetic elaborations illustrating the usefulness of the developed methods.

Despite conceptually distinct, the transformations detailed in the following chapters are somehow linked together by simple and recurring modes of activation, enantioinduction and reactivity, promoted by the catalysts employed.

2.1 Summary of the Thesis research

The following chapters describe how the intrinsic versatility of organocatalysts, combined with utilization of scaffolds previously unknown to organocatalysis, have been exploited to achieve new catalytic enantioselective processes. References can be found within each chapter.

In chapter **3** the first example of organocatalytic enantioselective dearomatization of *N*-alkylpyridinium salts is presented. Dearomatizations of highly reactive *N*-acylpyridinium salts is a well-established procedure, with asymmetric variants relying on metal catalysis and organocatalysis as well (one single example). The regiochemistry of these reactions

may change between the examples, however, a strong bias towards the C-2 (or C-6) functionalization is generally observed. On the other hand, *N*-alkylpyridiniums are bench-stable crystalline solids that undergo dearomatization less easily. Indeed, only one example of C-2 selective metal catalyzed asymmetric dearomatization exists. Non-enantioselective versions however were explored deeply and employed in diastereoselective alkaloid syntheses. Overcoming the poor reactivity (and dearomatized product instability) by placing an EWG group (such as nitro or cyano) at the 3-position, thus enhancing the electrophilicity of the cation, we were able to productively engage *N*-alkylpyridinium salts in nucleophilic dearomatizations, using indoles as reaction partners. The reaction displayed complete C-4 regioselectivity, an unusual feature that rendered our procedure complementary to previously disclosed methods. Chiral bifunctional thiourea derivatives were found to be the optimal catalysts for this reaction. Addressing the addition towards the C-3, rather than the N-1, of the indole and finding a base that could scavenge the HBr formed, without promoting a racemic background reaction, were the main challenges during the optimization process. A careful tuning of the stereoelectronic characteristics of the pyridinium salts was a prominent feature to improve the enantioselectivity. We were thus able to synthesize chiral dihydropyridine scaffolds in good yields and excellent stereoselectivities (Scheme 1). Importantly, the obtained heterocyclic compounds possess two reactive double bonds, which serve as a synthetic handle for further elaborations. Finally, some experimental investigations led us to propose a reaction pathway showing the catalyst involved in double (covalent and H-bond) activation of both the reaction partners.

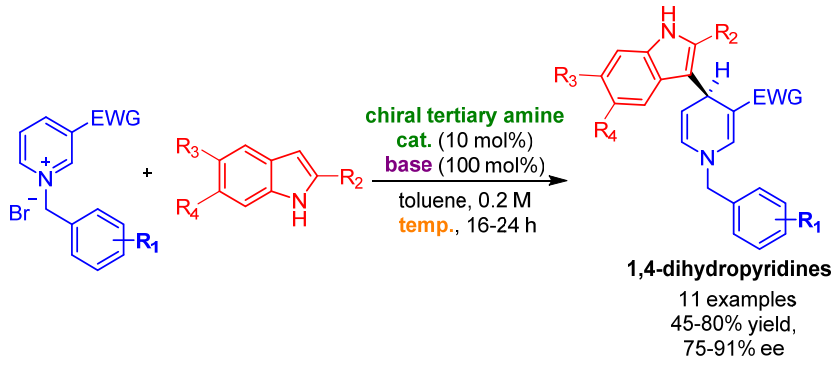

Scheme 1. Organocatalytic enantioselective dearomatization of *N*-alkyl pyridinium salts with indoles.

In chapter **4** the reactivity of *N*-alkyl-3-nitro- or 3-cyano-pyridinium halides towards asymmetric nucleophilic dearomatizations was extended by employing chiral enamines as nucleophiles. These were generated by reaction of chiral secondary amine organocatalysts with enolizable aldehydes. Dearomatizations of acridinium, quinolinium and isoquinolinium salts with chiral enamine nucleophiles have been developed by different groups. However, the dearomatization of benzo-fused azines is easier than the one of pyridine itself, as the largest part of the aromaticity (phenyl ring) does not get lost during the process. Indeed, no example of pyridinium salts dearomatizations with chiral enamines was disclosed. We therefore chose to employ our activated *N*-alkylpyridinium salts instead of highly reactive *N*-acyl analogues. Careful optimization of the reaction conditions enabled the achievement of a highly diastereo- and enantioselective process, displaying good yields and complete C-4 regioselectivity.

Importantly, the concomitant presence of the nitro and the aldehyde groups could be employed for cyclization processes that, after a series of chemoselective reductions, led to the formation of precious octahydropyrrolo-[2,3-*c*]pyridines, core structures of anticancer peptidomimetics (Scheme 2).

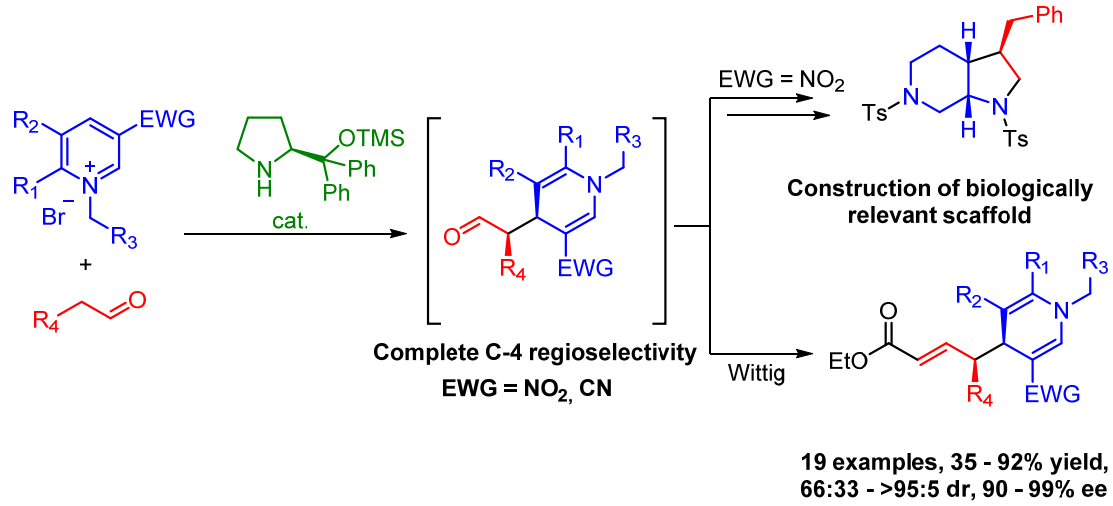

Scheme 2. Organocatalytic enantioselective dearomatization of *N*-alkyl pyridinium salts with chiral enamines.

Chapter **5** deals with the development of asymmetric organocatalytic α-heteroarylation of aldehydes with isoquinoline *N*-oxides (Scheme 3). Moving from pyridinium salts (and their dearomatization chemistry) and still being interested in involving azinium cations in organocatalytic enantioselective processes, we envisioned that aromatic *N*-oxides could, after proper activation, become powerful arylating species towards, for examples, chiral enamines. Indeed, previous examples of organocatalytic enantioselective arylation of

aldehydes either relied on non-aromatic electrophiles (such as quinones), employed metal co-catalysts or consisted in intramolecular processes (SOMO activation). The main challenges of devising such reactions are: finding a suitable arylating agent that does not quench the amine catalyst, and avoiding post-addition epimerization. We have found that isoquinoline-*N*-oxides, activated *in situ* by PyBroP, an exclusively oxophilic electrophile, underwent productive functionalization at the more reactive C-1, upon reaction with chiral enamines, resulting in α-heteroarylated aldehydes. Careful optimization of some reaction parameters enabled the achievement of good yields and high enantioselectivity values.

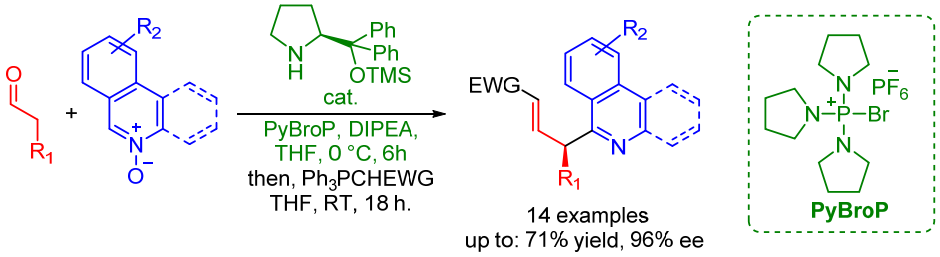

Scheme 3. Organocatalytic enantioselective α-heteroarylation of aldehydes with isoquinoline-*N*-oxides.

Chapter **6** deals with the development of organocatalytic asymmetric higher order cycloadditions. More specifically, the first catalytic [10+4] cycloaddition has been disclosed, by reaction of chiral 6-amino isobenzofulvenes (generated *in situ* from indene-2-carbaldehydes and aminocatalysts) with electron poor dienes. Overcoming the tendency of polyconjugated systems to undergo poorly periselective reactions (indeed amino isobenzofulvenes were demonstrated to act efficiently as 8π-components as well) we developed a robust procedure for this new [10+4] cycloaddition. The reaction rendered complex tetracyclic scaffolds with complete peri- and diastereoselectivity, following a predicted *exo*-approach, accompanied by excellent degrees of enantioselectivity and high yields (Scheme 4). During the optimization we found that the stereoselectivity of the process relied heavily on the presence of an acid additive and the removal of water. To address these particular features, both experimental and computational investigations were performed, leading to the hypothesis that the enantioselectivity of the present [10+4] cycloaddition arises from a kinetical preference for the formation of isobenzofulvene intermediates.

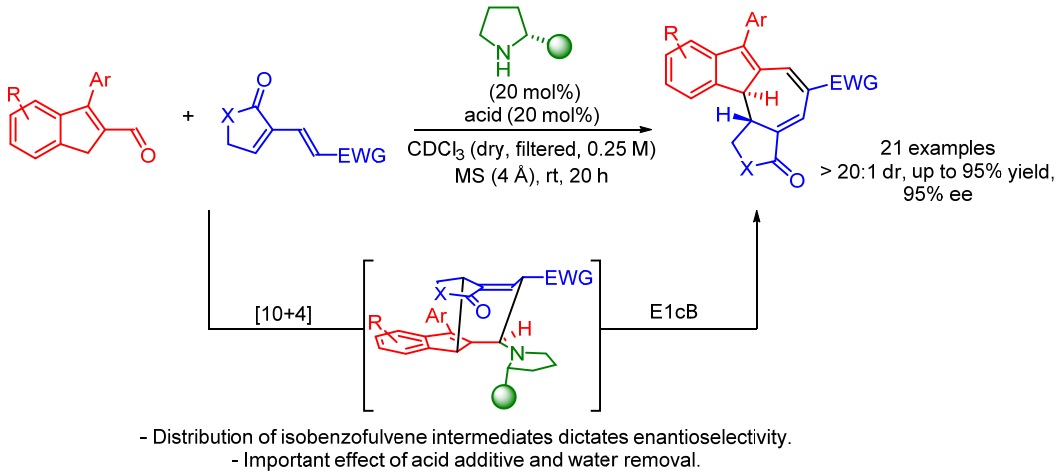

Scheme 4. Organocatalytic enantioselective [10+4] cycloadditions.

Finally, chapter **7** follows the path of higher order cycloadditions and moves from isobenzofulvenes as 10π-components to azafulvenes as hetero-6π-components. Indeed, only one example of organocatalytic enantioselective *aza*-higher order cycloaddition has been disclosed so far. Our strategy involved the catalytic transformation of pyrrole-2-carbaldehydes, imidazole-2-carbaldehyde, imidazole-4-carbaldehyde and pyrazole-5-carbaldehyde into the respective 6-amino (di)azafulvenes by reaction with chiral aminocatalysts. These electron rich hetero-6π-components could be productively engaged in [6+4] cycloadditions with two different classes of electron deficient dienes and [6+2] cycloadditions with nitroolefins (Scheme 5). The disclosed methodology represents a new and powerful tool for the stereoselective functionalization of different azoles, by the application of a common strategy. Careful optimization of the reaction conditions led to the formation of highly enantioenriched cycloadducts, exhibiting the structure of some natural compounds. A diversity-oriented procedure was also disclosed, showing the possibility to functionalize *in situ* some of the obtained products. Finally, observation by means of NMR spectroscopy of some putative intermediates allowed a deeper comprehension of the reaction pathways. Computational calculations are now ongoing to elucidate the exact role of the catalyst in the enantioinduction.

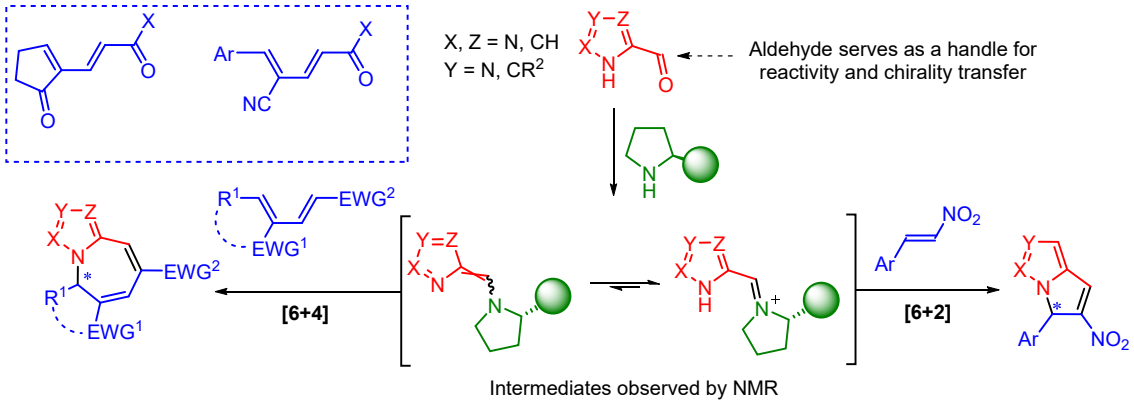

Scheme 5. Organocatalytic enantioselective *aza*-[6+4] and [6+2] cycloadditions.

3 Organocatalytic enantioselective dearomatization of *N*-alkylpyridinium salts with indoles as nucleophiles.

All the procedures and results here described are part of- and can be found in-:

- G. Bertuzzi, A. Sinisi, L. Caruana, A. Mazzanti, M. Fochi, L. Bernardi, "Catalytic Enantioselective Addition of Indoles to Activated *N*-Benzylpyridinium Salts: Nucleophilic Dearomatization of Pyridines with Unusual C-4 Regioselectivity". *ACS Catal.* **2016**, *6*, 6473.

ABSTRACT

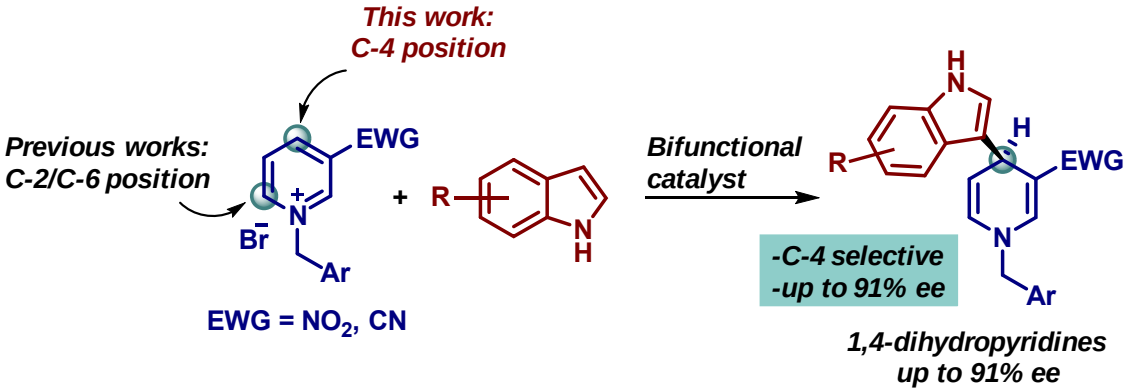

The catalytic enantioselective dearomatization of pyridines with nucleophiles represents a direct and convenient access to highly valuable dihydropyridines. Available methods, mostly based on *N*-acylpyridinium salts, give addition to the C-2/C-6 of the pyridine nucleus, rendering 1,2-/1,6-dihydropyridines. In this chapter, an alternative approach to this type of dearomatization reaction, employing activated *N*-benzylpyridinium salts in combination with a bifunctional organic catalyst is presented. Optically active 1,4-dihydropyridines resulting from the addition of the nucleophile (indole) to the C-4 of the pyridine nucleus are obtained as major products, rendering this method for nucleophilic dearomatization of pyridines complementary to previous approaches.

3.1 Background

Regio- and stereoselective dearomatization of pyridines represent one of the most powerful tools for the construction of complex and biologically relevant hydropyridine or piperidine scaffolds.[35] This process can be accomplished in two conceptually different

manners: namely, reductions and nucleophilic additions, both of which require pyridine as the electrophilic reaction partner. Reductions, i.e. addition of hydride nucleophiles, rely on the preparation of a pre-functionalized aromatic scaffold to be dearomatized in a late-stage process, whereas nucleophilic additions tackle the opportunity to build complexity during the same dearomatization reaction. In both cases however, the pyridine nucleus usually requires activation to undergo a successful dearomatization, since pyridine itself is usually not electrophilic enough (Scheme 1).[36]

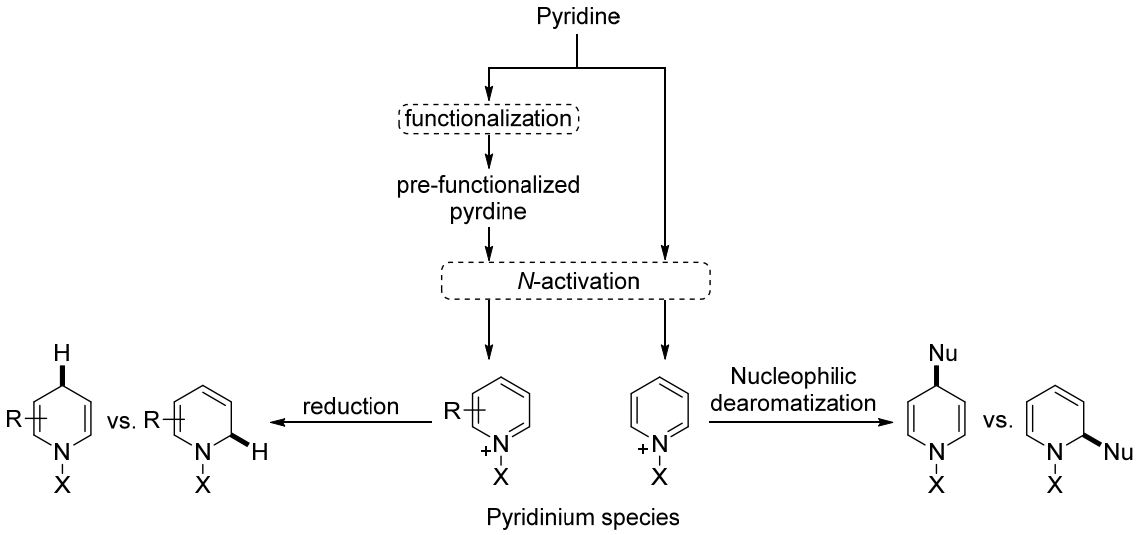

Scheme 1. Nucleophilic dearomatization and reduction of pyridinium cations.

Among the most useful activation methods, the preparations of pyridinium salts by reaction of the *N*-atom with various electrophiles has attracted much attention. Two categories of pyridinium cations can be synthesized and successfully employed in dearomatization processes, namely *N*-acyl- and *N*-alkylpyridinium salts.

N-Acylpyridinium salts, unstable species to be generated at low temperatures and reacted *in situ*, have been extensively employed in dearomatization reactions with a variety of nucleophiles. However, a regioselectivity issue arose from the two different positions (C-2 or C-6 and C-4) prone to nucleophilic attack present on the pyridine nucleus. Both steric bulk and hard or soft nature of the nucleophile were found to be factors determining the regiochemical outcomes of such additions.[37] Besides many exceptions, hard nucleophiles are usually found to be selective towards the C-2 position, while softer nucleophiles react selectively towards the C-4 position. However, when a bulky *N*-acyl activating group is present, the amount of C-4 functionalized product may increase (Scheme 2).

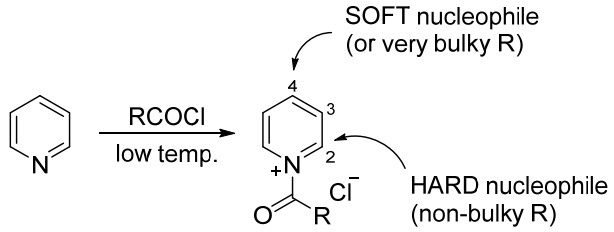

Scheme 2. Formation of *N*-acyl pyridinium salts and electrophilic sites.

For example, in 1981, Comins and Abdullah reported the reaction of various Grignard reagents, such as phenylmagnesium bromide, towards different *N*-acylpyridinium salts. Although in the absence of steric hindrance around the *N*-atom, the hard nature of the nucleophile rendered it selective towards position C-2, the presence of a pivaloyl activating agent gave a balanced regioisomeric mixture, favoring some extent of C-4 functionalization (Scheme 3, left).[38] In contrast, addition of soft nucleophiles, such as organocuprates[39] or silyl enol ethers,[40] was found to be almost exclusively C-4 regioselective (Scheme 3, right).

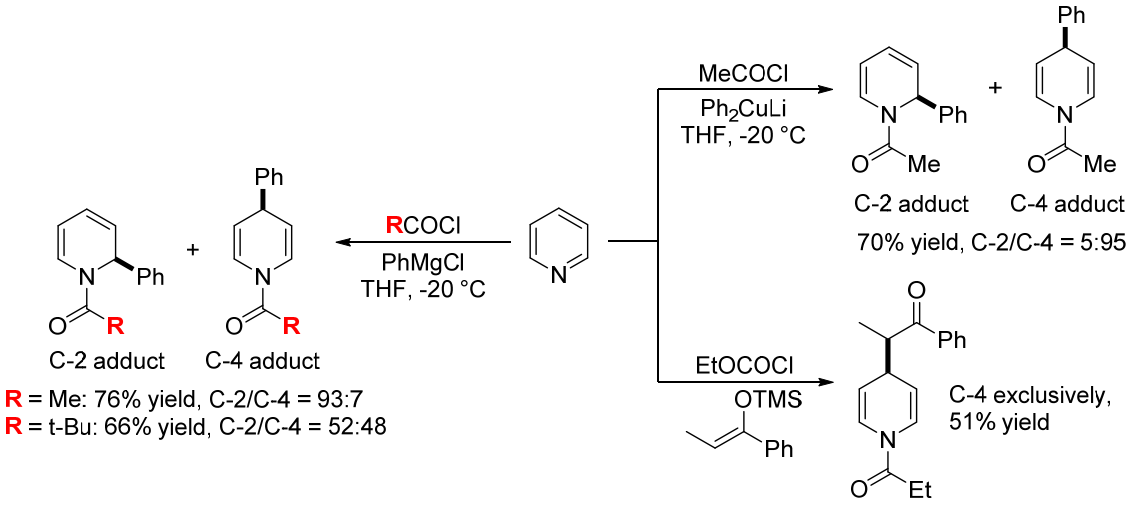

Scheme 3. Addition of hard and soft nucleophiles to *N*-acyl pyridinium salts: regiochemistry.

Substituted pyridines are even more challenging, presenting now three different electrophilic sites. On the other hand, substitution of the pyridine ring could also be employed to affect the regioselectivity of the nucleophilic addition. Thus, a bulky group at position C-3 for example, discourages functionalization at C-4 and C-2, rendering the C-6 the only carbon available for a nucleophilic attack. This strategy, relying on a 3-trisisopropylsilylpyridinium, in combination with a chiral *N*-acylating agent, was employed by Wanner, after the seminal work of Comins, to promote a regio- and diastereoselective addition of Grignard reagents (Scheme 4).[41]

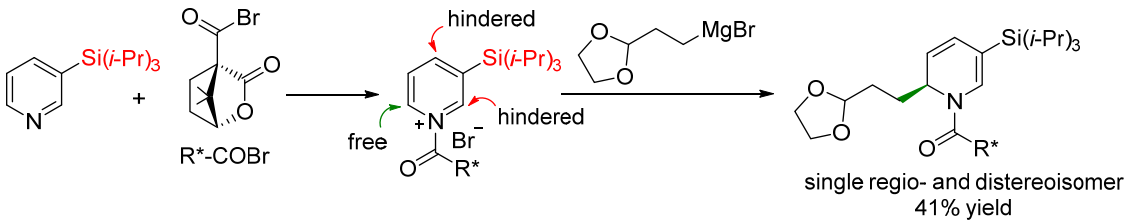

Scheme 4. C-6 selective functionalization of a hindered pyridinium salt.

In contrast with the unstable and transient nature of *N*-acyl species, the *N*-alkyl analogues are bench-stable crystalline solids that can be easily synthesized and isolated. On the other hand, *N*-acylpyridiniums rely on an enhanced electrophilicity and hydropyridinic product stability, while *N*-alkyl cations are more inert and deliver much less stable dearomatized products. For this reason, additional activation is often required to productively engage *N*-alkylpyridiniums in dearomatization reactions. This is commonly achieved by installing an electron-withdrawing group at the 3-position, resulting also in greater stability of the dearomatized products.[42]

Addition of organometallic reagents to this type of *N*-alkylpyridinium salts was predominantly carried out with organocuprates. While aryl nucleophiles reacted with good C-4 regioselectivities,[43] other type of substrates (such as alkynyl or alkyl) gave difficult to rationalize mixtures of regioisomers, depending on the nature of the organic residue or the cuprate moiety (Table 1).[44]

Table 1. Addition of various organocopper reagents to *N*-methylpyridinium iodide.

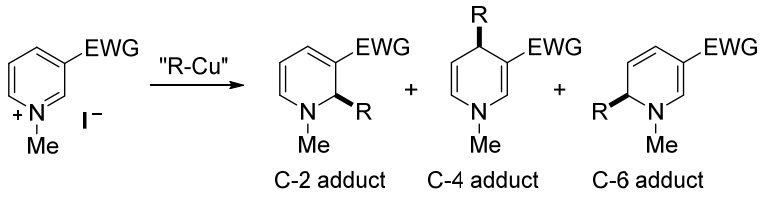

Entry	EWG	"RCu"	C-2/C-4/C-6	Combined yield (%)	ref.
1	CO_2Me	PhMgCl, CuI (cat.)	0:100:0	90	43a
2	CN	$Ph_2Cu(CN)Li_2$	0:100:0	90	43b
3	CO_2Me	Bu_2CuLi	0:90:10	77	44
4	CO_2Me	$(PhC{\equiv}C)_2Cu(CN)Li_2$	50:0:50	68	44
5	CO_2Me	$(PhC{\equiv}C)_2Cu(CN)(ZnCl)_2$	20:0:80	18	44
6	CO_2Me	PhC≡CMgBr, CuI (cat.)	100:0:0	65	44

Much attention has arisen also in the addition of other type of nucleophiles to this class of activated substrates, such as stabilized anions and indoles. As far as the first ones are concerned, both the nature of the EWG group and the nucleophile were found to affect the regiochemistry of the reactions and excellent degree of regiocontrol could be achieved with some specific combinations. For example, addition of malonate equivalents promoted by sodium methoxide in methanol to *N*-methyl-3-nitropyridinium iodide displayed full C-4 selectivities (Scheme 5, top left).[45] Addition to differently activated *N*-alkylpyridiniums resulted in: full C-6 selectivity in the case of bis(methylthio)methane, a balanced mixture in the case of butyrolactone, or full C-4 selectivity when methyl 2-(methylthio)butanoate where employed as nucleophile precursors (Scheme 5, bottom left).[46] Indole additions, on the other hand, were reported to be not only substrate-dependent, but to show also a dramatic influence of the reaction conditions on the regiochemical outcome. Thus, by changing the base or the solvent, the C-2/C-4 ratio could be favorably tuned (Scheme 5, right).[47]

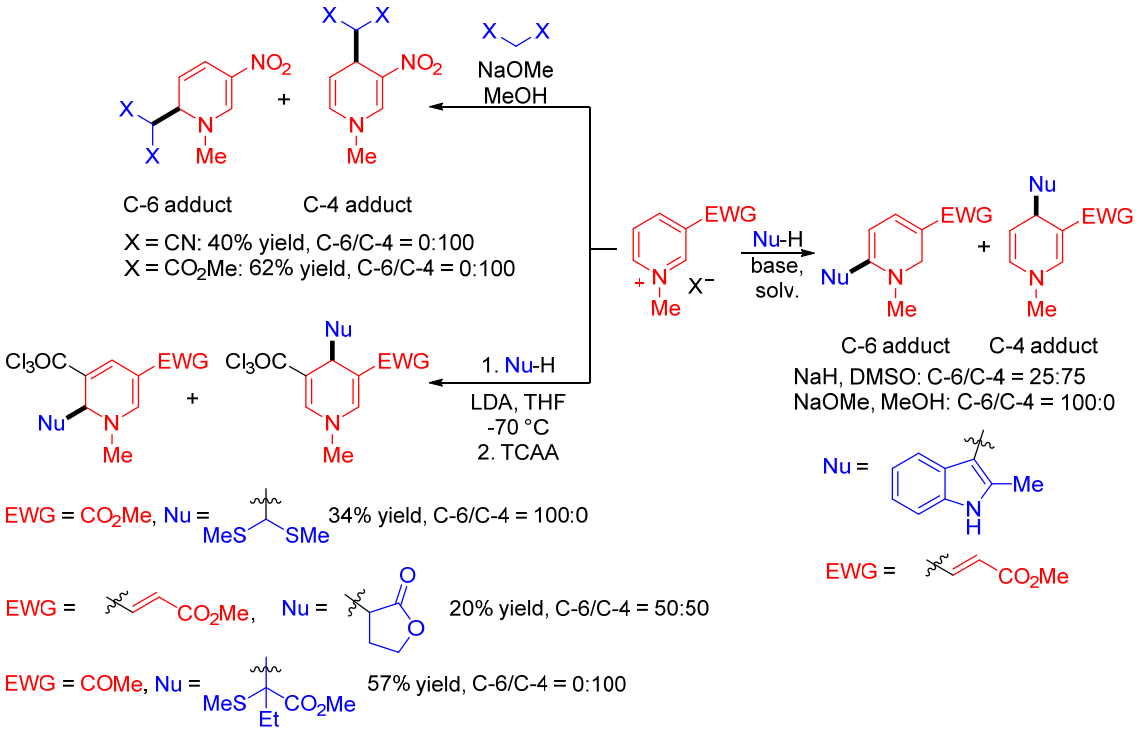

Scheme 5. Addition of stabilized anionic nucleophiles and 2-methylindole to *N*-methylpyridinium halides.

The utility of *N*-alkylpyridiniums dearomatization in organic synthesis is well demonstrated by its involvement in the total synthesis of several alkaloids; one of the most well-known and exploited methodology is undoubtedly the so-called "Wenkert

procedure". This consists in the construction of a tetracyclic hydrocarboline-like structure through a C-4 regioselective *N*-alkylpyridinium salts dearomatization, followed by a diastereoselective Pictet-Spengler cyclization. Two different variants of this procedure can be reported, depending on the relative position of the indole, the pyridinium and the nucleophile exploited for the dearomatization. The first type employs *N*-tryptyl pyridinium salts in combination with an external stabilized anionic nucleophile, leading to fused tetracycles. This was the first to be employed in 1973 (and revised in 1984) for the synthesis of vallesiachotamine (Scheme 6);[48] more than ten different alkaloids were later synthesized using the same methodology.[36]

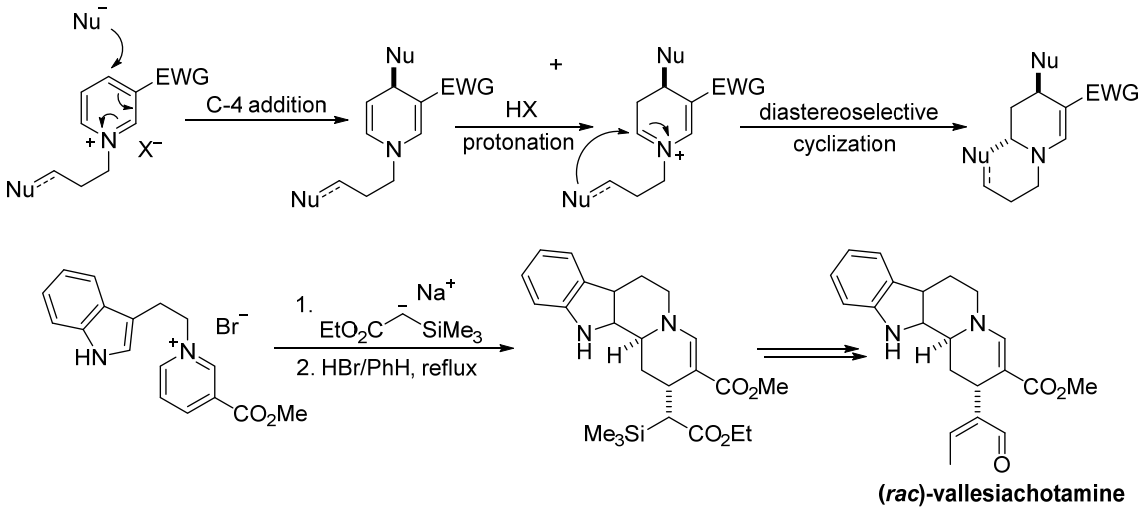

Scheme 6. Schematic strategy for one type of Wenkert procedure and application to the total synthesis of (*rac*)-vallesiachotamine.

On the other hand, the procedure can be employed for the preparation of bridged cycles, if the nucleophile is positioned at the C-2, C-3 or at the *N*-atom of the indole, instead of this being tethered to the alkyl substituent of the pyridinium ring. For example, the anions of methyl 1-, 2- or 3-indoloacetate were added to various activated pyridinium salts for the rapid total synthesis of different families of alkaloids (Scheme 7a). This was achieved by employing exactly the same strategy: namely, addition of the pre-formed anion, followed by an acid-promoted cyclization of one the one of the free nucleophilic positions of indole (C-3 or C-2). Methyl-1-indoloacetate lithium salt was employed for the synthesis of (*rac*)-vinoxine (Scheme 7b),[49] methyl 2-indoloacetate served as a precursor of the central core of the *Strychnos* alkaloids (Scheme 7c),[50] and methyl 3-indoloaceate produced a tetracyclic scaffold, characteristic of the akuammiline alkaloids (Scheme 7d).[51]

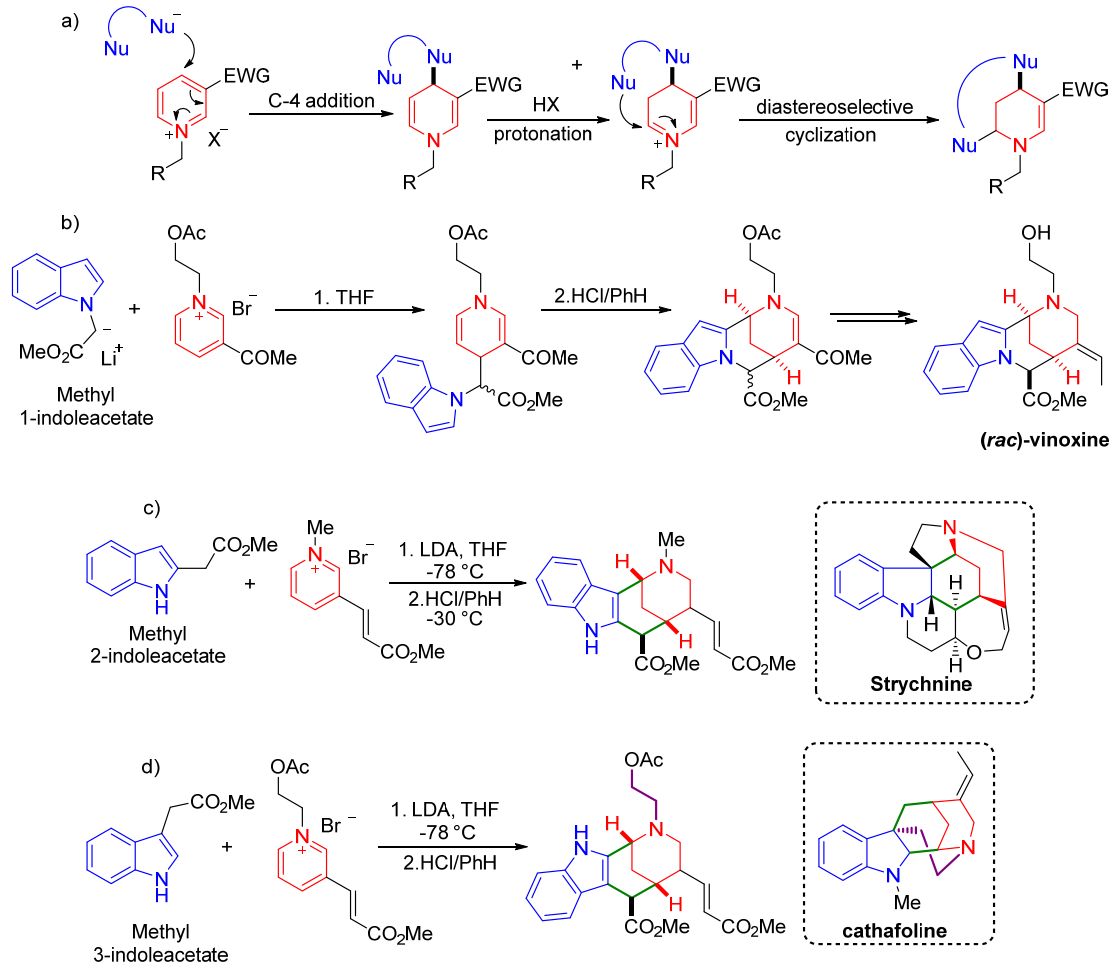

Scheme 7. Schematic strategy for the second Wenkert procedure and related examples.

Although the methodology granted accessibility to a great number of structurally diverse natural compounds, these were obtained exclusively in racemic form; the first enantioselective variant was indeed reported very recently, (subsequent to our works on organocatalytic pyridinium salts dearomatizations) by the group of Shu-Li You. The authors reported a "simplified" procedure, involving a C-4 regioselective reduction of *N*-tryptylpyridinium salts (thus not generating any chiral center at the 4-position) followed by chiral phosphoric acid catalyzed Pictet Spengler cyclization. This was also applied to the total synthesis of (+)-deplanceine (Scheme 8).[52]

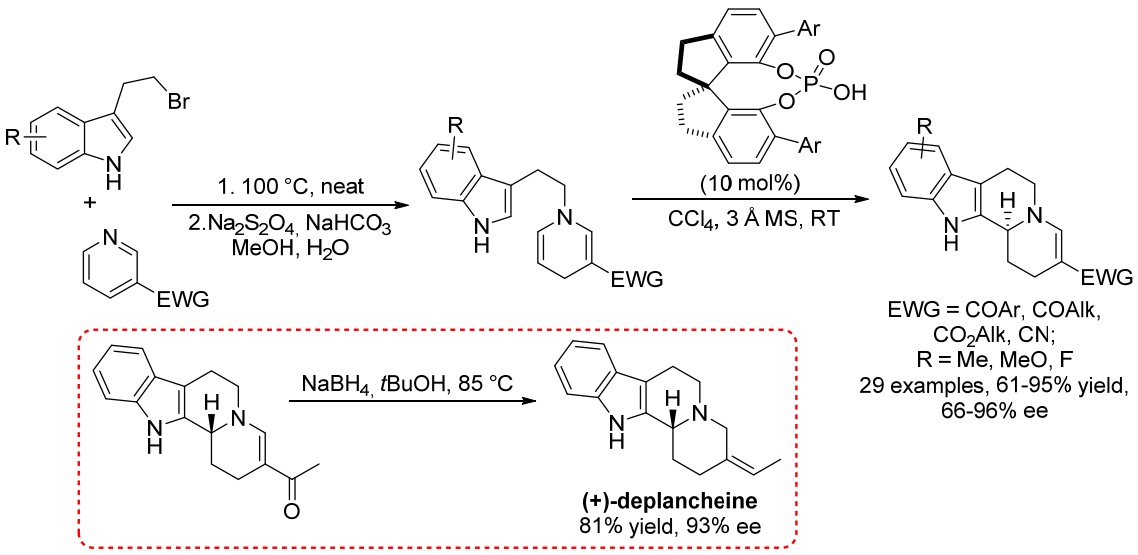

Scheme 8. Construction of chiral tetrahydro-β-carbolines by phosphoric acid catalyzed Pictet-Spengler reaction. Ar = 2,4,6-(*i*-Pr)$_3$C$_6$H$_2$.

Indeed, dearomatization processes represent a useful platform to introduce chiral information into organic molecules, starting from flat aromatic compounds. Various organometallic catalysts were reported to induce stereoselectivity in the addition of a certain variety of nucleophiles to the C-2 or C-6 of highly activated *N*-acylpyridinium salts. For example, chiral aluminum catalysts were found to efficiently promote an asymmetric Reissert reaction, namely the addition of cyanide nucleophiles to (activated) *N*-acylpyridinium cations. In this reaction, proceeding with almost exclusive C-6 regioselectivity, high yields and enantioselectivities were observed for a variety of *N*-alkoxycarbonyl nicotinamides, employing TMS-CN as the cyanide source. This procedure was then applied to a formal catalytic enantioselective synthesis of the dopamine D4 receptor-selective antagonist, CP-293,019 (Scheme 9).[53]

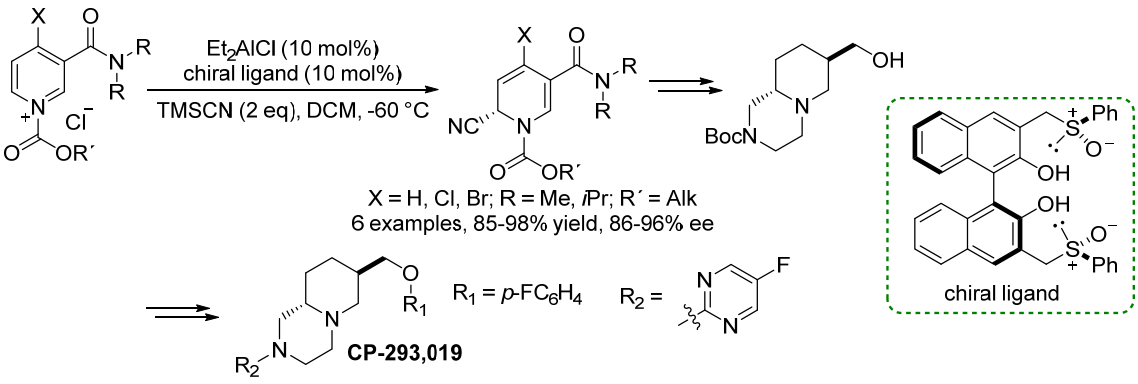

Scheme 9. Asymmetric Reissert reaction.

Organozinc reagents were also found to be productive nucleophiles for regio and enantioselective dearomatizations of *N*-acylpyridiniums. Feringa's group developed in 2009 a chiral copper/phosphoramidite catalyst for the asymmetric addition of various dialkylzinc nucleophiles to 4-methoxy-*N*-benzyloxycarbonyl pyridiniums, resulting in the formal total synthesis of the alkaloid (*R*)-coniine (Scheme 10).[54]

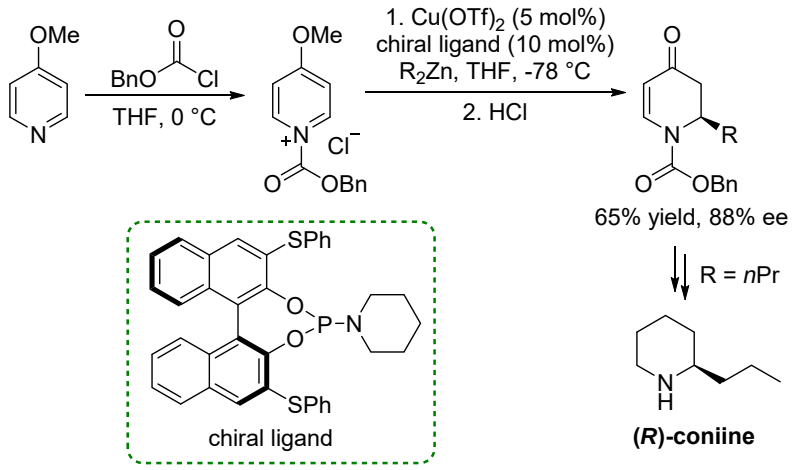

Scheme 10. Addition of organozinc reagents catalyzed by a chiral copper complex.

Doyle's group, on the other hand, relied on nickel catalysis when dealing with arylzinc reagents as nucleophiles. 4-Methoxypyridine and C-4 unsubstituted pyridines were productively dearomatized, after activation with chloroformates, under differently optimized reaction conditions. All these three examples, involving organozinc nucleophiles, proceeded with complete C-6 regioselectivity (Scheme 11).[55]

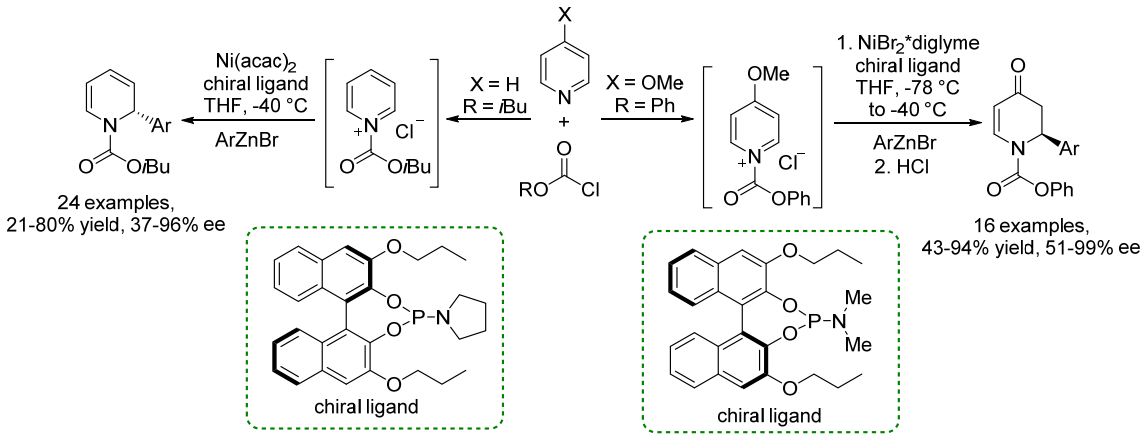

Scheme 11. Arylative dearomatizations catalyzed by chiral nickel complexes.

On the other hand, only one example of asymmetric dearomatization of *N*-alkylpyridinium salts had been reported, consisting in the highly enantioselective addition of aryl and alkenyl boronic acids to *N*-benzyl nicotinates, catalyzed by a chiral Rh-complex (Scheme 12).[56]

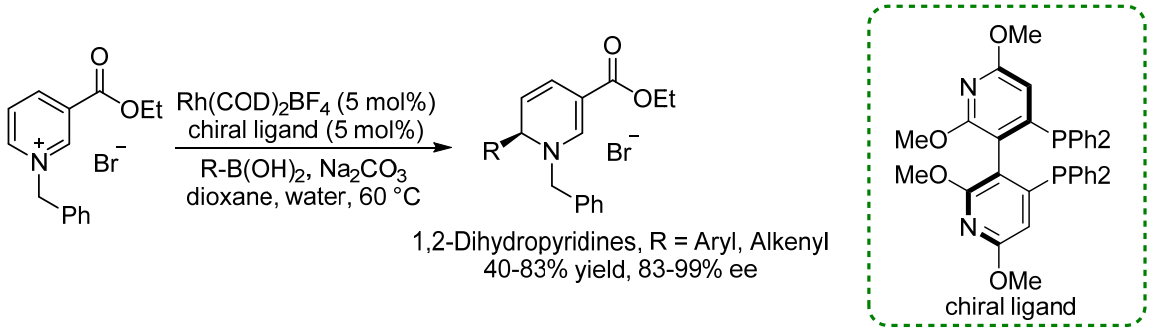

Scheme 12. Enantioselective dearomatization of *N*-alkyl pyridiniums catalyzed by a chiral rhodium complex.

A recent report introduced organocatalysis as a platform to induce stereoselectivity in pyridinium salts dearomatization. This disclosed anion binding by multiple hydrogen bond donors as a suitable approach to this type of reaction, using a silylketene acetal as nucleophilic partner. Variable C-2 or C-4 selectivities, depending on the substitution pattern at the pyridine ring, were observed and, for example, a 3-EWG substituted pyridine substrate gave C-2/C-4 regioisomers in 61:39 ratio. Previous asymmetric organocatalytic examples were all limited to less-demanding dearomatization of *N*-acylquinolinium and isoquinolinium substrates (Scheme 13).[57]

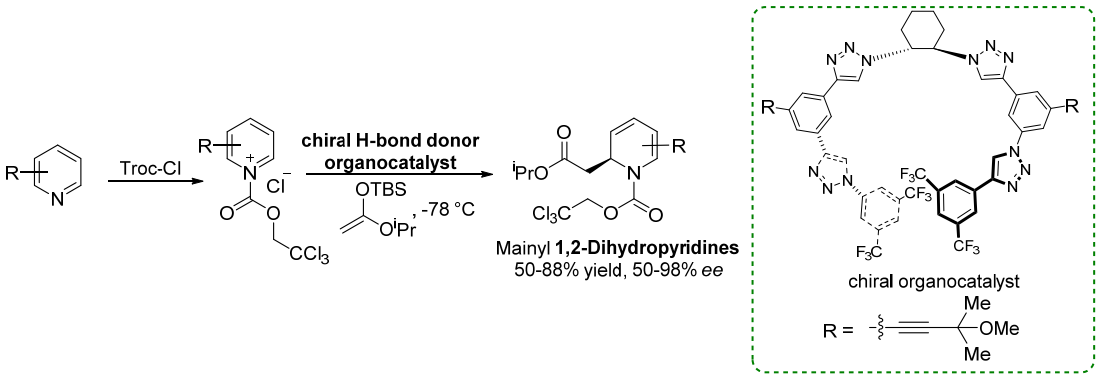

Scheme 13. Organocatalytic enantioselective dearomatization of *N*-acyl pyridiniums

We thus envisioned that *N*-alkylpyridinium salts, which are more stable and easier to handle, compared to their *N*-acyl analogues, may provide an alternative platform with unforeseen opportunities in catalytic enantioselective nucleophilic dearomatization of

pyridines. No report of organocatalytic enantioselective dearomatization of these substrates had been reported so far. In this context, our work on the development of *N*-alkyl pyridinium salts dearomatization reactions finds justification.

3.2 Aim of the work

The aim of the work described in this chapter has been the realization of the first organocatalytic enantioselective dearomatization of *N*-alkylpyridinium salts.

To our purposes, we have been conscious of the requirement of a suitable nucleophile and, as a consequence, a suitable catalytic system, capable of activation of at least one of the substrates. The choice however, was not obvious, as the literature precedents for the activation of pyridinium salts by organocatalysts were scarce and not existent for *N*-alkylpyridinium cations at all.

In addition, some synthetic challenges arise from this strategy: for instance, the aromaticity of pyridinium cations, along with the instability of dearomatized dihydropyridines, might lead to reversible addition of highly stabilized anionic nucleophiles, thus preventing an easily accessible enantioenriched addition. A judicious choice of the nucleophile, along with the activating EWG group, was thus important, in order to stabilize the dearomatized product and prevent re-aromatization. Moreover, as presented in the introduction, the regiochemistry of the nucleophilic dearomatization of pyridines is challenging and difficult to control, giving rise to poorly selective processes[46] or scarcely robust protocols.[47] Given this, one of the most exciting goals of this project was to find a process that delivered high regioselectivity towards the not easily accessible C-4 functionalized products, as most of the dearomatization of *N*-acyl (or alkyl) pyridinium salts presented above rendered C-2 (or C-6) products predominantly.[53-57] This is probably due to the enhanced electrophilicity of these positions, rendering thus 1,2- (or 1,6-) dihydropyridines as kinetic products, with the 1,4-dihydropyridines being the more stable thermodynamic compounds. However, reaching these products towards equilibration from the corresponding 1,2-dihydropyridines might imply difficulties in controlling the stereochemistry, leading to poor enantioselectivities.

Herein, it is possible to anticipate that *N*-alkyl pyridinium salts **1** were reacted with indoles **2** in the presence of bifunctional catalysts **3**, giving highly enantioenriched 1,4-dihydropyridnes **4**. This reaction represents the first example of organocatalytic enantioselective dearomatization of *N*-alkyl pyridinium salts (Scheme 14).

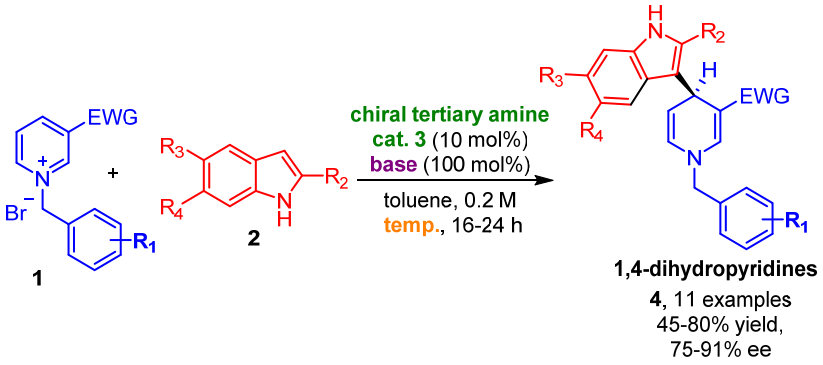

Scheme 14. *N*-alkylpyridinium salts dearomatization: project overview.

3.3 Results and discussion

The investigations on the asymmetric dearomatization of *N*-alkyl pyridinium salts started from the choice of the most promising substrate **1** and nucleophile combination. For example, attempts involving stabilized anionic nucleophiles such as the enolates derived from malonate or acetylacetone generated under different basic catalysis activation strategies, failed in rendering stable dearomatized compounds, probably due to the strong tendency of the pyridinium ring to undergo rearomatization. Moreover, pyridinium salts bearing an ester or a ketone at the C-3 positions were found to be poorly reactive, as the substituent was not electron-withdrawing enough to activate the substrate. However, indole **2a** was found to be a promising nucleophile, with less tendency to undergo reversible addition-elimination sequences; in addition, 3-nitro- or 3-cyano-substitued pyridinium salts proved to be more reactive substrates. Therefore, our screening started employing *N*-benzyl-3-nitropyridinium bromide **1a** and indole **2a** as model reaction partners. A key feature of this organocatalytic reaction is the formation of the 1,4-dihydropyridine regioisomers **4** as the major products, thus providing a new platform for nucleophilic pyridine dearomatization reactions, complementary in several aspects to existing methodologies.[56,57] All the preliminary screening experiments rendered adduct **4**, accompanied by substantial amounts of the indole *N*-alkylation product **5**, whereas C-2 or C-6 regioisomers were never detected in the reaction crude, revealing this system as a very promising fully regioselective strategy.

Our initial plan involved a reactivity enhancement of pyridinium salts **1a** by drifting apart the tightly bound halide counterion. Exploiting the low solubility of salts **1** in apolar organic solvents, an inverted phase-transfer catalytic approach was first

attempted.[58] However, no reaction was observed when the anion generated from a commonly employed BINOL-derived phosphoric acid and an inorganic base were employed as the catalytic system (Scheme 15).

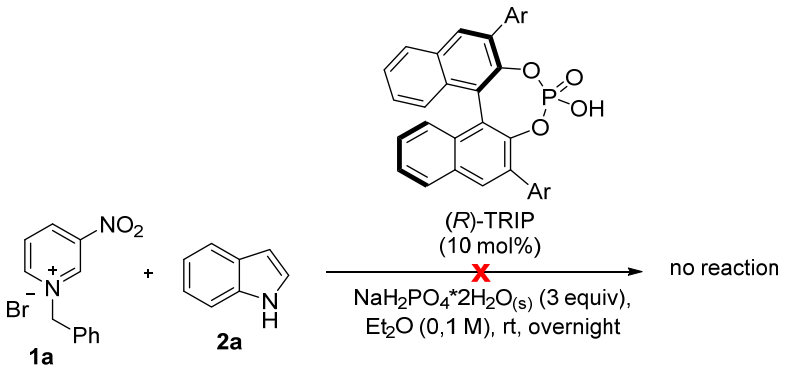

Scheme 15. Inverse phase-transfer catalytic approach. Reaction conditions: **1a** (0.05 mmol), **2a** (0.065 mmol), (*R*)-TRIP (10 mol%), $NaH_2PO_4*2H_2O$ (0.15 mmol), Et_2O (500 µL), RT, 18-24 h. Ar = 2,4,6-$(iPr)_3C_6H_2$.

We then tried an anion-binding activation strategy, using typical Jacobsen-type thioureas[59] and no reaction was observed in the absence of a base. Since it was clear that a stoichiometric amount of base is needed for the dearomatization to occur, as strongly acidic HBr is formed, we performed the same reaction with two different bases. A base-dependent selectivity was observed, since aqueous $NaHCO_3$ furnished only product **5aa**, while solid Na_2CO_3 rendered **4aa** as the sole product. However, in both cases, the products were found to be racemic, underlying that the reactions were promoted by the base alone (Table 2).

Table 2. Anion-binding activation approach.[a]

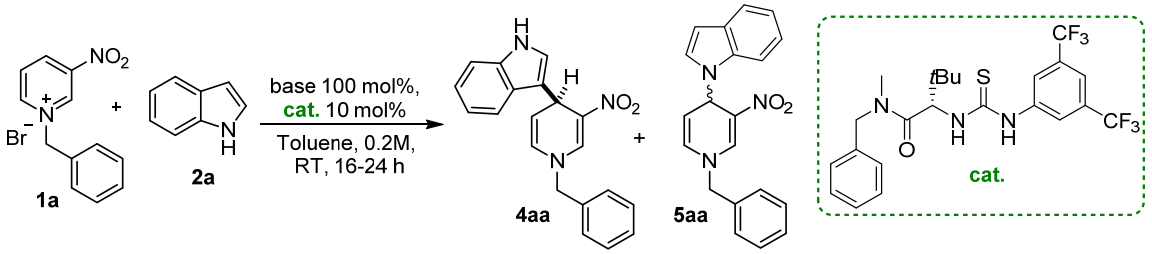

Entry	Base	Conversion[b,c] (%)	**4aa**/**5aa**	ee **4aa**/**5aa**[d] (%)
1	None	< 5	-	-
2	$NaHCO_{3\,(aq)}$ (5% wt.)	80	< 5:95	-/rac
3	$Na_2CO_{3\,(s)}$	70	> 95:5	rac/-

(**a**) Reaction conditions: **1a** (0.05 mmol), **2a** (0.065 mmol), catalyst (10 mol%), base (0.05 mmol), toluene (250 µL), RT, 18-24 h. (b) Determined on the crude mixture by ^{1}H NMR. (c) Overall conversion in products **4aa** and **5aa**. (d) Determined by chiral stationary phase HPLC.

Preliminary experiments showed that a catalyst bearing a tertiary amine basic moiety (quinine **3a**), was able to promote the reaction, rendering the C-4 addition product **4aa** with low yet promising enantioselectivity (Table 3, entry 1). Then, we carried out reactions with different base candidates and quinine **3a** as a preliminary catalyst. Both strong (entries 3,4) and weak (entry 2) organic bases, along with inorganic ones (entry 5) showed satisfactory conversions but very low ee values for adduct **4aa**, accompanied by variable amounts of indole *N*-alkylation product **5aa**, obtained as a racemate in all cases. These results suggested that these reactions were promoted by the auxiliary bases, rather than by the catalyst. Only an attempt performed with proton sponge (1,8-bis(dimethylamino)-naphthalene, PS),[60] rendered the same enantioselectivity obtained with quinine **3a** alone (compare entries 1 and 6). Although this positive result was accompanied by the formation of larger amounts of racemic **5aa**, we chose this base to perform a subsequent catalyst screening, postponing this selectivity problem to later optimization.

Table 3. Base screening.[a]

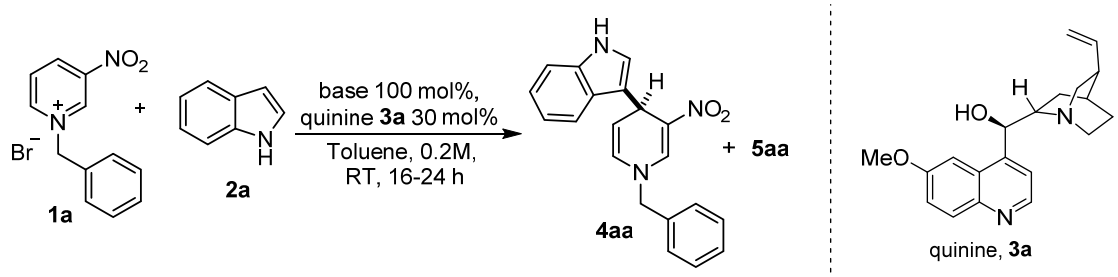

Entry	Base	Conversion[b,c] (%)	**4aa**/**5aa**[b]	ee[d] (%)
1	None	30	>95:5	25
2	Pyridine	75	>95:5	rac
3	Et_3N	60	65:35	rac
4	Quinuclidine	80	>95:5	rac
5	NaOAc	40	85:15	rac
6	Proton Sponge (PS)	47	35:65	25

(**a**) Reaction conditions: **1a** (0.05 mmol), **2a** (0.065 mmol), cat. **3a** (30 mol%), base (0.05 mmol), toluene (250 μL), RT, 16-24h. (**b**) Determined on the crude mixture by ^{1}H NMR. (**c**) Overall conversion in products **4aa** and **5aa**. (**d**) Of product **4aa**, determined by chiral stationary phase HPLC.

Among others, bifunctional catalysts bearing a basic functionality along with H-bond donor moieties, such as squaramide (**3b**, Table 4, entry 2), sulphonamide (**3c**, entry 3), urea (**3e**, entry 5) and thiourea (**3d** and **3f** entries 4 and 6) performed better than quinine **3a** (entry 1) in terms of enantioselectivity of **4aa**, with the most promising result obtained with catalyst **3f**.[61] The **4**/**5** selectivity of these reactions remained rather poor, with isomer **5aa** always produced in racemic form. As shown in Table 4, entries 7-15, the other cinchona alkaloid derivatives (**3g-n**) and cyclohexyldiamine **3o** tested (Figure 1) were found to be able to promote the reaction between **1a** and **2a**, but afforded lower enantioselectivities than catalyst **3f** (entry 6).

Table 4. Catalyst screening.[a]

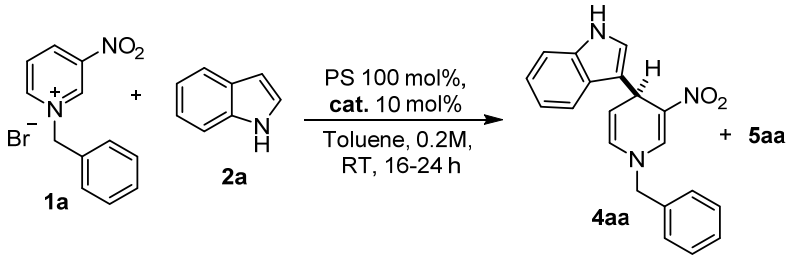

Entry	Catalyst	Conversion[b,c] (%)	**4aa**/**5aa**[b]	ee[d] (%)
1	**3a**	47	35:65	30
2	**3b**	64	40:60	40
3	**3c**	50	50:50	33
4	**3d**	49	35:65	30
5	**3e**	55	50:50	50
6	**3f**	60	65:45	68
7	**3g**	49	63:37	22
8	**3h**	50	75:25	rac
9	**3i**	51	69:31	10
10	**3j**	50	52:48	25
11	**3k**	51	48:52	13
12	**3l**	40	75:25	8
13	**3m**	45	62:38	18
14	**3n**	50	80:20	10
15	**3o**	56	25:75	rac

(**a**) Reaction conditions: **1a** (0.05 mmol), **2a** (0.065 mmol), **cat. 3** (10 mol%), PS (0.05 mmol), toluene (250 µL), RT, 16-24h. (b) Determined on the crude mixture by ^{1}H NMR. (c) Overall conversion in products **4aa** and **5aa**. (d) Of product **4aa**, determined by chiral stationary phase HPLC.

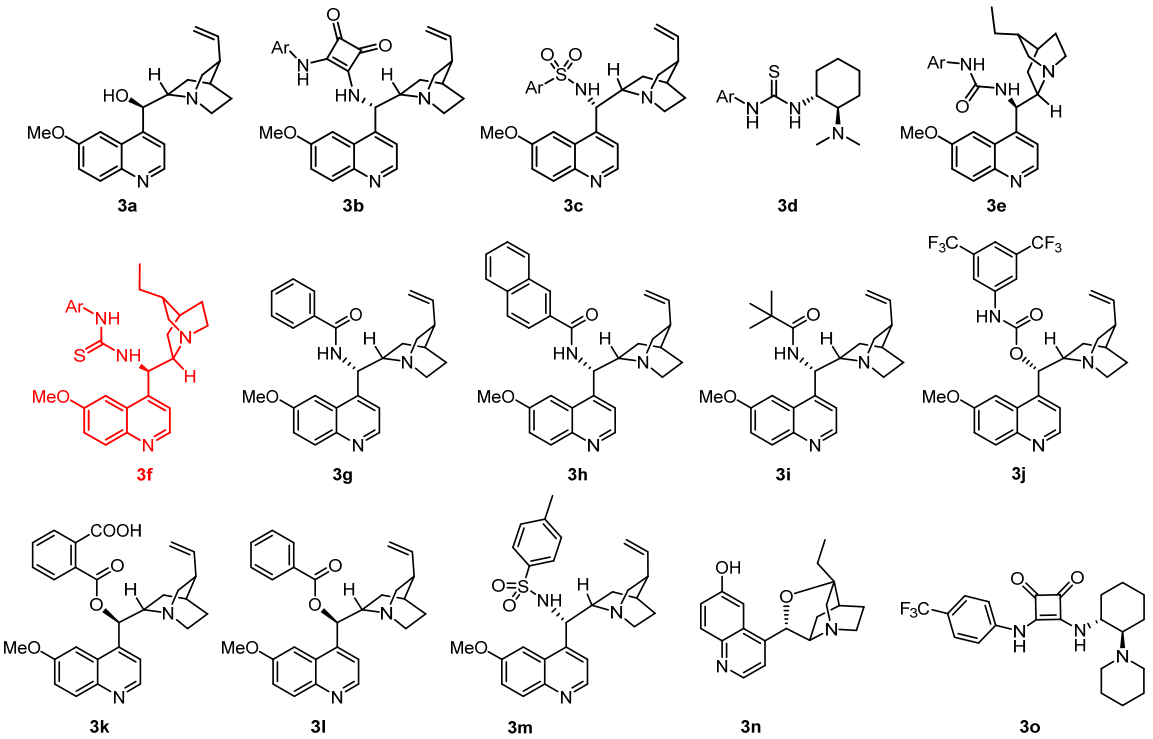

Figure 1. Catalysts screened in Table 4; Ar = 3,5-$(CF_3)_2$-C_6H_3.

Further optimization showed that lowering the reaction temperature gave better enantioselectivity in **4**, without giving a great detriment in conversion (entries 1−3 in Table 5). The **4**/**5** ratio was also slightly improved. Variations in the aryl ring of the *N*-benzyl substituent were then explored. Substrates **1b**−**e** bearing electron-withdrawing groups (**1b**, entry 4 and **1c**, entry 5) and additional aromatic rings (**1d**, entry 6 and **1e**, entry 7) gave lower enantioselectivities, compared to the unsubstituted substrate **1a** (entry 3), accompanied by variable conversions. In contrast, an electron-donating methoxy substituent (**1f**, entry 8) incremented slightly the enantioselectivity. Interestingly, the reaction outcome worsened considerably when employing the pyridinium salt **1′f**, bearing chloride, instead of bromide, as the counterion (entry 9, compared to entry 8). We were instead pleased to find that a bulky substituent, such as *t*-Bu (**1g**), gave remarkable improvement in both reactivity and enantioselectivity, along with a promising selectivity for product **4ga** vs **5ga** (entry 10). This positive result may be rationalized, considering the sandwich-like structure of substrates **1**, inferred from the X-ray structure of related *N*-benzylpyridinium salts, in which the halide is fitted between the two aromatic rings.[62] A bulky (and electron-rich) substituent may open this structure, rendering the Br anion more available for thiourea coordination (*vide infra*). Finally, we found that the undesired isomer **5** is apparently generated as a background PS-promoted

process. Thus, we envisioned that a controlled addition of this auxiliary base would have resulted in an improvement in selectivity. Indeed, when PS was added portion-wise over 10 h, a good 91:9 ratio in favor of the desired product **4ga**, along with a satisfactory 91% enantiomeric excess (ee), was achieved (entry 11 in Table 1). Multiple solvent screenings were also performed, affording similar or worse results, compared to toluene (results not shown).

Table 5. Temperature and benzyl group screening[a]

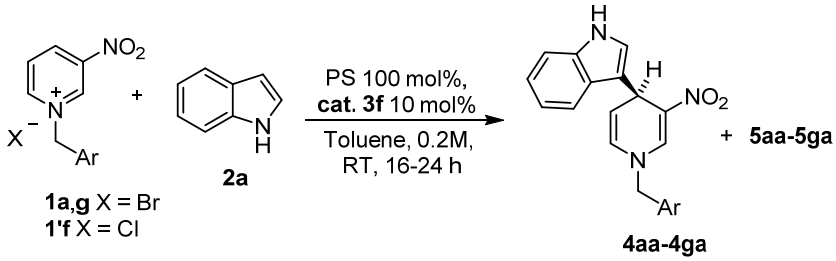

Entry	T (°C)	**1a-g**, Ar	Conversion[b,c] (%)	**4/5**[b]	ee[d] (%)
1	RT	**1a**, Ph	60	55:45	68
2	0	**1a**, Ph	50	55:45	75
3	-20	**1a**, Ph	50	70:30	75
4	-20	**1b**, 4-BrC_6H_4	52	80:20	70
5	-20	**1c**, 3,5-$(CF_3)_2C_6H_3$	89	71:29	63
6	-20	**1d**, 2-naphthyl	51	88:12	67
7	-20	**1e**, 4-PhC_6H_4	13	95:5	45
8	-20	**1f**, 4-MeOC_6H_4	52	82:18	82
9	-20	**1'f**, 4-MeOC_6H_4	31	76:24	58
10	-20	**1g**, 4-*t*-C_6H_4	88	71:29	87
11[e]	-20	**1g**, 4-*t*-C_6H_4	92	91:9	91

(**a**) Reaction conditions: **1** (0.05 mmol), **2a** (0.065 mmol), **cat. 3f** (10 mol%), PS (0.05 mmol), toluene (250 µL), temp, 16-24h. (**b**) Determined on the crude mixture by ^{1}H NMR. (**c**) Overall conversion in products **4aa** and **5aa**. (**d**) Of product 4aa, determined by chiral stationary phase HPLC. (**e**) 0.2 equiv of PS were added every 2 h: overall 1 equiv in 10 h.

Having identified reaction conditions and substrate requirements for optimal results, the reaction scope was investigated (Scheme 16). Variation of the bulky substituent in the *N*-benzyl moiety afforded dearomatized products **4ha** and **4ia** in similar yields (75-70%) and enantioselectivities (91-90%) to adduct **4ga**. Variation at the indole **2** reaction partner showed that methoxy and methyl substituents at the 5-position were well tolerated (**4gb** and **4gc** 73-76% yield and 91-87% ee).

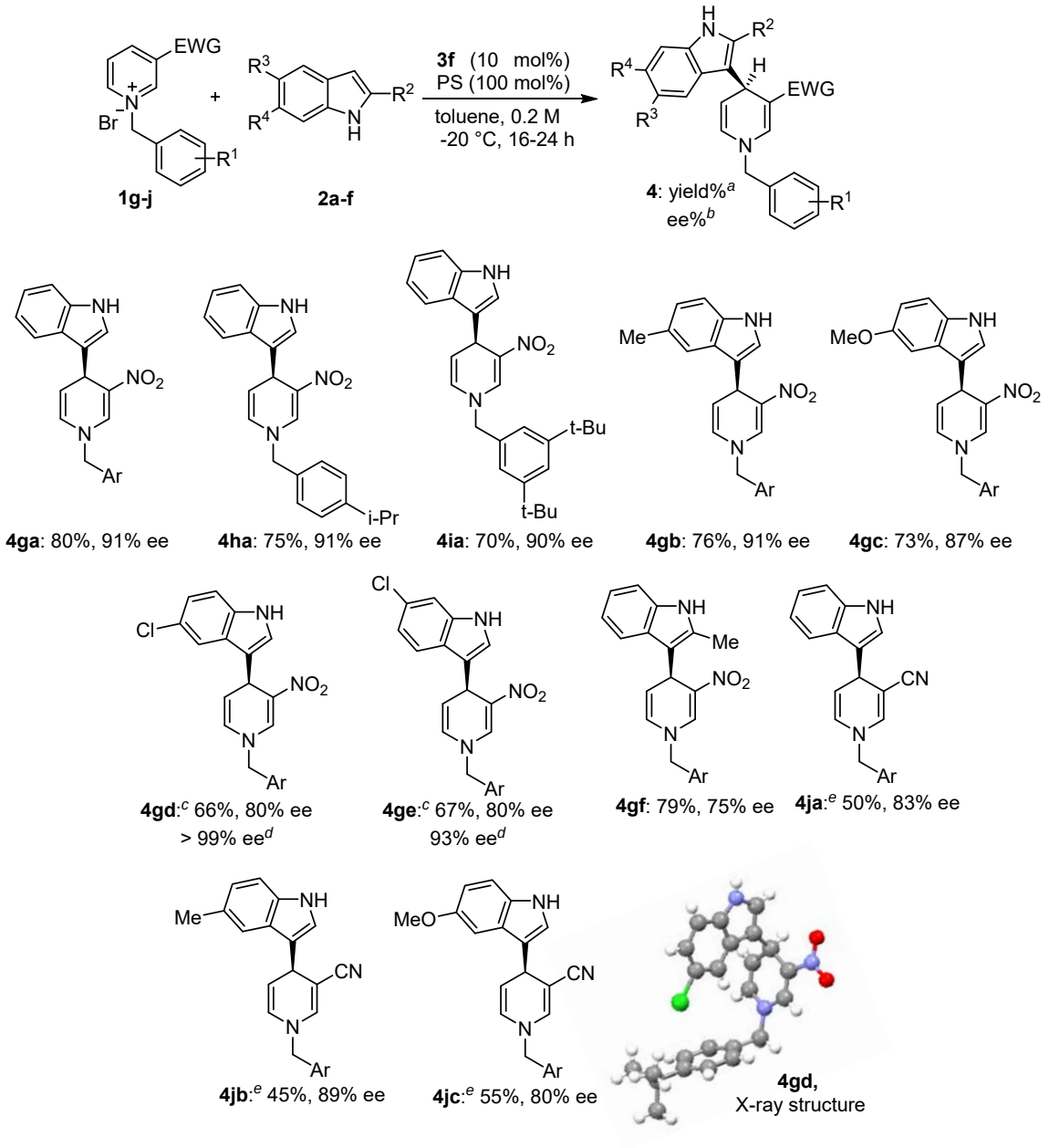

Scheme 16. Scope of the reaction. Conditions: **1g-j** (0.15 mmol), **2a-f** (0.195 mmol), **3f** (10 mol%), toluene (750 µL), -20 °C. Reaction was set up without PS, then 0.2 equiv. (0.03 mmol) of PS were added every 2 h: overall 1 equiv. (**a**) Yields of isolated products **4**. (**b**) ee determined by chiral stationary phase HPLC. (**c**) Reaction performed at 0 °C with 15 mol% **3f**. (**d**) After one crystallization. (**e**) Reaction performed at RT with 15 mol% **3f**. Ar = 4-*t*-BuC_6H_4.

Indoles **2d**,**e** bearing an electron withdrawing group (Cl) at both 5- and 6- positions afforded the desired adducts **4gd** and **4ge** with moderate enantiomeric excess (80% ee). Their lower reactivity required 15 mol% catalyst **3f** and a reaction temperature of 0 °C to afford satisfactory yields (66-67%). Crystallization of compound **4gd** afforded enantiopure single crystals which, upon X-ray analysis, provided the absolute configuration S at the C-4-stereocenter, extended by analogy to all other compounds **4**. Also the more challenging 2-methylindole **2f** was a suitable nucleophile for the present reaction, affording product **4gf** in very good yield and a moderate ee value of 75%. We then explored the possibility of changing the EWG at the C-3 of pyridinium salts **1**. To our pleasure, compound **1j** bearing a cyano group was found to be a sufficiently activated substrate for the present nucleophilic dearomatization. Although its lower reactivity forced us to increase the reaction temperature and the catalyst loading (15 mol%), dihydropyridines **4ja-jc** were obtained with useful results (45-55% yield, 80-89% ee) in the reactions with indoles **2a-c**. Possibly due to the higher temperature, the isomeric ratios **4**/**5** of these reactions were found to be lower than in the previous examples, accounting for the lower yields obtained with this less activated substrate **4j**. Other EWG (acetyl and methoxycarbonyl) at the 3-position were tested, but did not show sufficient reactivity.

Once demonstrated the generality of the present dearomatization reaction, resulting in 11 different examples, dihydropyridine **4ga** was then subjected to some synthetic elaborations, involving the two endocyclic double bonds, summarized in Scheme 17.

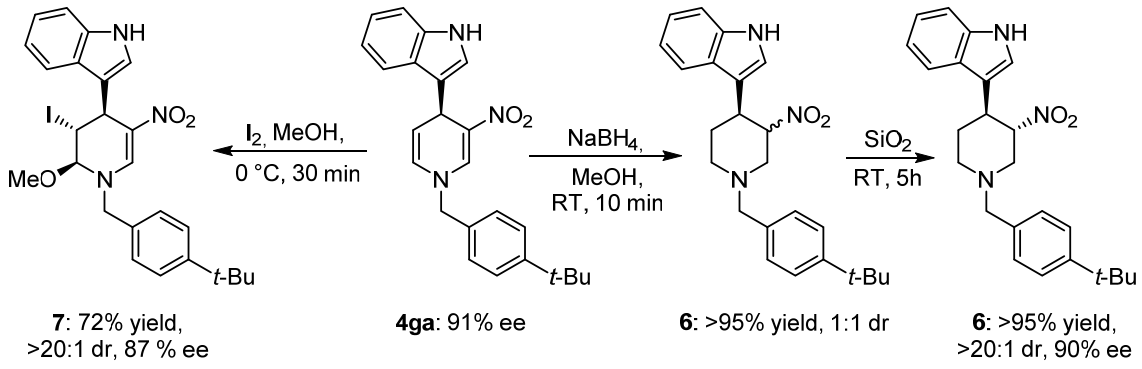

Scheme 17. Synthetic elaborations on product **4ga**.

By exposing product **4ga** to sodium borohydride reduction in methanol, piperidine **6** was readily obtained as a balanced mixture of diastereoisomers. Upon adsorption and standing on dry silica however, epimerization of the labile stereocenter bearing the nitro

group was possible, leading quantitatively to the most stable 3,4-*trans* diastereoisomer in high yield and complete retention of the enantiomeric excess.

On the other hand, following an "oxidative" protocol reported in literature,[63] functionalization of the sole electron-rich double bond of dihydropyridine **4ga** was possible. By treating this compound with a methanolic solution of molecular iodine, tetrahydropyridine **7** was in fact synthesized. This highly functionalized product bears three contiguous stereocenters and was obtained as a single diastereoisomer in good yield and 87% ee. These brief synthetic elaborations showed the possibility to achieve, by the present method, all the three possible degree of saturation of the pyridine ring, starting from aromatic pyridinium ions **1**: dihydropyridines **4**, tetrahydropyridine **7** and piperidine **6**. This broadens the flexibility of the disclosed dearomatization strategy and shows its utility as a synthetic procedure.

3.3.1 Mechanistic proposal

We initially believed the reaction to proceed by simple halide-extraction performed by the thioureidic portion of catalyst **3f**; in other words, coordination of the bromide counterion by the two N-H bonds would render the substrate soluble in the reaction medium, and at the same increase its reactivity.[58] This reasoning was preliminary supported by the complete insolubility of substrate **1g** in toluene.

In order to support this initial hypothesis with experimental ^{1}H NMR data, we mixed product **1g** and catalyst **3f** in toluene-*d8*. Whereas pyridinium salt alone did not give signals, due to its insolubility, in the presence of the catalyst a new species soluble in toluene appeared. This was identified as covalent adduct **I** (Scheme 18) resulting from the addition of the tertiary amine moiety of catalyst **3f** to the C-6 of the pyridinium ring (for more details see section 3.3.2). We therefore envisioned that activation of the pyridinium ion by the catalyst was beyond the initially hypothesized halide coordination – solid phase extraction. We therefore believe that catalyst **3f**, which bears both the thioureidic and the quinuclidinic moieties, acts in this way: nucleophilic addition at C-6 and bromide coordination.

On these grounds, we can propose the reaction pathway sketched in Scheme 18, involving the intermediacy of adduct **I** undergoing an S_N2'-like reaction with indole.[64] A concerted S_N2' mechanism does not seem likely, and an addition-elimination pathway has to be excluded (stabilization of the resulting negative charge is not possible due to

the loss of conjugation with EWG group). An elimination-addition sequence seems instead more reasonable. In other words, attack of the indole would occur either as the catalyst is already leaving its position, on an electrophile that resembles more the free cation (**III**) than the dihydropyridine **I**, or even on the free pyridinium (**II**). Even if, according to the latter hypothesis, intermediate **I** is not involved in the regio- and stereo-determining step of the reaction (the addition of indole), its formation plays a crucial role in the catalytic cycle, "increasing" the concentration of the electrophile in the reaction medium.

To complete the proposed mechanism, we investigated if the indole had some interactions with the catalyst in the enantiodetermining step. Since the catalytic reaction performed with *N*-methylindole afforded only a small amount of product (<15%), in racemic form, it is likely that the N-H plays a crucial role in the catalytic mechanism. To account for these experimental data, we can propose two ways of coordination of the indole N-H moiety: either to the bromide anion exclusively, in its turn coordinated by the thiourea, as previously proposed by Porco and Jacobsen,[65] while the nitrogen of the quinuclidinic portion is leaving the previously attached C-6 position (**II**); or by the quinuclidine nitrogen and the bromide anion coordinated by the thiourea together (**III**, in this case addition of indoles **2** occurs on free pyridinium cation **1**).

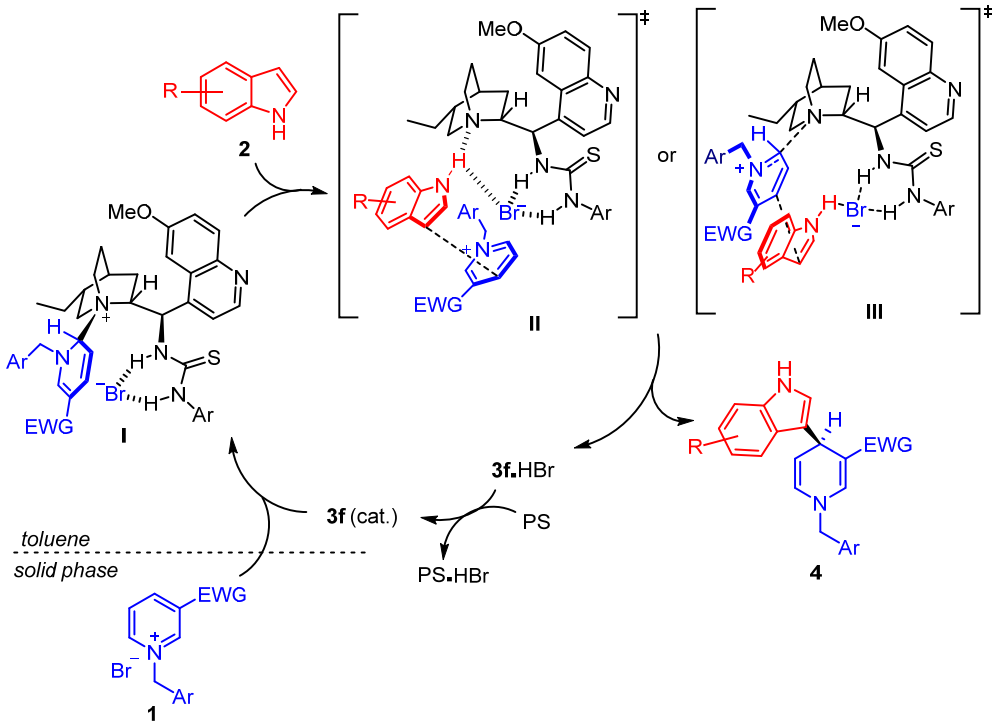

Scheme 18. Proposed reaction pathway and transition state.

Coordination of the thiourea to the EWG can be instead excluded, considering the similar results obtained with substrates **1g-i** where EWG = NO_2, and **1j** where EWG = CN.

Regarding the regioselectivity of the addition: the C-6 position of substrates **1** is generally considered to be the most reactive, while the C-4 gives the thermodynamically favored 1,4-dihydropyridine adducts. However, the regioselectivity in nucleophilic additions to *N*-alkyl pyridinium salts as **1** is often highly depending on the nature of the nucleophiles, with soft ones preferentially undergoing addition at C-4, and hard ones at C-6.[36] From the collected NMR data it seems that the C6-adduct **I** of a tertiary amine catalyst to pyridinium ions **1** is favored both kinetically and thermodynamically. In contrast, indoles **2** react selectively at C-4. It has been previously reported that the regioselectivity in addition of indoles to pyridinium ions **1** depends on reaction conditions (inorganic base and solvent).[47] While it can be concluded that the mild reaction conditions used in our work guarantee full regioselectivity towards C-4, the reasons for this selectivity are not fully clear. Different speculations can be done, one of which is the possibility of "C-6-intermediates" **I** undergoing an S_N2'-like reaction (through **III**, Scheme 18). In this case, the regioselectivity of the process might be controlled by the catalyst.

Finally, to give some mechanistic explanation for the formation of isomers **5**, a reaction was performed with proton sponge only. Exclusively *N*-alkylation products were observed in the crude mixture by ^{1}H NMR: **5aa**, isolated and characterized (section 3.3.2), along with a highly unstable, not isolable isomer that was tentatively assigned to the C-6 adduct **5'aa**. Since additions to such type of pyridinium ions can occur first at the C-6 position in a reversible fashion, yielding an unstable C-6 adduct which slowly isomerizes to the most stable C-4 isomer, we propose that the same equilibration occurs in this PS-promoted reaction (Scheme 19). However, if it can be concluded that PS alone is responsible for the formation of these *N*-alkylated products **5**, the reasons for the selectivity against C-alkylated **4**, displayed by these reactions, are not clear at this stage.

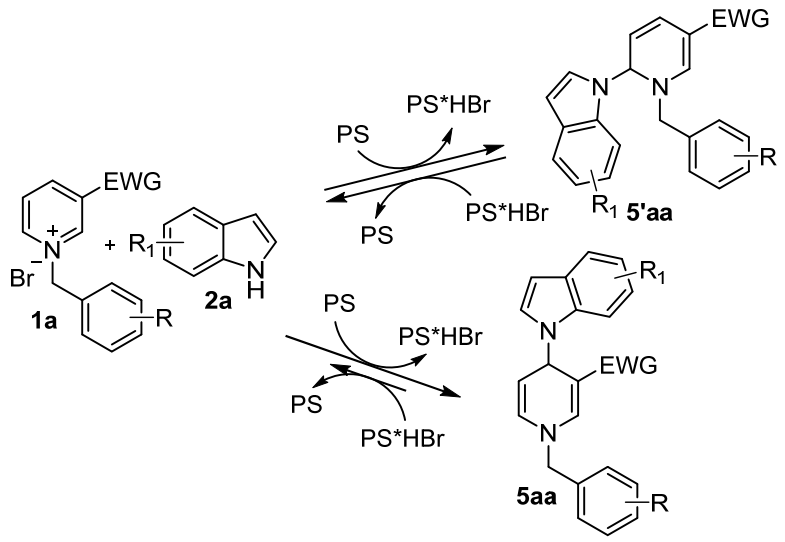

Scheme 19. Formation of product **5aa**

3.3.2 Structural identification of compound 5aa and intermediate I.

The structure of the isomer of interest (C-4) was confirmed by means of X-ray diffraction analysis on a single crystal of product **4gd**[66] and extended by analogy to all other similar structures. A further strong confirmation of this assignment was the presence of a peak between 30 and 40 ppm in the ^{13}C NMR spectra of all products **4** isolated, indicating that the sp^3 carbon atom of the dihydropyridine ring does not bear a *N*-atom.

Byproduct 5aa. Isomer **5aa**, the major side-product of the dearomatization process, was selectively prepared by reacting pyridinium salt **1a** with indole **2a** in the presence of the sole PS (for further details see the experimental details). This was preliminary identified as an *N*-alkylation adduct of indole **2a** on the pyridinium ring, for the absence of the characteristic signal of the indole N-H in the ^{1}H NMR spectrum (bs at about 8 ppm, present for **4aa**). Moreover, an additional signal in the vinylic region (6.46 ppm, dd), not belonging to the dihydropyridine, indicated the presence of a proton at the 3-position of the indole ring, absent for **4aa** (analogous to the signal of free indole **2a** at 6.51 ppm). However, to claim on the complete C-4 regioselectivity of our process, we found it important to assign the correct regiochemistry to this by-product as well. The presence of a signal at 8.26 ppm (doublet with a very small J constant of 1.1 Hz), deshielded by the conjugation with the nitro-group, rules out addition at the more hindered C-2 of the pyridinium ring. Between the two remaining conceivable regioisomers, the structure of

adduct **5aa** was confirmed by means of DPFGSE-NOE NMR spectroscopy, as follows (Figure 2 and Figure 3).

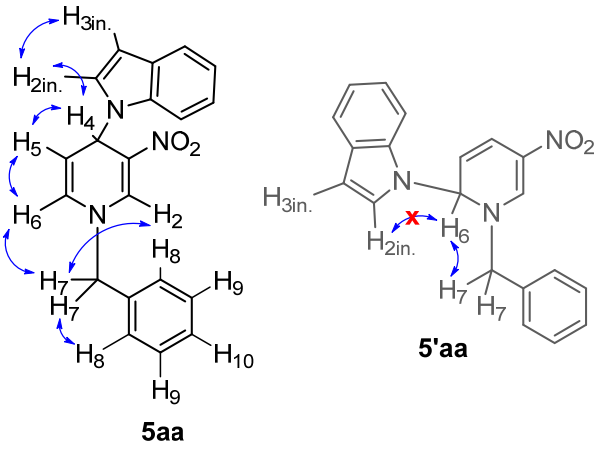

Figure 2. Product **5aa** and possible regioisomer **5'aa**. Blue arrows indicates DPFGSE-NOE spatial correlations.

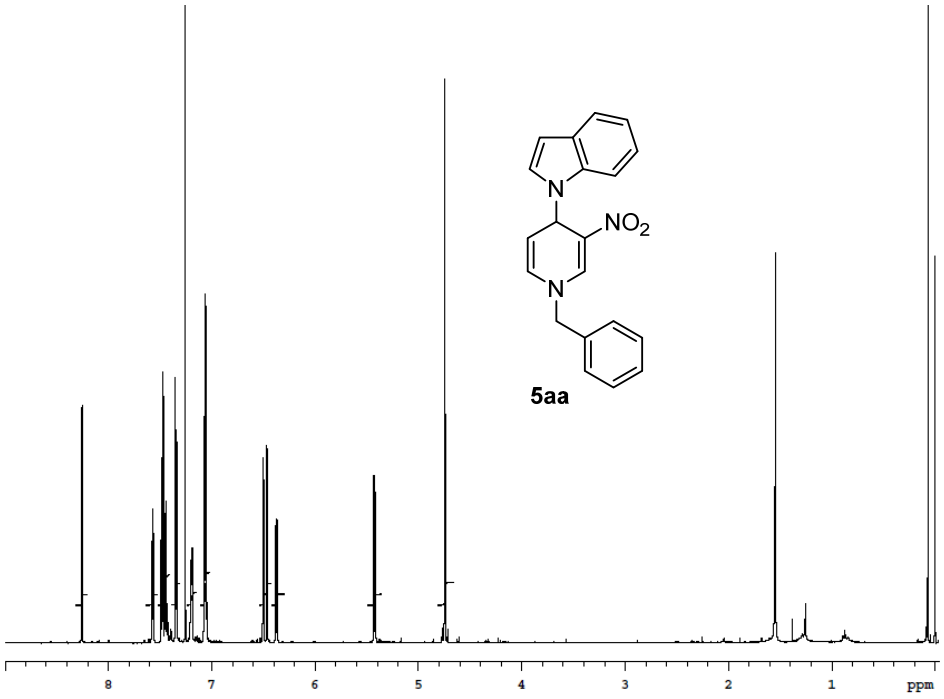

Figure 3. ^{1}H NMR Spectrum of byproduct **5aa**.

Saturation of H-7 (Figure 4, A) resulted in the enhancement of signals relative to H-2, and the ones assigned to H-8 and H-6. Saturation of H-6 (Figure 4, B) showed enhancement of signals relative to H-7and the one assigned to H-5. Saturation of H-5 showed enhancement (Figure 4, C) of signals relative to H-6 and the one assigned to H-4. The only rimaning signal in the vinylic region (6.46 ppm) was therefore attributed to H-

3in for exclusion (proton at the C-3 position of the indole ring is usually more shielded than the other ones). Saturation of the signal relative to H-4 alone was not possible, due to its close proximity with the signal of H-3in. However, the simultaneous saturation (Figure 4, D) showed NOE enhancement of a multiplet, generated by the overlap of three different signals, one of which had to be H-2in. This is not useful for the regiochemistry assignment, since enhancement of H-2in may be due only to saturation of the H-3in signal, but allowed to identify the position of the H-2in signal in the spectrum.

Saturation of the multiplet containing H-2in showed enhancement (Figure 4, E) of signals relative to H-3in and H-4, clearly showing the regiochemistry of product **5aa**.

Structure **5'aa**, on the other hand, would have showed enhancement of the H-2in upon saturation of H-6 (the proton near the H-7 protons of the benzyl moiety), which was not observed. Moreover, gHSQC experiment showed H-4 correlating with a carbon signal at 48.4 ppm (C-4), perfectly in agreement with an sp^3 carbon deshielded by the *N*-atom,

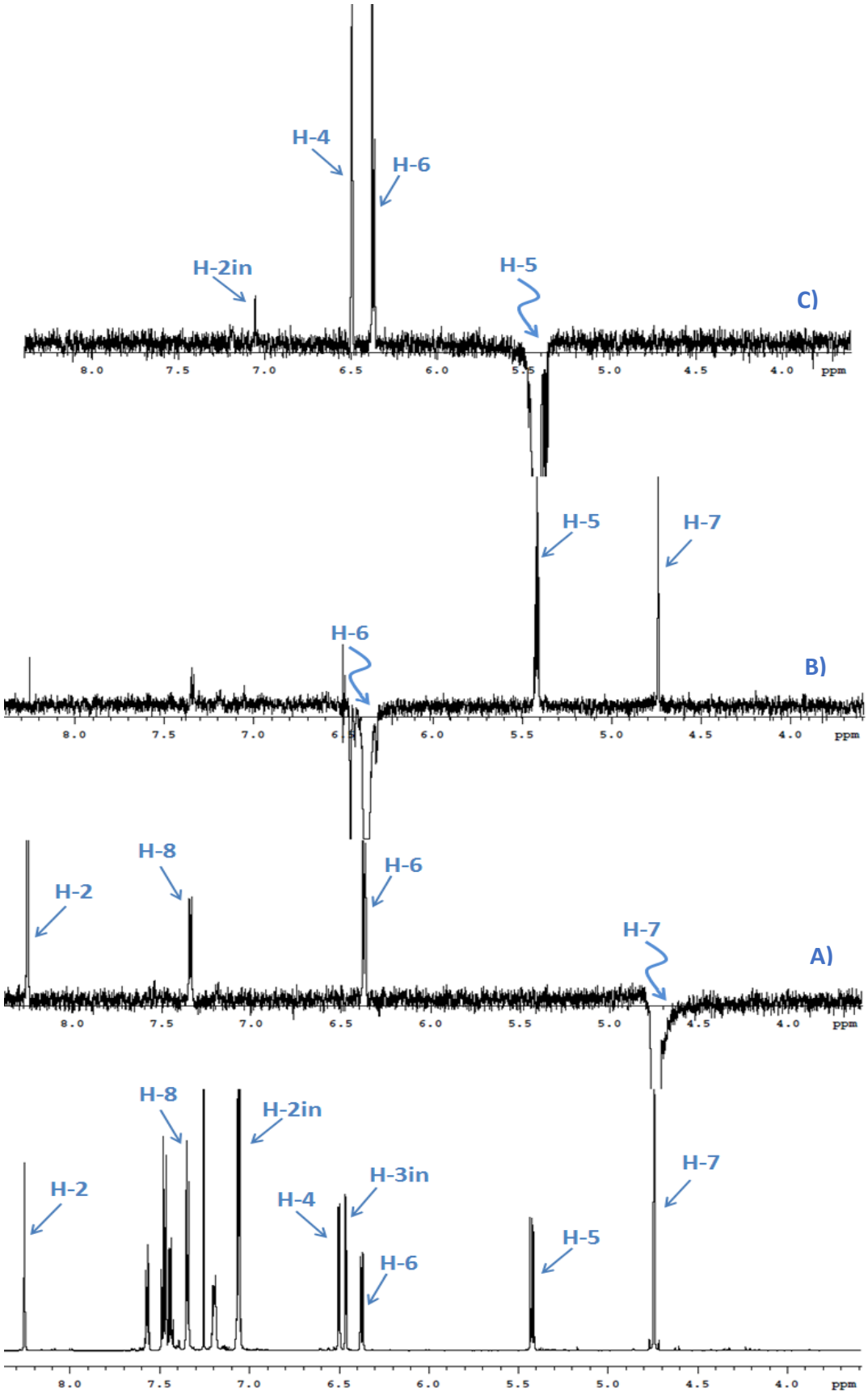

Figure 4. NOE spectra of product **5aa**.

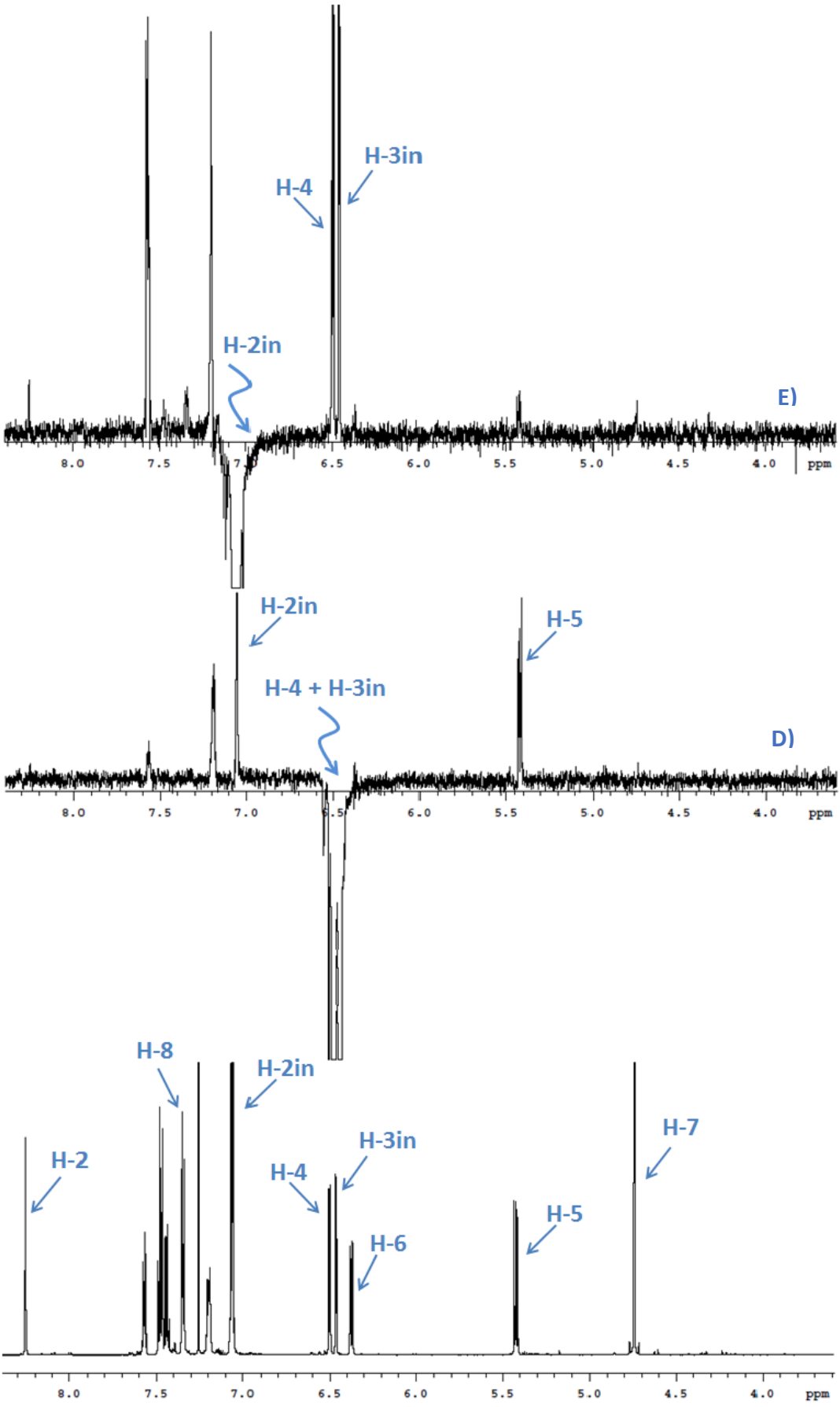

Figure 4. DPFGSE-NOE spectra of product **5aa** (continuation).

while H-6 correlates with a carbon signal at 128.7 ppm (C-6), typical of a vinylic carbon. This is consistent with structure **5aa**, while **5'aa** would have shown H-6 correlating with a signal at about 70 ppm (sp^3 deshielded by two nitrogen atoms) and H-4 with a signal in the vinylic region.

Intermediate I. Upon mixing pyridinium salt **1g** and catalyst **3f** in toluene-*d8* a complicated spectrum appeared, showing anomalous signals in the vinylic region. A nucleophilic attack of the quinuclidinic nitrogen of the catalyst on the electrophilic pyridinium cation **1g** was thus considered (Figure 5).

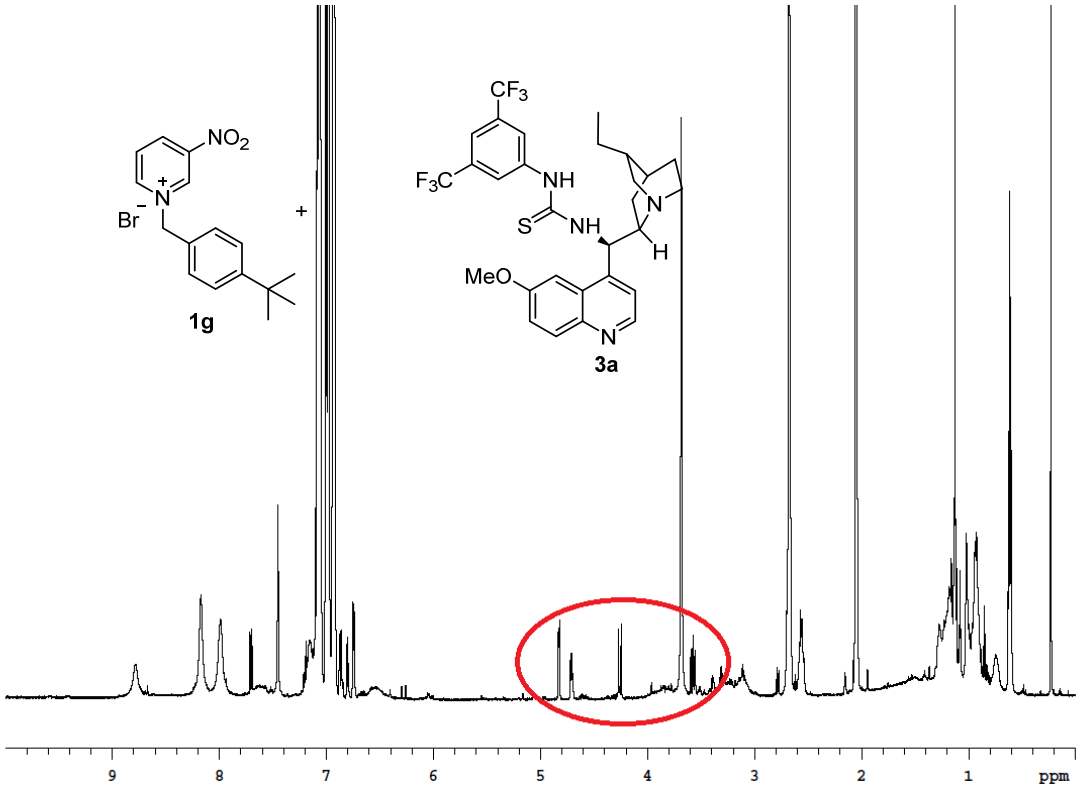

Figure 5. ^{1}H NMR spectrum resulting from mixing equimolar amounts of catalyst **3f** and pyridinium salt **1g** in toluene-*d*8.

Therefore, we decided to repeat the experiment by mixing equimolar amounts of pyridinium **1g** and quinuclidine in toluene-*d*8, in order to obtain a simpler spectrum (Figure 6), after having verified that quinuclidine behaved similarly to catalyst **3f** in the reaction between **1g** and **2a** (complete regioselectivity towards C-4 addition product **4ga**). This showed clearly the typical pattern of a dihydropyridine along with the signals of quinuclidine, shifted from the original position. This proved the hypothesis that the catalyst, which also bears a quinuclidine ring, besides possibly coordinating the bromide

anion, also binds the substrate **1** by nucleophilic addition. This would lead to the formation of an intermediate dihydropyridine, (subsequently captured by the nucleophilic indole). We then moved to characterize the regiochemistry of this intermediate (i.e. structure A vs structure B, Scheme 20).

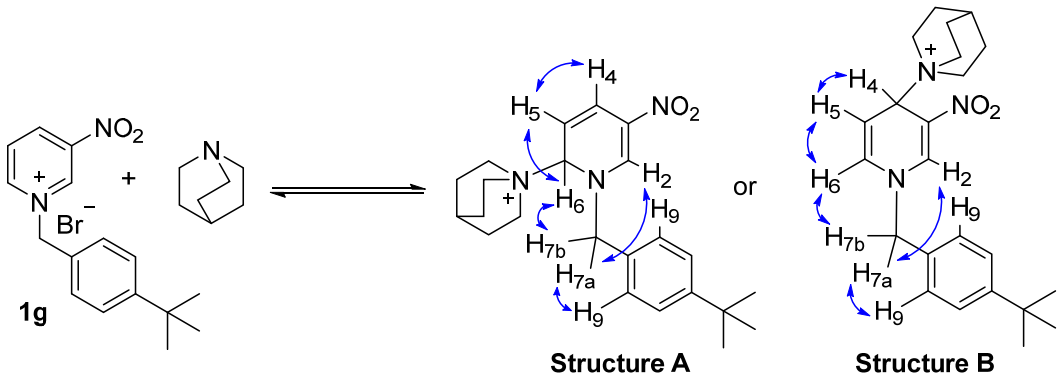

Scheme 20. Addition of quinuclidine to substrate **1g**, leading to dearomatized structures **A** or **B**.

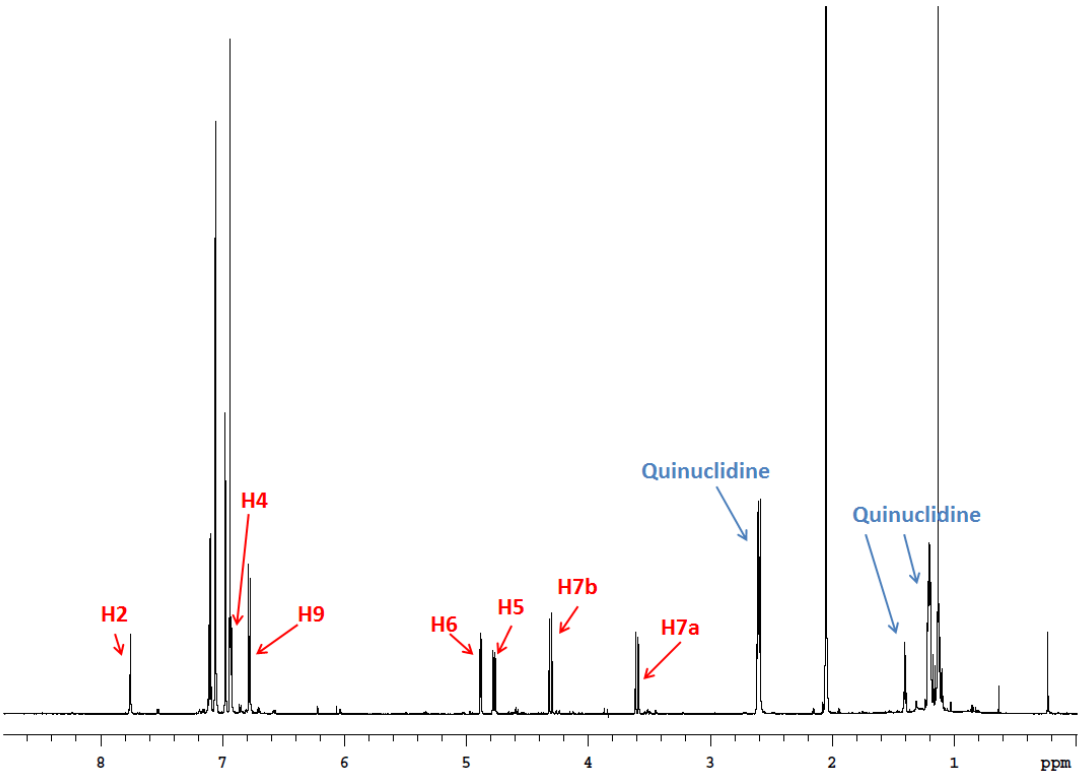

Figure 6. ^{1}H NMR spectrum resulting from mixing equimolar amounts of quinuclidine and pyridinium salt **1g** in toluene-*d*8 (dihydropyridine intermediate).

We initially tried to see correlations between protons of the quinuclidine and the dihydropyridine, either by DPFGSE-NOE or gHMBC experiments. This proved to be

unsuccessful, probably due to a rapid interconversion between the dearomatized (structures A or B) and the aromatic (**1g**) forms. Absence of NOE between quinuclidine protons and dihydropyridine portion of **I** might indicate a fast equilibration between adduct **I** and the two parent species, thus confirming that **I** is also the thermodynamic addition product.

Nevertheless, a complete characterization and signal assignment of the dihydropyridinic portion was performed by ^{1}H NMR, DPFGSE-NOE and gHSQC NMR experiments (with a strategy similar to the one adopted for compound **5aa**, sketched in Scheme 20 but not reported fully for brevity sake). In particular, we focused on the chemical shift of C-6 at 77.2 ppm, which contrasts with the other CH carbons of the dihydropyridine ring. This led us to consider that this may be the sp^3-hybridized carbon. To support this hypothesis, we found that a previously reported product (Figure 7), bearing a C-H moiety between a cationic and a neutral nitrogen atom showed analogous ^{13}C and ^{1}H NMR chemical shifts.[67]

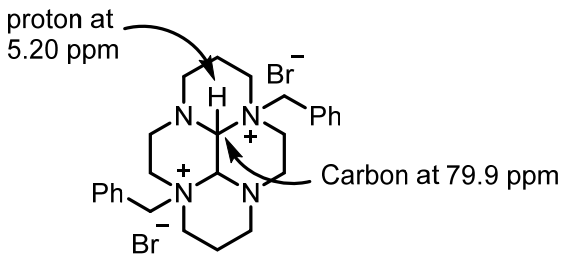

Figure 7. Product reported in ref. 67.

We therefore propose **structure A** to be correct, resulting from the addition of quinuclidine to the more reactive C-6 of the pyridinium ring (Scheme 20).

Since a coordination of the thiourea portion of the catalyst to the bromide can be envisioned, we performed an additional experiment adding an achiral thiourea (*N*,*N*′-bis[3,5-bis(trifluoromethyl)phenyl]thiourea, Schreiner's thiourea) to this dihydropyridine-quinuclidinium intermediate. We observed a substantial shift (1.4 ppm) in the signals of the thiourea (compared to the spectrum of thiourea alone in toluene-*d*8), suggesting a strong coordination of the bromide anion. All these features led us to the structural identification of intermediate **I**, which we proposed have a substantial role in the catalytic cycle of the present dearomatization.

3.4 Conclusion

In summary, the first organocatalytic enantioselective *N*-alkylpyridinium salts **1**, promoted by chiral bifunctional bases, has been developed. The unanticipated pathway followed by this new catalytic reaction implies addition of the nucleophile to the C-4 of the pyridinium ring. Enantiomerically enriched 1,4-dihydropyridines **4** were accordingly obtained as major products, rendering this method for nucleophilic dearomatization of pyridines complementary to previous approaches. Preliminary investigations on the reactivity of readily available *N*-benzyl 3-nitropyridinium halides **1** have identified indole derivatives **2** as most suitable nucleophilic partners. Among others, bifunctional catalysts bearing a basic functionality along with H-bond donor moieties resulted in the most promising results, enlightening thiourea derivative **3f** as the best catalyst. A stoichiometric amount of an auxiliary base was required in order to neutralize the HBr formed and achieve catalyst turnover. Proton sponge (1,8-dimethylamino naphthalene, PS), often described as "thermodynamic base" (strong, yet non-nucleophilic proton scavenger) was found to be the optimal candidate. Further optimization showed that lowering the reaction temperature gave better enantioselectivity in **4**, without giving a great detriment in conversion. A bulky substituent on the *N*-benzyl moiety, such as *t*-Bu, gave a remarkable improvement in both reactivity and enantioselectivity. In most of the cases products **4** were formed along with a certain amount of undesired racemic *N*-alkylation products **5**, apparently generated as a background PS-promoted process. Indeed, when PS was added portion-wise, a good 91:9 ratio in favor of the desired product **4**, along with a satisfactory 91% ee and 91% conversion, was achieved for the model compound **4ga**. With the optimal conditions in hand, the generality of the reaction was evaluated varying the substitution of both the indole nucleus and the benzyl ring, along with the EWG-group on the pyridinium moiety. The dihydropyridines obtained were also amenable of various synthetic manipulations through the two enamine-type double bonds. Many control experiments were also conducted in order to propose a mechanism for the reaction, accounting for both the full C-4 selectivity and the absolute configuration showed by X-ray analysis on product **4gd**. ^{1}H and ^{13}C NMR studies pointed to the extraction of the insoluble pyridinium salt **1** in the apolar reaction medium through formation of a covalent adduct with the catalyst. Reaction of indole **2** with this ammonium intermediate might proceed in an S_N2' or S_N1 fashion, accounting for the

formation of the C-4 adducts – the 1,4-dihydropyridines 4 – as the major products. All the experimental and mechanistic results are summarized in Scheme 21.

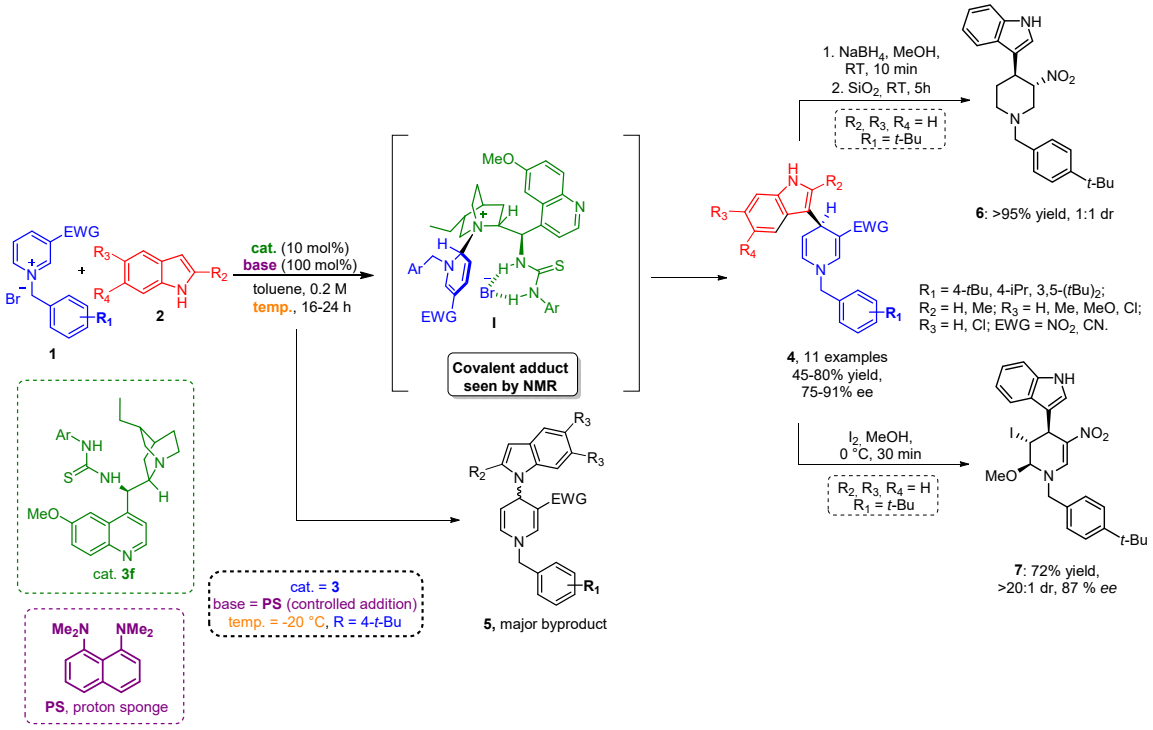

Scheme 21. Organocatalytic enantioselective *N*-alkyl pyridinium salts dearomatization: optimization, observed intermediate, scope and synthetic elaborations.

3.5 Experimental details

3.5.1 General methods and materials

General Methods. ^{1}H and ^{13}C NMR spectra were recorded on a Varian Inova 300, Mercury 400 or Inova 600 spectrometer. Chemical shifts (δ) are reported in ppm relative to residual solvents signals for ^{1}H and ^{13}C NMR. ^{13}C NMR were acquired with ^{1}H broad-band decoupled mode. Chromatographic purifications were performed using 70-230 mesh silica. Mass spectra were recorded on a micromass LCT spectrometer using electrospray (ESI) ionization techniques. Optical rotations were measured on a Perkin Elmer 241 Polarimeter provided with a sodium lamp and are reported as follows: $[\alpha]_{\lambda}^{T\,(^{\circ}C)}$ (c = g/100 mL, solvent). The enantiomeric excess of the products (ee) were determined by chiral stationary phase HPLC (Daicel Chiralpak AD-H, AS or Chiralcel OD columns), using an UV detector operating at 254 nm. Below the general procedures the characterization of the model compound only is reported. For the complete description of all the products reported see the Supporting Information of *ACS Catal.* **2016**, *6*, 6473.

Materials. Analytical grade solvents and commercially available reagents were used as received, unless otherwise stated. Pyridinium salts **1a-j** were synthesized from commercially available 3-nitropyridine or 3-cyanopyridine and the respective benzyl bromides (4-methoxybenzyl bromide was prepared according to a literature procedure). 1,8-Bis(dimethylamino)naphthalene (proton sponge PS) was obtained from Sigma-Aldrich and used as received. Catalyst **3f** was prepared following literature procedures.

Preparation of the racemic products. In a test tube equipped with a magnetic stirring bar, pyridinium salts **1a-k** (0.05 mmol), indoles **2a-f** (0.065 mmol), quinuclidine (5.6 mg, 0.05 mmol) and *N*,*N*′−bis[3,5−bis(trifluoromethyl)phenyl]−thiourea (Schreiner's thiourea) (2.5 mg, 0.005 mmol) were stirred in toluene (0.250 mL) at room temperature for 2 hours. DCM was then added and the resulting solution was passed through a short plug of silica and washed with Et_2O (4x). Evaporation of the solvents afforded the crude product, which was purified by column chromatography on silica gel (*n*-hexane/EtOAc). Products **4** were thus obtained as red solids in nearly quantitative yields.

Preparation of byproduct 5aa. In a test tube equipped with a magnetic stirring bar, product **1a** (15 mg, 0.05 mmol), indole **2a** (7.6 mg, 0.065 mmol) and PS (10.4 mg, 0.05 mmol) were vigorously stirred in toluene (0.125 mL) for 18 hours. DCM was then added and the organic layer was passed through a short plug of silica, and the plug flushed with Et_2O (4x). Evaporation of the solvents afforded the crude product, which was purified by column chromatography on silica gel (*n*-hexane/EtOAc 2:1). Product **5aa** was thus obtained as a light yellow solid in 70% yield. ^{1}H NMR ($CDCl_3$, 600 MHz) δ = 8.26 (d, J = 1.4 Hz, 1H), 7.58-7.56 (m, 1H), 7.49-7.43 (m, 3H), 7.35-7.33 (m, 2H), 7.21-7.18 (m,

1H), 7.08-7.04 (m, 3H), 6.50 (d, J = 4.9 Hz, 1H), 6.46 (dd, J_1 = 3.3 Hz, J_2 = 0.9 Hz, 1H), 6.37 (dt, J_1 = 7.8 Hz, J_2 = 1.4 Hz, 1H), 5.42 (dd, J_1 = 7.7 Hz, J_2 = 5.0 Hz, 1H), 4.75 (s, 2H) ppm.

Racemic **6** and **7** were synthesized by employing racemic **4ga** in the respective reactions.

3.5.2 General procedure for the catalytic enantioselective pyridinium salts dearomatization

In a test tube equipped with a magnetic stirring bar, catalyst **3a** (0.015 mmol; 9.0 mg; 10 mol% or 0.023 mmol; 13.8 mg; 15 mol%) and indole **2a-f** (0.195 mmol; 1.3 equiv.) were dissolved in toluene (0.75 mL). The resulting mixture was stirred at the desired temperature for 5 minutes, after which pyridinium salt **1** (0.15 mmol) was added in one portion. Then, every 2 hours PS (0.03 mmol; 6.4 mg; 0.2 equiv.) was added as solid, until, after 10 hours, 1 equivalent was reached. The resulting mixture was then left stirring overnight.

Hereafter, CH_2Cl_2 was added (5 mL), the solution was filtered through a short plug of silica gel, and the plug was washed with Et_2O (4x). After removal of the solvents, the reaction crude was analyzed by ^{1}H NMR spectroscopy to determine the isomeric ratio of the dihydropyridines (**4**/**5**). The residue was then purified by chromatography on silica gel (*n*-hexane/EtOAc mixtures) to afford the desired products **4**. Finally, the enantiomeric excess was determined by chiral stationary phase HPLC (*n*-hexane/*i*-PrOH mixtures).

(*S*)-3-(1-(4-(*tert*-Butyl)benzyl)-3-nitro-1,4-dihydropyridin-4-yl)-1*H*-indole (4ga)

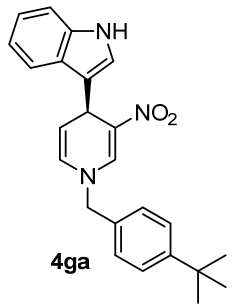

4ga

Following the general procedure (T = **-**20 °C, **3a** 10 mol%), from *N*-(4-*tert*-butylbenzyl)-3-nitropyridinium bromide (**1g**) and indole (**2a**), product **4ga** was obtained as a bright yellow solid in 80% yield after column chromatography on silica gel (*n*-hexane/EtOAc = 2.5:1). Isomeric ratio **4ga**/**5ga** was evaluated from the ^{1}H NMR spectrum of the crude mixture and was found to be 91:9. The enantiomeric excess of **4ga** was determined by chiral stationary phase HPLC (AS, *n*-hexane/*i*-PrOH 70:30, 1.00 mL/min, λ = 254 nm, t_{maj} = 15.3 min, t_{min} = 21.9 min, 91% *ee*). $[\alpha]_D^{25\ °C}$ = -279.1 (c = 0.4, $CHCl_3$); ^{1}H NMR (400 MHz, $CDCl_3$) δ = 8.10 (d, J = 1.4 Hz, 1H), 8.06 (bs, 1H), 7.51 (d, J = 8.0 Hz, 1H), 7.48-7.45 (m, 2H), 7.33 (d, J = 8.2 Hz, 1H), 7.30-7.26 (m, 2H), 7.15 (t, J = 7.6 Hz, 1H), 7.07 (s, 1H), 6.98 (t, J = 7.4 Hz, 1H), 6.01 (dt, J_1 = 7.8 Hz, J_2 = 1.2 Hz, 1H), 5.31 (dd, J_1 = 8.2 Hz, J_2 = 5.0 Hz, 1H), 5.25 (d, J = 4.8 Hz, 1H), 4.57 (s, 2H), 1.36 (s, 9H) ppm; ^{13}C NMR (100 MHz, $CDCl_3$) δ = 151.9, 138.9, 136.5, 132.3, 127.5, 126.2, 126.0, 125.6, 125.3, 122.7, 121.8, 119.4, 119.2, 118.5, 113.0, 111.4, 58.5, 34.7, 31.5, 31.3 ppm; ESI-MS: 410 [M + Na^+].

3.5.3 General procedures for elaborated products 6 and 7.

3-((3*S*,4*S*)-1-(4-(*tert*-butyl)benzyl)-3-nitropyridin-4-yl)-1*H*-indole (6)

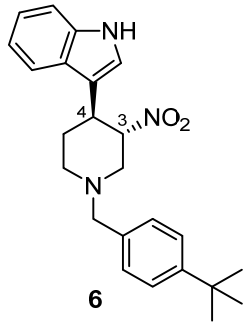

6

In a small vial, equipped with a magnetic stirring bar, product **4ga** (91% *ee*; 31.4 mg, 0.08 mmol) was suspended in MeOH (0.75 mL). $NaBH_4$ was then added in small portions until TLC showed complete conversion of the reagent (overall 37.8 mg added, 10 mmol). A saturated solution of NH_4Cl (5 mL) and DCM (5 mL) were added and the organic layer separated, washed again with a saturated solution of NH_4Cl (5 mL), dried over $MgSO_4$ and filtered. To this crude solution (containing a 50/50 diastereomeric mixture, by ^1H NMR analysis) SiO_2 (3.50 g) was added and the solvent was evaporated *in vacuo*. The product was left standing adsorbed on SiO_2 for 5 h. Then, $CHCl_3$ (20 mL) was added and the resulting suspension was stirred for 30 min. SiO_2 was filtered off and washed repeatedly with $CHCl_3$. The solvent was finally evaporated to afford 32.0 mg (quantitative yield) of pure product **6** as a white solid. Diastereomeric ratio was evaluated from the ^1H NMR spectrum and was found to be > 20:1. The enantiomeric excess of the product was determined by chiral stationary phase HPLC (ADH, *n*-hexane/*i*-PrOH 80:20, 0.75 mL/min, λ = 254 nm, t_{maj} = 8.8 min, t_{min} = 10.2 min, 90% *ee*). $[\alpha]_D^{25\ °C}$ = -7.3 (c = 0.4, $CHCl_3$); ^1H NMR ($CDCl_3$, 400 MHz) δ = 8.03 (bs, 1H), 7.66 (d, J = 8.0 Hz, 1H), 7.39-7.36 (m, 2H), 7.34 (dt, J_1=8.0 Hz, J_2 = 0.8 Hz, 1H), 7.28-7.25 (m, 2H), 7.19 (ddd, J_1 = 8.1 Hz, J_2 = 7.1 Hz, J_3 = 1.2 Hz, 1H), 7.12 (ddd, J_1 = 8.0 Hz, J_2 = 7.1 Hz, J_3 = 1.1 Hz, 1H), 7.06 (d, J = 2.4 Hz, 1H), 5.03 (td, J_1 = 10.9 Hz, J_2 = 4 Hz, 1H), 3.68 (d, J = 13.1 Hz, 1H), 3.58 (d, J = 13.1 Hz, 1H), 3.54 (td, J_1 = 11.0 Hz, J_2 = 5.4 Hz, 1H), 3.43 (ddd, J_1 = 10.4 Hz, J_2 = 4.0 Hz, J_3 = 1.7 Hz, 1H), 3.06-3.01 (m, 1H), 2.59 (t, J = 10.4 Hz, 1H), 2.31 (td, J_1 =11.4 Hz, J_2 = 3.5 Hz, 1H), 2.14-2.04 (m, 2H), 1.34 (s, 9H) ppm; ^{13}C NMR (100 MHz, $CDCl_3$) δ = 150.4, 136.3, 134.2, 128.8, 126.1, 125.3, 122.3, 121.2, 119.7, 118.9, 115.0, 111.4, 88.1, 62.2, 57.0, 53.2, 38.5, 34.5, 31.7, 31.4 ppm; ESI-MS: 414 [M + Na^+]. HRMS(ESI) calcd. for $C_{24}H_{30}N_3O_2$ (M + H^+): 392.2338; found: 392.2338.

The relative configuration of the two stereogenic centers was determined by means of ^1H NMR spectroscopy, on the basis of the coupling constants of the signal at 5.03 ppm, belonging to H-3 (α to the nitro group, assigned for the chemical shift). A value of 10.9 Hz for J_t clearly indicates two *trans*-diaxial relationships, of which one must be between H-3 and H-4 (proton α to the indole). In a chair-like conformation of the piperidine ring, this configuration allows the two bulky substituents at C-3 and C-4 (indole and the nitro group) to occupy the most favorable equatorial positions. This assignment also takes into account the major stability of this product, obtained after thermodynamic equilibration of the diastereomeric mixture.

3-((2*S*,3*R*,4*S*)-1-(4-(*tert*-butyl)benzyl)-3-iodo-2-methoxy-5-nitro-1,2,3,4-tetrahydropyridin-4-yl)-1*H*-indole (7)

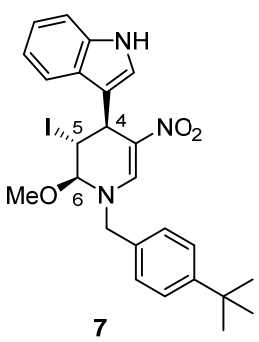

7

In a round bottomed flask equipped with a magnetic stirring bar and under N_2 flow, product **4ga** (91% *ee*, 31.4 mg, 0.08 mmol) was suspended in MeOH (1.6 mL). The resulting mixture was cooled to 0 °C and a solution of I_2 (38.5 mg, 0.152 mmol) in MeOH (4.4 mL) was added dropwise by means of an addition funnel, over a period of 15 minutes. The resulting mixture was stirred for additional 15 minutes at 0 °C, after which a saturated solution of $NaHCO_3$ was added dropwise (10 mL). The precipitated yellow solid was dissolved by addition of DCM (10 mL) and the two layers formed were separated. The aqueous layer was extracted again with DCM (2 x 10 mL). The organic extracts were then washed with a diluted solution of $Na_2S_2O_3$ (2 x 10 mL), dried over $MgSO_4$, filtered and evaporated *in vacuo*. Product **7** was obtained as a red solid in 72% yield (31.4 mg) after column chromatography on silica gel (*n*-hexane/EtOAc = 3:1). The diastereomeric ratio was evaluated from the ^{1}H NMR spectrum of the crude mixture and was found to be > 20:1. The enantiomeric excess of the product was determined by chiral stationary phase HPLC (ADH, *n*-hexane/*i*-PrOH 80:20, 0.75 mL/min, λ = 254 nm, t_{maj} = 11.9 min, t_{min} = 11.0 min, 87% *ee*). $[\alpha]_D^{25\ °C}$ = -77.9 (c = 0.450, $CHCl_3$); ^{1}H NMR ($CDCl_3$, 400 MHz) δ = 8.41 (s, 1H), 8.02 (bs, 1H), 7.68-7.64 (m, 1H), 7.45-7.41 (m, 2H), 7.36-7.31 (m, 3H), 7.20 (dt, J_1 = 7.0 Hz, J_2 = 1.5 Hz, 1H), 7.16 (td, J_1 = 7.0 Hz, J_2 = 1.5 Hz, 1H), 6.87 (dd, J_1 = 2.5 Hz, J_2 = 0.9 Hz, 1H), 5.08-5.06 (m, 2H), 4.56 (s, 2H), 4.51 (t, J = 1.8 Hz, 1H), 2.67 (s, 3H), 1.34 (s, 9H) ppm; ^{1}H NMR (CD_3CN, 600 MHz) δ = 9.15 (bs, 1H), 8.47 (s, 1H), 7.62 (d, J = 8.1 Hz, 1H), 7.51-7.49 (m, 2H), 7.44-7.42 (m, 2H), 7.41 (d, J = 8.4 Hz, 1H), 7.17 (ddd, J_1 = 8.2 Hz, J_2 = 7.0 Hz, J_3 = 1.2 Hz, 1H), 7.11 (ddd, J_1 = 7.9 Hz, J_2 = 7.2 Hz, J_3= 1.0 Hz, 1H), 6.64 (dd, J_1 = 2.8 Hz, J_2 = 0.9 Hz, 1H), 5.13 (t, J = 2.0 Hz, 1H), 4.92 ("pseudo-q" or ddd $J_1 = J_2 = J_3$ = 1.5 Hz, 1H), 4.69 (d, J = 14.6 Hz, 1H), 4.64 (t, J = 1.7 Hz, 1H), 4.62 (d, J = 14.6 Hz, 1H), 2.73 (s, 3H), 1.34 (s, 9H) ppm; ^{13}C NMR (100 MHz, $CDCl_3$) δ = 152.0, 142.5, 136.3, 130.9, 128.8, 125.9, 122.6, 122.2, 121.9, 119.9, 117.9, 114.9, 111.6, 90.3, 57.8, 55.0, 38.7, 34.7, 31.3, 21.9 ppm; ESI-MS: 568 [M + Na^+].

The relative configuration of the three stereogenic centers was assigned by means of NMR spectroscopy, after a complete characterization and signal assignment was performed by^{1}H NMR, DPFGSE-NOE and gHSQC NMR experiments (with a strategy similar to the one adopted for compound **5aa**, but not reported fully for brevity sake. In particular, since the coupling constants of the signal corresponding to H-5 with signals corresponding to H-4 and H-6 are the same (the formal doublet of doublets has in fact the shape of a triplet; ^3J = 2.0 Hz), the same dihedral angle between H-5 and H-6 is observed between H-5 and H-4. Building upon what was reported by Lavilla *et al.*,[63] the MeO and I substituents are in a *trans* relationship (*i.e.* H-5 and H-6 are *anti*): this implies that also H-5 and H-4 have to be *anti* to each other (*i.e.* the I and the indole substituents are *trans*).

3.5.4 Crystallographic data

Suitable crystal of compound **4gd**, which possesses an appropriate heavy atom (Z > Si using standard Mo-Kα radiation), were obtained by slow diffusion of a layer of *n*-hexane into an ethyl acetate solution.

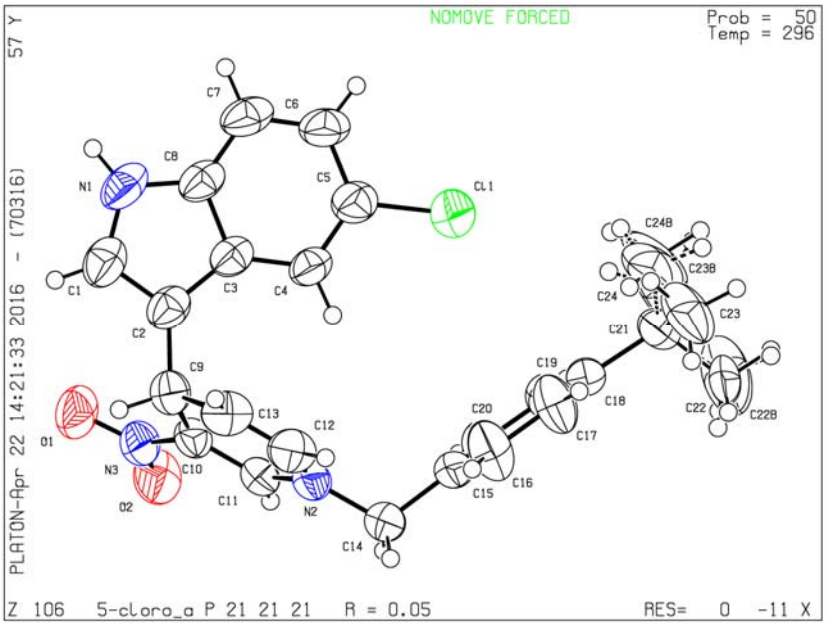

Molecular formula: $C_{24}H_{24}N_3O_2Cl$; M_r = 421.91, orthorhombic, space group $P2_12_12_1$ (19), a = 10.4050(4), b = 14.2652(6), c = 14.6935(6) Å; V = 2180.95(15) Å^3, T = 296(2) K, Z = 4, ρ_c = 1.285 g cm^{-3}, $F(000)$ = 888, graphite-monochromated $Mo_{K\alpha}$ radiation (λ = 0.71073 Å), $\mu(Mo_{K\alpha})$ = 0.200 mm^{-1}, yellow brick (0.40 × 0.30 × 0.015 mm^3), empirical absorption correction with SADABS (transmission factors: 0.924 – 0.997), 2400 frames, exposure time 20 s, 1.99 ≤ θ ≤ 26.00, –12≤ h ≤ 12, –17 ≤ k ≤ 17, –18 ≤ l ≤ 18, 20389 reflections collected, 4133 independent reflections (R_{int} = 0.0223), solution by intrinsic phasing method and subsequent Fourier syntheses, full-matrix least-squares on F_o^2 (SHELXL-2014/7), hydrogen atoms refined with a riding model, data / restraints / parameters = 4133/ 3/ 309, $S(F^2)$ = 0.964, $R(F)$ = 0.0639 and $wR(F^2)$ = 0.1719 on all data, $R(F)$ = 0.0466 and $wR(F^2)$ = 0.1365 for 3259 reflections with $I > 2\sigma(I)$, weighting scheme $w = 1/[\sigma^2(F_o^2) + (0.1053P)^2 + 0.7766P]$ where $P = (F_o^2 + 2F_c^2)/3$, largest difference peak and hole 0.415 and –0.394 e Å^{-3}. Flack parameter: 0.034(18) for *S* configuration at C9. The *t*-butyl group was found to be disordered over two positions and it was accordingly modelled with separate parts (53:47 optimized ratio). Crystallographic data have been deposited with the Cambridge Crystallographic Data Centre as supplementary publication no. CCDC-1476006. Copies of the data can be obtained free of charge on application to CCDC, 12 Union Road, Cambridge CB21EZ, UK (fax: (+44) 1223-336-033; e-mail: deposit@ccdc.cam.ac.uk).

4 Asymmetric Nucleophilic Dearomatization of Pyridinium Salts under Enamine Catalysis

The procedures and results here described are part of- and can be found in-:

- G. Bertuzzi, A. Sinisi, D. Pecorari, L. Caruana, A. Mazzanti, L. Bernardi, M. Fochi "Nucleophilic Dearomatization of Pyridines under Enamine Catalysis: Regio-, Diastereo-, and Enantioselective Addition of Aldehydes to Activated N-Alkylpyridinium Salts" *Org. Lett.* **2017**, *19*, 834.

ABSTRACT

Catalytic addition of chiral enamines to azinium salts is a powerful tool for the synthesis of enantioenriched heterocycles. An unprecedented asymmetric dearomative addition of aldehydes to activated *N*-alkylpyridinium salts is presented. The process exhibits complete C-4 regioselectivity along with high levels of diastereo- and enantiocontrol, achieving a high-yielding synthesis of a broad range of optically active 1,4-dihydropyridines. Moreover, the presented methodology enables the synthesis of functionalized octahydropyrrolo[2,3-c]pyridines, the core structure of anticancer peptidomimetics.

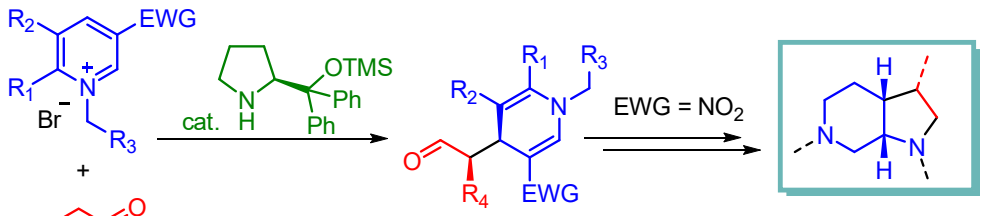

4.1 Background

Having explored the first organocatalytic enantioselective dearomatization of *N*-alkylpyridinium salts employing indoles as nucleophiles and a bifunctional chiral base as the catalyst, we envisioned that the reported strategy might be applicable to other processes. This implies the use of a different nucleophile and, accordingly, a different catalytic system.

Indeed, activated *N*-alkylpyridinium salts were employed in catalytic dearomatizations requiring other approaches, in concomitance or shortly after the development of the present and the previously reported process.

For example, Waser's group reported a Lewis acid catalyzed dearomatization of azinium electrophiles, including activated pyridiniums, promoted by the reaction with donor–acceptor aminocyclopropanes.[68] Both the electrophilic *N*-alkyl azinium cation and the nucleophile responsible for the dearomatization are generated simultaneously by the addition of the nucleophilic *N*-atom to the electrophilic cyclopropane. An intramolecular dearomatization thus follows, resulting in a formal (3+2)-cyclization. The process served for the synthesis of diverse tetrahydroindolizine derivatives with high *anti* diastereoselectivities (Scheme 1). For pyridine derivatives, the presence of at least one strong (or two weak) electron-withdrawing groups was necessary to observe a productive dearomatization (otherwise the zwitterionic intermediate was isolated). However, pyridines bearing exceedingly electron poor substrates (e.g. two strong EWG groups) were not nucleophilic enough to even commence the reaction sequence.

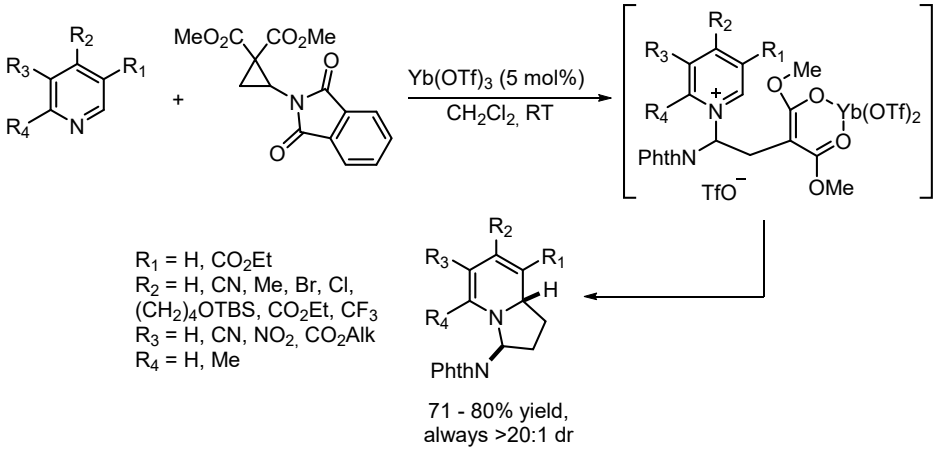

Scheme 1. Dearomatization of pyridines through (3+2)-cyclizations.

On the side of asymmetric catalysis, two examples of *N*-alkylpyridinium salts dearomatizations were developed, employing chiral *N*-heterocyclic carbenes as catalysts and aldehydes as pro-nucleophiles. In 2017 Rovis' group reported an enantioselective β-functionalization of enals employing 3-cyanopyridinium cations as electrophiles.[69] The reaction produced 1,4-dihydropyridines as the major (but not sole) regioisomer with modest diastereoselectivities and generally good enantioselectivity values (Scheme 2).

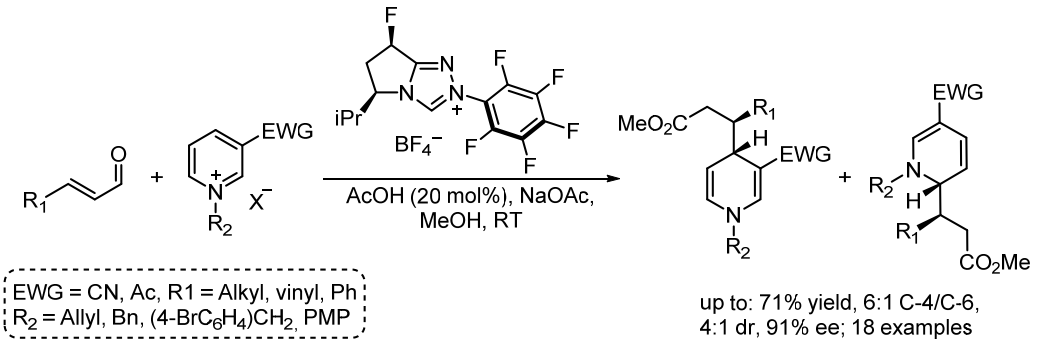

Scheme 2. Dearomatization of *N*-alkylpyridinium salts with α,β-unsaturated aldehydes catalyzed by chiral NHCs.

Shortly after, Massi and coworkers developed an analogous process employing simple aldehydes as pro-nucleophiles. 4-Acyl-1,4-dihydropyridines were obtained as the sole regioisomers, in useful synthetic yields and up to 78% ee.[70] In this case as well, 3-cyanopyridinium halides were employed as activated *N*-alkyl pyridiniumsalts (Scheme 3).

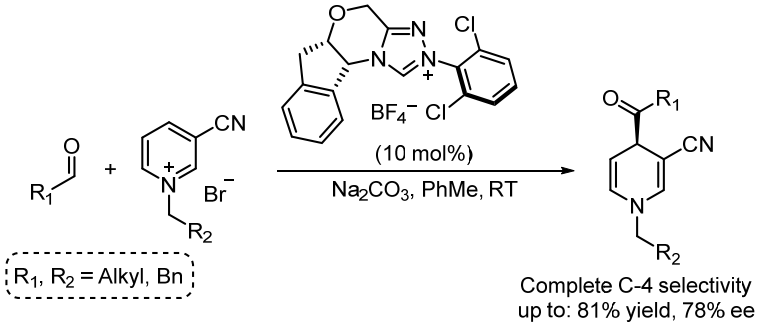

Scheme 3. Dearomatization of *N*-alkyl pyridinium salts with simple aldehydes catalyzed by chiral NHCs.

These three examples demonstrate that *N*-alkylpyridiniums are competent electrophiles for a diverse number of catalytic methodologies. Chiral enamines, derived from the condensations of enantiopure secondary amine catalysts on enolizable aldehydes, are arguably one of the most largely employed nucleophiles in organocatalytic reactions. Their enantioselective α-functionalization is indeed a reliable and robust process, realized with a large variety of different electrophiles.[71,30,33] This served for the preparation of diverse classes of substituted aldehyde derivatives, often employed in the stereoselective synthesis of natural compounds or biologically active ingredients.

Chiral enamines served indeed as nucleophiles in the organocatalytic dearomatization of benzo-fused azinium salts such as acridinium, isoquinolinium, phthalazinium and quinolinium species. It is important to stress that the dearomatization of such compounds

is easier than the dearomatization of pyridinium cations, as the aromaticity of the fused rings does not get completely lost. Indeed, the benzene ring is not involved in the dearomatization process, thus preserving the major contribute of the aromaticity intact. On the other hand, as a simple pyridine gets dearomatized, all the aromatic stabilization is lost in the process, rendering these reactions more difficult, both kinetically and thermodynamically.

Similar to anthracene, possessing only little aromaticity on the central ring, acridinium cations are very easily dearomatized, as the azinium nucleus can be functionalized leaving the two side rings aromatic. Indeed, dearomatization of *N*-alkylacridinium salts was first developed by Cozzi in 2010 showing regrettably low enantiomeric excesses under the optimized reaction conditions (Scheme 4, top).[72] Great improvement to the same reaction was brought by Li and co-workers, developing a way to obtain highly enantioenriched chiral acridane derivatives (Scheme 4, bottom).[73]

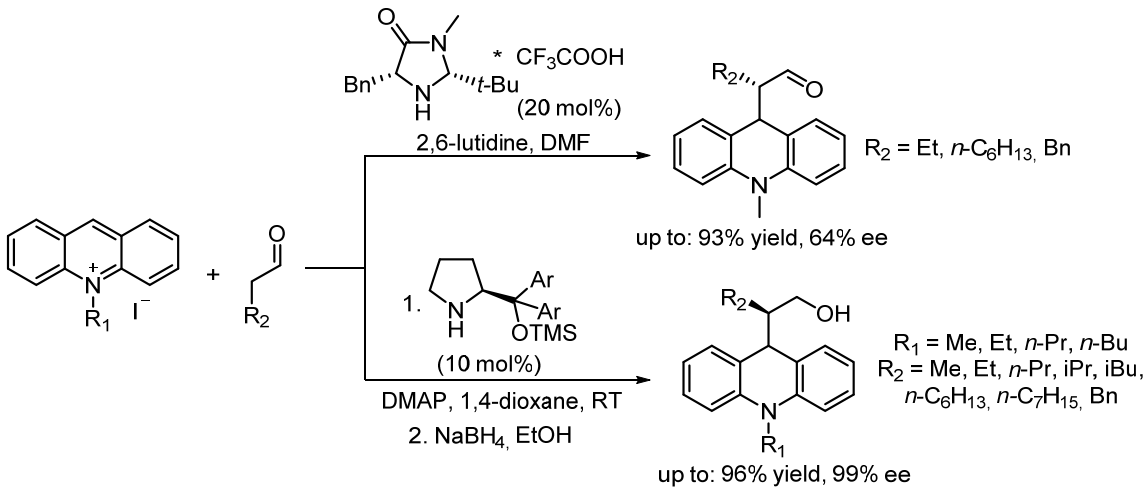

Scheme 4. Dearomatization of acridinium salts with chiral enamines.

The first example of isoquinolinium-like substrates dearomatization was reported by Jørgensen and co-workers in 2005 and consisted in the intramolecular dearomatization of *N*-alkyl isoquinolinium and phthalazinium salts, employing a conveniently tethered aldehyde, connected to the heteroaromatic nucleus through an alkyl chain, serving at the same time as alkylating residue for the *N*-atom.[74] The unstable annulation products could be conveniently transformed into stable 1,2-dihydroisoquinolines under treatment with trifluoroacetic anhydride and $NaBH_4$ (Scheme 5).

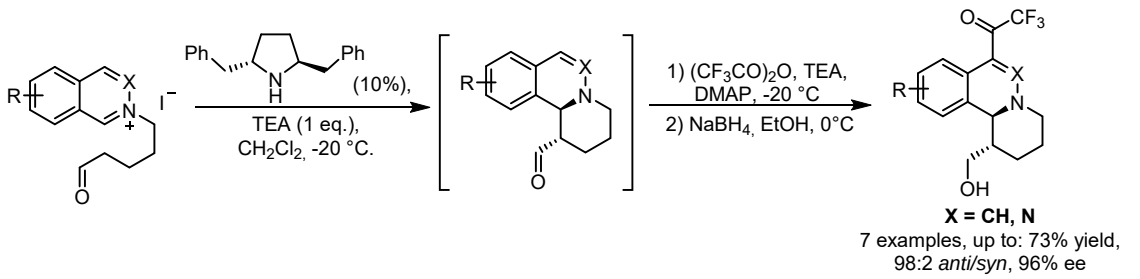

Scheme 5. Intramolecular dearomatization of isoquinolinium and phthalazinium salts with chiral enamines.

The first intermolecular example was reported later by Cozzi's group. This relied on highly activated *N*-acyl isoquinolinium salts as electrophilic partners.[75] The need to generate these reactive species *in situ* implied problems related to catalyst deactivation, due to irreversible reaction between the catalyst N-H moiety and the electrophilic activating agent (benzyl chloroformate). This was circumvented by slow addition of this species (Scheme 6).

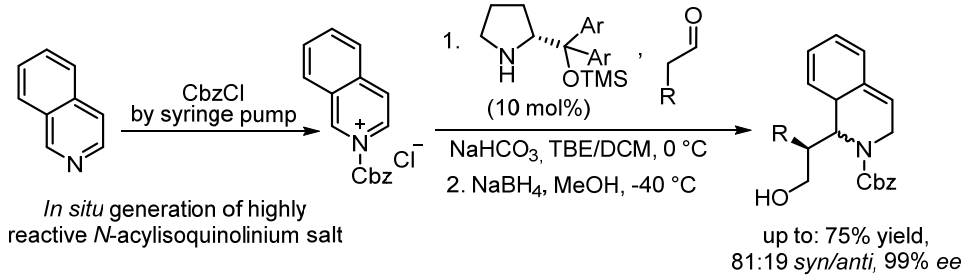

Scheme 6. Intermolecular dearomatization of isoquinolinium salts with chiral enamines. Ar = 3,5-$(CF_3)_2C_6H_3$

Isoquinolinium salts present enhanced electrophilic character at benzylic C-1, rendering functionalized products with exclusive C-1 regioselectivity. On the other hand, quinolinium derivatives, similar to pyridinium ones, present sometimes regioselectivity issues, due to the possibility of an attack on C-2 or C-4. However, position C-2 is often more reactive and preferably functionalized.

Three simultaneous approaches by Pineschi (Table 1, entry 3),[76] Rueping (entry 1)[77] and Liu (entry 2)[78] realized the enantioselective dearomatization of *N*-acylquinolinium salts by addition of chiral enamines. The highly activated aromatic electrophile was generated not by alkylation of the heterocyclic *N*-atom, but by acid promoted alkoxide elimination of a stable quinoline-*N,O*-acetal. This conveniently avoided catalyst deactivation, as no electrophilic activator was needed. Modest diastereoselectivities, along with very high enantioselectivity values and good yields were obtained in most of the cases for 1,2-

dihydroquinoline derivatives, obtained as the sole regioisomers (or accompanied by trace amounts of the C-4 adducts). While Rueping and Liu employed a Lewis acid co-catalyst to promote the elimination leading to the cationic electrophile, a Brønsted acid was employed by Pineschi.

Table 1. Dearomatization of *N*-acyl isoquinolinium salts with chiral enamines. Reports by Pineschi, Rueping and Liu.

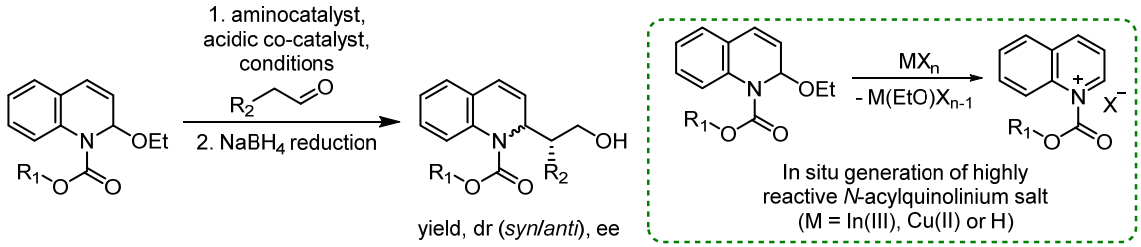

Entry (ref.)	Aminocatalyst	Acidic cocatalyst	Conditions	Yield, dr, ee
1 (77)	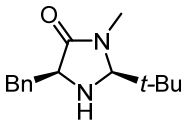	$In(OTf)_3$	Toluene, -30 °C	up to: 83%, 4:1 dr, 97% ee
2 (78)	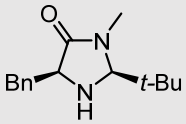	$Cu(OTf)_2$	Et_2O, EtOH (1 equiv), RT	up to: 91%, 4:1 dr, 99% ee
3 (76)	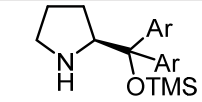 Ar = 3,5-$(CF_3)_2C_6H_3$	TsOH	Toluene, 0 °C	up to: 85%, 9:1 dr, 99% ee

Pineschi and coworkers envisioned to employ a similar strategy for non-benzo-fused scaffolds; however, this did not proceed through a pyridinium cation dearomatization but through an α-selective alkylation of an acyl-iminium ion, generated *in situ* (Scheme 7a). The versatility of the reported methodology was demonstrated by the different synthetic elaborations reported: while Liu proved that the dearomatization process was applicable to isoquinoline-like substrates as well, involving, for example, a β-carbolinium cation (Scheme 7b), Rueping was able to obtain complex bicyclic scaffolds in one step, by treating the reduced products with trimethylsilyl iodide. It was also possible to obtain a formal heteroarylated product, after carbamate hydrolysis and spontaneous air-oxidation of the resulting free dihydroquinoline (Scheme 7c).

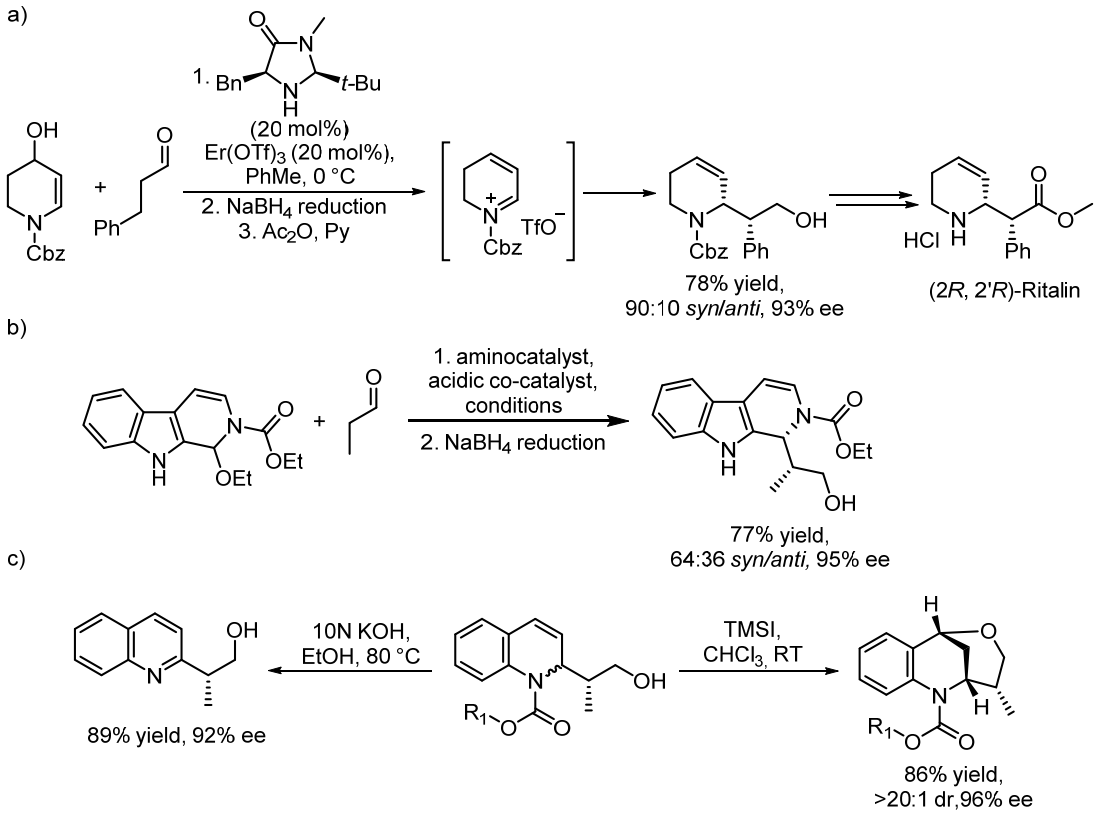

Scheme 7. Selected synthetic elaborations.

Based on a more typical activation strategy, Cozzi and co-workers proposed a quinolinium salt dearomatization process, analogous to the one reported for isoquinoliniums.[79] In this case, non-neglectable amounts of undesired C-4 regioisomers were formed in some cases (Scheme 8).

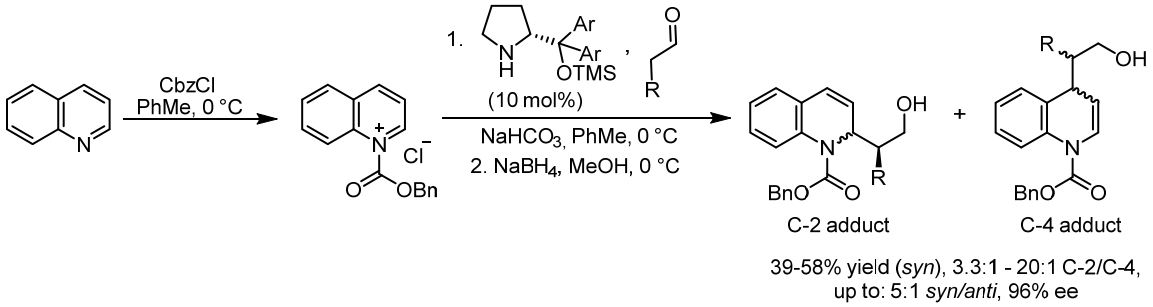

Scheme 8. Dearomatization of *N*-acylquinolinium salts. Report by Cozzi.

While the dearomatization of benzo-fused azines with chiral enamines as nucleophiles is demonstrated to be a well-established procedure, no example of pyridine dearomatization with such a strategy was present in literature. On the other hand, the activation of aldehydes by chiral amine catalysts could be employed for the synthesis of enantioenriched 1,4-dihydropyridines, presenting an EWG group at the 3-position. This

consisted in a multi-step reaction sequence involving the nucleophilic addition of enaminones or β-amino esters to chiral iminium ions, followed by hydrolysis and cyclization *via* intramolecular enamine formation (Scheme 9).[80]

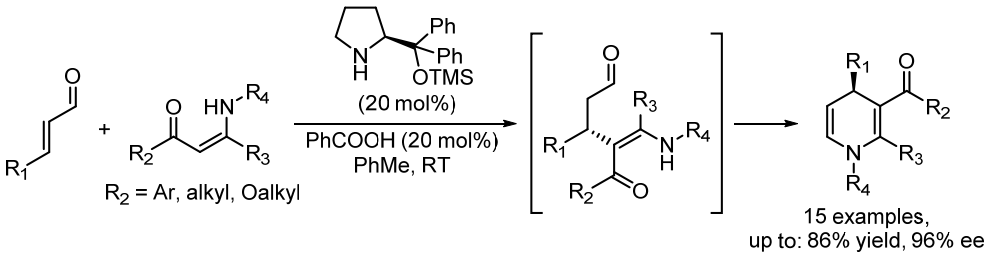

Scheme 9. Construction of 1,4-dihydropyridines through a multistep sequence.

However, the presented strategy was not extended to β-amino nitroolefins, probably due to the poor nucleophilicity of their double bond. Nitro groups, on the other hand, represent useful precursors for the synthesis of amines. Indeed, 4-alkyl-3-aminopiperidines,[81] potentially derived from the C-4 regioselective dearomatization of 3-nitropyridinium salts, represent common scaffolds of some medicinally relevant compounds. This is exemplified in Figure 1 for piperidine quinolones **I**, a class of antibacterial agents,[82] and tofacitinib **II**,[83] a potent Janus Kinase inhibitor commercialized as Xeljanz and Jakvinus for the treatment of rheumatoid arthritis. Furthermore, the presence of a formyl group on the nucleophile and the nitro function on the dearomatized product can be exploited for further manipulations. For example, cyclization processes would render synthetically challenging bicyclic motives related to octahydropyrrolo[2,3-c]pyridines **III**, core structures of anticancer peptidomimetics.[84]

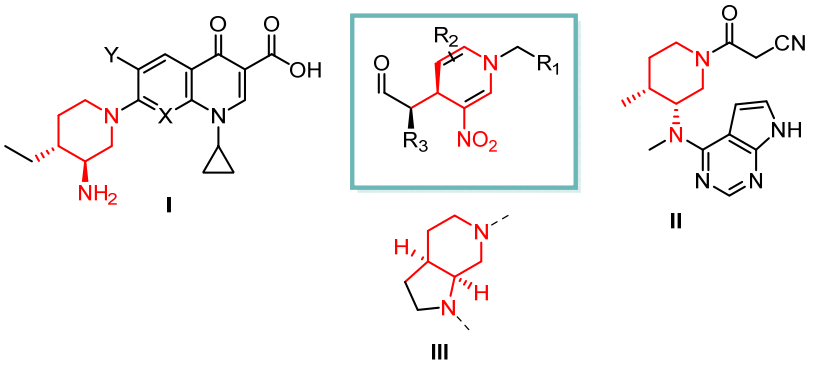

Figure 1. 4-Alkyl-3-nitrodihydropyridines as precursors of biologically relevant structures.

It is now clearer how, both in the contest of pyridinium salts dearomatization and of valuable hydropyridines preparation, regio-, diastereo- and enantioselective

dearomatizations of *N*-alkyl-3-nitropyridinium salts with chiral enamines become an appealing process.

4.2 Aim of the work

Being interested in the possibility to expand the methodology for organocatalytic enantioselective pyridinium salts dearomatizations, we have devoted our efforts to the disclosure of a procedure involving chiral enamines, generated catalytically by aldehydes and secondary amine catalysts **3**, as nucleophiles. In this chapter, an asymmetric addition of aldehydes **2** to pyridinium salts **1**, catalyzed by secondary amine **3a** (Scheme 10) and furnishing highly enantioenriched 1,4-dihydropyridines **4**, is presented.

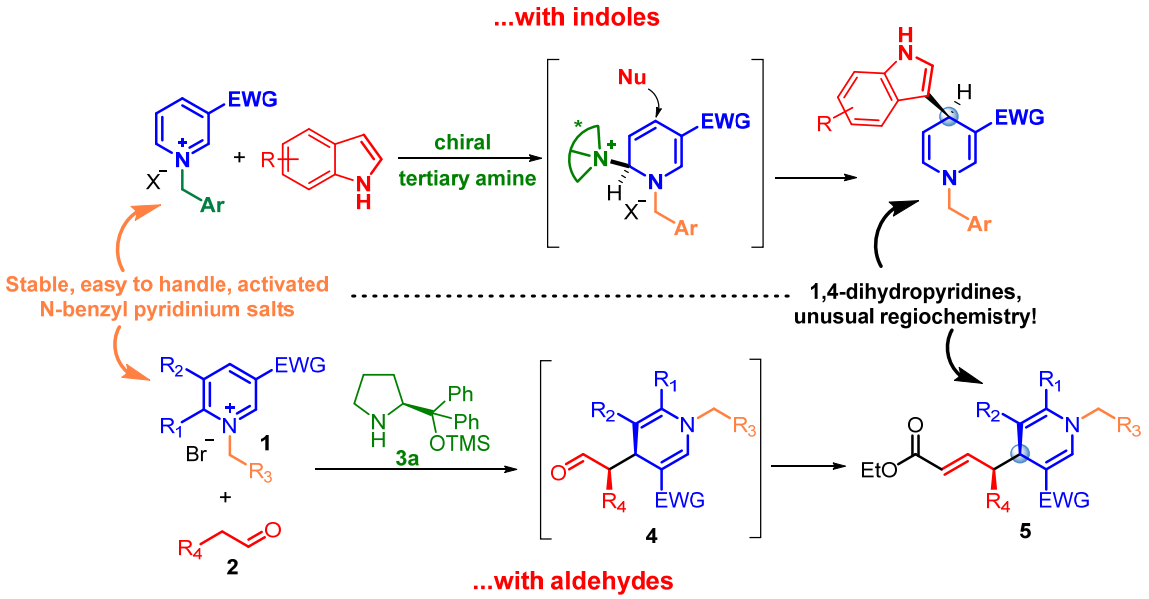

Scheme 10. Dearomatization of *N*-alkylpyridinium salts with indoles and chiral enamines.

This merges one of the most reliable and commonly employed activation strategy in organocatalysis with the newly discovered class of electrophiles. Some challenges however, derived from the combination of these elements. First of all, the regioselectivity issues, intrinsic in pyridinium salts dearomatizations. C-4 Alkylated products, besides being valuable for the reasons explained in section 3, where also the only ones having the aldehyde and the nitro group in the correct position for a cyclization process, leading to compounds **III** (Figure 1). Moreover, as it is possible to notice in all the examples reported in the previous section, low diastereoselectivities were obtained for azinium salts dearomatizations with aldehydes, leading to non-separable mixtures of isomers or, where the separation became possible, to low isolated yields. The presence of the nitro

group however, peculiar characteristic of the chosen class of electrophiles **1**, might induce a higher degree of diastereoselectivity, as it will be explained later.

More importantly, the reversibility of the dearomatization, derived from the aromaticity of the starting material, might be a more challenging issue in this case, compared to the previously described methodology (section 3). Indeed, the addition of indoles is rendered irreversible by restoring their aromaticity after nucleophilic attack (which is expected to be a fast step). On the other hand, recondensation of catalysts **3** on the dearomatized product **4** would lead to an iminium ion, acting as a good leaving group for dihydropyridine rearomatization. Thus, with the catalyst enabling both dearomatization and rearomatization pathways, the whole process might fall under thermodynamic control, losing possibly diastereo- and enantioselectivity (Scheme 11).

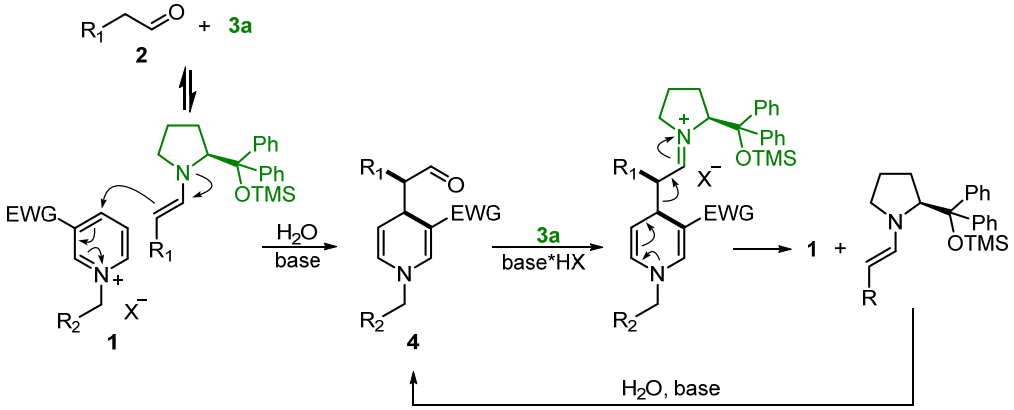

Scheme 11. Equilibration pathway in the dearomatization of pyridinium salts with chiral enamines.

Overcoming all these issues by careful optimization of the reaction conditions will lead to the development of an organocatalytic nucleophilic dearomatization of activated *N*-alkylpyridinium salts **1** with aldehydes **2**, under chiral enamine catalysis. The process will exhibit complete C-4 regioselectivity along with high levels of diastereo- and enantiocontrol, enabling a good yielding synthesis of a broad range of optically active 1,4-dihydropyridines.

4.3 Organocatalytic reactions between *N*-alkyl pyridinium salts 1 and aldehydes 2: results and discussion

Initially, we treated pyridinium salt **1a** with 2 equivalents of 3-phenylpropionaldehyde **2a** in the presence of 20 mol% of catalyst **3a** and 1 equivalent of TEA (Et_3N) as stoichiometric base (HBr is formed as the reaction proceeds) in DCM for 6 hours.

Although the process proved to be feasible (complete conversion), no diastereo- or enantioselectivity was observed (Table 2, entry 1). Since the reaction seemed to be almost instantaneous, we tried to reduce considerably the reaction time and the temperature. This would prove beneficial, suppressing two important side reactions, leading to the erosion of the stereoselectivity. First of all, post-addition epimerization, which can be a considerable issue in chiral enamine-catalyzed α-alkylation of aldehydes.[85] Secondly, the abovementioned rearomatization process, leading to thermal equilibration. Indeed, the diastereomeric ratio increased considerably but the maximum value of enantiomeric excess (40% ee for *syn*-**4aa**), observed at -30 °C, remained unsatisfactory (entries 2, 3 and 4). Gratifyingly, upon changing the reaction solvent from DCM to toluene, very good values of diastereoselectivity (92:8) and enantioselectivity (92% ee for *syn*-**4aa**) were reached for the first time (entry 5). At this point, many different auxiliary bases were tested, giving similar or worse results compared to TEA, which was thus confirmed as optimal (*vide infra*, Table 3). However, at this stage of optimization, the reaction protocol did not prove to be much robust, as, for example, simply increasing the reaction time from 1 to 2 hours led to significant erosion in both diastereo- and enantioselectivity values (compare entry 6 with entry 5). We then found that an acidic co-catalyst (phenylacetic acid, equimolar with **3a**) led to better results in terms of enantiocontrol (92:8 dr, 96% ee for *syn*-**4aa**, entry 7) and that lowering the catalyst loading to 10 mol% led only to slightly inferior results (90:10 dr, 92% ee for *syn*-**4aa**, entry 8). Under these latter conditions, the process proved to be much more robust than before: upon prolonging the reaction time to 2.5 h only a very small detriment in the enantiomeric excess and the diastereomeric ratio (88:12 dr, 90% ee for *syn*-**4aa**) was observed (compare entries 8-9 to entries 5-6). We thus found that the acidic additive takes an important role in stabilizing the reaction product, slowing the erosion of the diastereo- and enantioenrichment obtained. Given this experimental feature, it can be hypothesized that such epimerization is accelerated by the concomitant presence of the base (TEA), necessary for the HBr scavenging, and the free catalyst acting on products **4**. In fact, if TEA alone was responsible for this isomerization, this would take place predominantly at the beginning of the reaction, when the amount of base is larger (not yet reacted with the HBr developed). It would be therefore impossible to obtain good diastereoselections. On the other hand, in the early stages of the process the catalyst is sequestered into the catalytic cycle and does not react with **4**. As the reaction reaches higher degrees of completion, such epimerization becomes competitive. The acid may

then buffer the yet unreacted amount of base, slowing post-addition epimerization of **4** and rendering the process more robust and reliable.

Table 2. Optimization of the dearomatization reaction between **1a** and **2a**: overview.

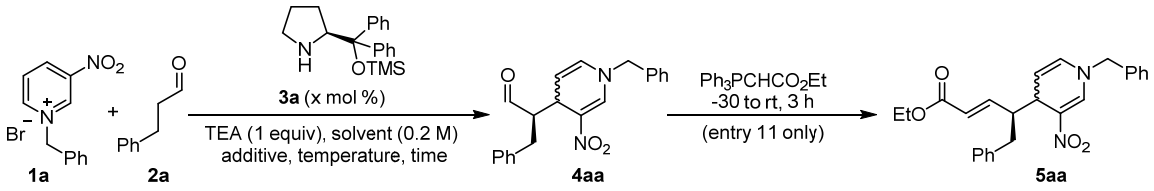

Entry[a]	Solvent	Temperature (°C)	Time (min)	**3a** (mol%)	Additive[b]	Conversion (%)[c,d]	dr[c] (*syn*/*anti*)	ee[e] (%)
1	DCM	RT	360	20	none	> 95	50:50	rac
2	DCM	RT	10	20	none	> 95	75:25	6
3	DCM	-30	35	20	none	60	86:14	40
4	DCM	-60	90	20	none	> 95	90:10	35
5	PhMe	-30	60	20	none	> 95	92:8	92
Base screening: see Table 3								
6	PhMe	-30	120	20	none	> 95	86:14	73
7	PhMe	-30	60	20	$PhCH_2COOH$	83	92:8	96
8	PhMe	-30	60	10	$PhCH_2COOH$	> 95	91:9	92
9	PhMe	-30	150	10	$PhCH_2COOH$	> 95	88:12	90
10	PhMe	-30	60	5	$PhCH_2COOH$	41	93:7	37
Catalyst screening: see Table 4								
11[f]	PhMe	-30	60	10	$PhCH_2COOH$	86[g]	> 95:5[h]	99[i]/-

(**a**) Reaction conditions: **1a** (0.05 mmol), **2a** (0.1 mmol), TEA (0.05 mmol), **3a** (0.01 or 0.005 or 0.0025 mmol), solvent (250 µL). (**b**) Equimolar with **3a**. (**c**) Determined on the crude mixture by ^{1}H NMR. (**d**) Overall conversion in the two diastereoisomers. (**e**) Enantiomeric excess of crude ***syn* 4aa** determined by CSP HPLC. (**f**) Reaction conditions as before, then, Ph_3PCHCO_2Et (0.6 mmol), -30 °C to RT, 3 h. (**g**) Isolated yield of product **5aa** after column chromatography. (**h**) Diastereomeric ratio of isolated **5aa** (93:7 in the crude mixture). (**i**) Enantiomeric excess of isolated **5aa** by chiral stationary phase HPLC.

On the other hand, by further diminishing the catalyst loading to 5 mol% all the results dropped considerably (entry 10). We therefore chose 10 mol% as the best value. Finally,

to avoid small deviations from the primary outcomes of the reaction during isolation, due to the instability of product **4aa**, we chose to transform the aldehyde group into a less labile α,β-unsaturated ester, by Wittig reaction. Product **5aa** proved thus to be stable enough for column chromatography and was isolated as a single diastereoisomer in 86% yield and 99% ee (entry 11).

Table 3. Optimization of the dearomatization reaction between **1a** and **2a**: base screening.

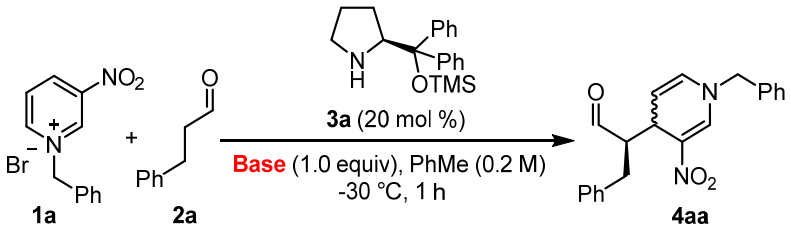

Entry[a]	base	Conversion[b,c] (%)	dr[c] (*syn*/*anti*)	ee[d] *syn* (%)
1	TEA	> 95	92:8	92
2	proton sponge	> 95	63:37	55
3	quinuclidine	> 95	76:24	25
4	pyridine	60	90:10	82
5	DIPEA	> 95	90:10	89
6	2,6-(*t*-Bu)$_2$-pyridine	43	86:14	82
7	*N,N*-(Me)$_2$-aniline	37	83:17	77
8	DMAP	> 95	83:17	60
9	DABCO	> 95	88:12	77
10	DBU	69	86:14	84
11	$NaHCO_3$	< 5	-	-
12[e]	$NaHCO_3$	> 95	50:50	rac

(**a**) Reaction conditions: **1a** (0.05 mmol), **2a** (0.1 mmol), base (0.05 mmol), **3a** (0.005 mmol), PhMe (250 µL), -30 °C, 1h. (**b**) Determined on the crude mixture by ^{1}H NMR. (**c**) Overall conversion in the two diastereoisomers. (**d**) Enantiomeric excess of crude ***syn* 4aa** determined by CSP HPLC. (**e**) Reaction run at RT overnight.

Different organic bases (Table 3, entries 1-10) were tested in the reaction between salt **1a** and aldehyde **2a** catalyzed by **3a** in toluene at -30 °C. It can be speculated that (except from DBU, entry 10), stronger bases achieved complete conversion (entries 1-3, 5, 8, 9)

while weaker ones (entries 4, 6, 7) were less able to regenerate the catalyst from the HBr developed. The diastereomeric ratios obtained were rather good while the enantiomeric excesses ranged from poor to very good. However, the initially chosen TEA was confirmed as the best base for the present dearomatization process. This highlights how the tendency of the substrate to undergo reversible addition-elimination reactions is part of a base-catalyzed process and is responsible for the low enantioselectivities observed in some cases. Sodium bicarbonate ($NaHCO_3$), previously employed in similar dearomatization processes, failed to give any conversion under the standard reaction conditions (entry 11), while rising the temperature to RT and prolonging the time to 18 hours provided the desired product in a racemic equimolar diastereomeric mixture (entry 12).

Different catalysts were also screened, with TEA as optimal base. Similarly to catalyst **3a** (Table 4, entry 1), **3b** gave excellent values of enantio- and diastereoselectivity with good conversion (entry 2). On the contrary, **3c** gave poor results in terms of enantiomeric excess and diastereomeric ratio, along with a quite diminished conversion (entry 3). Unprotected prolinol **3d** and proline **3e** were not able to promote the reaction (entries 4 and 5 respectively), as MacMillan's type catalysts **3f** and **3g** (entries 6 and 7). Prolinol-squaramide **3h,** tested to investigate if anion-binding motifs could be involved in the reaction pathway, as well as coordination of the nitro group, was found to be unsuitable for the present process (entry 8).

Table 4. Optimization of the dearomatization reaction between **1a** and **2a**: catalyst screening.

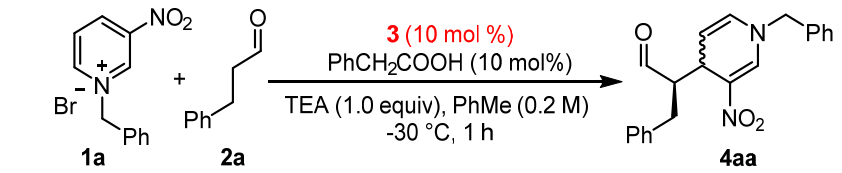

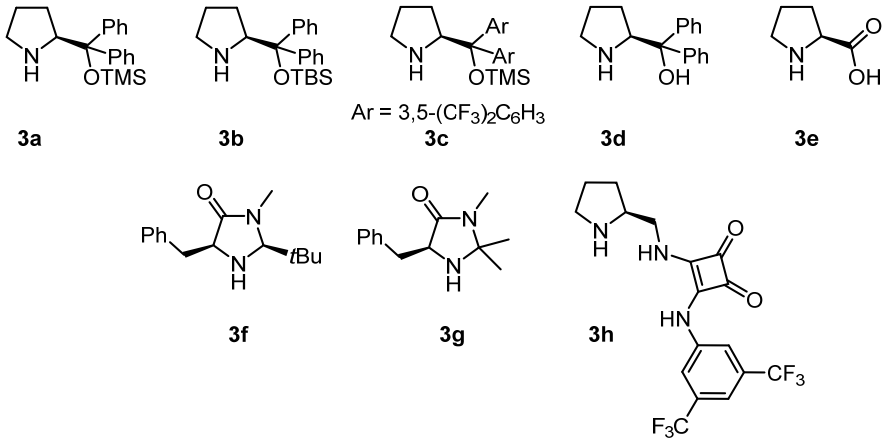

Entry[a]	catalyst **3**	Conversion[b,c] (%)	dr[c] (*syn*/*anti*)	ee[d] *syn* (%)
1	**3a**	83	92:8	96
2	**3b**	81	93:7	96
3	**3c**	51	80:20	60
4	**3d**	< 5	-	-
5	**3e**	< 5	-	-
6	**3f**	< 5	-	-
7	**3g**	< 5	-	-
8	**3h**	< 5	-	-

(**a**) Reaction conditions: **1a** (0.05 mmol), **2a** (0.1 mmol), TEA (0.05 mmol), catalyst **3** (0.005 mmol), $PhCH_2COOH$ (0.005 mmol), PhMe (250 µL), -30 °C, 1h. (**b**) Determined on the crude mixture by ^1H NMR. (**c**) Overall conversion in the two diastereoisomers. (**d**) Enantiomeric excess of crude ***syn* 4aa** determined by CSP HPLC. (**e**) Reaction run at RT overnight.

Having thus optimized the parameters required for optimal results, we sought to verify the reaction scope. Along with 3-phenylpropanal **2a**, a variety of aldehydes was successfully employed in the disclosed dearomatization (Scheme 12). Short- (*n*-butanal **2b**), medium- (*n*-hexanal **2c**) and long-chained (*n*-dodecanal **2d**) linear aldehydes, as well as 4-methylpentanal **2e** and 3-cyclohexylpropanal **2f** furnished in good yields (65%-

89%) and excellent enantiomeric excesses (96%-99% ee) the respective dearomatized products **5ab**-**5af** isolated as single diastereoisomers. Isovaleraldehyde **2g** proved to be less reactive than the other aldehydes employed. Therefore, the reaction temperature had to be raised to 0 °C and the time prolonged to 2 h. Since in this case the Wittig olefination proved to be quite slow and thus inefficient in preventing epimerization, product **6ga** was obtained through acetalization of the formyl group. This was achieved in moderate yield (43%) but good enantiomeric excess (94%). Other aldehydes, bearing functional groups on the β-carbon, such as heterocycles (**2h**), aromatic polycycles (**2i**), and ethers (**2j**) could also be employed, without loss in reaction efficiency or diastereo- and enantiocontrol, showing a broad functional group tolerance and a generally robust process.

Thereafter, we tested the possible changes on pyridinium partner **1**. Since the nitrogen protecting group strongly influenced the reaction outcomes in the dearomatization between salts **1** and indoles (see Section 3), we thought that exploration of this moiety could be of some interest. Both an electron-poor (**1b**) and an electron-rich (**1c**) aromatic ring, along with simple aliphatic chains (**1d**) were all suitable for the present process, giving products **5ba-5da** with excellent results (83%-91% yield, 90%-99% ee). This shows the robustness of the disclosed procedure, relying on a less substrate-dependent activation of the reactants. We next moved to the exploration of the substitution pattern on the pyridinium ring. Salt **1e**, bearing a methyl substituent on the C-6, proved to be a particularly challenging substrate, given the observed tendency of this electrophile to undergo side reactions under the basic conditions required in this dearomatization. The acidity of the methyl hydrogens of some nitro aromatic systems was indeed successfully exploited for the generation of aryl methane nucleophiles.[86] Nevertheless, we were able to isolate product **5ea**, albeit in moderate yield (35%), as a single diastereoisomer and with excellent optical purity (98% ee). Substitution on the C-5 was also explored: products **5fa** and **5ga** were obtained in useful synthetic yields (70%-50%) and high enantiomeric excesses (94%-91% ee for the *syn* isomer), although with decreased diastereoselectivity. The possibility of changing the EWG on the pyridinium ring was also investigated. A cyano group was found to be activating enough the pyridinium cation to promote the dearomatization. Substrate **1h** was therefore reacted with aldehydes **2a** and **2b** to render products **5ha** and **5hb**, as diastereomeric mixtures, in 75% and 60% yield respectively. The enantiomeric excesses of both diastereoisomers were very good

(>90% ee) in both cases. Unfortunately, less activated substrates such as *N*-Benzyl-3-acetylpyridinium and *N*-benzyl-3-methoxycarbonyl pyridinium bromides did not show sufficient reactivity.

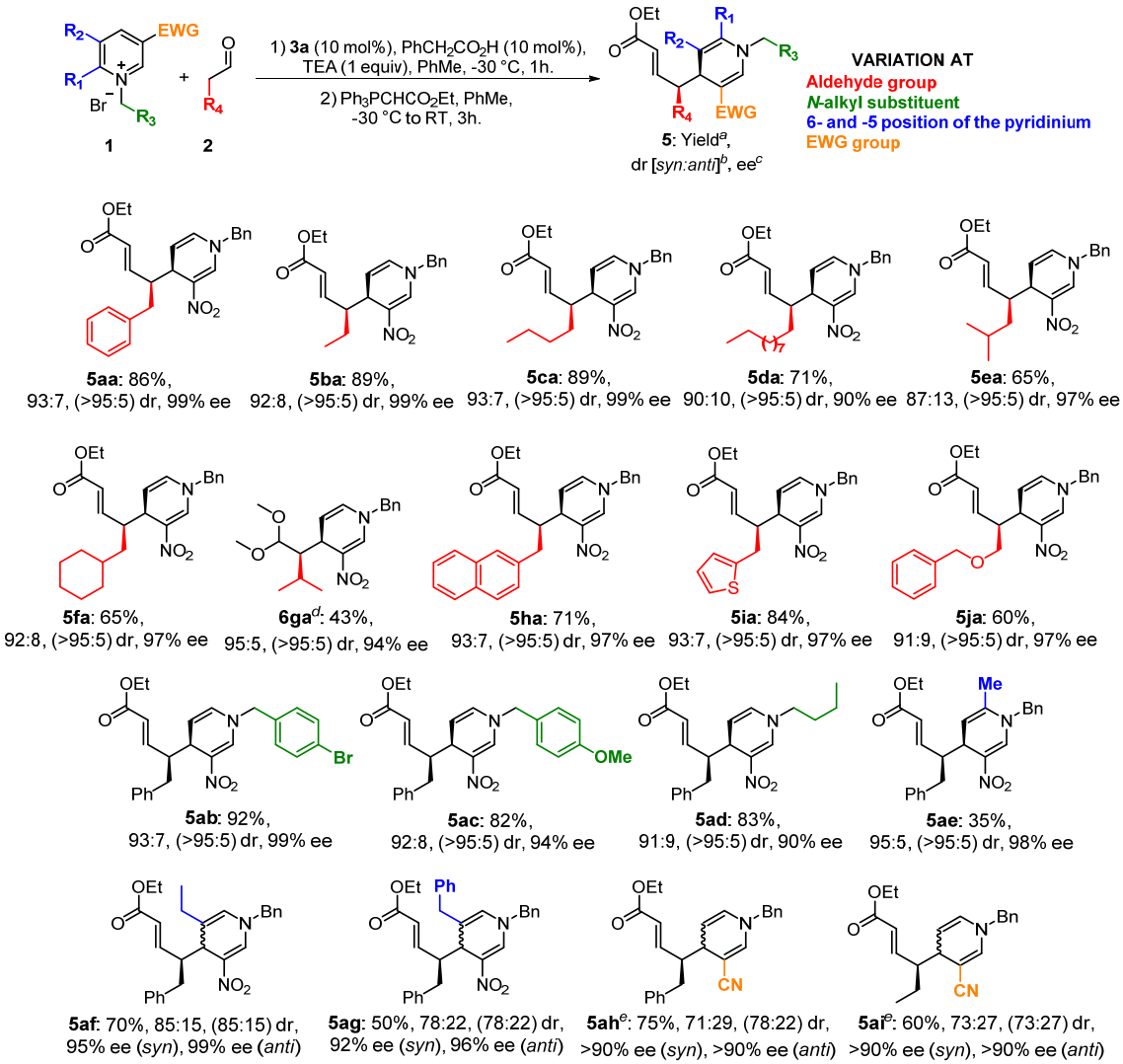

Scheme 12. Reaction scope. Reaction conditions: **1** (0.1 mmol), **2** (0.3 mmol), **3a** (0.01 mmol), phenylacetic acid (0.01 mmol), triethylamine (0.1 mmol), PhMe (500 µL), 0 °C, 1 h, then Ph_3PCHCO_2Et (0.6 mmol), 0 °C to RT, 3 h (products **5**). (**a**) Isolated yield after column chromatography. (**b**) Measured on the crude mixture by ^1H NMR spectroscopy e (dr of isolated product after column chromatography shown in parentheses). (**c**) Measured by CSP HPLC on isolated products **5** and **6**. (**d**) Reaction run at 0 °C for 2 h. Acetalization conditions: SiO2 plug, then HCO(Me)3 (1.0 mmol), p-TSA (0.15 mmol), MeOH (250 µL), 0 °C to rt, 2 h. (**e**) Reaction run at 0 °C for 2 h; ee determined by ^1H NMR spectroscopy using a chiral shift reagent (Pirkle's alcohol).

As mentioned, taking advantage of the concomitant presence of the nitro- and the aldehyde groups in the obtained dihydropyridines **4**, we envisioned that the present dearomatization would be suitable for the construction of medicinally relevant bicyclic structures of type **III**. These synthetically challenging frameworks have been prepared in enantioenriched form by intramolecular 1,3-dipolar cycloadditions followed by chiral

resolution or with a chiral auxiliary approach.[84] In our projected synthesis, the pyrrole ring would derive from intramolecular reductive amination of intermediate **IV**, in turn arising from progressive selective reductions of product **4** (Scheme 13).

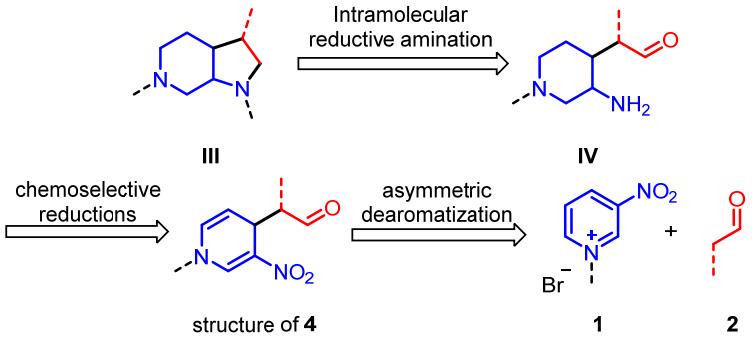

Scheme 13. Retrosynthetic analysis towards bicyclic structures.

Therefore, after applying the standard addition protocol to salt **1a** and aldehyde **2a**, product **4aa** was transformed into acetal **6aa**, obtained as a single diastereoisomer in 76% yield and 95% ee, under conditions similar to the ones applied for **6ag**, (*vide supra*). This allowed, besides obtaining a stable and isolable product, to preserve the masked aldehydic function during the subsequent reductions. Treatment of **6aa** with excess $NaBH_4$ in methanol afforded fully saturated piperidine **7** (89% yield, 95% ee) with complete diastereocontrol of the newly formed stereocenter, which was found to be in an 1,2-*cis* relationship with the contiguous one (assigned by consistency with the absolute configuration of product **10**, *vide infra*). Under standard hydrogenation conditions (ammonium formate and Pd/C in methanol), **7** underwent simultaneous nitro-group reduction and benzyl group cleavage to afford 3-aminopiperidine **8**. Crude **8** was directly subjected to acetal deprotection-cyclization by reaction with aqueous HCl. Partial epimerization of the imine α-stereocenter was observed during preliminary attempts, caused by slow thermodynamic equilibration of the product in the acidic reaction medium. After some optimization, we found that conducting the reaction at 0° C for 18 h, then at room temperature for 1h, was the optimal compromise between diastereopurity (93:7 dr) and conversion (95% by ^{1}H NMR). Crude bicyclic imine **9** was hydrogenated to obtain a diamine, conveniently isolated as ditosylated product **10** in 30% overall yield (4 steps, 75% yield per step) and 95% ee (i.e. complete retention from **6aa**). Product **10** afforded enantiopure single crystals which, upon X-rays diffraction analysis, provided its absolute configuration as 3R, 3aR, 7aS (Scheme 14).[87] This, along with the structural

assignments performed by NMR analysis (see Section 4.3.1) provided the absolute (and relative) configuration of compounds **5** and **6** for consistency.

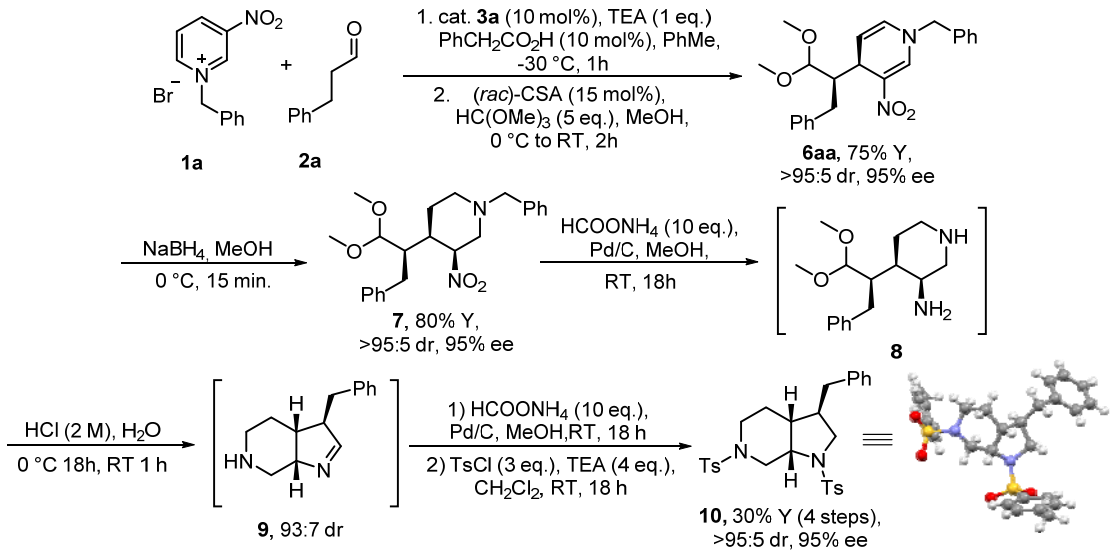

Scheme 14. Preparation of compound **10**.

4.3.1 Determination of the regiochemistry and relative configuration of compounds *syn* and *anti* 5aa

In order to make sure that the disclosed dearomatization was exclusively C-4 regioselective, we carefully characterized both the two isomers detected in the crude reaction mixtures, in order to show that they are in fact diastereoisomers and not regioisomers. For the preparation and isolation of these compounds see the dedicated section.

Isomer *syn* 5aa, regiochemistry. Isomer ***syn* 5aa** (for relative configuration assignment *vide infra*) showed first of all a singlet at 8.09 ppm in the ^{1}H NMR spectrum (Figure 2), which was assigned to H-2 due to the chemical shift and multiplicity (triplet, formally doublet of doublets, with a coupling constant of 1.1 Hz, conjugation with the nitro-group). This signal rules out addition at the more hindered C-2 of the pyridinium ring. Between the remaining conceivable regioisomers (C-4 or C-6), the regiochemistry of diastereoisomer ***syn* 5aa** was confirmed as follows.

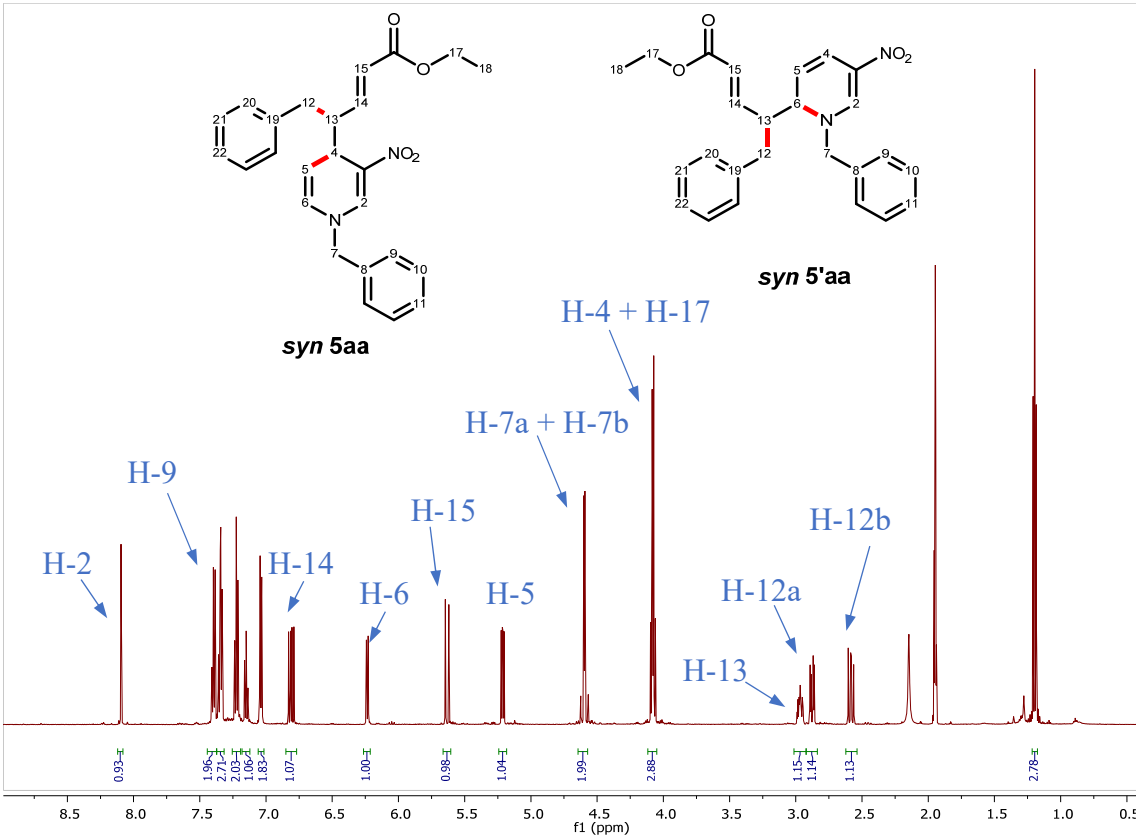

Figure 2 ^{1}H NMR spectrum of product ***syn* 5aa** in CD_3CN (with the structures and numberings of the possible regioisomers ***syn* 5aa** and ***syn* 5'aa**).

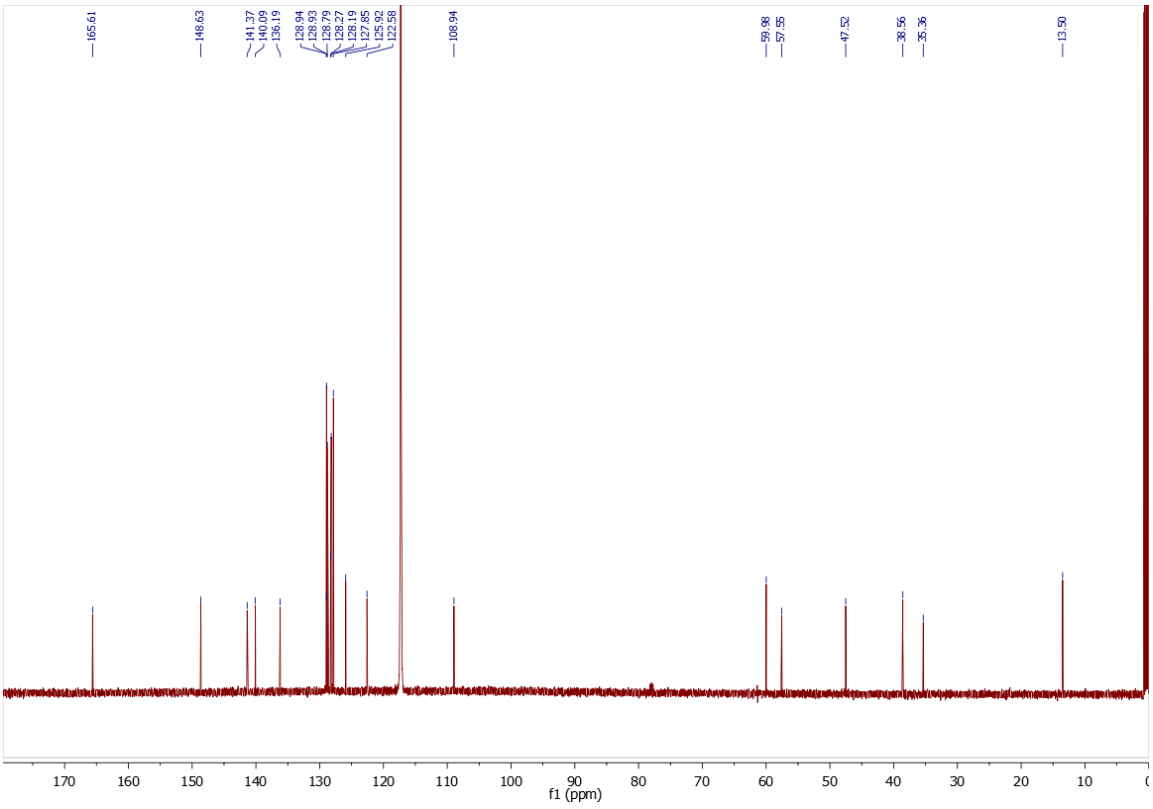

Figure 3. ^{13}C NMR spectrum of product ***syn* 5aa** in CD_3CN.

The signals found at 4.61 and 4.58 ppm were assigned to H-7a and H-7b due to the multiplicity (AB system with small chemical shift difference between the two diastereotopic hydrogens) and its integral value. The signal at 6.81 ppm (dd, trans coupling J = 15.7 and vicinal coupling with H-13 = 8.8 Hz) was assigned at H-14 due to the chemical shift and multiplicity. The same large coupling constant (15.7 Hz) was found in the signal at 5.63 ppm, which was assigned to H-15. This proton as well couples with H-13, but with a much smaller ^{4}J = 1.1 Hz. The signal at 5.21 ppm was assigned to H-5 due to its multiplicity: doublet of doublets with two similar constants (coupling with H-4 and H-6). Therefore, the signal at 6.24 ppm was assigned to H-6 (product ***syn* 5aa**) or H-4 (product ***syn* 5'aa**).

The signal at 2.97 ppm was assigned to H-13, due to the coupling system showed by a gCOSY experiment (as discussed before, in addition to coupling with H-12a and H-12b; (Figure 4) and the signal at 4.08 ppm (overlapped with H-17) was assigned to H-4 (***syn* 5aa**) or H-6 (***syn* 5'aa**) as the only remaining sp^3-CH (correlation with a CH carbon at 38.6 ppm in the gHSQC spectrum, Figure 5). The signals at 2.88 and 2.58 ppm were therefore assigned to H-12a and H-12b due to the correlation with the same CH_2 carbon at 35.4 ppm in the gHSQC spectrum (Figure 5). In addition, ^{13}C chemical shifts corresponding to C-14 (148.7 ppm), C-6 for ***syn* 5aa** or C-4 ***syn* 5'aa** (129.0 ppm), C-15 (122.6 ppm), C-5 (109.0 ppm), C-7 (57.6 ppm) and C-13 (47.6 ppm) were assigned by gHSQC experiment, along with the previous assignments of the ^{1}H NMR signals. In the gHMBC experiment (Figure 6), C-7 (57.6 ppm) correlates with the signals at 8.09 ppm (H-2), 7.34 ppm (H-9) and 6.24 ppm (H-6). Only structure ***syn* 5aa** is compatible with this experimental data, and was therefore taken as the correct one. On the other hand, in structure ***syn* 5'aa** the only additional correlation with a $^{3}J_{C\text{-}H}$ (except for H-2 and H-9) would have been detected with the signal at 4.08 ppm (H-6 of this structure). If it is true that the regiochemistry of this particular isomer could be assessed from the X-ray structure obtained from compound **10**, the previous structural assignments were also useful for the relative configuration finding discussed below. This too might have been deduced from the crystal structure, however, since epimerization of one of the chiral centers has been demonstrated to occur during the preparation of **10**, this might have brought to a misleading result.

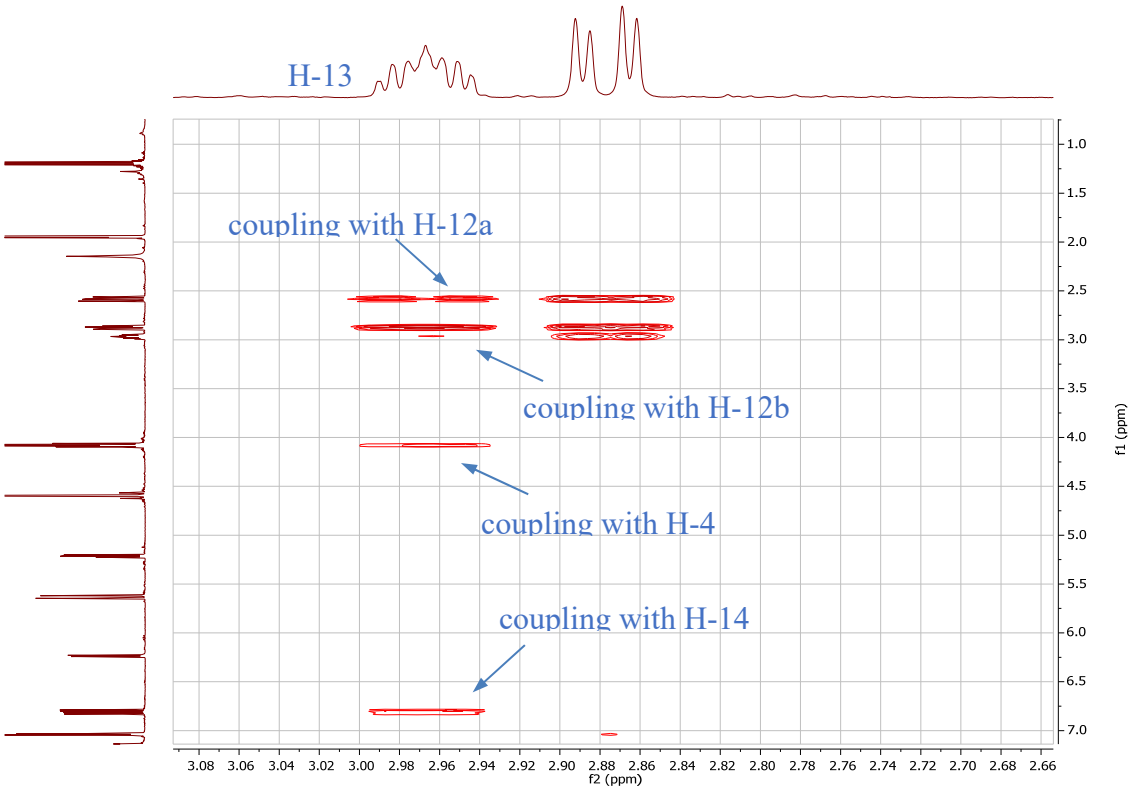

Figure 4. Couplings of H-13 in the gCOSY spectrum of product ***syn* 5aa** in CD_3CN.

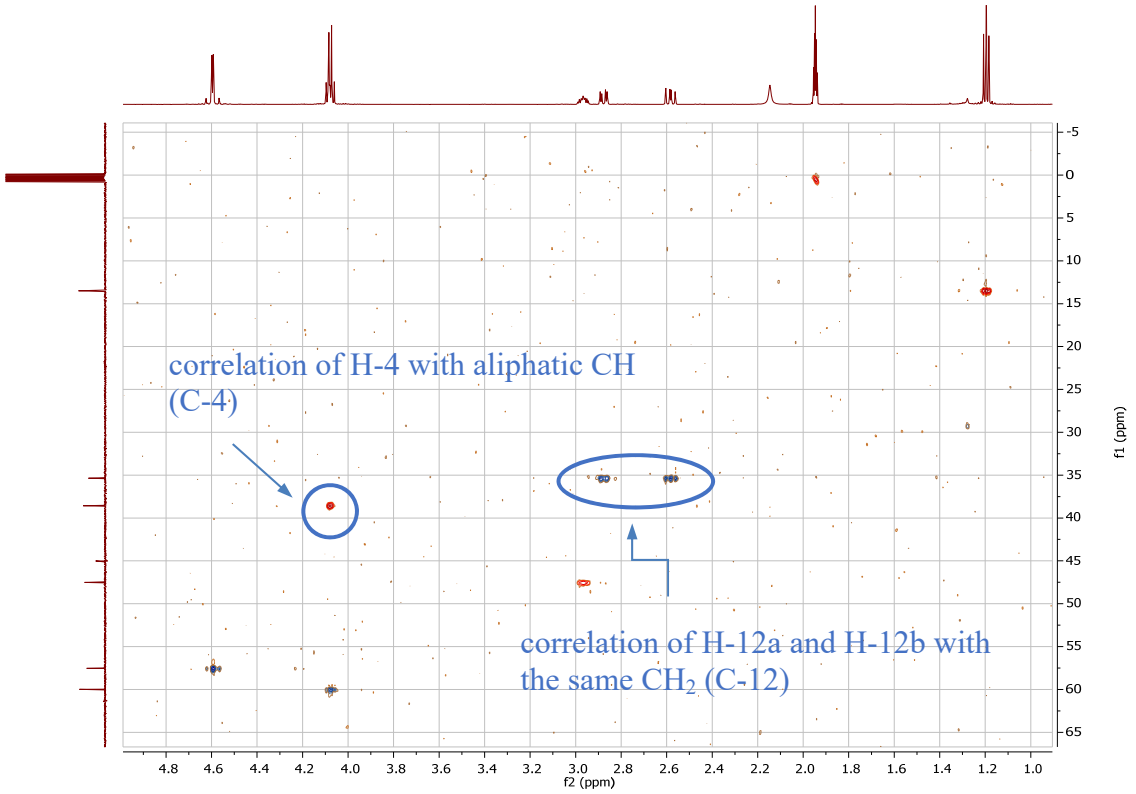

Figure 5. Expansion of the aliphatic region in the gHSQC spectrum of product ***syn* 5aa** in CD_3CN.

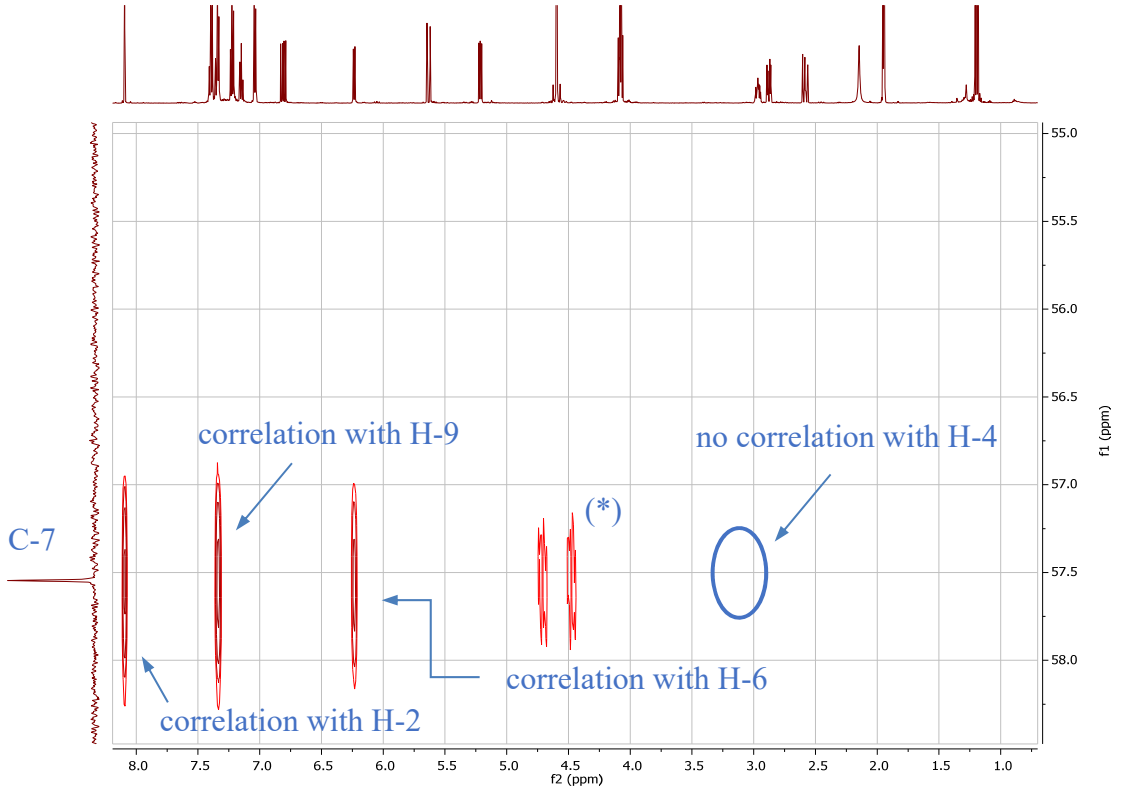

Figure 6. C-H Correlations of C-7 in the gHMBC spectrum of product ***syn* 5aa** in CD_3CN. (*) Indicates the unfiltered ^1J coupling constant.

Isomer *anti* 5aa, regiochemistry. As far as diastereoisomer ***anti* 5aa** is concerned, the presence of a signal at 8.05 ppm (singlet) in the ^1H NMR spectrum (Figure 7), deshielded by the conjugation with the nitro-group, rules out again addition at the more hindered C-2 of the pyridinium ring. Between the remaining conceivable regioisomers (C-4 or C-6), the regiochemistry of diastereoisomer ***anti* 5aa** was confirmed analogously to diastereoisomer ***syn* 5aa**.

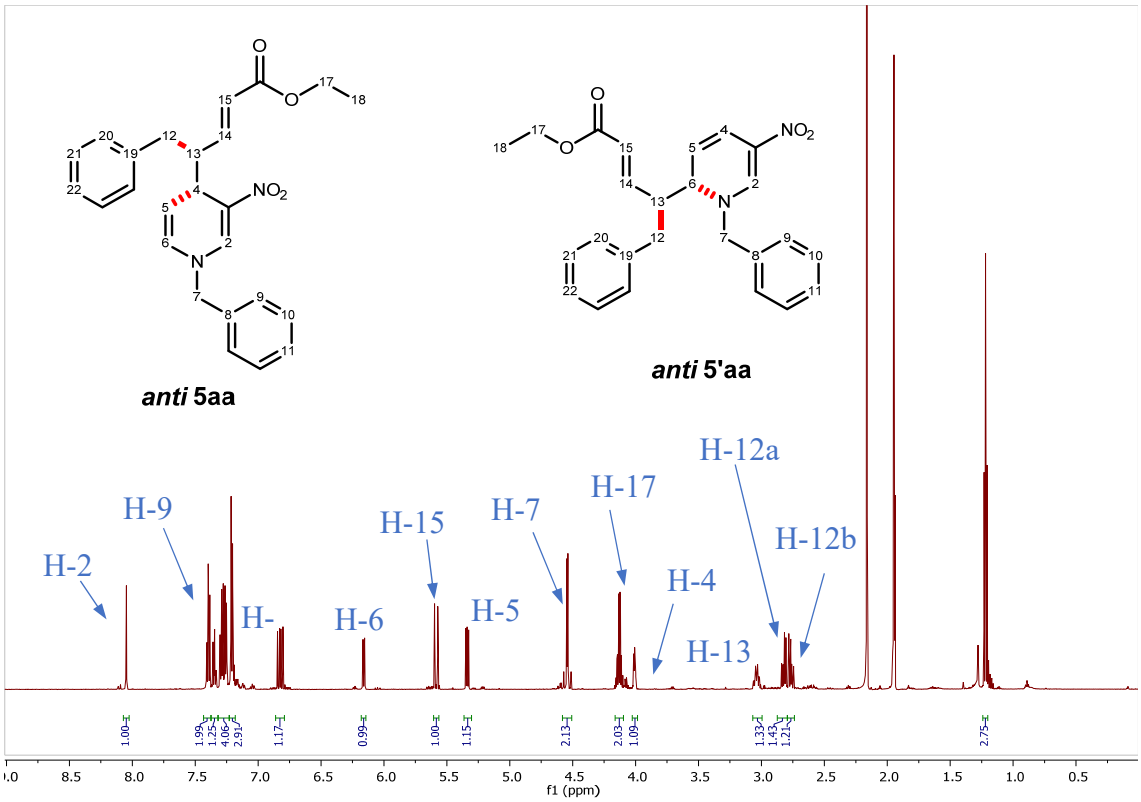

Figure 7. ^{1}H NMR spectrum of product ***anti* 5aa** in CD_3CN (with the structures and numberings of the possible regioisomers ***anti* 5aa** and ***anti* 5'aa**).

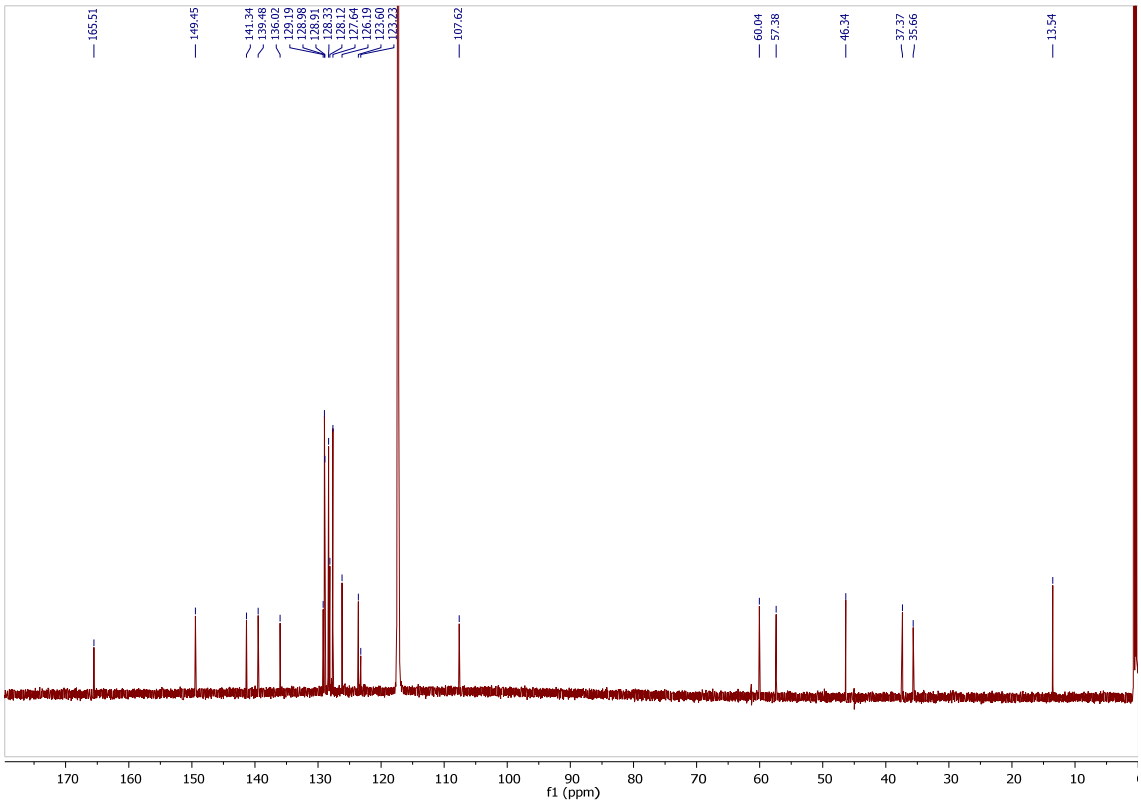

Figure 8. ^{13}C NMR spectrum of ***anti* 5aa** in CD_3CN.

^{1}H Chemical shifts corresponding to H-2 (8.05 ppm), H-7 (4.54 ppm), H-14 (6.83 ppm), H-15 (5.59 ppm), H-5 (5.34 ppm), H-6 for ***anti* 5aa** or H-4 for ***anti* 5'aa** (6.16 ppm), H-13 (3.04 ppm), H-4 for ***anti* 5aa** or H-6 for ***anti* 5'aa** (4.01 ppm), H-12a (2.82 ppm) and H-12b (2.76 ppm) and ^{13}C chemical shifts corresponding to C-2 (141.4 ppm), C-7 (57.5 ppm), C-14 (149.6 ppm), C-5 (107.8 ppm), C-6 for ***anti* 5aa** or C-4 for ***anti* 5'aa** (129.3 ppm), C-13 (46.4 pm), C-4 for ***anti* 5aa** or C-6 for ***anti* 5'aa** (37.4 ppm) and C-12 (35.8 ppm) were assigned analogously to ***syn* 5aa**. In this case too, in the gHMBC experiment (Figure 9) C-7 (57.5 ppm) correlates with the signals at 8.05 ppm (H-2), 7.26 ppm (therefore assigned to H-9) and 6.16 ppm. Only structure ***anti* 5aa** renders this correlation ($^{3}J_{C-H}$) possible (signal at 6.16 ppm attributed to H-6) and was therefore taken as the correct one. On the other hand, in structure ***anti* 5'aa** the only additional correlation with a $^{3}J_{C-H}$ (except for H-2 and H-9) would have been with the signal at 4.01 ppm (H-6 of this structure).

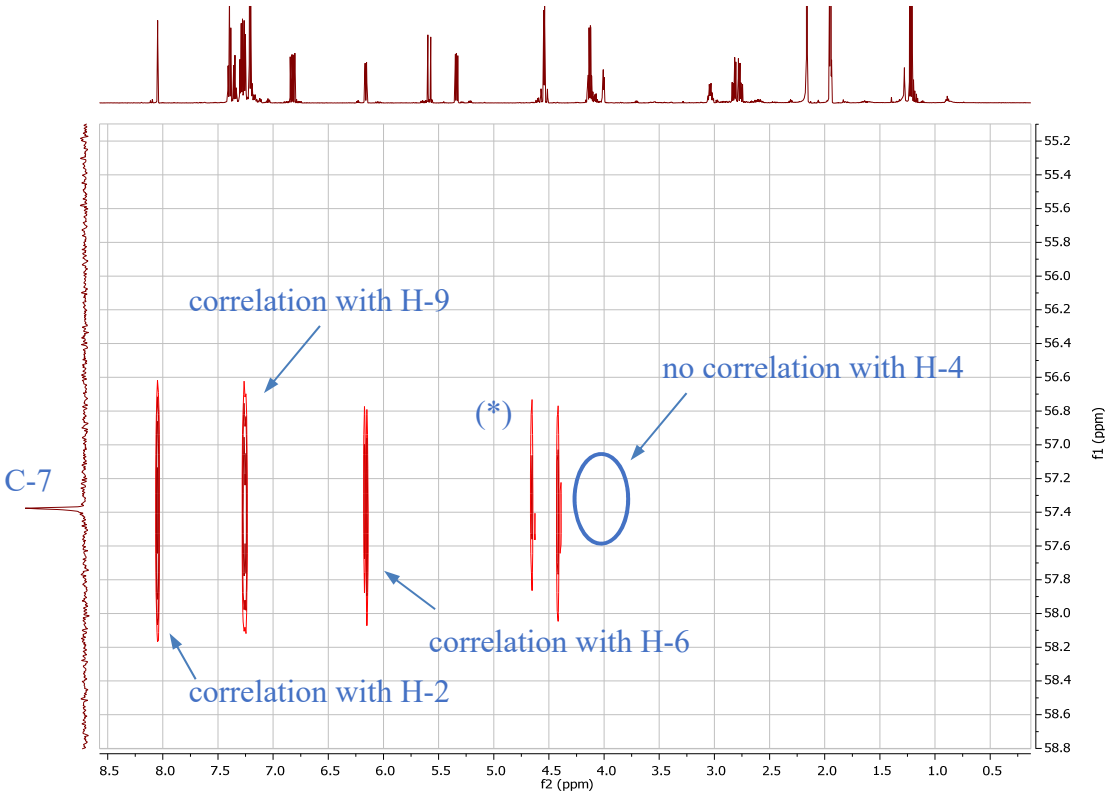

Figure 9. C-H Correlations of C-7 in the gHMBC spectrum of product ***anti* 5aa** in CD_3CN. (*) Indicates the unfiltered ^{1}J coupling constant.

These spectroscopic data indicate that the two isomers observed in the dearomatization reaction are diastereoisomers sharing the same regiochemistry, demonstrating that the process displays full C-4 regioselectivity.

Isomers *syn* and *anti* 5aa, relative configuration. The relative configurations of ***syn* 5aa** and ***anti* 5aa** were derived from NOE-NMR spectra.[88]

The NMR signal of H-5, H-4 and H-13 were selected for the NOE spectra of the major diastereoisomer. Saturation of H-5 (trace a in Figure 10) at 5.20 ppm shows that H-13 on the second stereogenic carbon is far away from H-5 (weak NOE), while H-14 is closer. At the same time, the two diastereotopic hydrogens of the CH_2 (H-12) have weak NOE with similar intensity. They are thus located far and at the same distance from H-5. When saturating H-4 at 4.05 ppm (trace b), the NOE signal of H-5 sets a "control" distance (i.e. a NOE that must be observed because of the chemical structure), and it is found that H-13 has the same distance from H-4. The smaller NOE observed on H-14 confirms that H-14 is on the same side of H-5. Again, the two weak and similar NOEs observed on the hydrogens of the CH_2 suggest that the two hydrogens are located far and at the same distance from H-4. On saturation of H-13 at 2.97 ppm (the second chiral center, trace c) the intense NOE observed on H-15 fixes the conformation of the α,β-unsaturated system. As a last information, the two coupling constants of H-13 with H-12a and H-12b are quite different, being 4.4 and 10.6 Hz. The latter values is typical of an *anti* conformation (dihedral angle between H-13 and H-12a close to 180°). This occurrence suggests that only a conformation of the benzyl group is populated. DFT calculation (B3LYP/6-31G(d) level) indeed suggested that the second-best conformation of the benzyl group is much higher in energy (1.80 kcal/mol) and it should not be populated.

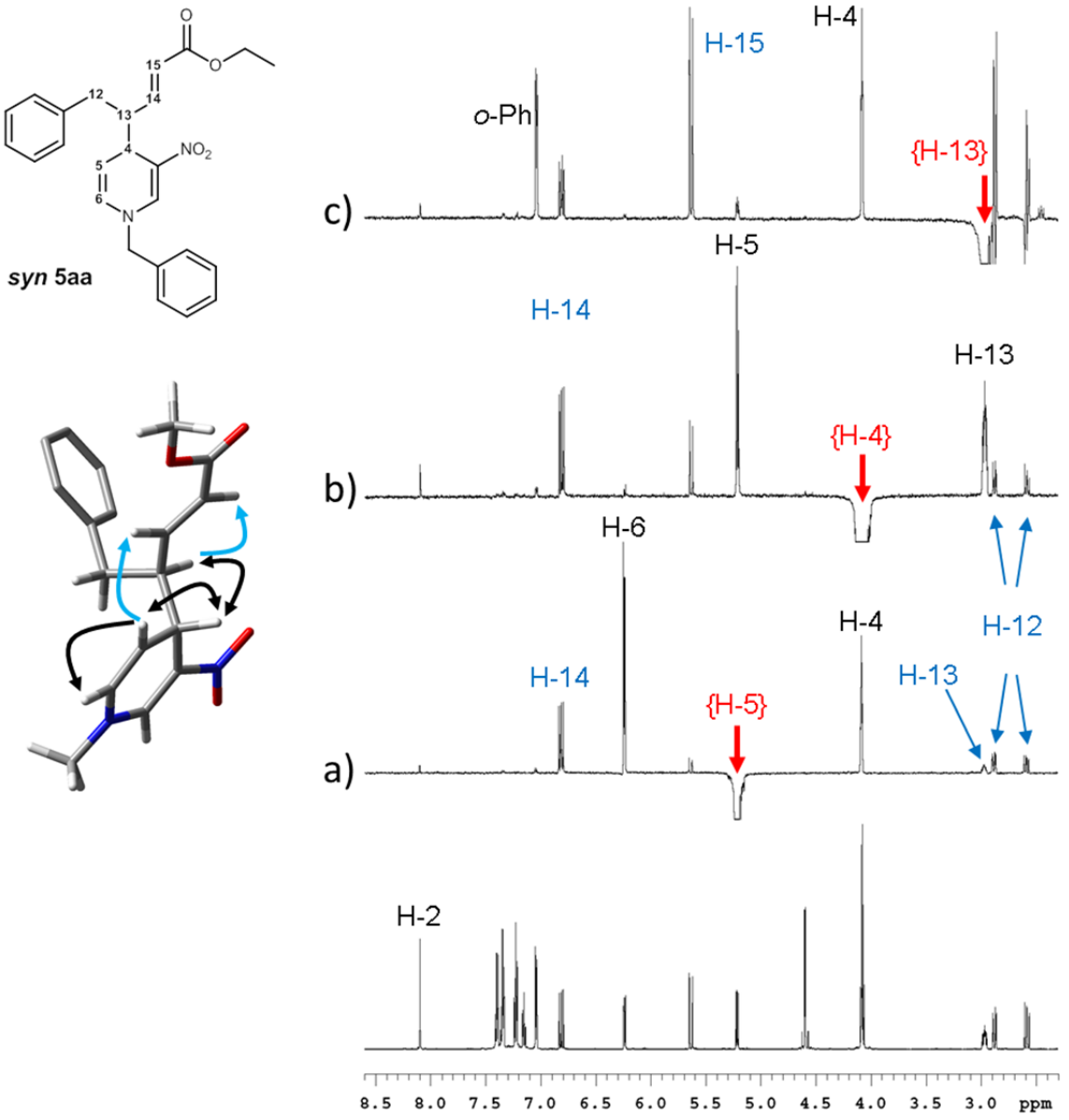

Figure 10. NOE spectra of compound **syn 5aa**. The bottom spectrum is the standard ^{1}H spectrum. Traces a-c show the NOE spectra on saturation of H-5, H-4 and H-13. The 3D structure on the left is for a model compound where the *N*-benzyl moiety has been replaced by a *N*-Me and the OEt moiety has been replaced by an OMe.

When the second diastereoisomer is considered, the saturation of H-5 at 5.32 ppm (trace a in Figure 11) yields a control NOE on H-4, a strong NOE on the two diastereotopic hydrogens of CH_2 (H-12a and H-12b) and a weak enhancement on H-14. As in the case of the major diastereoisomer, the NOE on H-13 is very weak. This suggests that in the second diastereoisomer H-13 is again far from the H-5 (thus close to the nitro group), but H-5 is close to the CH_2 and far from the α,β-unsaturated system. When H-4 (trace b) is saturated, the NOE observed on the CH_2 is similar to the control enhancement of H-5 and H-13, while the NOE on H-14 is weak. This again localizes the CH_2 close to H-5 and H-

4. The NOE obtained by saturation of H-13 (trace c) is similar to that of the major diastereoisomer, and it confirms the disposition of the α,β-unsaturated system with respect to H-13. At a variance with the major diastereoisomer, here the two vicinal coupling constants of the CH_2 are similar (6.8 and 8.7 Hz). This suggests the presence of two populated conformations of the benzyl group. After DFT optimization, two conformations were found to have the same energy, and they exchange the dihedral angle of the two diastereotopic hydrogens with H-13, thus explaining the similarity of the two coupling constants, that are due to conformational averaging.

The data obtained for the two diastereoisomers converge, when compared to the structures obtained through the DFT calculations, in the assignment of the *syn* configuration of the two vicinal chiral centers to the main diastereoisomer (***syn* 5aa**) and the *anti* to the second diastereoisomer (***anti* 5aa**).

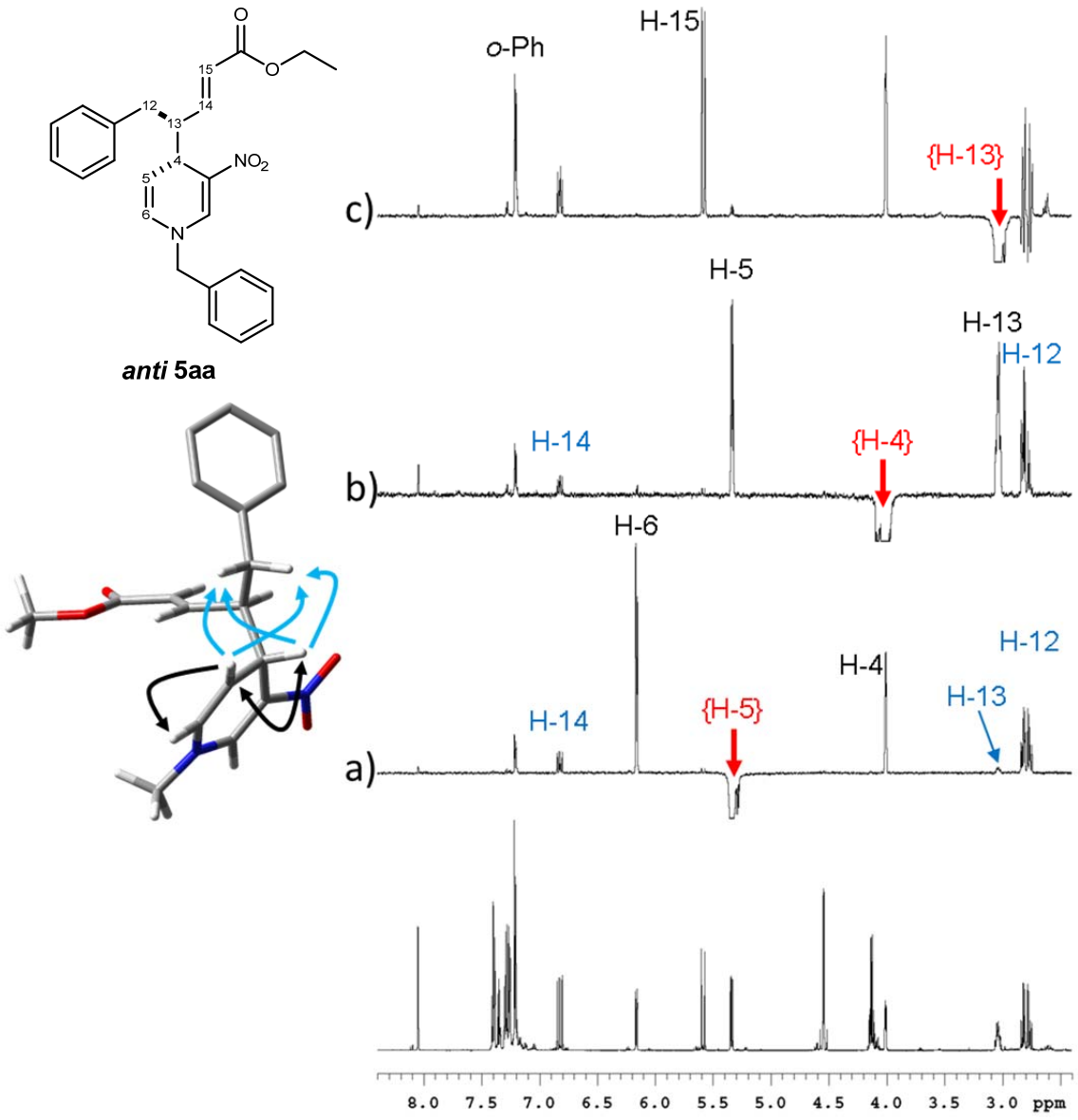

Figure 11. NOE spectra of the minor diastereoisomer of ***anti* 5aa**. The bottom spectrum is the standard ^{1}H spectrum. Traces a-c show the NOE spectra on saturation of H-5, H-4 and H-13. The 3D structure on the left is for a model compound where the *N*-benzyl moiety has been replaced by a *N*-Me and the OEt moiety has been replaced by an OMe.

4.3.2 Proposed reaction pathway

With both the relative and the absolute configuration of the major isomers in hand, a plausible catalytic cycle for the cascade reaction between salts **1** and aldehydes **2** was envisioned.

The high diastereoselectivity and the excellent enantioselectivity values shown by the reaction may be explained taking into account the transition state model invoked for the

conjugate additions of aldehydes to nitroolefins, catalyzed by **3a**. The relative and absolute configurations of the obtained products **4** (lately transformed into esters **5** or acetals **6**) are in fact in agreement with the ones reported for enantioenriched γ-nitroaldehydes. For simplicity, the acyclic synclinal transition state proposed by Seebach and Golinski[89] and invoked by Hayashi[33] in the first report of such additions (Scheme 15, top equation), is presented herein, applied to the present reaction (Scheme 15, bottom equation). Later on, many efforts have been done by different authors, to elucidate the catalytic cycle and the intermediates formed in this process.[34] At this stage of investigation, however, whether these features, derived more closely from the specific reactivity of the precise reaction partners, are applicable or not to our reaction, is not certain.

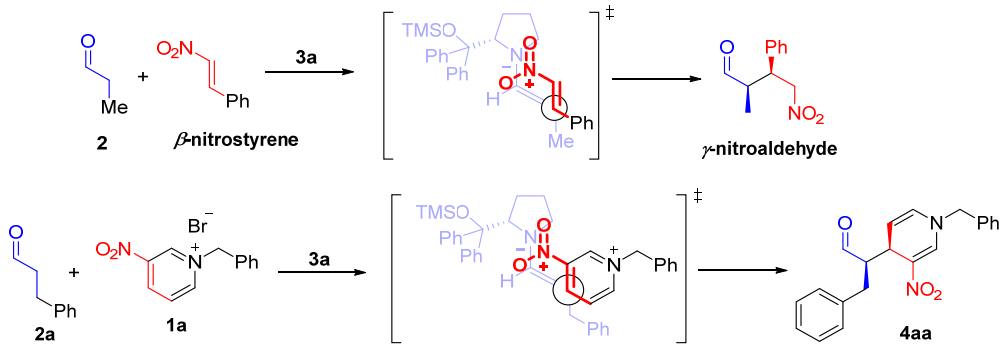

Scheme 15. Transition state models proposed by Hayashi (top line). Same transition state, proposed for the present reaction (bottom line).

Regarding the role of the acid in this reaction, irrespective of the intervention of cyclic intermediates in the catalytic cycle (e.g. cyclobutanes, oxazines, etc.), it should be noted that in the benchmark addition of aldehydes to nitroalkenes, protonation of a nitronate intermediate is necessary at some stage of the catalytic cycle.[85] The acidic additive is supposed to assist this step, which has indeed been proposed as the rate-determining step of the cycle (Scheme 16, top equation). In our case the electrophile is cationic, thus protonation is not required (Scheme 16, bottom equation).

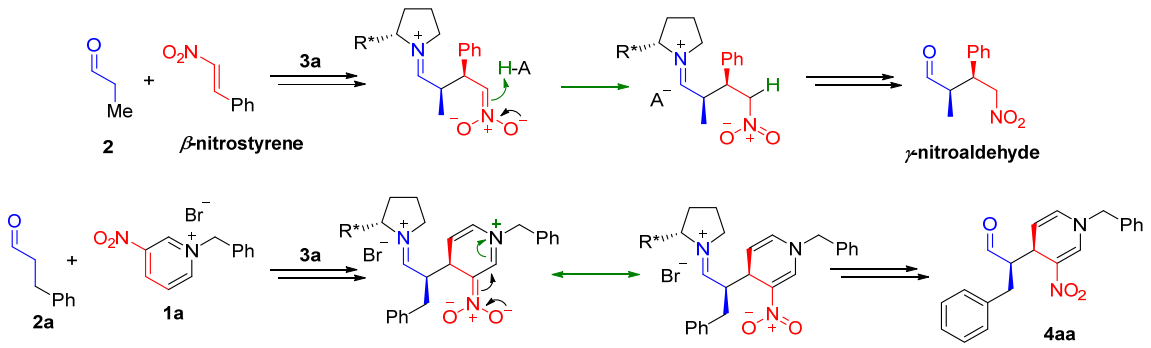

Scheme 16. Some intermediates of the benchmark (top) and present (bottom) reaction catalytic cycle (top). R* = CPh_2OTMS.

4.4 Conclusion

After the first organocatalytic enantioselective dearomatization of *N*-alkylpyridiniums was successfully developed, we sought to envision if other nucleophiles, requiring different activation modes, could be productively engaged in the same process. Our attention focused primarily on chiral enamines, generated catalytically from aldehydes **2** and enantiopure secondary amines **3**. In contrast with the large number of examples involving quinolinium and isoquinolinium salts dearomatization by chiral enamine catalyzed addition of aldehydes, pyridinium cations, more challenging substrates for dearomatization reactions, have not been employed so far in such processes. The first asymmetric addition of aldehydes **2** to pyridinium salts **1**, catalyzed by chiral secondary amines **3**, was therefore developed. The process furnished highly enantioenriched 1,4-dihydropyridines **4** (Scheme 17). The reaction conditions were carefully optimized until satisfactory results in terms of product stability, yield, diastereo- and enantioselectivity were reached. A short reaction time and a low temperature led to very good values of diastereoselectivity and enantioselectivity, when toluene was employed as the solvent. It was then found that an acidic co-catalyst (phenylacetic acid) led to better results in terms of enantiocontrol. Finally, to avoid small deviations from the primary outcomes of the reaction during isolation, we chose to transform the aldehyde group in products **4** into a less labile α,β-unsaturated ester (**5**) by Wittig reaction. The reaction scope was investigated and was found to be broad in terms of functional groups toleration on the aldehyde counterpart **2** and substitution pattern on the pyridinium ring **1**. Moreover, both $–NO_2$ and –CN moieties were found to be suitable activating groups for the present

dearomatization. Furthermore, the aldehyde and nitro functions of products **4** could be exploited for further manipulations. For example, cyclization processes rendered synthetically challenging bicyclic motives related to octahydropyrrolo[2,3-*c*]pyridines, core structures of anticancer peptidomimetics. Employing the previously described dearomatization, starting from *N*-benzyl-3-nitropyridinium bromide and 3-phenylpropionaldehyde, this scaffold was built in a 7-steps sequence, leading to product **10**, bearing three contiguous stereocenters, isolated as single diastereoisomer in 95% ee.

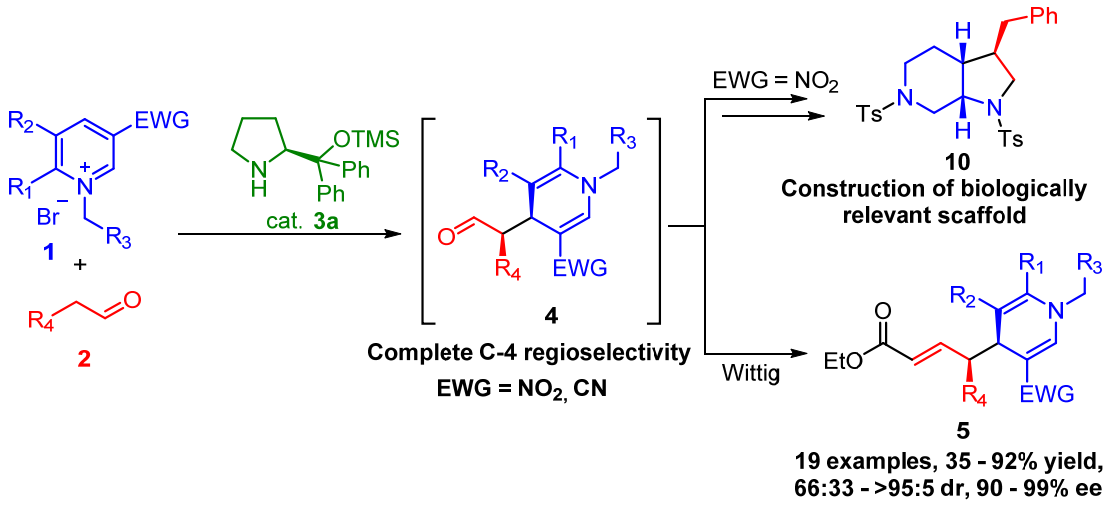

Scheme 17. Organocatalytic enantioselective *N*-alkyl pyridinium salts dearomatization with chiral enamines: summary of the project.

4.5 Experimental details

4.5.1 General methods and materials

General Methods. ^{1}H and ^{13}C NMR spectra were recorded on a Varian Inova 300, Mercury 400 or Inova 600 spectrometer. Chemical shifts (δ) are reported in ppm relative to residual solvents signals for ^{1}H and ^{13}C NMR. ^{13}C NMR were acquired with ^{1}H broad-band decoupled mode. Chromatographic purifications were performed using 70-230 mesh silica. Mass spectra were recorded on a Waters Xevo Q-TOF spectrometer. Optical rotations were measured on a Perkin Elmer 241 Polarimeter provided with a sodium lamp and are reported as follows: $[\alpha]_{\lambda}^{T\ (°C)}$ (c = g/100 mL, solvent). IR spectra were recorded on an Agilent Cary 630 FTIR spectrometer. Melting points were measured on a Stuart Scientific melting point apparatus SMP3 and are not corrected. The enantiomeric excess of the products (ee) were determined by chiral stationary phase HPLC (Daicel Chiralpak AD-H or AS columns), using an UV detector operating at 254 nm. Below the general procedures, the characterization of the model compound only is reported. For a full description of all the products reported see the Supporting Information of *Org. Lett.* **2017**, *19*, 834.

Materials. Analytical grade solvents and commercially available reagents were used as received, unless otherwise stated. Pyridinium salts **1a-j** were synthesized from 3-nitropyridine or 3-cyanopyridines and the respective benzyl bromides (4-methoxybenzyl bromide was prepared according to a literature procedure). Catalyst **3a** was purchased from Sigma Aldrich and used as received. Commercially available aldehydes **2**: **2a** was purified by column chromatography on silica gel (CH_2Cl_2) prior to use; **2b** was distilled and dried over $MgSO_4$ prior to use; **2c**, **2d** and **2g** were used as received. Aldehydes **2e**, **2f** and **2j** were prepared by oxidation of the corresponding commercially available alcohols with PCC (pyridinium chlorochromate) in CH_2Cl_2. Aldehydes **2g** and **2h** were prepared adapting a literature procedure as previously reported. Racemic products **5** and **6** were prepared following **general procedure A** or **B** (*vide infra*) employing racemic catalyst **3a**. Racemic product **7** was prepared from racemic **6aa** and racemic **10** from racemic **7** following the same procedures reported for the enantioenriched products (*vide infra*).

4.5.2 General procedures

General procedure A (to obtain Wittig products **5**)**.** In a test tube equipped with a magnetic stirring bar, a 0.02 M solution of catalyst **3a** in toluene (3.2 mg, 0.01 mmol, 10 mol % in 500 µL) was added to pyridinium salt **1** (0.10 mmol), followed by Et_3N (13.4 µL, 0.10 mmol, 1 equiv) and a 0.5 M solution of phenylacetic acid in toluene (1.4 mg, 0.01 mmol, 10 mol % in 20 µL). The resulting suspension was stirred at the desired

temperature for 2 minutes, after which aldehyde **2** (0.2 mmol, 2 equiv) was added in one portion and the reaction mixture was stirred for 1 h or 2 h. Hereafter, ethyl (triphenylphosphoranilidene)acetate (0.6 mmol, 209 mg) was added and the reaction was stirred at the same temperature of the previous step for 10 minutes, at 0 °C for 1 h and at room temperature for 2 h. To this suspension, CH_2Cl_2 (500 μL) was added and the resulting solution[90] was directly purified by column chromatography on silica gel (*n*-hexane/EtOAc mixtures) to afford the desired products **5**. Finally, the enantiomeric excess was determined by chiral stationary phase HPLC (*n*-hexane/*i*-PrOH mixtures).

Ethyl (*S*,*E*)-4-((*S*)-1-benzyl-3-nitro-1,4-dihydropyridin-4-yl)-5-phenylpent-2-enoate (5aa)

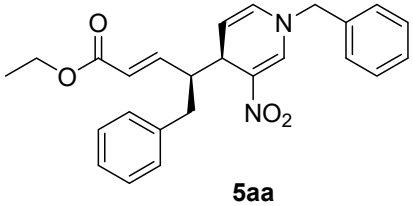

5aa

Following **general procedure A** (T = -30 °C, t = 1 h), from *N*-benzyl-3-nitropyridinium bromide (**1a**) and 3-phenylpropanal (**2a**), product **5aa** was obtained as a yellow sticky oil in 86% yield (35.9 mg) after column chromatography on silica gel (*n*-hexane/EtOAc = 4.5:1). Diastereoisomeric ratio was evaluated from the ^{1}H NMR spectrum of the crude mixture and was found to be 93:7 (>95:5 after column chromatography). The enantiomeric excess of **5aa** was determined by chiral stationary phase HPLC (AD-H, *n*-hexane/*i*-PrOH 80:20, 0.75 mL/min, λ = 254 nm, t_{maj} = 26.4 min, t_{min} = 17.7 min, 99% *ee*). $[\alpha]_D^{25\ °C}$ = +417 (c = 0.44, $CHCl_3$); ^{1}H NMR ($CDCl_3$, 400 MHz) δ = 7.96 (dd, J_1 = 1.5 Hz, J_2 = 0.8 Hz, 1H), 7.42-7.33 (m, 3H), 7.24-7.20 (m, 4H), 7.17-7.12 (m, 1H), 7.04-7.01 (m, 2H), 6.87 (dd, J_1 = 15.7 Hz, J_2 = 8.4 Hz, 1H), 6.07 (dt, J_1 = 7.9 Hz, J_2 = 1.1 Hz, 1H), 5.76 (dd; J_1 = 15.8 Hz, J_2 = 1.2 Hz, 1H), 5.14 (dd, J_1 = 7.9 Hz, J_2 = 5.1 Hz, 1H), 4.49 (s, 2H), 4.18-4.15 (m, 1H), 4.13 (q, J = 7.2 Hz, 2H), 3.20-3.13 (m, 1H), 2.85 (dd, J_1 = 14.0 Hz, J_2 = 4.3 Hz, 1H), 2.61 (dd, J_1 = 14.1 Hz, J_2 = 10.7 Hz, 1H), 1.25 (t, J = 7.2 Hz, 3H) ppm; ^{13}C NMR ($CDCl_3$, 100 MHz) δ = 166.2, 148.2, 140.9, 139.4, 134.8, 129.3, 128.80, 128.76, 128.6, 128.3, 127.5, 126.1, 123.4, 123.2, 109.3, 60.3, 58.5, 45.9, 39.0, 35.7, 14.2 ppm; HRMS(ESI): calcd. for $C_{25}H_{26}N_2O_4Na$ ($M + Na^+$): 441.1790; found: 441.1790; IR (neat) ν = 1708, 1665, 1582, 1477, 1265, 1175 cm^{-1}.

General procedure B (to obtain acetals **6**)**.** In a test tube equipped with a magnetic stirring bar, a 0.02 M solution of catalyst **3a** in toluene (3.2 mg, 0.01 mmol, 10 mol % in 500 μL) was added to pyridinium salt **1** (0.10 mmol), followed by Et_3N (13.4 μL, 0.10 mmol, 1 equiv) and a 0.5 M solution of phenylacetic acid in toluene (1.4 mg, 0.01 mmol, 10 mol % in 20 μL). The resulting suspension was stirred at the desired temperature for 2 minutes, after which aldehyde **2** (0.2 mmol, 2 equiv) was added in one portion and the reaction mixture was stirred for 1 h or 2 h. Hereafter, CH_2Cl_2 was added (5 mL) and the **cold** solution was **rapidly** filtered through a short plug of silica gel; the plug was washed with cold CH_2Cl_2 and cold Et_2O (3x). After careful removal of the solvents *in vacuo* (water bath temperature below 10 °C) the residue was cooled to 0 °C and treated with

$HC(OMe)_3$ (110 μL, 1.0 mmol) and a 0.06 M solution of *p*-TSA or (*rac*)-CSA in methanol (0.015 mmol, 15 mol % in 250 μL). The reaction was then stirred at 0 °C for 1 h and at room temperature for 1 h. After removal of the solvents *in vacuo*, the residue was analysed by ^{1}H NMR spectroscopy to determine the diastereomeric ratio of the reaction, and purified by column chromatography on silica gel (*n*-hexane/EtOAc mixtures) to afford the desired products **6.** Finally, the enantiomeric excess was determined by chiral stationary phase HPLC (*n*-hexane/*i*-PrOH mixtures).

(*R*)-1-Benzyl-4-((*R*)-1,1-dimethoxy-3-methylbutan-2-yl)-3-nitro-1,4-dihydropyridine (6ag)

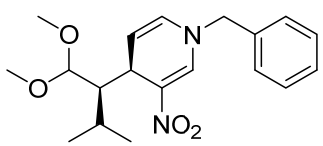

6ag

Following **general procedure B** (T = **0** °C, t = 2 h), from *N*-benzyl-3-nitropyridinium bromide (**1a**) and isovaleraldehyde (**2g**), product **6ag** was obtained as a yellow sticky oil in 43% yield (14.9 mg) after column chromatography on silica gel (*n*-hexane/EtOAc = 6.5:1). Diastereoisomeric ratio was evaluated from the ^{1}H NMR spectrum of the crude mixture and was found to be 95:5 (>95:5 after column chromatography). The enantiomeric excess of **6ag** was determined by chiral stationary phase HPLC (AS, *n*-hexane/*i*-PrOH 70:30, 0.75 mL/min, λ = 254 nm, t_{maj} = 9.1 min, t_{min} = 23.4 min, 94% *ee*). $[\alpha]_D^{25\ °C}$ = +415 (c = 0.33, $CHCl_3$); ^{1}H NMR ($CDCl_3$, 400 MHz) δ = 8.01 (d, J = 1.0 Hz, 1H), 7.42-7.33 (m, 3H), 7.28-7.26 (m, 2H), 5.91 (dt, J_1 = 8.1 Hz, J_2 = 1.1 Hz, 1H), 5.12 (dd, J_1 = 8.0 Hz, J_2 = 5.1 Hz, 1H), 4.48 (s, 2H), 4.36 (d, J = 7.6 Hz, 1H), 4.08 (bd, J = 5.1 Hz, 1H), 3.17 (s, 3H), 3.15 (s, 3H), 2.10-1.93 (m, 1H), 1.86 (ddd, J_1 = 7.5 Hz, J_2 = 4.2 Hz, J_3 = 1.4 Hz, 1H), 1.09 (d, J = 7.1 Hz, 3H), 0.96 (d, J = 7.0 Hz, 3H) ppm; ^{13}C NMR ($CDCl_3$, 100 MHz) δ = 140.8, 135.1, 129.2, 128.7, 127.7, 127.0, 126.1, 112.2, 105.8, 58.4, 53.7, 52.3, 47.8, 32.3, 27.0, 21.2, 20.0 ppm; HRMS(ESI): calcd. for $C_{19}H_{26}N_2O_4Na$ ($M + Na^+$): 369.1791; found: 369.1792; IR (neat) ν = 2960, 2927, 1655, 1578, 1259, 1177, 1065 cm^{-1}.

Isomer *anti* 5aa. In a test tube equipped with a magnetic stirring bar, a 0.02 M solution of catalyst **3a** in toluene (3.2 mg, 0.01 mmol, 10 mol% in 500 μL) was added to pyridinium salt **1a** (0.10 mmol), followed by $NaHCO_3$ (25.2 mg, 0.30 mmol, 3 equiv) and a 0.5 M solution of phenylacetic acid in toluene (1.4 mg, 0.01 mmol, 10 mol% in 20 μL). The resulting suspension was stirred at room temperature for 2 minutes, after which 3-phenylpropanal **2a** (0.2 mmol, 2 equiv) was added in one portion and the reaction mixture was stirred for 18 h.

Hereafter, CH_2Cl_2 was added (5 mL) and the solution was filtered through a short plug of silica gel; the plug was washed with CH_2Cl_2 and Et_2O (3x). After removal of the solvents *in vacuo*, the residue (containing ***syn* 5aa** and ***anti* 5aa** in 1:1 ratio) was dissolved in toluene and treated with ethyl (triphenylphosphoranilidene)acetate (209 mg, 0.6 mmol). The reaction was then stirred at room temperature for 2 h. To this suspension, CH_2Cl_2 (500 μL) was added and the resulting solution was directly purified by column

chromatography on silica gel (*n*-hexane/EtOAc 5:1) to separate the two diastereoisomers (R_f of ***anti* 5aa** > R_f of ***syn* 5aa**). Product ***anti* 5aa** was obtained as a yellow sticky oil in 25% yield (10.5 mg).

Ethyl (*S*,*E*)-4-((*R*)-1-benzyl-3-nitro-1,4-dihydropyridin-4-yl)-5-phenylpent-2-enoate (*anti* 5aa)

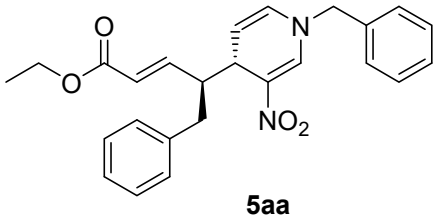

5aa

^{1}H NMR (CD_3CN, 600 MHz) δ = 8.05 (s, 1H), 7.4-7.37 (m, 2H), 7.37-7.32 (m, 1H), 7.31-7.24 (m, 4H), 7.24-7.18 (m, 3H), 6.82 (dd, J_1 = 15.6 Hz, J_2 = 9.8 Hz, 1H), 6.16 (dt, J_1 = 8.0 Hz, J_2 = 1.2 Hz, 1H), 5.58 (dd, J_1 = 15.6 Hz, J_2 = 0.9 Hz, 1H), 5.34 (dd, J_1 = 8.0 Hz, J_2 = 5.3 Hz, 1H), 4.56 (d, J = 15.4 Hz, 1H), 4.53 (d, J = 15.4 Hz, 1H), 4.16-4.10 (m, 2H), 4.01 (ddt, J_1 = 5.2 Hz, J_2 = 3.2 Hz, J_3 = 1.0 Hz, 1H), 3.11-2.99 (m, 1H), 2.82 (dd, J_1 = 13.9 Hz, J_2 = 6.9 Hz, 1H), 2.76 (dd, J_1 = 13.9 Hz, J_2 = 8.8 Hz, 1H), 1.22 (t, J = 7.1 Hz, 3H).; ^{13}C NMR (CD_3CN, 150 MHz) δ = 165.5, 149.4, 141.3, 139.5, 136.0, 129.2, 129.0, 128.9, 128.3, 128.1, 127.6, 126.2, 123.6, 123.2, 107.6, 60.0, 57.4, 46.3, 37.4, 35.7, 13.5 ppm.

4.5.3 Preparation of (3R,3aR,7aS)-3-benzyl-1,6-ditosyloctahydro-1H-pyrrolo[2,3-c]pyridine (10)

(*R*)-1-benzyl-4-((*R*)-1,1-dimethoxy-3-phenylpropan-2-yl)-3-nitro-1,4-dihydro pyridine (6aa)

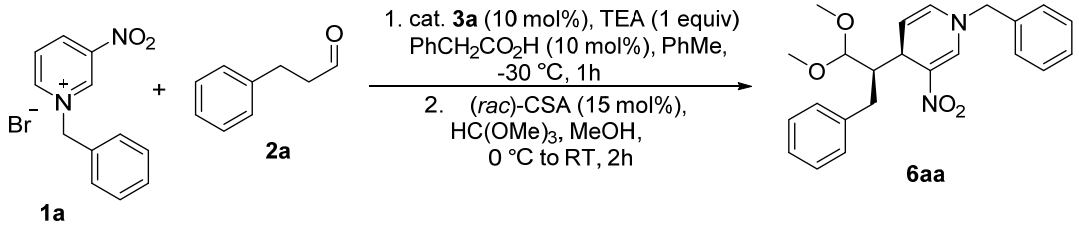

1a **2a** **6aa**

Compound **6aa** was prepared following **general procedure B** (scaled for 0.33 mmol of substrate **1a**, T = -30 °C, t = 1 h, CSA as acid in the acetalization step) from *N*-benzyl-3-nitropyridinium bromide (**1a**) and 3-phenylpropanal (**2a**), product **6aa** was obtained as a yellow sticky oil in 75% yield (0.25 mmol, 97.6 mg) after column chromatography on silica gel (*n*-hexane/EtOAc = 4.5:1). Diastereoisomeric ratio was evaluated from the ^{1}H NMR spectrum of the crude mixture and was found to be 95:5 (>95:5 after column chromatography). The enantiomeric excess of **6aa** was determined by chiral stationary phase HPLC (AD-H, *n*-hexane/i-PrOH 80:20, 0.75 mL/min, λ = 254 nm, t_{maj} = 18.8 min, t_{min} = 10.9 min, 95% ee). $[\alpha]_D^{25\ °C}$ = +479 (c = 0.53, $CHCl_3$); ^{1}H NMR ($CDCl_3$, 400 MHz) δ = 7.75 (dd, J_1 = 1.4 Hz, J_2 = 0.5 Hz, 1H), 7.40-7.30 (m, 3H), 7.25-7.18 (m, 4H), 7.17-7.12 (m, 1H), 7.10-7.05 (m, 2H), 5.95 (dt, J_1 = 8.1 Hz, J_2 = 1.3 Hz, 1H), 5.28 (dd, J_1 = 8.1 Hz, J_2 = 1.3 Hz, 1H), 4.41 (d, J = 15.1 Hz, 1H), 4.36 (d, J = 15.1 Hz, 1H), 4.37-4.32 (m,

1H), 4.10 (d, J = 4.8 Hz, 1H), 3.35 (s, 3H), 3.31 (s, 3H), 2.82-2.60 (m, 3H) ppm; ^{13}C NMR ($CDCl_3$, 100 MHz) δ = 141.0, 140.8, 134.9, 129.2, 128.7, 128.6, 128.1, 127.5, 127.4, 125.8, 124.0, 112.0, 106.4, 58.3, 54.8, 54.5, 43.2, 33.7, 33.0 ppm; HRMS(ESI): calcd. for $C_{23}H_{26}N_2O_4Na$ (M + Na^+): 417.1791; found: 417.1790; IR (neat) ν = 2930, 2831, 1667, 1583, 1474, 1265, 1174 cm^{-1}.

(3S,4R)-1-benzyl-4-((R)-1,1-dimethoxy-3-phenylpropan-2-yl)-3-nitropiperidine (7)

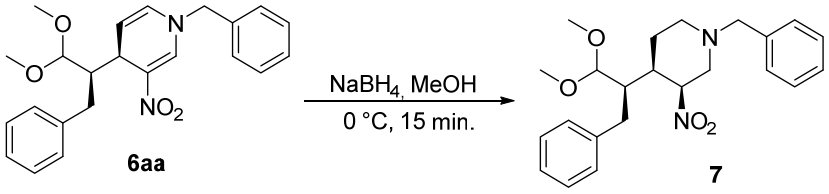

In a small vial equipped with a magnetic stirring bar, compound **6aa** (97.6 mg, 0.25 mmol, 95% ee) was dissolved in MeOH (2 mL) and the resulting solution was cooled to 0 °C. Then, $NaBH_4$ was added in small portions until complete conversion was reached, as judged by TLC analysis (ca. 67 mg, 1.75 mmol). Hereafter, a saturated solution of NH_4Cl (10 mL) and CH_2Cl_2 (10 mL) were added, and the organic layer separated, washed again with a saturated solution of NH_4Cl (5 mL), dried over $MgSO_4$, filtered and evaporated in vacuo. Diastereoisomeric ratio was evaluated from the ^{1}H NMR spectrum of this crude mixture and was found to be >95:5. The residue was then purified by column chromatography on silica gel (*n*-hexane/EtOAc 9:1) to afford compound **7** (single diastereoisomer) as a colorless wax in 80% yield (0.20 mmol, 78.9 mg). The newly formed stereocenter was found to be in an 1,2-*cis* relationship with the contiguous one, assigned by consistency with the absolute configuration of product **10** (*vide infra*). The enantiomeric excess of **7** was determined by chiral stationary phase HPLC (AD-H, *n*-hexane/*i*-PrOH 80:20, 0.75 mL/min, λ = 254 nm, t_{maj} = 8.3 min, t_{min} = 6.2 min, 95% *ee*). $[\alpha]_D^{25\ °C}$ = +2 (c = 1.5, $CHCl_3$); ^{1}H NMR ($CDCl_3$, 400 MHz) δ = 7.33-7.27 (m, 4H), 7.25-7.20 (m, 4H), 7.19-7.14 (m, 2H), 5.16-4.99 (m, 1H), 3.85 (d, J = 1.2 Hz, 1H), 3.59-3.44 (m, 3H), 3.32 (s, 3H), 3.00 (s, 3H) overlapped with 3.10-2.91 (m, 2H), 2.52-2.22 (m, 4H), 2.08 (ddd, J_1 = 12.2 Hz, J_2 = 11.2 Hz, J_3 = 3.0 Hz, 1H), 1.85 (ddt, J_1 = 16.0 Hz, J_2 = 8.5 Hz, J_3 = 3.8 Hz, 1H), 1.81-1.73 (m, 1H) ppm; ^{13}C NMR ($CDCl_3$, 100 MHz) δ = 140.3, 137.7, 128.9, 128.6, 128.5, 128.2, 127.1, 126.1, 107.5, 83.5, 62.1, 57.7, 56.7, 55.4, 53.7, 42.7, 38.0, 35.6, 25.2 ppm; HRMS(ESI): calcd. for $C_{23}H_{31}N_2O_4$ (M + H^+): 399.2284; found: 399.2284; IR (neat) ν = 2981, 1537, 1074 cm^{-1}.

(3*R*,3a*R*,7a*S*)-3-benzyl-1,6-ditosyloctahydro-1H-pyrrolo[2,3-c]pyridine (10)

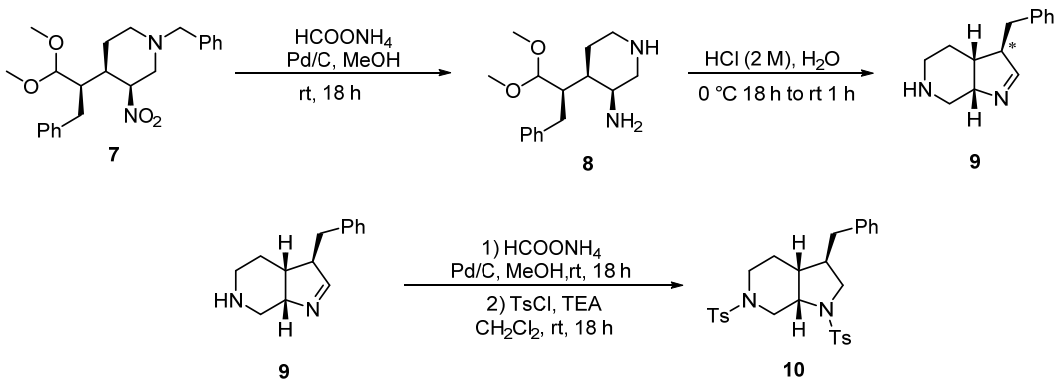

In a small vial equipped with a magnetic stirring bar, to a suspension of compound **7** (46.0 mg, 0.12 mmol, 95% *ee*) in MeOH (1.0 mL) ammonium formate (78 mg, 1.2 mmol, 10 equiv) and Pd/C 10% wt. (40.5 mg) were subsequently added. The resulting mixture was stirred at room temperature for 18 h, diluted with CH_2Cl_2 (5 mL) and filtered through a short plug of Celite. The solvents were removed *in vacuo* to afford product **8**.

Crude **8** was dissolved in a 2 M solution of HCl in water (250 µL) and stirred at 0 °C for 18 h and at room temperature for 1 h. Then, CH_2Cl_2 (5 mL) was added, followed by water (5 mL) and a saturated solution of Na_2CO_3 (until pH 12 was reached). The organic phase was then separated, the aqueous phase was back extracted with CH_2Cl_2 (2x), the collected organic phases were washed with brine, dried over $MgSO_4$, filtered and evaporated *in vacuo* to afford product **9**. ^{1}HNMR of the crude mixture revealed that, under these reaction conditions, minimum epimerization occurred at the carbon α to the imine (*): the diastereoisomeric ratio of **9** was found to be 93:7. Substantial epimerization of the imine α stereocenter was instead observed during preliminary attempts, caused by slow thermodynamic equilibration of product **8** in the acidic reaction medium (66:33 dr at 70 °C for 20 minutes or at RT for 18 h).

Crude **9** was dissolved in MeOH (1.0 mL) and to this solution ammonium formate (78 mg, 1.2 mmol, 10 equiv) and Pd/C 10% wt. (40.5 mg) were subsequently added. The resulting mixture was stirred at room temperature for 18 h, diluted with CH_2Cl_2 (5 mL) and filtered through a short plug of Celite. The solvents were removed *in vacuo*. The residue was then dissolved in CH_2Cl_2 (600 µL), TEA (55 µL, 0.48 mmol) and TsCl (64 mg, 0.36 mmol) were added in this order and the resulting mixture was stirred at room temperature for 18 h. The crude solution was directly purified by column chromatography on silica gel (CH_2Cl_2) to afford compound **10** (single diastereoisomer) as a white solid in 30% yield (19.0 mg) after 4 steps. The enantiomeric excess of **10** was determined by chiral stationary phase HPLC (AD-H, *n*-hexane/*i*-PrOH 70:30, 1.00 mL/min, λ = 254 nm, t_{maj} = 20.4 min, t_{min} = 30.9 min, 95% *ee*). $[\alpha]_D^{25\ °C}$ = +4.5 (c = 0.36, $CHCl_3$); ^{1}H NMR ($CDCl_3$, 400 MHz) δ = 7.71-7.67 (m, 2H), 7.67-7.63 (m, 2H), 7.37-7.28 (m, 4H), 7.25-7.16 (m, 3H), 7.01-6.95 (m, 2H), 3.96-3.78 (m, 2H), 3.55-3.41 (m, 1H), 3.39 (dd, J_1 = 9.8 Hz, J_2 = 6.6 Hz, 1H), 2.78 (dd, J_1 = 9.7 Hz, J_2 = 8.8 Hz, 1H), 2.70-

2.58 (m, 1H), 2.45 (s, 3H), 2.44 (s, 3H), 2.43-2.30 (m, 2H), 2.29-2.14 (m, 2H), 1.86 (ddt, J_1 = 14.4 Hz, J_2 = 11.2 Hz, J_3 = 5.4 Hz, 1H), 1.64 (dq, J_1 = 14.5 Hz, J_2 = 3.4 Hz, 1H), 1.57-1.48 (m, 1H) ppm; ^{13}C NMR ($CDCl_3$, 100 MHz) δ = 143.7 (C), 143.6 (C), 138.6 (C), 134.3 (C), 133.4 (C), 129.81 (CH), 129.78 (CH), 128.6 (CH), 128.5 (CH), 127.7 (CH), 127.4 (CH), 126.6 (CH), 57.1 (CH), 52.9 (CH_2), 48.4 (CH_2), 42.1 (CH_2), 40.3 (CH), 39.5 (CH), 37.4 (CH_2), 23.7 (CH_2), 21.57 (CH_3), 21.55 (CH_3) ppm; HRMS(ESI): calcd. for $C_{28}H_{32}N_2O_4S_2Na$ ($M + Na^+$): 547.1701; found: 547.1701; IR (neat) ν = 2981, 1343, 1160 cm^{-1}.

Slow evaporation of a diluted $CHCl_3$ solution afforded enantiopure single crystals (m.p. = 123-125 °C of $CHCl_3$ solvate crystals) suitable for X-rays analysis.

4.5.4 Crystal structure of compound 10

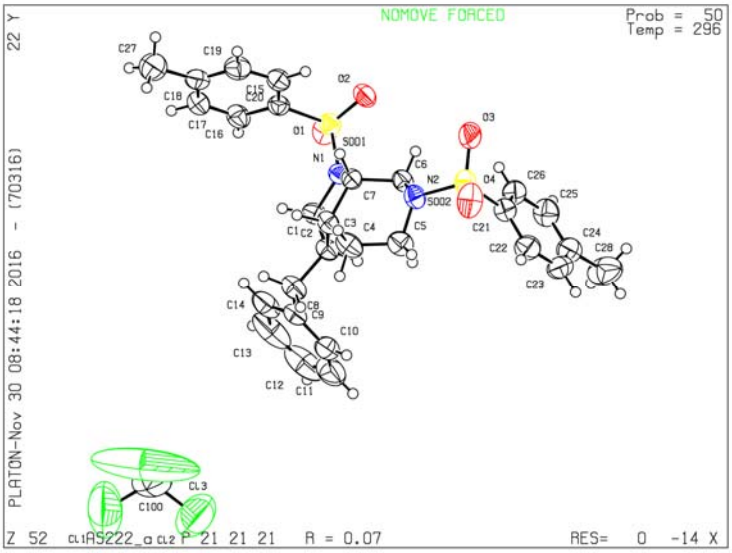

Molecular formula: $C_{28}H_{32}N_2O_4S_2{\cdot}CHCL_3$; M_r = 644.04, orthorhombic, space group $P2_12_12_1$, a = 10.6471(8), b = 17.0945(12), c = 17.2371(12) Å, V = 3137.3(9) Å^3, T = 298(2) K, Z = 4, ρ_c = 1.364 g cm^{-3}, F(000) = 1344, graphite-monochromated $Mo_{K\alpha}$ radiation (λ = 0.71073 Å), μ($Mo_{K\alpha}$) = 0.462 mm^{-1}, colourless brick (0.35 × 0.30 × 0.12 mm^3), empirical absorption correction with SADABS (transmission factors: 0.851 – 0.945), 2400 frames, exposure time 30 s, 1.678 ≤ θ ≤ 26.00, –13≤ h ≤ 13, –21 ≤ k ≤ 21, –21 ≤ l ≤ 21, 40258 reflections collected, 6130 independent reflections (R_{int} = 0.0250), solution by intrinsic phasing method and subsequent Fourier syntheses, full-matrix least-squares on F_o^2 (SHELXL-2014/7), hydrogen atoms refined with a riding model, data / restraints / parameters = 6130/ 0/ 363, $S(F^2)$ = 1.075, $R(F)$ = 0.0773 and $wR(F^2)$ = 0.2165 on all data, $R(F)$ = 0.0735 and $wR(F^2)$ = 0.2111 for 5721 reflections with $I > 4\sigma$ (I), weighting scheme $w = 1/[\sigma^2(F_o^2) + (0.1458P)^2 + 2.0539P]$ where $P = (F_o^2 + 2F_c^2)/3$, largest difference peak and hole 0.947 and –0.822 e Å^{-3}. Flack parameter for 2R, 3R, 7S

configuration = 0.047(11) using 2350 quotients. The unit cell contains a disordered molecule of $CHCl_3$. Crystallographic data have been deposited with the Cambridge Crystallographic Data Centre as supplementary publication no. CCDC-1522977. Copies of the data can be obtained free of charge on application to CCDC, 12 Union Road, Cambridge CB21EZ, UK (fax: (+44) 1223-336-033; e-mail: deposit@ccdc.cam.ac.uk).

5 Organocatalytic enantioselective direct α-heteroarylation of aldehydes with isoquinoline *N*-oxides

The procedures and results here described are part of- and can be found in-:

- G. Bertuzzi, D. Pecorari, L. Bernardi, M. Fochi "An organocatalytic enantioselective direct α-heteroarylation of aldehydes with isoquinoline *N*-oxides" *Chem. Commun.* **2018**, *54*, 3977.

ABSTRACT

A new protocol for the enantioselective direct α-heteroarylation of aldehydes with isoquinoline *N*-oxides, *via* chiral enamine catalysis, has been successfully developed. High enantiomeric excesses and moderate to good yields were achieved for a variety of a-heteroarylated aldehydes. The employment of a strictly oxophilic chemoselective activator of the *N*-oxide moiety was the key feature to achieve an efficient methodology.

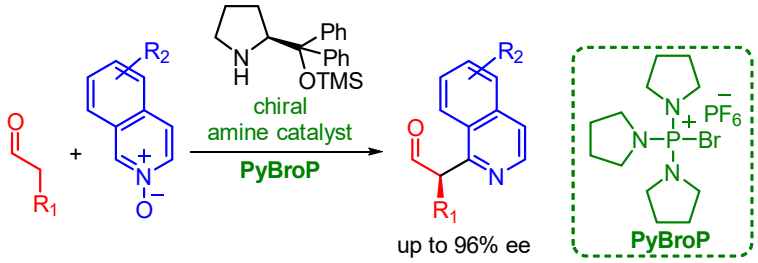

5.1 Background

As part of our interest in the employment of azine electrophiles in new organocatalytic enantioselective reactions, we moved from *N*-alkyl pyridinium salts, displaying a dearomatization chemistry, to another class of compounds, namely azine *N*-oxides. These scaffolds are nucleophilic in nature thanks to the delocalization of the negative charge of the oxygen atom into the aromatic ring (Scheme 1, red path). They are indeed employed in nucleophilic aromatic substitutions, difficult to perform on the otherwise unactivated heterocycle. C-4 regioselective nitration of pyridine relies indeed on this strategy. On the other hand, if the oxygen atom reacts first with an electrophilic activator, the heterocycle becomes cationic and electrophilic, prone to undergo nucleophilic additions and temporary loss of aromaticity.[36] Nonetheless, this activation of the oxygen usually turns it into a good leaving group, undergoing elimination and, at the same time,

rearomatization of the system. An equivalent of a strong mineral acid is usually formed during this process and a base is thus required as a scavenger. The *N*-oxide moiety is now lost and the reaction results in the heteroarylation of the nucleophile (Scheme 1, blue path).

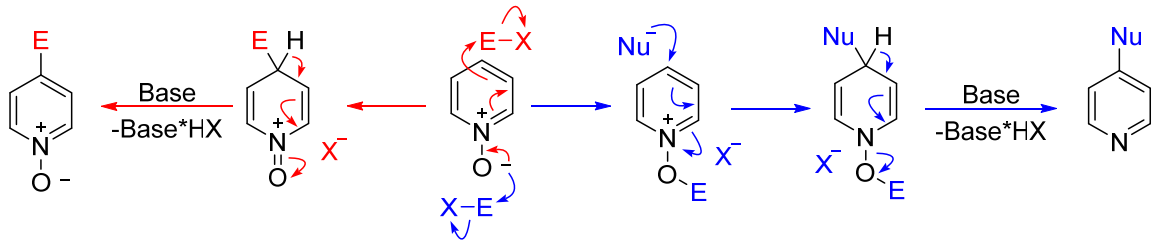

Scheme 1. Nucleophilic and electrophilic nature of azine *N*-oxides.

This is a fascinating procedure, posing a valid alternative to classical arylations, such as metal catalyzed cross-couplings that usually require the installation of a leaving group on the desired carbon, or the generation of an organometallic reagent from the aromatic moiety. Indeed, no functionalization of the carbon interested in the nucleophilic addition has to be performed if the abovementioned strategy is applied; this is indeed sometimes very difficult, especially with heteroarenes, where, for example, installation of a halogen into certain positions might be not trivial. On the contrary, the only pre-functionalization required in the former case is the transformation of the desired azine into the corresponding *N*-oxide, which is a very chemoselective and easy process. A large variety of oxidants was successfully applied to this transformation, in order to develop cheap, mild and easy to purify or scale-up methodologies (Scheme 2).

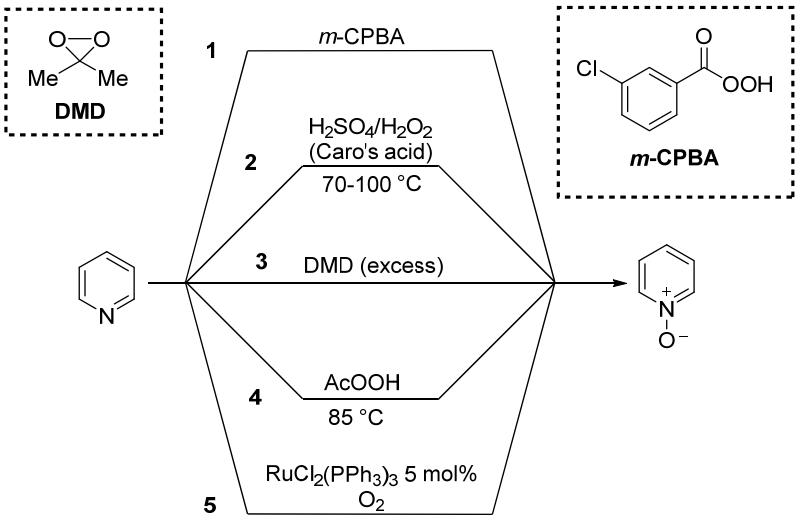

Scheme 2. Different methods for the preparation of pyridine *N*-oxide.

An alternative to commonly employed *m*-CPBA,[91] might be the employment of Caro's acid, dioxiranes,[92] or peracetic acid,[93] generating water-soluble byproducts, or molecular oxygen as a green oxidant in combination with Ru salts.[94]

As far as the activating electrophilic agent is involved, many protocols have been developed, relying on different moieties. Sulfonyl chlorides such as tosyl chloride have been applied for this purpose in the reaction with pyridine *N*-oxides and stabilized anions derived from azlactones, to render heteroarylated quaternary stereocenters in racemic form with synthetically useful yields and mixed regioselectivities (Scheme 3a).[95] Anhydrides, such as acetic or triflic anhydride, were also employed for various transformations of azine *N*-oxides. For example, triflic anhydride could easily activate pyridine *N*-oxides towards the nucleophilic attack of silyl ketene acetals. However, when the anhydride was added in excess, transformation of the expected product into a highly reactive *N*-acylpyridinium salt was observed, undergoing subsequent dearomatization, upon capture by another equivalent of nucleophile (Scheme 3b).[96]

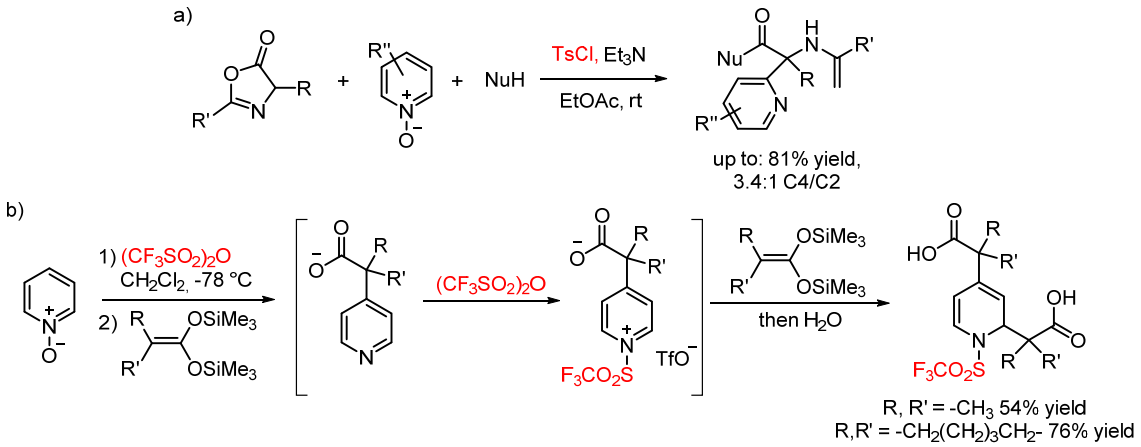

Scheme 3. Examples of reactions employing activation of pyridine *N*-oxides with TsCl and triflic anhydride.

However, in general, the formation of chlorinated pyridines as byproducts is usually a drawback of the activation with TsCl, as chloride anions are usually nucleophilic enough towards activated azine *N*-oxides. Moreover, if the desired nucleophile is heteroatom-based, like alcohols or, even worse, amines, huge chemoselectivity problems arise, as the nucleophile, instead of the *N*-oxide, might react preferentially with TsCl or anhydrides, leading to poor yields in the desired products.[97]

It is to avoid the issues of the commonly employed electrophilic activators with amine nucleophiles that the development of more chemoselective processes was considered. Indeed, preparation of 2-aminopyridine, a commodity for the synthesis of many APIs, from the corresponding *N*-oxide and *tert*-butylamine was considered an appealing strategy, as elucidated in a report by Davies' group at Merck (Scheme 4).[97] Nevertheless, the process, with common activators such as tosyl anhydride, was difficult and poor performing, forcing the employment of a large excess of the amine, to obtain useful yields. However, the major product of the reaction was the tosylated amine in all the cases; if it was not an important drawback in this case, as *tert*-butylamine is cheap and abundant, on the contrary, the optimized reaction is demonstrated to be completely unsuitable for the coupling of expensive or non-commercially available amines.

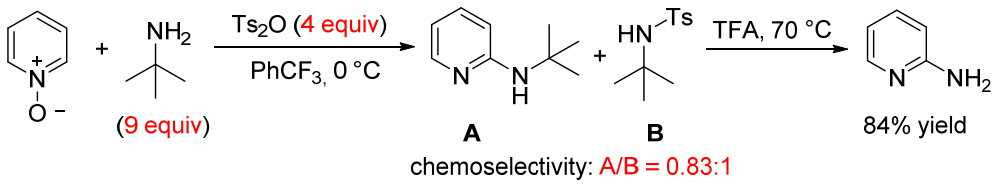

Scheme 4. Preparation of 2-aminopyridine following Davies' procedure

To circumvent these issues, PyBroP (bromotrispyrrolidinium hexafluorophosphate),[98] was employed as an exclusively oxophilic activating agent by Londregan's group at Pfizer, starting from 2010.[99] This commercially available phosphonium salt, originally developed as a peptidic coupling agent, relies on the strong affinity between phosphorus and the anionic oxygen of the *N*-oxide.

While remaining unreactive toward amine (or other) nucleophiles, it works in excellent balance to activate the *N*-oxide moiety and perform the subsequent elimination, as a strong P=O bond is formed in the phosphoramide co-product, enhancing the driving force of the rearomatization process. Moreover, under no circumstances, bromide addition onto the pyridine was observed. A general, mild and expedient preparation of 2-aminoazines was thus developed, presenting in all the cases excellent C-2 regioselectivities (Scheme 5).

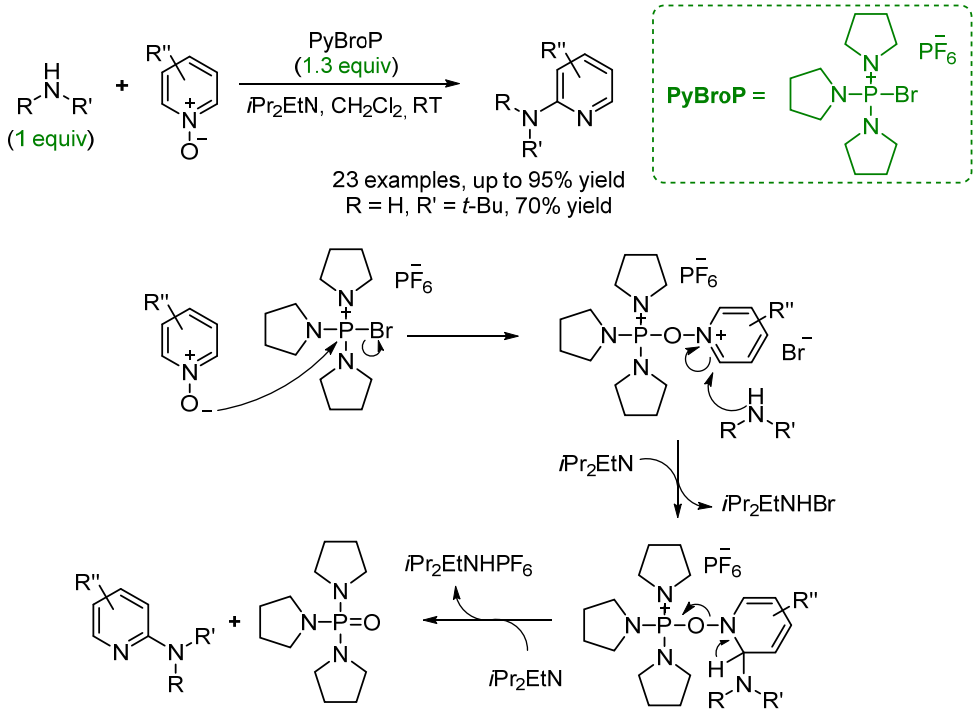

Scheme 5. Amination of pyridine with PyBroP and specific activation-elimination mechanism.

Shortly after, the applicability of this method to the preparation of differently substituted azine *N*-oxides was demonstrated. Phenols, amides, 1,3-dicarbonyls, thiols, nitrogen heterocycles,[100] silyl enol ethers,[101] alcohols[102] and water[103] were found to be competent nucleophiles (Scheme 6). It is important to remark that the presence of oxygen-based nucleophiles is well tolerated, as phosphonium salts, species of strongly hard nature, selectively bind to the anionic oxygen of the *N*-oxide, leaving the less charged hydroxyl moiety untouched and free to react at the carbon atom of the heterocycle.

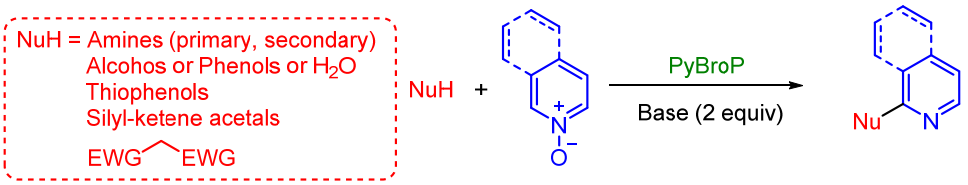

Scheme 6. Nucleophilic additions to azine *N*-oxides activated by PyBroP.

It is in this contest that we became interested in the activation of azine *N*-oxides as a powerful tool to realize new organocatalytic asymmetric heteroarylation reactions. Indeed, to the best of our knowledge, the field of asymmetric heteroarylations employing azine *N*-oxides is very much underexplored. A single report appeared very recently, as we were developing the present methodology, dealing with a highly enantioselective

copper-catalyzed alkylation of quinoline and other azine *N*-oxides with vinylarenes (Scheme 7).[104]

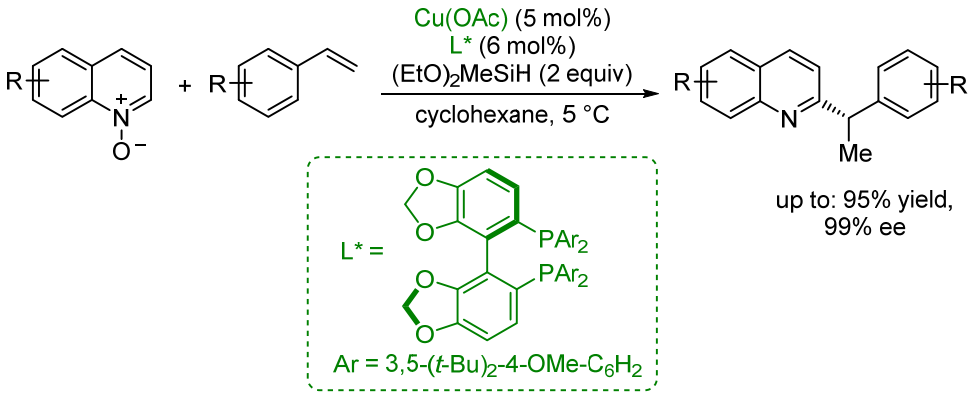

Scheme 7. Copper-catalyzed asymmetric alkylation of quinoline *N*-oxides.

To prove that activated azine *N*-oxides are competent arylating agents in organocatalytic reactions, we chose to employ chiral enamines, generated catalytically *in situ* from enolizable aldehydes and chiral secondary amine catalysts, as reaction partners.

The products of the reaction between activated azine *N*-oxides and chiral enamines is an α-heteroarylated aldehyde. Besides metal-catalyzed asymmetric α-arylation of aldehydes, not relying on organocatalytic activation *via* enamine, the first organocatalytic enantioselective arylation of aldehydes, activated *via* enamine catalysis, was achieved by Jørgensen in 2007, employing quinones as arylating agents (Scheme 8).[105] Upon Michael reaction on the electrophilic double bond and subsequent tautomerization, the quinone turns into an aromatic hydroquinone, which triggers an intramolecular ring closure on the aldehyde group, rendering stable hemiacetals in high yields and enantioselectivities.

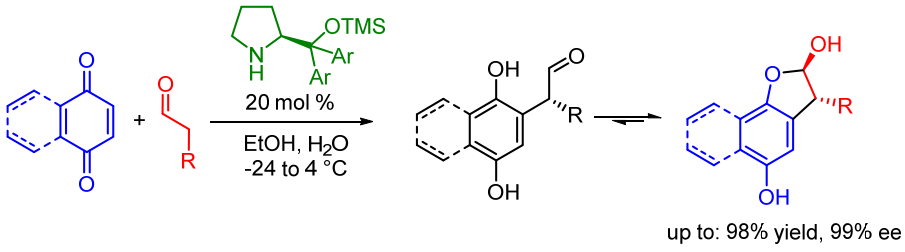

Scheme 8. Asymmetric arylation of aldehydes with quinones.

Shortly after, MacMillan[106] and Nicolau[107] reported an organo-SOMO intramolecular arylation of δ-aryl-aldehydes, employing the same organocatalytic activation. Oxidation of the enamine with an external oxidant gives an electrophilic radical cation, trapped intramolecularly by the aryl ring. The radical formed on the former arene is further

oxidized to a cation, suffering rearomatization through proton abstraction. In Scheme 9, the reaction is exemplified for 3-anisole pentanaldehyde (showing exclusive *ortho*-selectivity) treated under the conditions optimized by MacMillan.

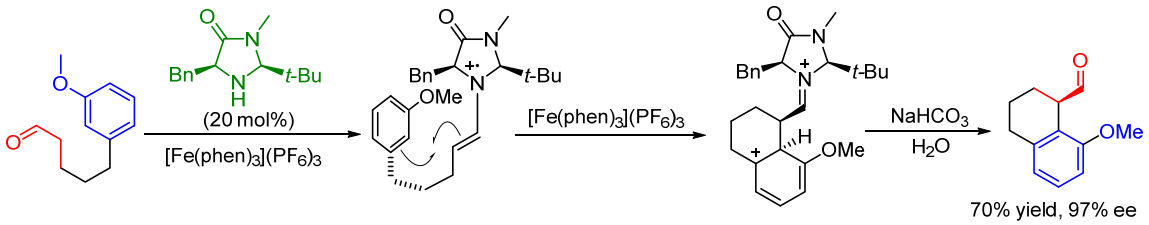

Scheme 9. Asymmetric SOMO-catalyzed intramolecular arylation of aldehydes.

Finally, in 2011 MacMillan reported an intermolecular arylation of aldehydes employing diaryliodonium salts activated with a catalytic amount of Cu(I). The elegant strategy relied on the generation of aryl electrophiles that selectively underwent addition onto the enamine.[108] When substituted rings had to be transferred, a mesityl group was introduced onto the hypervalent iodine as a "dummy" ligand, achieving the exclusive transfer of the less bulky substituent (Scheme 10).

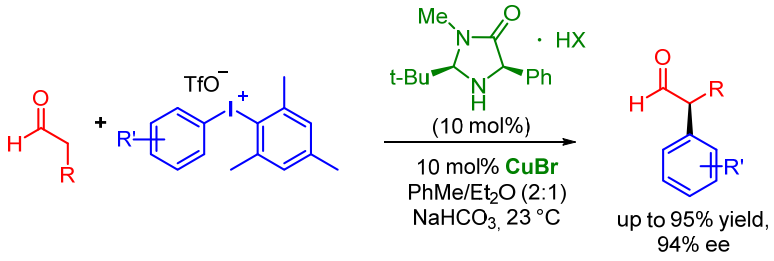

Scheme 10. Asymmetric arylation of aldehydes with diaryliodonium salts.

5.2 Aim of the work

Chiral enamines, generated *in situ* from secondary amines and aldehydes, were demonstrated to react smoothly with pyridinium salts in dearomatization reactions (Section 4) and we found interesting to investigate if, upon changing the type of electrophilic azine, different functionalizations of the same structures were feasible (Scheme 11).

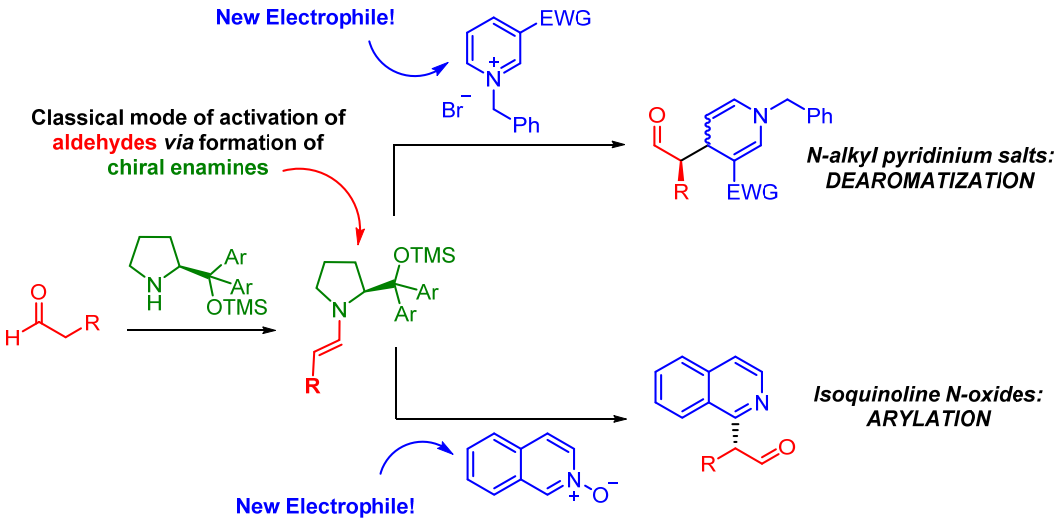

Scheme 11. Organocatalytic asymmetric functionalization of aldehydes with azinium cations: from dearomatization to arylation reactions.

In this case, the desired α-heteroarylation reaction poses some challenges. First of all, the non-trivial devise of an aryl electrophile with the right reactivity to suffer enamine addition and not quenching the amine catalyst. As broadly discussed previously, the activation of azine *N*-oxides with electrophiles such as tosyl chloride or anhydrides is not compatible with amine nucleophiles in amination reactions. The same problem arises from the strategy employed by us, as the catalyst might get deactivated from irreversible reaction with this electrophile. Similar issues were observed, and finally overcame, by Cozzi in developing isoquinolinium salts dearomatization (see Section 3).[75] Moreover, deactivation of the catalyst might also occur by reaction with the activated azine *N*-oxide, as hindered secondary amines were reported to be competent nucleophiles in heteroarenes aminations, relying on the reported strategy (Scheme 12).[100] With two different deactivation pathways, one of which also erodes the reagent available for the desired reaction, the possibility to reach high yields becomes an intriguing challenge.

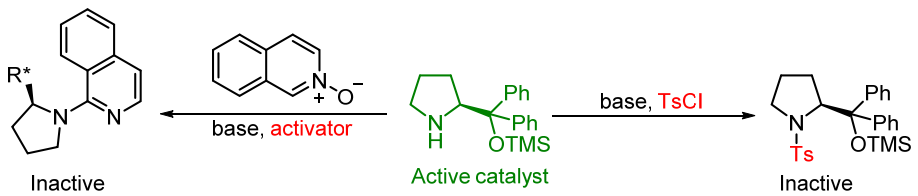

Scheme 12. Possible catalyst deactivation pathways.

Secondly, if the desired reaction is kindly unlikely to undergo thermal equilibration, as the rearomatization step should render it completely irreversible, the tendency to post-

addition racemization is still a significant problem. The acidity of the α-proton of arylated aldehydes is indeed much higher than simple alkyl ones, as the enol form, in conjugation with aryl moiety, is quite stable. Considering the necessity to add to the reaction mixture 2 equivalents of a strong base, as mineral acids are developed during the reaction course, and the predictable need to employ high catalyst loading, due to the abovementioned deactivation pathways, this racemization poses a serious obstacle to the achievement of high enantioselectivities.

Here it is possible to anticipate that, by careful optimization of the reaction conditions, the development an organocatalytic direct α-heteroarylation of aldehydes with isoquinoline *N*-oxides was possible, enabling a good yielding synthesis of a broad range of optically active α-heteroarylated aldehydes. This represents a novel and complementary protocol, as it differentiates from the previously reported strategies not only for the type of electrophile employed, but also because it represents the first strictly organocatalytic (no metal salts employed, see Scheme 10) intermolecular (Scheme 9) arylation of aldehydes with aromatic electrophiles (Scheme 8).

5.3 Results and discussion

At the outset of this work, we started our investigation by reacting 3-phenylpropanal **1a** and isoquinoline *N*-oxide **2a** in the presence of 20 mol% of catalyst **3a**,[71,30c,33] different activating agents and auxiliary bases in THF as solvent (Table 1). Since product **4aa** may exhibit modest configurational stability, due to the enhanced acidity of the proton on the newly generated stereogenic center, we decided to conveniently transform the aldehyde group into a less labile α,β-unsaturated ester (**5aa**) through Wittig reaction.

When tosyl chloride was employed as the activating agent, in the presence of DIPEA or Na_2CO_3 as bases (HCl and TsOH are generated during the course of the reaction), in THF at room temperature for 18 h, only traces of the desired product **5aa** were observed (entries 1 and 2). This was probably due to irreversible tosylation of catalyst **3** under the reaction conditions, as speculated before. Chemoselective activation of the azine *N*-oxide moiety in the presence of amines as nucleophilic partners was recently achieved, employing PyBroP as an exclusively oxophilic reagent, as stated in detail before. Indeed, when PyBroP was employed under the previous reaction conditions (DIPEA as base) the desired product **5aa** was formed in 48% yield and 70% ee (entry 3). Nevertheless, as

previously foreseen, another possible pathway for catalyst deactivation is its reaction with the activated heterocycle. Indeed, it is reported that hindered cyclic secondary amines react efficiently with activated azine *N*-oxides to render *N*-heteroarylated derivatives. To avoid this additional unwanted side-reaction, leading to catalyst deactivation and substrate consumption, we decided to add PyBroP portion-wise. As reported in entry 4, the process, run under these new conditions, exhibited a higher conversion. The greater availability of the catalyst ensured thus a shorter reaction time, preventing racemization and ultimately rendering product **5aa** with a much higher enantioenrichment (89% ee). Different bases were then tested, giving less satisfactory outcomes (entries 5-7). A thorough solvent and catalyst screening (see Table 2) was performed, confirming THF and **3a** as optimal. Importantly, diminishing the temperature to 0 °C and employing a slight excess of PyBroP resulted in improved conversion and enantioselectivity (65% isolated yield and 93% ee, entry 8). A further decrease of the temperature was instead detrimental (entry 9).

Table 1. Optimization of the reaction conditions between isoquinoline *N*-oxide **2a** and 3-phenylpropanal **1a**. Overview.

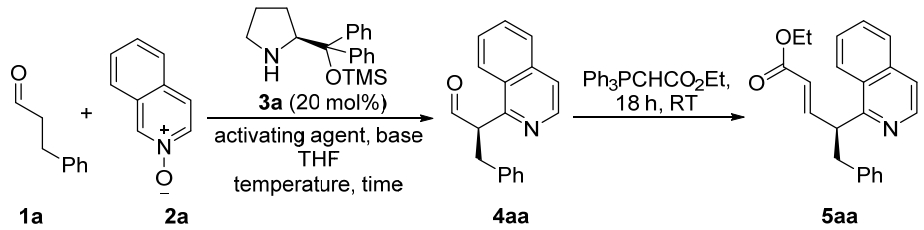

Entry[a]	Activating agent	Base	Temperature	Time (h)	Conversion (%)[b]	ee[c] (%)
1	TsCl	Na_2CO_3	RT	18	Traces	n.d.
2	TsCl	DIPEA	RT	18	Traces	n.d.
3	PyBroP	DIPEA	RT	18	48	70
4[d]	PyBroP	DIPEA	RT	5	62	89
5[d]	PyBroP	Na_2CO_3	RT	5	61	81
6[d]	PyBroP	Proton sponge	RT	5	40	83
7[d]	PyBroP	2,6-lutidine	RT	5	27	n.d.
Solvent and catalyst screening: see Table 2 (entries 1-6)						
8[e]	PyBroP	DIPEA	0	6	71 (65[f])	93
Additional solvent and catalyst screening: see Table 2 (entries 7-13)						
9[e]	PyBroP	DIPEA	-15	6	58	91

(**a**) Reaction conditions: **1a** (0.3 mmol), **2a** (0.1 mmol), base (0.2 mmol), **3a** (0.02 mmol), THF (500 µL), activating agent (0.1 mmol), temp., time, then Ph_3PCHCO_2Et (0.7 mmol), RT, 18h. (**b**) Determined on the crude mixture by ^1H NMR. (**c**) Determined by CSP HPLC. (**d**) 0.02 mmol of PyBroP was added hourly until 1.0 equiv. was reached (five additions). (**e**) 0.02 mmol of PyBroP was added hourly until 1.2 equiv. were reached (six additions). (**f**) Isolated yield after column chromatography.

Different chiral secondary amine catalysts such as **3b** (Table 2, entry 1) and **3c** (entry 2) resulted in decreased conversion and enantioselectivity values. Different solvents (entries 3-6) did not afford any improvement in the described arylation, confirming THF as the optimal choice. This is probably due to the greater stability of the activated intermediate in THF than, for example, in DCM, as reported by Londregan.[102] Different ethereal solvents were then screened in a fine-tuning optimization, leading again to less unsatisfactory results (entries 7-9). Furthermore, variations in the catalytic loading did not improve the reaction outcomes (entries 10 and 11). Finally, both strictly anhydrous

conditions or deliberate water addition decreased the conversion slightly but did not prevent the reaction to occur (entries 12 and 13).

Table 2. Optimization of the reaction conditions between isoquinoline *N*-oxide **2a** and 3-phenylpropanal **1a**. Solvent, catalyst and additive screening.

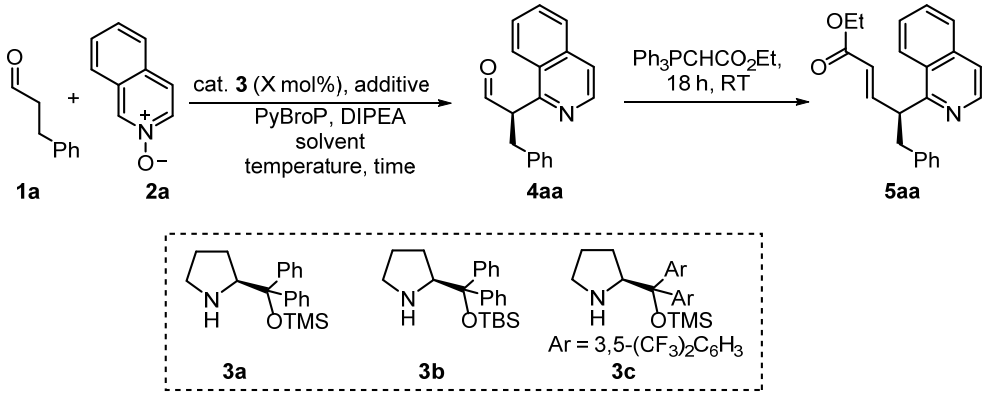

Entry[a]	Catalyst (mol%)	Additive	Solvent	Temperature	Time (h)	Conversion (%)[b]	ee (%)[c]
1	**3b** (20)	none	THF	RT	5	< 5	n.d.
2	**3c** (20)	none	THF	RT	5	50	n.d.
3	**3a** (20)	none	DCM	RT	5	60	73
4	**3a** (20)	none	PhMe	RT	5	20	75
5	**3a** (20)	none	EtOAc	RT	5	20	73
6	**3a** (20)	none	PhMe/Et_2O	RT	5	73	71
7	**3a** (20)	none	MTBE	0	6	< 5	n.d.
8	**3a** (20)	none	Dioxane	0	6	33	80
9	**3a** (20)	none	CPME	0	6	< 5	n.d.
10	**3a** (10)	none	THF	0	6	40	85
11	**3a** (30)	none	THF	0	6	60	85
12	**3a** (20)	$MgSO_4$[d]	THF	0	6	47	85
13	**3a** (20)	H_2O	THF	0	6	34	86

(**a**) Reaction conditions: **1a** (0.3 mmol), **2a** (0.1 mmol), DIPEA (0.2 mmol), **3a** (0.02 mmol), 0.02 mmol of PyBroP was added hourly until 1.2 equiv. were reached (six additions). solvent (500 μL), temperature, time. (**b**) Determined on the crude mixture by ^{1}H NMR. (**c**) Determined by CSP HPLC. (**d**) $MgSO_4$ was thermally activated *in vacuo* prior to use, anhydrous THF was employed and the reaction was run under a N_2 flow.

Using the optimized reaction conditions, we evaluated various aldehydes and isoquinoline *N*-oxides to verify the generality of our procedure. As outlined in Scheme 13, besides 3-phenylpropanal **1a**, a variety of aldehydes was productively engaged in this heteroarylation protocol. The isoquinoline moiety was successfully introduced onto linear (**1b** and **1c**) and γ-branched (**1d** and **1e**) aliphatic aldehydes, rendering the respective products **5ba-5ea** in moderate to good yields (50-70%) and high enantiomeric excesses (88-93% ee). More sterically demanding isovaleraldehyde **1f** was also found to be a suitable partner for the present reaction, although requiring a less hindered and more reactive ylide, such as (triphenylphosphoranylidene)acetonitrile, for the Wittig reaction.

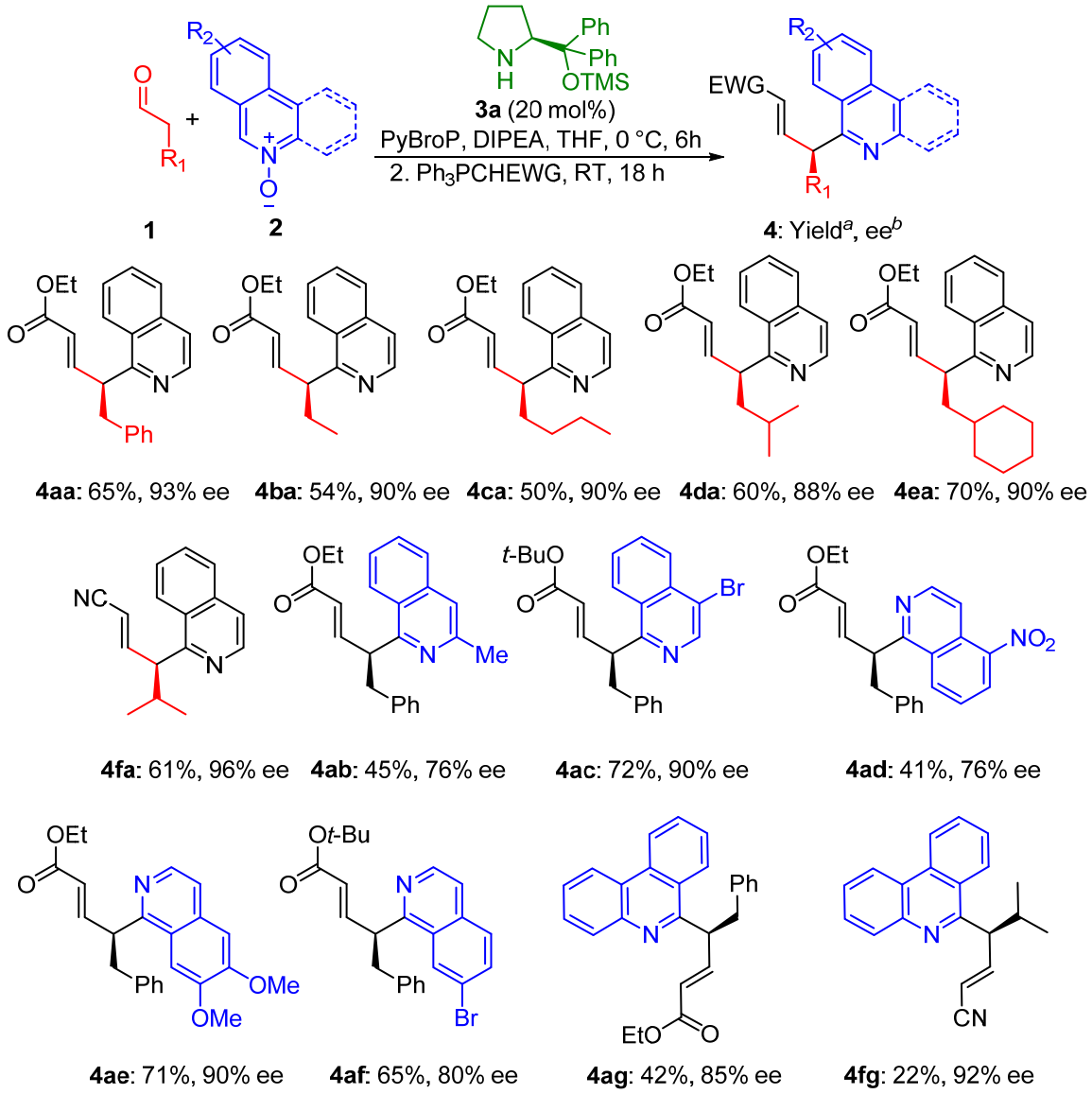

Scheme 13. Reaction scope. Reaction conditions: **1a** (0.3 mmol), **2a** (0.1 mmol), **3** (0.02 mmol), PyBroP (0.02 mmol added hourly until 1.2 equiv. were reached), DIPEA (0.2 mmol), THF (0.5 mL), 0 °C, 6 h, then $Ph_3PCHEWG$ (0.7 mmol), RT, 18 h. (**a**) Yield of isolated products after column chromatography. (**b**) Determined by chiral stationary phase (CSP) HPLC on isolated products **5**.

Arylated acrylonitrile **5fa** was thus isolated in 61% yield and excellent enantiomeric excess (96% ee).

As far as the *N*-oxides **1** are concerned, we have found that a substituent at the C-3 position, vicinal to the *N*-O reactive site, does not impair the reactivity, although causing a slight decrease in both the yield and the enantioselectivity (**5ab**). A halogen atom is well tolerated at positions C-4 (**2c**) and C-7 (**2f**) affording respective products **5ac** and **5af** in good yields and enantioselectivities. However, in these cases, a much slower Wittig reaction was observed and a more reactive ylide (bearing a *tert*-butyl ester) was necessary to achieve an effective procedure. Notably, we were delighted to find that *N*-oxides of both electron-poor (**2d**), and electron-rich (**2e**) nature were found to be suitable substrates for the disclosed protocol. Moreover, it was possible to successfully introduce the hindered phenanthridine backbone onto aldehydes **1a** and **1f**, affording products **5ag** and **5fg** in good enantioselectivities and in moderate yields.

Different azine *N*-oxides such as pyridine 1-oxide, 4-methylquinoline 1-oxide, phthalazine 2-oxide and quinazoline 3-oxide did not show any reactivity under the optimized reaction conditions (Scheme 14). Pyridine 1-oxide did not probably undergo the first dearomatization step (see section 4) and 4-methylquinoline 1-oxide was less electrophilic than isoquinoline-*N*-oxide **1** (the activated position, next to the nitrogen, is not benzylic). Phthalazine 2-oxide and quinazoline 3-oxide probably reacted faster with catalyst **3a** than with the condensed enamine, as some traces of substituted heterocycles were detected in the crude reaction mixtures.

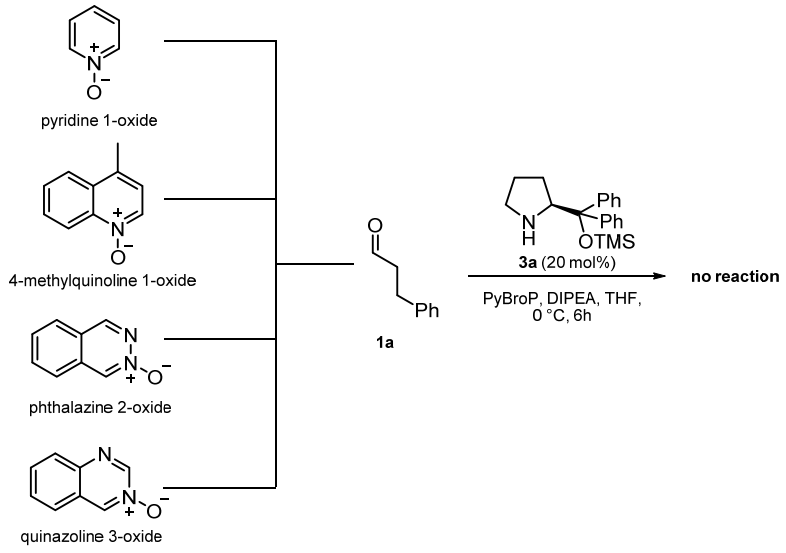

Scheme 14. Unreactive azine *N*-oxides.

5.3.1 Determination of the absolute configuration of compounds 5

The absolute configuration of products **4** (*R*), and **5** (*S*) for consistency, was determined by synthesizing known alcohol **6**, readily obtained by reduction with $NaBH_4$ of product **4ga**, prepared from propanal **1g** and *N*-oxide **2a** under the standard reaction conditions. This compound was obtained in 60% yield and 93% ee, demonstrating that the disclosed procedure was suitable for the preparation of β-heteroaryl alcohols, along with α,β-unsaturated esters **5**. The optical rotation $[\alpha]_D$ value of **6** was then compared with literature data (Scheme 15).[75] The absolute configuration of **6** was thus determined to be (*R*), as the corresponding literature product (also 93% ee) exhibiting an $[\alpha]_D$ = -52 (c = 1.7 in $CHCl_3$) was reported to be (*S*). This absolute configuration was extended to all products **4** (*R*) and **5** (*S*) for analogy. It is worth to stress that (*R*)-aldehydes **4** render, through Wittig olefination, (*S*)-α,β-unsaturated esters and nitriles **5**, as the as the C.I.P. priority of the substituents bonded to the chiral center changes. The obtained absolute configuration of aldehydes **4** was the expected one and is in agreement with the reported catalytic cycles, since the formation of the stereogenic center involves the addition of the enamine intermediate through the less hindered face.[71,30c,33]

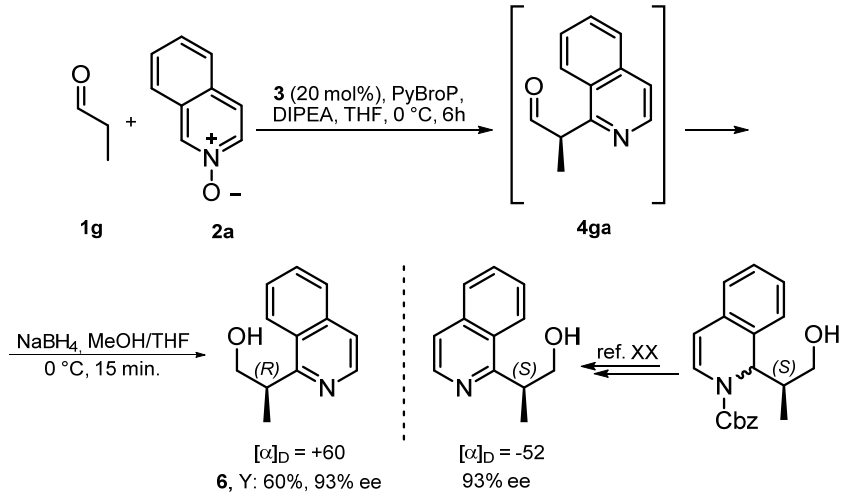

Scheme 15. Preparation of alcohol **6** and optical rotation value comparison with literature data.

5.3.2 Mechanistic proposal

Finally, a possible reaction pathway can be devised (Scheme 16). In accordance with previous reports on the addition of nucleophiles to azine *N*-oxides activated by PyBroP,[99] we propose intermediate **A** as the key mechanistic feature in this transformation. This electrophilic intermediate reacts with the enamine, generated by condensation of the aldehyde with catalyst **3**, at its less hindered face (enantio-determining step), rendering

dearomatized intermediate **B**. Subsequent base-promoted rearomatization, followed by hydrolysis of the resulting iminium ion, affords the desired heteroarylated aldehyde **4** and free catalyst **3**.

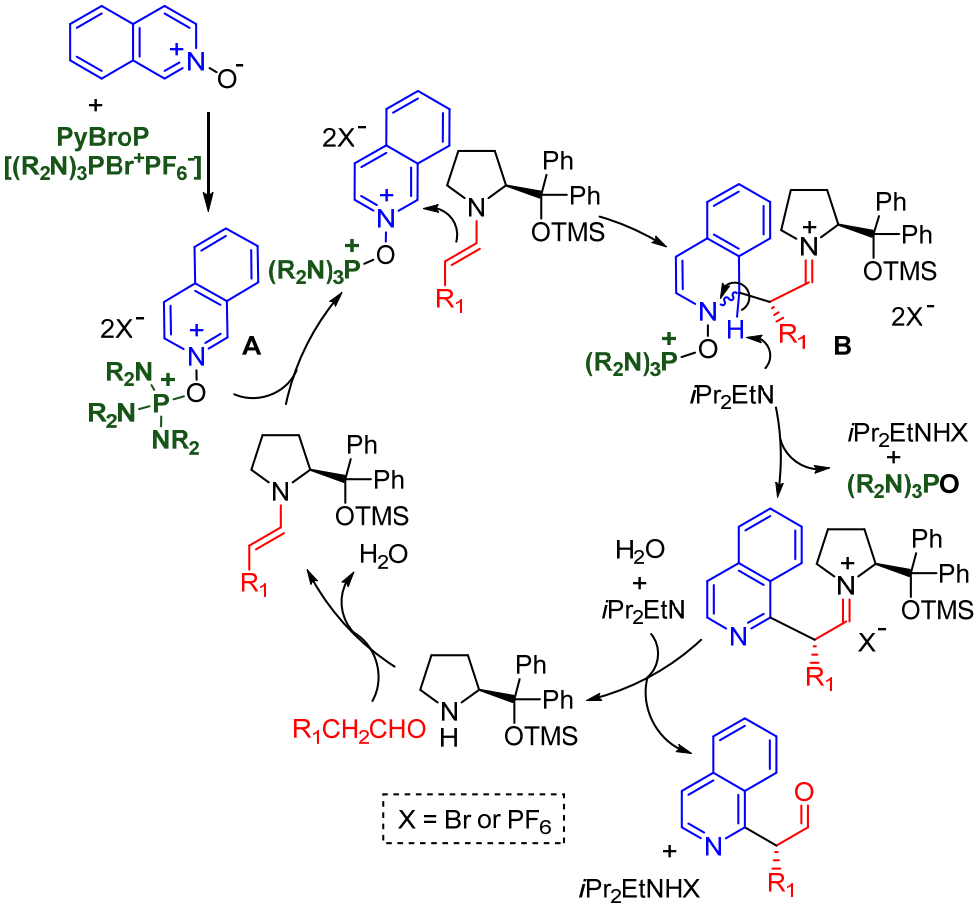

Scheme 16. Proposed reaction pathway (X = Br or PF_6).

5.4 Conclusion

To sum up, moving from pyridinium salts to different azinium electrophiles, we started being interested in activated *N*-oxides **2** as novel substrates for new organocatalytic transformations. Those compounds were widely employed to build functionalized azines through addition (dearomatization) – elimination (rearomatization) sequences. It was thus envisioned that they could be turned into powerful arylating agents towards, for example, nucleophilic chiral enamines, generated *in situ* from enolizable aldehydes **1**. Therefore, an unprecedented direct strictly organocatalytic α-heteroarylation of aldehydes was developed. This led to a new approach to enantioenriched α-heteroaryl aldehydes,

tackling several challenges related to catalyst quench and product racemization. This direct arylation approach combines typical catalytic enamine chemistry with isoquinoline *N*-oxides **2** as aromatic reaction partners. PyBroP (bromotripyrrolidinophosphonium hexafluorophosphate) is used to activate the isoquinoline *N*-oxides for the reaction, which occurs at the more reactive C-1 of the isoquinoline nucleus. The same activating agent ensures rearomatization *via* a base promoted elimination, ultimately resulting in a substituted azine. Most importantly, the employment of an exclusively oxophilic activating agent, such as PyBroP, avoided irreversible catalyst quench and allowed a smooth transformation. A short reaction time and a moderately low temperature (0 °C) were sufficiently mild conditions to avoid product racemization. Ultimately, a controlled addition of the activating agent was found to improve the yield greatly, probably due to a reduced tendency of the activated species to react with the amine catalyst. The present protocol was applied both to different aliphatic aldehydes **1** and to isoquinoline *N*-oxides **2** bearing substituents of various electronic nature located at different positions of the aromatic nucleus, rendering the respective arylated products **5** in useful yields (41–72%) and very good enantioselectivities (75–96% ee). The presented protocol, exhibiting good yields, high enantiomeric excesses and wide substrate scope, thus represents the first organocatalytic enantioselective direct α-heteroarylation of aldehydes (Scheme 17).

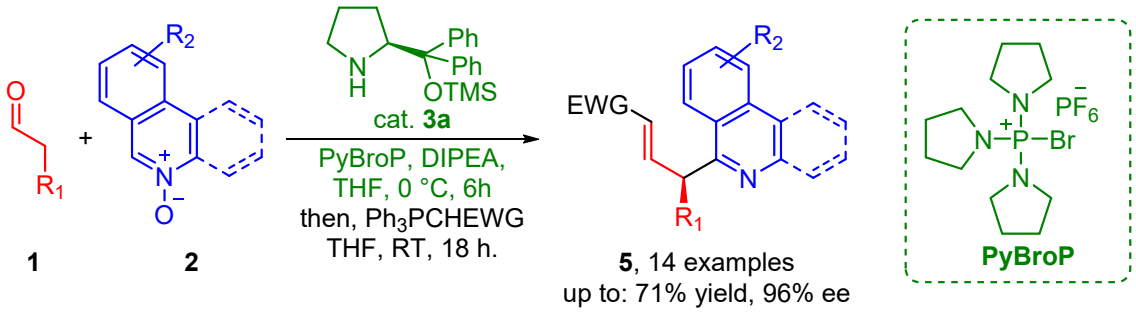

Scheme 17. Organocatalytic enantioselective α-heteroarylation of aldehydes with isoquinoline *N*-oxides. Summary of the project.

5.5 Experimental details

5.5.1 General methods and materials

General Methods. ^{1}H and ^{13}C NMR spectra were recorded on a Varian Inova 300 or Mercury 400 spectrometer. Chemical shifts (δ) are reported in ppm relative to residual solvents signals for ^{1}H and ^{13}C NMR. Signal patterns are indicated as follows: br s, broad singlet; s, singlet; d, doublet; t, triplet; q, quartet; m, multiplet. Coupling constants (J) are given in hertz (Hz). ^{13}C NMR were acquired with ^{1}H broad-band decoupled mode. Chromatographic purifications were performed using 70-230 mesh silica. Mass spectra were recorded on a micromass LCT spectrometer using electrospray (ES) ionization techniques or on a FOCUS/DSQ using electron impact (EI) ionization techniques (relative intensity are given in bracket). Optical rotations were measured on a Perkin Elmer 241 polarimeter provided with a sodium lamp and are reported as follows: $[\alpha]_{\lambda}^{T(°C)}$ (c = g/100 mL, solvent). The enantiomeric excess of the products (ee) were determined by chiral stationary phase HPLC (Daicel Chiralpak AD-H, IC, or Chiralcel OD, OD-H columns), using an UV detector operating at 254 or 214 nm r). Below the general procedures, the characterization of the model compound only is reported. For a full description of all the products reported see the Supporting Information of *Chem. Commun.* **2018**, *54*, 3977.

Materials. Analytical grade solvents and commercially available reagents were used as received, unless otherwise stated. Aldehydes **1d** and **1e** were prepared by oxidation of the corresponding commercially available alcohol with PCC (pyridinium chlorochromate) in DCM. *N*-oxides **2a** and **2f** are commercially available products. 6,7-Dimethoxyisoquinoline (see product **2e**) was prepared following a literature procedure. 3-Chloroperoxybenzoic acid (*m*-CPBA) (50-55%, cont. ca 10% 3-chlorobenzoic acid, balance water) was purchased by Alfa Aesar and used as received. Racemic products **5** were prepared following the same general procedure for the enantioenriched ones but using an equimolar mixture of **(*S*)-3a** and **(*R*)-3a** as catalyst.

5.5.2 General procedure for the preparation of products 5.

In a test tube equipped with a magnetic stirring bar, aldehyde **1** (0.3 mmol) is added to a 0.04 M solution of catalyst **(*S*)-3** in THF (0.5 mL, corresponding to 6.54 mg of **(*S*)-3**, 0.02 mmol, 20 mol%). Isoquinoline *N*-oxide **2** (0.1 mmol) is added, followed by *N*,*N*-diisopropylethylamine (DIPEA, 34.2 μL, 0.2 mmol) and the resulting suspension is cooled to 0 °C Then, every hour, bromotripyrrolidinophosphonium hexafluorophosphate (PyBroP, 0.02 mmol, 9.2 mg, 0.2 equiv) was added as solid, until, after 5 hours, 1.2

equivalents were reached (six additions). One hour after the latest addition (total reaction time 6 hours), the appropriate ylide (0.7 mmol) is added and the reaction mixture is stirred at room temperature overnight. Hereafter, CH_2Cl_2 is added (5 mL), the solution is filtered through a short plug of silica gel, and the plug is washed with Et_2O (4x). The residue was then purified by chromatography on silica gel (*n*-hexane/Et_2O mixtures) to afford the desired products **5**. Finally, the enantiomeric excess was determined by chiral stationary phase HPLC (*n*-hexane/*i*-PrOH mixtures).

Ethyl (*S*,*E*)-4-(isoquinolin-1-yl)-5-phenylpent-2-enoate 5aa

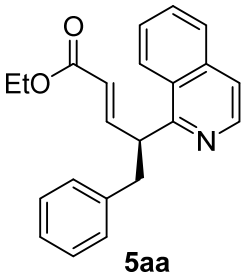

5aa

Following the general procedure from isoquinoline *N*-oxide **2a**, 3-phenylpropanal **1a** and ethyl (triphenylphosphoranylidene)acetate, product **5aa** was obtained as a pale-yellow oil in 65% yield (22 mg) after column chromatography on silica gel (*n*-hexane/Et_2O = 6:1). The enantiomeric excess of **5aa** was determined by chiral stationary phase HPLC (OD, *n*-hexane/*i*-PrOH 95:5, 0.75 mL/min, λ = 254 nm, t_{maj} = 10.0 min, t_{min} = 8.9 min, 93% *ee*). $[\alpha]_D^{25\ °C}$ = -16 (c = 1.2, $CHCl_3$); ^{1}H NMR (400 MHz, $CDCl_3$) δ = 8.56 (d, *J* = 5.7 Hz, 1H), 8.04 (br d, *J* = 8.3 Hz, 1H), 7.81 (ddd, *J* = 8.2, 1.3, 0.6 Hz, 1H), 7.64 (ddd, *J* = 8.1, 6.8, 1.1 Hz, 1H), 7.57 – 7.50 (m, 2H), 7.34 (dd, *J* = 15.7, 8.0 Hz, 1H), 7.21 – 7.08 (m, 5H), 5.71 (dd, *J* = 15.8, 1.1 Hz, 1H), 4.80 – 4.70 (m, 1H), 4.16-4.08 (m, 2H), 3.51 (dd, *J* = 13.9, 7.2 Hz, 1H), 3.31 (dd, *J* = 13.7, 7.6 Hz, 1H), 1.22 (t, *J* = 7.1 Hz, 3H) ppm; ^{13}C NMR (101 MHz, $CDCl_3$) δ = 166.3, 160.2, 149.7, 142.0, 139.5, 136.4, 129.8, 129.1, 128.2, 127.6, 127.3, 126.9, 126.2, 124.1, 122.1, 119.8, 60.3, 47.1, 40.4, 14.2 ppm; EI-MS (m/z, relative intensity): 331 (M^+, 35%), 258 (M^+- CO_2Et, 100).

5.5.3 Preparation of alcohol 6

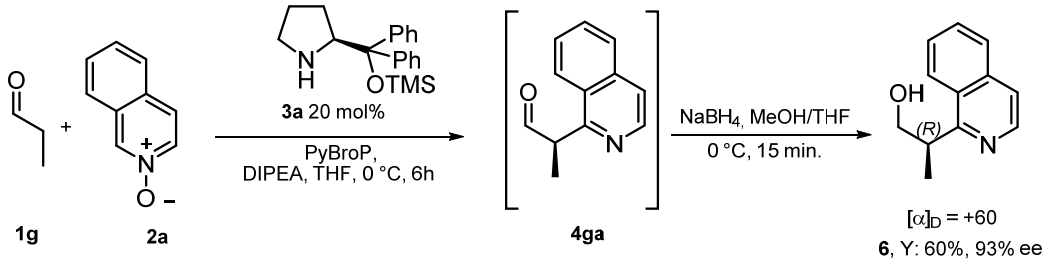

In a test tube equipped with a magnetic stirring bar, propanal **1g** (21.5 µL, 0.3 mmol) is added to a 0.04 M solution of catalyst **(*S*)-3** in THF (0.5 mL, corresponding to 6.54 mg of **3**, 0.02 mmol, 20 mol%). Isoquinoline *N*-oxide **2a** (14.5 mg, 0.1 mmol) is added, followed by DIPEA (34.2 µL, 0.2 mmol) and the resulting suspension is cooled to 0 °C. Then, every hour, PyBroP (0.02 mmol, 9.2 mg, 0.2 equiv) was added as solid, until, after 5 hours, 1.2 equivalents were reached. One hour after the latest addition (total reaction time 6 hours), MeOH (0.5 mL) is added followed by $NaBH_4$ (26.5 mg, 0.7 mmol) and the resulting suspension is stirred at 0 °C for 15 minutes.

Hereafter DCM (5 mL) and a saturated aqueous solution of Na_2CO_3 (5 mL) are added, the phases separated and the aqueous layer extracted three times with DCM (3x5 mL). The combined organic extracts are dried with $MgSO_4$, filtered and evaporated *in vacuo*. The crude residue is then purified by column chromatography on silica gel (*n*-hexane/EtOAc 3:1) to obtain product **6** as a pale-yellow oil (60% yield, 12 mg). The enantiomeric excess of **6** was determined by chiral stationary phase HPLC (IC, *n*-hexane/*i*-PrOH 90:10, 0.70 mL/min, λ = 214 nm, t_{maj} = 22.8 min, t_{min} = 21.3 min, 93% *ee*). NMR analytical data are in complete accordance to the ones reported in literature; $[\alpha]_D$ = +60 (c = 0.5 in $CHCl_3$).

6 Organocatalytic Enantioselective [10+4] Cycloadditions.

The procedures and results here described are part of- and can be found in-:

- B. S. Donslund, N. I. Jessen, G. Bertuzzi, M. Giardinetti, T. Palazzo, M. L. Christensen, K. A. Jørgensen. *Angew. Chem. Int. Ed.* **2018**, *57*, 13182.

This work was carried out at the Department of Chemistry, University of Aarhus, Denmark, supported by "Marco Polo" fellowship of the University of Bologna, Italy. The author of this Doctoral Thesis gratefully acknowledges.

ABSTRACT

The first peri- and stereoselective [10 +4] cycloaddition between catalytically generated amino isobenzofulvenes and electron-deficient dienes is described. The highly stereoselective catalytic [10+4] cycloaddition exhibits a broad scope with high yields, reflecting a unusually robust higher-order cycloaddition. Experimental and computational investigations support a kinetic distribution of intermediate rotamers dictating the enantioselectivity, which relies heavily on additive effects.

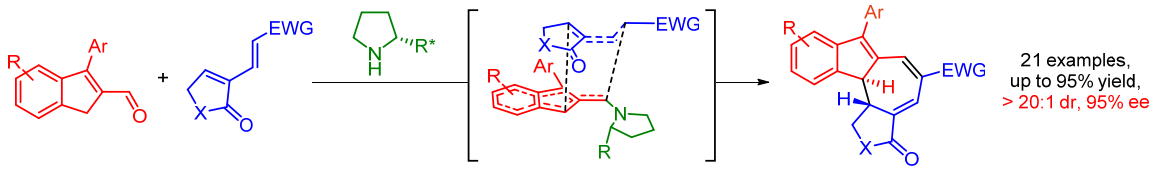

6.1 Background

Higher-order cycloadditions are cycloaddition (HOC) reactions that involve more than six π-electrons (Diels-Alder) and represent a powerful and intriguing tool for the construction of complex polycyclic scaffolds in a single synthetic step. In the first papers by Woodward and Hoffmann, stating the rules for symmetry allowed thermal and photochemical concerted pericyclic reactions, the authors did not limit their rule to known [4+2]-cycloadditions, but made predictions about other pericyclic reactions, stating, for example, that [6+4] and [8+2]-cycloadditions would be thermal processes.[109] Furthermore, based on the orbital symmetry rules, the [6+4] cycloaddition was predicted to proceed with *exo*-selectivity, whereas the [8+2] and [4+2] cycloadditions should both be *endo*-selective.[110] No experimental report was available at the time about [6+4]-

cycloadditions, while one [8+2] already existed. One year later, Morrison, Cookson and Drake published the first [6+4] cycloaddition, reacting tropone and cyclopentadiene (Scheme 1a).[111] In 1970, Houk and Woodward discovered other [6+4] cycloadducts between the products of the reaction of cycloheptatrienes with a substituted cyclopentadienone (Scheme 1b).[112] Those cycloadditions proceeded indeed with high *exo*-selectivity, showing not only that the predictions were correct, but demonstrating how powerful those elegant rules could be.

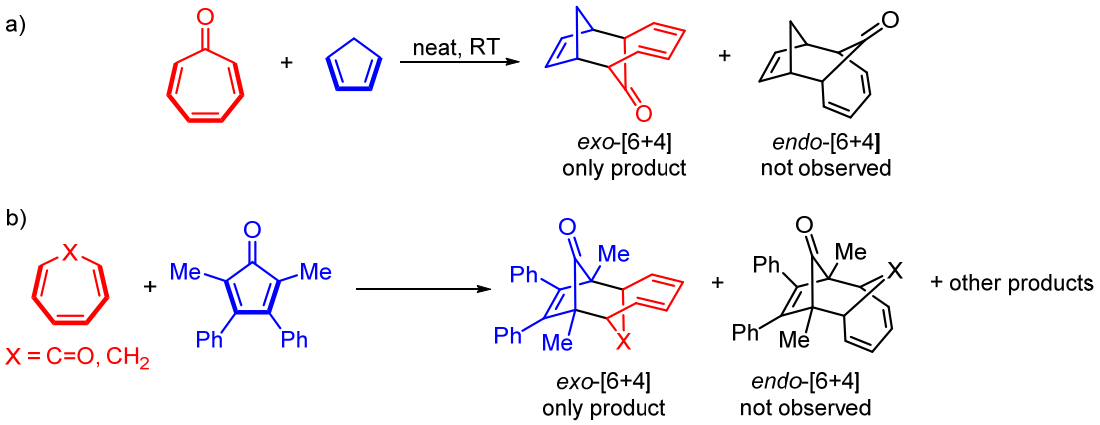

Scheme 1. First examples of [6+4] cycloaddition.

It is not by case that the conjugated systems undergoing these first [6+4]-cycloadditions are both strained in a cycle. The only examples of higher-order cycloadducts found in the literature are, in fact, polycyclic systems. In principle, monocyclic ten-membered rings stemming from ten-electron concerted cycloadditions are conceivable. However, the additional degrees of freedom in longer polyene systems result in increased entropic barriers towards reactivity, and these usually undergo intramolecular electrocyclizations, rather than intermolecular cycloadditions.[113] All the following examples will in fact deal with at least one of the polyconjugated component being cyclic, the processes developed by us being no exceptions.

Besides tropone (*vide infra*), one of the most popular cyclic polyenes, engaged in HOCs, are isobenzofulvenes. With a total of 10π-electrons, they can be involved in a *plethora* of different cycloaddition pathways.[114] For example, 6,6-dimethylisobenzofulvene, generated *in situ* from a series of [4+2] cycloadditions and cycloreversions between an alkylidene benzonorbornene and a tetrazine, was found to dimerize in a perispecific manner through a [10+8] cycloaddition (Scheme 2a).[115] Moreover, 6-amino isobenzofulvene could be generated *in situ*, reacting indene with Vilsmeier salt, and

subsequently captured by *N*-phenylmaleimide in a [10+2] cycloaddition. An amino substituent on the exocyclic carbon atom was reported to stabilize the isobenzofulvene, by increasing the aromatic character (Scheme 2b).[116]

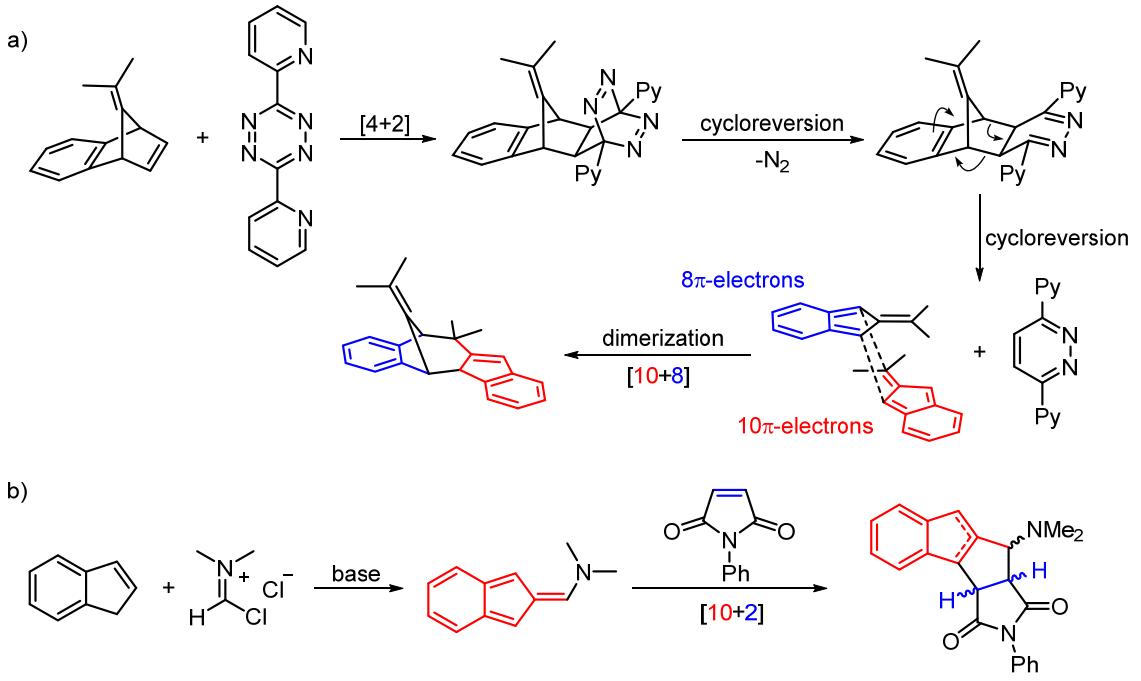

Scheme 2. HOCs of isobenzofulvenes.

One of the most intriguing, yet challenging feature of HOCs is periselectivity. When the number of electrons involved in a cycloaddition moves from six to ten (or more) the different type of conceivable pathways increases. For a reaction involving a 4π-component and a 6π-component, for example, [4+2], [2+4], [4+6] and [6+4]-thermal cycloadditions are possible. Every reaction pathway might, in principle, render two different diastereoisomers, depending on the *endo* or *exo* approach. The number of different products possibly arising from those two reagents might then become discouraging. Indeed, it is probably due to the usual lack of periselectivity and the fact that no general guidelines to control the reaction pathway of higher-order cycloadditions are known, that these reactions have been largely neglected for the past 50 years.

One of the most "chimeric" components of HOCs is tropone. This polyconjugated cyclic ketone was in fact demonstrated to behave as a 2π-component in [2+4],[117] 4π-component in [4+2][118] and [4+6], 6π-component in [6+4] and [6+6][119] and 8π-component in [8+2]-cycloadditions,[120] depending on the different reaction partners (Scheme 3).

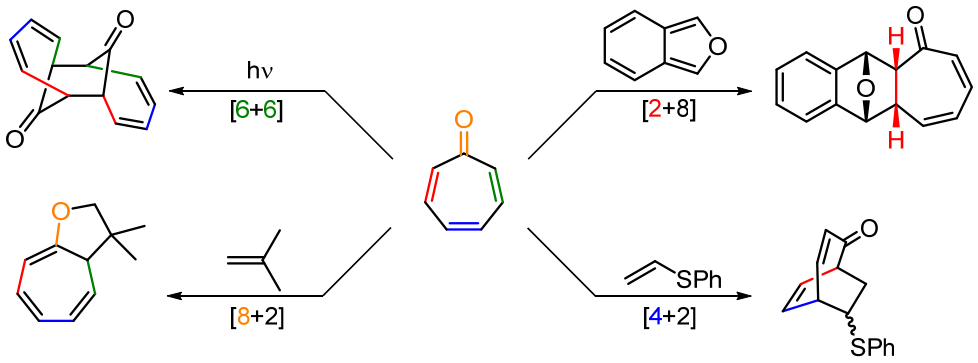

Scheme 3. Tropone acting as a 2, 4, 6 or 8π-component in HOCs.

It is worth stressing that all the possible cycloaddition products from a single system are often in thermal equilibrium between each other through electrocyclic rearrangement pathways. When multiple products are observed as a result of a HOC, it is always uncertain if the cycloadducts might lie on thermally allowed conversion pathways or on the occurrence of three separate concerted cycloadditions, or both.[121]

Periselectivity switches are also possible under kinetic control, as the same two reagents might render, upon variation of the reaction conditions, products arising from two different cycloaddition pathways. This was observed by Yamamoto and Li in the reaction between tropone and ketene acetals: while $B(C_6F_5)_3$ favored a classical [4+2]-cycloaddition, some other Lewis acids, such as $TiCl_4$, selectively promoted the formation of a product arising from the [8+2]-pathway (Scheme 4).[122] This tunability of the periselectivity is optimal for regiodivergent approaches, opening the possibility to synthesize different scaffolds, starting from the same reagents.

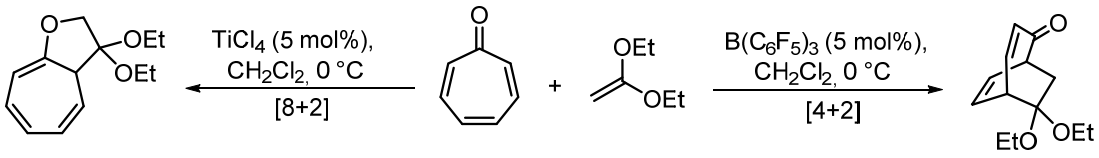

Scheme 4. Periselectivity switch depending on the Lewis acid catalyst.

The control of the stereoselectivity of HOCs is the ultimate goal of overcoming the huge complexity of these reactions. Very few examples existed, until 2017, of enantiocontrolled HOCs, relying on different methodologies. Rigby *et al.* adopted a chiral auxiliary strategy for the photochemical [6+4] cycloaddition between an electron-poor diene and a cycloheptatriene-chromium(0) complex, obtaining up to 92:8 dr (Scheme 5).[123] The coordination of the cyclic triene to the transition metal center

provided a stepwise mechanism to the reaction, guided by the coordination of the conjugated systems to the chromium. This was indeed a powerful strategy to force the [6+4]-periselectivity to such systems, widely employed by the same authors in many reports.

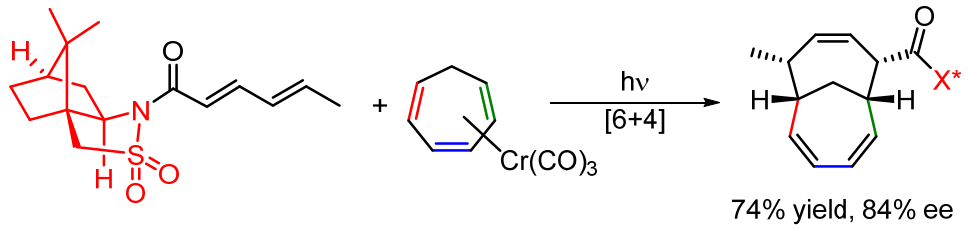

Scheme 5. Chiral ausiliary strategy employed by Rigby to impart stereoselectivity to a [6+4] cycloaddition

To impart enantioselectivity to an intramolecular [6+4]-cycloaddition of a diene-tethered cycloheptatriene (tropone in this case), leading to a valuable bicyclic scaffold, a chiral Al complex was chosen as catalyst. Following a retrosynthetic analysis, the authors envisioned that the Ingenol skeleton could be quickly constructed using a [6+4] cycloaddition in conjunction with isomerization of the double bond systems. Of particular note, the entire stereochemistry of the southern perimeter of Ingenol is envisioned to be derived from the *exo*-transition state of the cycloaddition event. Unfortunately, the results in terms of enantioselectivity were quite poor, as the desired product was obtained with less than 40% ee (Scheme 6).[124]

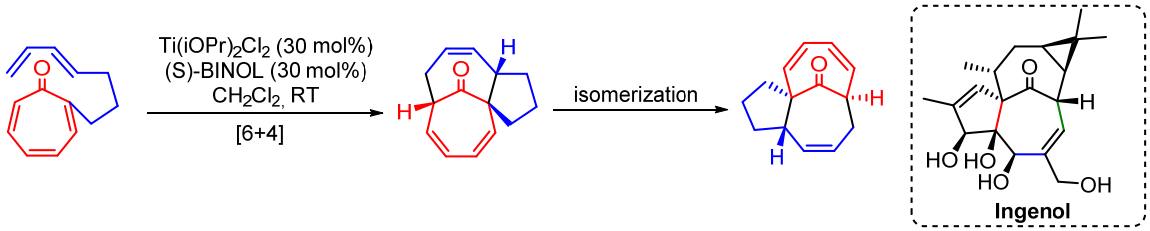

Scheme 6. Chiral Lewis acid strategy for the asymmetric construction of Ingenol core through [6+4] cycloaddition.

Finally, a catalytic asymmetric *aza*-[8+2] cycloaddition reaction of azaheptafulvenes with alkylidene malonates was developed by Feng and coworkers. When employing catalytic amounts of a chiral *N*,*N*′-dioxide–Ni(II) complex, the reaction afforded functionalized cycloheptatriene-fused pyrrole derivatives in excellent yields, diastereoselectivities and enantioselectivities (Scheme 7).[125]

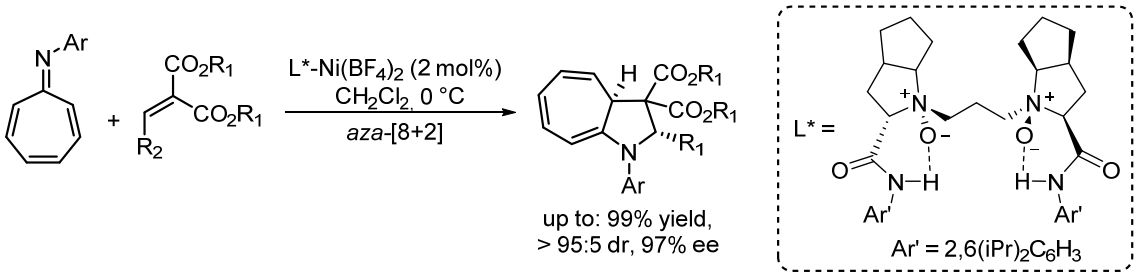

Scheme 7. Nickel-catalyzed asymmetric [8+2] cycloaddition

Organocatalysis was introduced as a tool to induce stereoselectivity in intermolecular HOCs in 2017 by Jørgensen's group, disclosing for the first time highly stereoselective [6+4] and [8+2]-cycloadditions, catalyzed by simple organic molecules.[126] The employed strategy involves the activation of cycloalkenones by primary amine catalysts for the formation of cyclic dienamines. By changing the size of the cycle, discrimination between a cross or linear dienamine was possible, triggering the periselective [6+4]-cycloaddition with tropone or [8+2]-cycloaddition with electron-poor heptafulvenes respectively (Scheme 8).

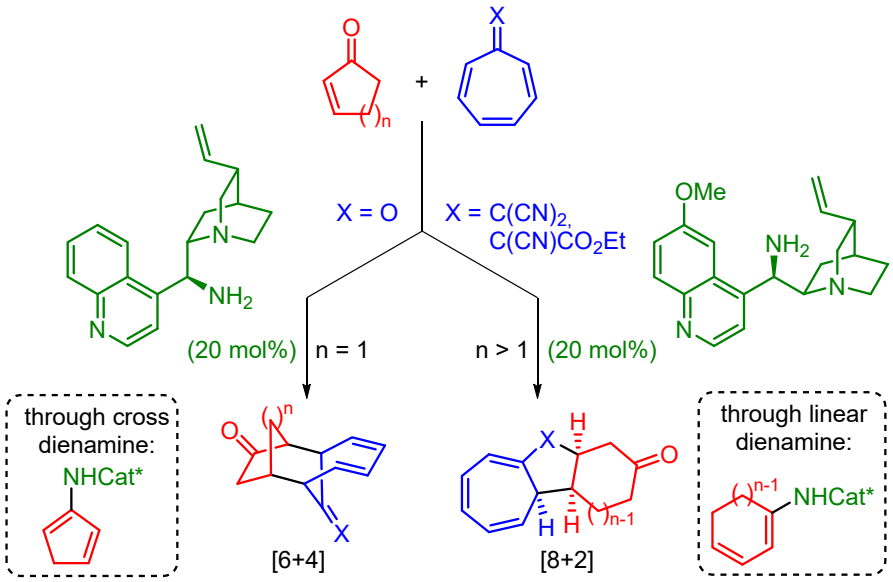

Scheme 8. Organocatalytic asymmetric [6+4] and [8+2] cycloadditions of cycloalkenones and tropone derivatives.

An intramolecular organocatalytic higher order cycloaddition was disclosed earlier by Hayashi and coworkers: activation *via* enamine of a fulvene-tethered enolizable aldehyde enabled a highly diastereo and enantioselective [6+2]-cycloaddition for the construction of a tricyclic scaffold (Scheme 9).[127]

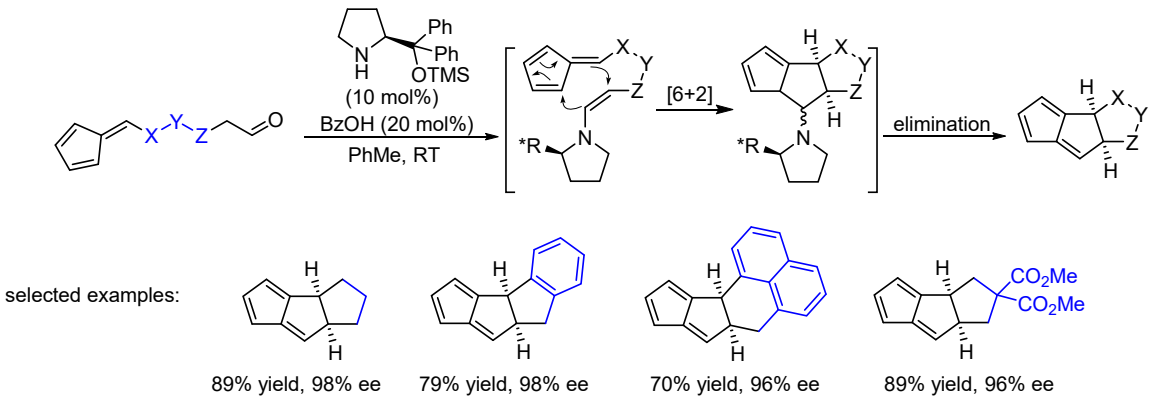

Scheme 9. Organocatalytic enantioselective intramolecular [6+2] cycloaddition.

In 2017 Chen disclosed an organocatalytic enantioselective intramolecular formal [6+2]-cycloaddition between *in situ* generated 4-aminofulvenes and alkylidene oxindoles, catalyzed by *Cinchona* alkaloids-derived primary amine catalysts.[128] A periselectivity switch was also observed when a catalytic amount of thiosalicylic acid was added to the reaction mixture. The thio-Michael addition of the co-catalyst onto the alkylidene cycloalkenone prevented the formation of the 4-aminofulvene, upon subsequent reaction with the amine catalyst, forcing the process to follow an alternative [4+2]-pathway (Scheme 10).

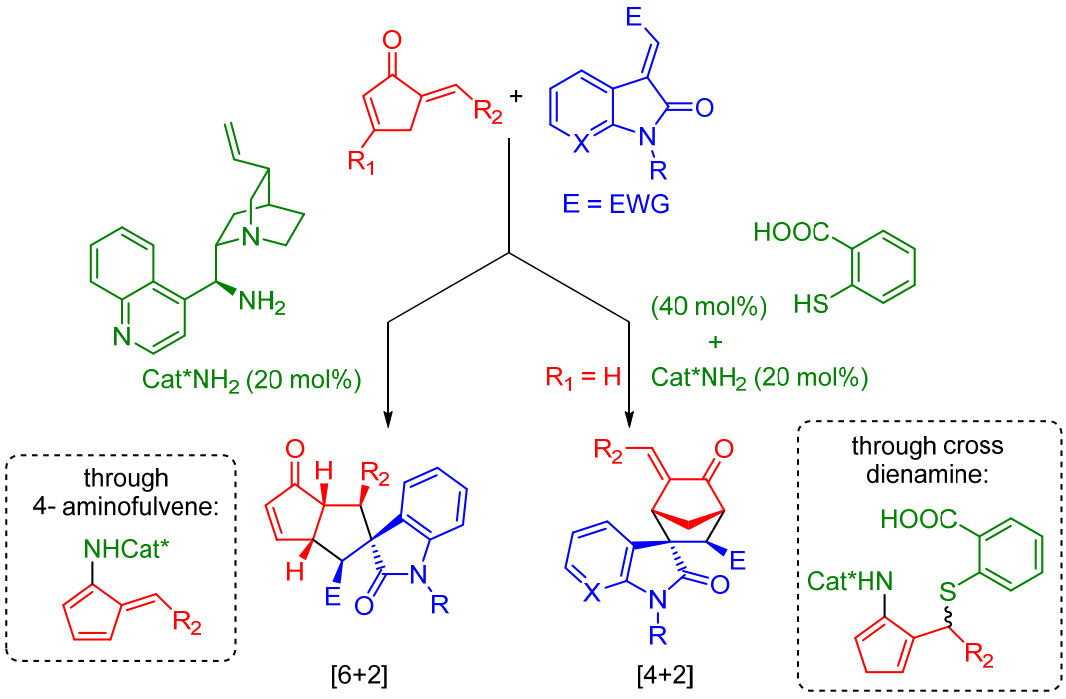

Scheme 10. Organocatalytic enantioselective [6+2] and [4+2] cycloadditions of alkylidene cycloalkenones and alkylidene oxindoles.

Two new examples of organocatalytic enantioselective [8+2]-cycloadditions appeared between late-2017 and early-2018. Pericàs reported the production of enantiomerically enriched cycloheptatrienes fused to a pyrrolidone ring, on the basis of an immobilized recyclable isothiourea-catalyzed periselective [8+2] cycloaddition reaction between chiral ammonium enolates (generated in situ from carboxylic acids) and azaheptafulvenes (Scheme 11).[129]

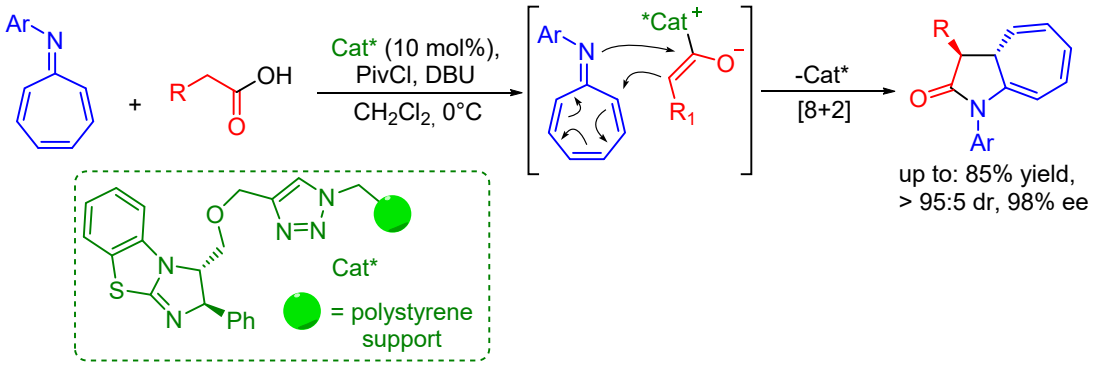

Scheme 11. Organocatalytic enantioselective *aza*-[8+2] cycloaddition

Jørgensen and coworkers disclosed the first catalytic generation of amino isobenzofulvenes by reaction of indene-2-carbaldehydes and chiral secondary amines. These were their productively reacted with nitroolefins in [8+2]-cycloadditions for the rapid and efficient construction of functionalized benzonorbornene scaffolds in a highly peri-, diastereo-, and enantioselective fashion (Scheme 12).[130]

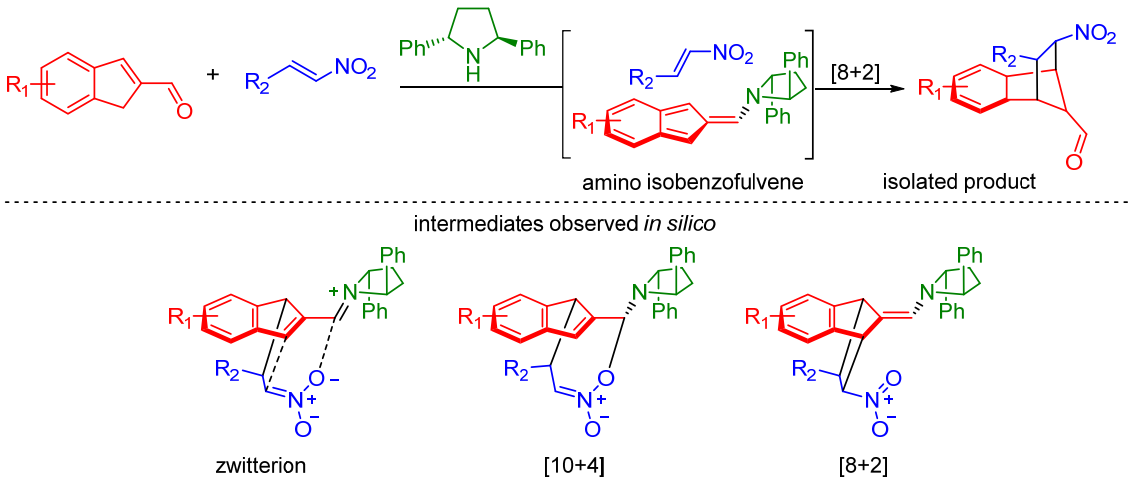

Scheme 12. Organocatalytic enantioselective [8+2] cycloaddition between amino isobenzofulvenes and nitroolefins with some relevant intermediates observed *in silico*.

During the computational studies about the stereo- and periselectivity of this reaction, the calculations indicated a [10+4] cycloadduct as the kinetically favored intermediate.

However, this proposed off-pathway species was not observed experimentally. We then became interested in the possibility to harness this predicted reactivity and develop a catalytic enantioselective [10+4] cycloaddition.

Indeed, to the best of our knowledge, [10+4] cycloadditions have been reported in two instances in noncatalytic reactions employing dialkyl isobenzofulvenes, without control of enantioselectivity. If transient 6,6-dimethylisobenzofulvene is generated with the "tetrazine" method (Scheme 13a) using tropone as solvent, efficient trapping occurs through a [10+4] cycloaddition.[131] An alternative route to generate 6,6-dimethylisobenzofulvene was the 14π-electrons electrocyclic fragmentation of a transient 1,3-dipolar intermediate formed by ring-opening of a fused aziridinocyclobutane. 6,6-Dimethyl isobenzofulvene, generated in this way, reacted with its 1,3-dipole precursor to form a [10+4]-cycloadduct. However, this compound was obtained as a by-product in very low yield (Scheme 13b).[132]

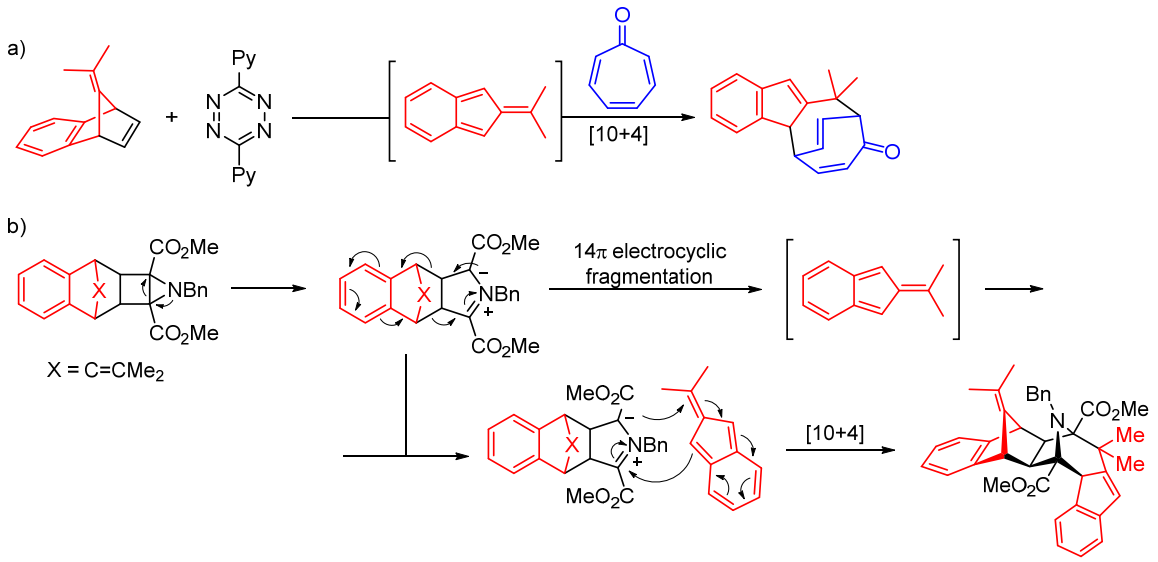

Scheme 13. Precedents for [10+4] cycloadditions.

6.2 Aim of the work

As anticipated previously, the interest in a catalytic enantioselective [10+4] cycloaddition, arose from the prediction of a [10+4] cycloadduct between nitroolefins and amino isobenzofulvenes *in silico*. The choice of the 10π component fell clearly on this amino isobenzofulvene for multiple reasons. First of all, its catalytic generation from indene-2-carboxaldehydes and chiral amine catalysts was proven possible. Secondly, participation of isobenzofulvenes in [10+n] cycloaddition was documented in the

literature.[116] The choice of the 4π component was however not trivial. Indeed, differently from the [8+2] reaction, regeneration of the catalyst is not possible by hydrolysis, unless the cycloaddition proceeds in a very stepwise manner and hydrolysis occurs prior to cyclization. However, a more general strategy would be the design of a diene capable of eliminative catalyst release after the cycloaddition events. The formation of a double bond in this particular position excludes, for example, 4π components leading to bridged cycles (such as tropone), as an unstable bridgehead double bond would be formed. Moreover, the presence of an EWG group on the terminal double bond of such diene might promote the elimination enabling an E1cB pathway, rendering, for example, the relative position of the catalyst and the substituent next to it completely irrelevant for this step to occur. Finally, enclosing part of the conjugated system into a cycle, might render the whole structure more rigid and prone to adopt an *s-cis* conformation, favorable for the cycloaddition reaction All these features considered, we envisioned that indene-2-carbaldehydes **1**, turned into electron rich amino isobenzofulvenes by reaction with aminocatalysts **3**, might render stable [10+4] cycloaddition products upon reaction with electron-poor dienes **2** (Scheme 14). If the control of the diastereoselectivity of the reaction might be facilitated by the natural tendency of these cycloaddition to undergo *exo* or *endo* approaches selectively, the control of the enantioselectivity is more challenging. In a polyconjugated system in fact, controlling the exact geometry of the enamine is more difficult than with those derived from simple aldehydes. Indeed, some computational calculations will be presented, in order to address the role of some additives and the origins of the stereoselectivity of this novel [10+4] cycloaddition.

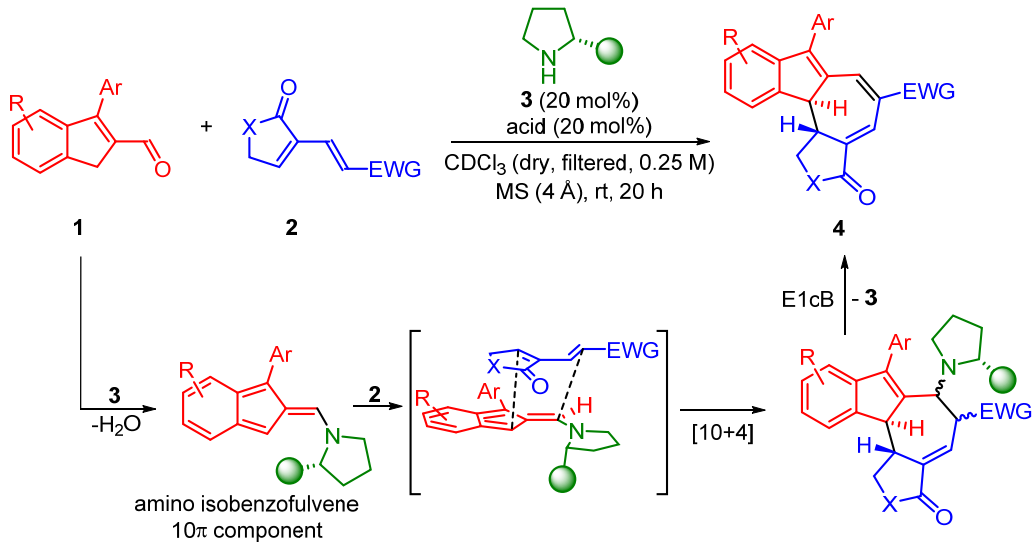

Scheme 14. Project overview.

6.3 Results and discussion

Initially, the reaction between 1*H*-indene-2-carbaldehyde **1a** and diene **2a** (1.5 eq) catalyzed by diphenylprolinol silyl ether **3a**[71,30c,33] (20 mol%) in $CDCl_3$ was probed.[133] The reaction afforded a complex product mixture including mainly Michael adducts, the desired [10+4] cycloadduct **4aa** and traces of a presumed [8+2] cycloadduct (Table 1, entry 1). Reaction analysis was complicated by isomerization of the indene double bond in **4aa**, leading to byproduct **4'aa**. Nevertheless, small amounts of non-racemic **4aa** were isolated. 3-Phenyl substituted indene **1b** was found to ease analysis of the reaction mixture. Notably, no double-bond isomerization and no Michael- or [8+2] adducts were observed. Furthermore, the yield and enantioselectivity were improved and only one diastereoisomer of cycloadduct **4ba** was observed (entry 2). In both these reactions molecular sieves were applied, since catalyst release does not rely on hydrolysis and removal of water might be beneficial, speeding up the reaction; however, the real benefit of their presence will be verified deeply later (*vide infra*). After observing the [10+4]-reactivity of indene-2-carbaldehyde **1b** with electron-deficient diene **2a**, a screening of seven aminocatalysts (**3a**-**g**) was conducted, revealing catalyst **3b** as optimal (entry 3). In some cases, reappearance of byproduct **4'** (**4'ba**) was noted (entries 6 and 7). Notably, *C2*-symmetric catalyst **3c** was also quite efficient in promoting the reaction (entry 4) and thiourea-derivative **3g** produced, as expected the opposite enantiomer compared to **3a** or **3b**, however with less satisfactory results (entry 8).

Table 1. Initial investigations and catalyst screening in the [10+4] cycloaddition between aldehydes **1** and dienes **2**.[a]

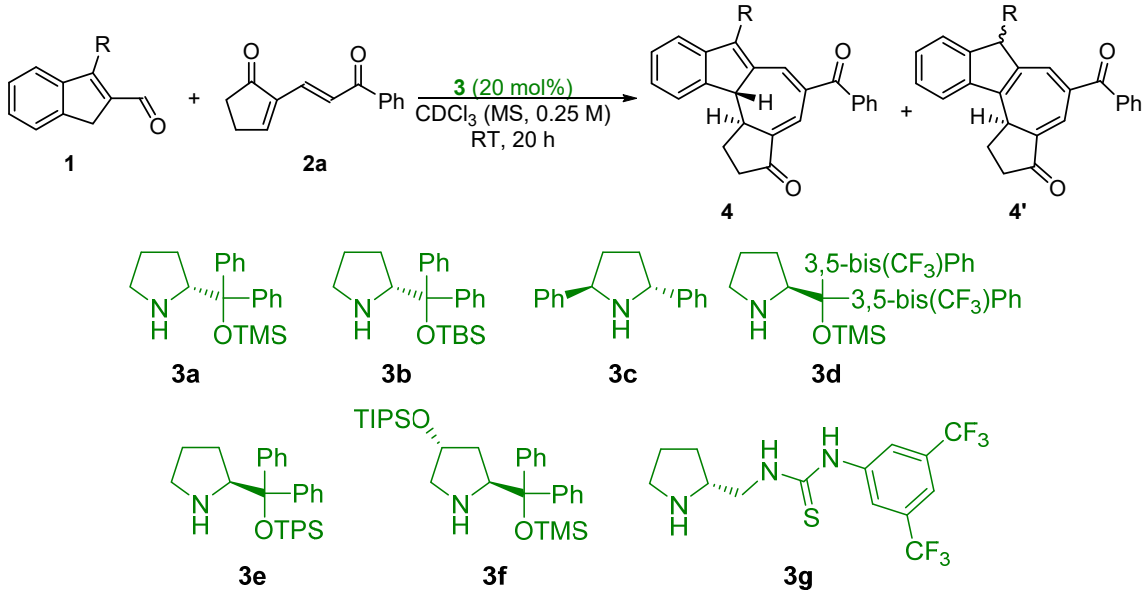

Entry	**1**, R	Catalyst	Consumption[b] (%)	NMR yield[c] (%)	ee[d] (%)
1	**1a**, H	**3a**	> 95	5[e]	11
2	**1b**, Ph	**3a**	75	57	82
3	**1b**, Ph	**3b**	60	41	87
4	**1b**, Ph	**3c**	75	56	84
5	**1b**, Ph	**3d**	44	< 5	-
6	**1b**, Ph	**3e**	75	43[e]	55[f]
7	**1b**, Ph	**3f**	> 95	38[e]	62[f]
8	**1b**, Ph	**3g**	70	40	30[f]

(**a**) Reaction conditions: **1** (0.05 mmol), **2a** (0.075 mmol), **3** (0.01), $CDCl_3$ (200 µL), RT, 20 h. (**b**) Consumption of the limiting reagent **1**, determined on the crude mixture by ^1H NMR in comparison to $SiEt_4$ as internal standard. (**c**) Determined on the crude mixture by ^1H NMR in comparison to $SiEt_4$ as internal standard. (**d**) Determined by CSP UPCC on the isolated product **4**. (**e**) Formation of **4'** was observed (**f**) The major enantiomer of product **4**

Since the results, in terms of enantioselectivity and conversion, were still not completely satisfactory, we investigated the influence of different solvents; at the same time, the effect of MS was tested, repeating some of the reactions in their absence. Surprisingly, the postulated positive effect was observed only in $CDCl_3$, where they were found to be beneficial for the enantioselectivity (Table 2, entry 7). On the other hand, in the presence

of MS, the reaction run in THF barely proceeded (entry 3), the one in acetonitrile showed a significant loss in yield and enantioselectivity (entry 5) and the one in DCM gave improved yields but lower enantiomeric excesses (entry 2).

Table 2. Solvent screening.[a]

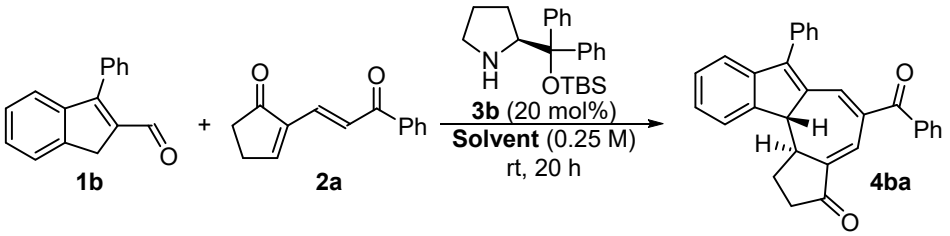

	Reactions run without MS				Reactions run with MS			
Entry	Solvent	Cons.[b] (%)	Yield[c] (%)	ee[d] (%)	Solvent	Cons.[b] (%)	Yield[c] (%)	ee[d] (%)
1	**Toluene**	85	56	58	-[e]	-	-	-
2	**CH_2Cl_2**	70	44	81	**CH_2Cl_2**	74	68	74
3	**THF**	94	69	69	**THF**	43	trace	-
4	**Et_2O**	100	54	64	-[e]	-	-	-
5	**MeCN**	100	92	58	**MeCN**	100	68	5
6	**MeOH**	94	74	-[7[e]]	-[e]	-	-	-
7	**$CDCl_3$**	55	41	73	**$CDCl_3$**	60	41	87

(**a**) Reaction conditions: **1b** (0.05 mmol), **2a** (0.075 mmol), **3** (0.01), $CDCl_3$ (200 µL), RT, 20 h. (**b**) Consumption of the limiting reagent **1**, determined on the crude mixture by ^{1}H NMR in comparison to $SiEt_4$ as internal standard. (**c**) Determined on the crude mixture by ^{1}H NMR in comparison to $SiEt_4$ as internal standard. (**d**) Determined by CSP UPCC on the isolated product **4ba**. (**e**) Reactions in PhMe, Et_2O and MeOH were not repeated in the presence of MS.

At this point, it was hypothesized that a protic additive, such as water, was essential for the cycloaddition to proceed, as strongly suggested by the reactions run in THF, and was also beneficial for the enantioselectivity, as shown by the reactions run in acetonitrile. This might explain the singular behavior of $CDCl_3$, as it may contain traces of DCl, a strong mineral acid, capable of promoting the reaction. When water is removed, the acidity of DCl in $CDCl_3$ is increased, as it does not get "solvated" from water. In all the other solvents, where traces of acid are not present, the water, generated from the reaction, takes the role of this protic additive.

This hypothesis was proven in multiple ways. First of all, since DCl is produced from $CDCl_3$ upon standing in air, $CDCl_3$ from two different batches was employed as the solvent for two otherwise identical reactions. As it is possible to see in Table 3, results obtained from a freshly opened bottle (blue) resembled more closely the ones obtained in CH_2Cl_2, while the ones from the "old" batch (red) matched the previously obtained ones. Again, the presence of MS (entry 2) was beneficial only when a significant amount of DCl was present (old batch). Secondly, upon filtering the $CDCl_3$ through a short plug of activated basic alumina (thus removing DCl) and running the reaction in the presence of MS (removing water as well) the reactivity was completely suppressed, in both cases (entry 3).

Table 3. Results obtained when $CDCl_3$ from two different batches was employed as solvent.[a]

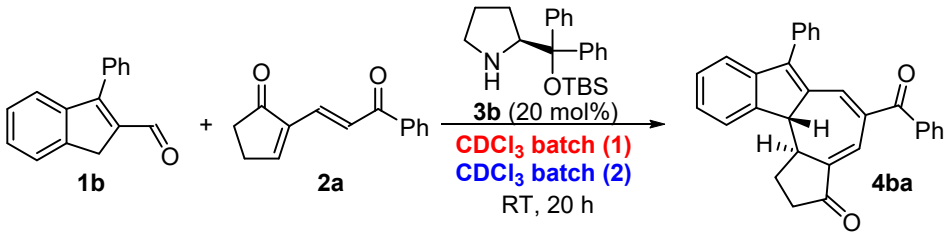

Results from different bottles of $CDCl_3$: old batch (1), freshly opened batch (2)

Entry	Solvent treatment	Consumption[b] (%)	NMR yield[c] (%)	ee[d] (%)
1	-	55, 43	37, 17	73, 51
2	**MS**[e]	73, 46	50, 7	85, 44
3	**MS**[e], **F**[f]	35, 35	trace, trace	-, -

(**a**) Reaction conditions: **1b** (0.05 mmol), **2a** (0.075 mmol), **3** (0.01), $CDCl_3$ (200 µL), RT, 20 h. (**b**) Consumption of the limiting reagent **1**, determined on the crude mixture by ^{1}H NMR in comparison to $SiEt_4$ as internal standard. (**c**) Determined on the crude mixture by ^{1}H NMR in comparison to $SiEt_4$ as internal standard. (**d**) Determined by CSP UPCC on the isolated product **4ba**. (**e**) MS added to the reaction mixture. (**f**) Solvent filteret through a short plug of activated basic Al_2O_3 prior to reaction setup.

All these features considered, important hints for optimizing the reaction could be achieved. First, an acid additive is essential for the reaction to proceed and improves the enantioselectivity greatly. Secondly, although in the absence of the acid MS showed a detrimental role, in its presence they helped both with reactivity and stereoselectivity.

Thus, acid additives were found to restore reactivity in a reproducible fashion. Catalyst **3b** with benzoic acid (BA, 20 mol%) provided **4ba** in 77% yield and 90% *ee* (Table 4, entry 1). In order to verify that a bulky catalyst was still necessary, **3a** was tested again

under the optimized reaction conditions, giving **4ba** in 80% yield and 83% *ee* (entry 2), confirming **3b** as the optimal choice. The nature of the acid additive was found to be important as well. For example, exceeding the aminocatalyst loading was detrimental both to the yield and the enantioselectivity (compare entry 3 and 1), very strong acids such as trifluoroacetic acid (TFA) impaired the reaction at all (entry 4), such as phenols (2,4-dinitrophenol, 2,4-DNP, entry 5), acetic acid performed worse than benzoic acid (entry 6). Having identified in benzoic acids the most promising motif, some different substituents were tested. While *p*-nitrobenzoic (entry 7) acid and *o*-fluorobenzoic (entry 8) acids gave less satisfactory results, *p*-methoxybenzoic acid was found to be the optimal choice, rendering product **4ba** in 69% yield and 92% ee (entry 9). Importantly, diminishing the acid loading to 10 mol% resulted in decreased yield but equally high enantiomeric excess (compare entries 9 and 10). It was found at the same time that reversing the stoichiometry of the reaction in favor of **1a** (1.5 equiv) improved the isolated yield to 82% and eased the purification process, maintaining an optimal 92% ee value (entry 11). Ultimately, the importance of the MS was checked again under the very last optimized conditions, and it was confirmed to be beneficial both in terms of yield and stereoselectivity (compare entries 10 and 12).

Table 4. Acid additive screening.[a]

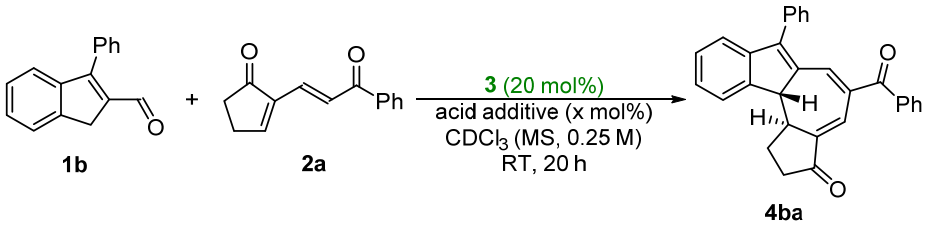

Entry	Catalyst	$CDCl_3$[b]	Additive (mol%)	Consumption[c] (%)	Yield[d] (%)	ee[e] (%)
1	**3b**	MS, F	BA (20)	> 95	77	90
2	**3a**	MS, F	BA (20)	> 95	80	83
3	**3b**	MS, F	BA (40)	90	60	77
4	**3b**	MS, F	TFA (20)	39	< 5	-
5	**3b**	MS, F	2,4-DNP (20)	36	< 5	-
6	**3b**	MS, F	AcOH (20)	48	41	85
7	**3b**	MS, F	*p*-NO_2-BA (20)	50	31	78
8	**3b**	MS, F	*o*-F-BA (20)	82	69	82
9	**3b**	MS, F	*p*-MeO-BA (20)	93	69	92
10	**3b**	MS, F	*p*-MeO-BA (10)	69	41	92
11[f]	**3b**	MS, F	*p*-MeO-BA (20)	> 95	82[g]	92
12[f]	**3b**	F	*p*-MeO-BA (20)	70	64	84

(**a**) Reaction conditions: **1b** (0.05 mmol), **2a** (0.075 mmol), **3** (0.01), $CDCl_3$ (200 µL), RT, 20 h. (**b**) MS means that molecular sieves were added to the reaction mixture. F means that solvent was filtered through a short plug of activated basic Al_2O_3 prior to reaction setup. (**c**) Consumption of the limiting reagent **1b** (or **2a**), determined on the crude mixture by ^1H NMR in comparison to $SiEt_4$ as internal standard. (**d**) Determined on the crude mixture by ^1H NMR in comparison to $SiEt_4$ as internal standard. (**e**) Determined by CSP UPCC on the isolated product **4ba**. (**f**) Reaction conditions: **1a** (0.15 mmol), **2a** (0.1 mmol), **3** (0.02), $CDCl_3$ (400 µL), RT, 20 h. (**g**) Isolated yield.

The substrate scope was then investigated (Scheme 15). In general, excellent diastereoselectivity was observed. Phenyl groups of various electronic nature on the 3-position of 1*H*-indene-2-carbaldehydes **1** led to the formation of [10+4] cycloadducts **4ba-ea** in high yields and enantioselectivities. *ortho*-Tolyl and 1-naphthyl substituted indenes delivered **4fa** and **4ga**, respectively, in high yields and enantioselectivities, as 1:1 diastereomeric mixtures due to hindered axial rotation. 2-Naphthyl and 5-(1,3-

(benzodioxyl)) substituted **4ha** and **4ia** were achieved in high yields and enantioselectivities as single diastereomers. A heteroaromatic substituent was well-tolerated and **4ja** was formed in excellent yield and enantioselectivity. In a 10-fold scale-up with no procedural modifications, the excellent stereoselectivity was maintained and a slight improvement to 95% yield was achieved. Unfortunately, only indenes **1** carrying aromatic substituents at position 3 were found to be reactive towards **2a** (Me-, *t*-Bu- and vinyl-substituted indenes were tested).

Successful variations of the benzofused ring were performed with indenes bearing methoxy-, chloro- and methyl substituents granting access to cycloadducts **4ka**-**na** in high yields and enantioselectivities. An attempt to introduce a methyl substituent at position 11 or a chlorine in position 8 resulted only in trace product formation.

Various 4π-components **2** were also tested and it was found that the phenyl ketone could be decorated with halogens, electron-donating, and electron-withdrawing groups affording **4ab**-**4ad** in good to high yields and enantioselectivities. Similar good results were obtained with a methyl ketone (**4ae**). Employment of esters as electron-withdrawing groups resulted in slightly lower enantioselectivity, however, the high yield was maintained (**4af** and **4ag**). The nitrile containing cycloadduct **4ah** was also obtained, albeit in low yield and enantioselectivity. As an alternative to the cyclopentenone core of the 4π-component, a lactone was found to deliver cycloadduct **4ai** with an enantioselectivity comparable to other esters (**4af** and **4ag**). However, similarly to nitrile substituted 4π-component **2h**, extensive degradation of the lactone substrate **2i** occurred, resulting in low yield. The absolute configuration of **4ka** was determined by X-ray crystallographic analysis and the stereochemistry of the remaining cycloadducts **4** was assigned analogously.

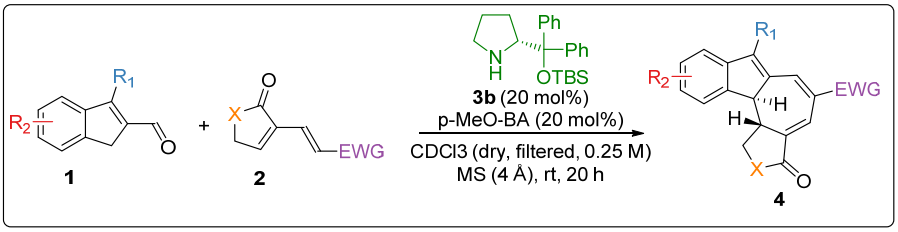

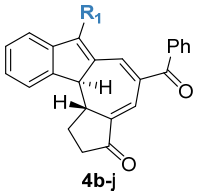

4b-j

R_1 = H,
R_1 = Me
R_1 = *t*-Bu
R_1 = vinyl
} product not observed

4ba; Ph	85%, >20:1 dr, 92% *ee*
4ca; p-MeO-C_6H_4	89%, >20:1 dr, 92% *ee*
4da; p-F-C_6H_4	89%, >20:1 dr, 90% *ee*
4ea; p-CF_3-C_6H_4	84%, >20:1 dr, 92% *ee*
4fa[a]; o-Me-C_6H_4	84%, 1:1 dr (rotamers), 85/84% *ee*
4ga; 1-naphthyl	82%, 1:1 dr (rotamers), 81/74% *ee*
4ha; 2-naphthyl	81%, >20:1 dr, 90% *ee*
4ia[b]; 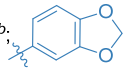	83%, >20:1 dr, 95% *ee*
4ja; 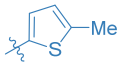	91%, >20:1 dr, 95% *ee* [c]95%, >20:1 dr, 94% *ee* (0.42 g)

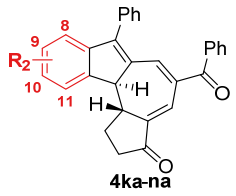

4ka-na

4ka; 10-Cl	86%, >20:1 dr, 90% *ee*
4la; 10-MeO	83%, >20:1 dr, 95% *ee*
4ma[a]; 9-MeO	82%, >20:1 dr, 92% *ee*
4na[b]; 9-Me	79%, >20:1 dr, 95% *ee*

R_2 = 11-Me
R_2 = 8-Cl
} product not formed

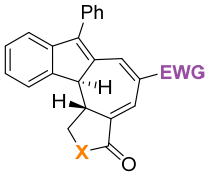

4ab-ai

4ab; CO(p-Br-C_6H_4), CH_2	88%, >20:1 dr, 93% *ee*
4ac[b]; CO(p-MeO-C_6H_4), CH_2	84%, >20:1 dr, 89% *ee*
4ad; CO(p-NO2-C_6H_4), CH_2	70%, >20:1 dr, 88% *ee*
4ae; COMe, CH_2	79%, >20:1 dr, 90% *ee*
4af; CO_2Et, CH_2	81%, >20:1 dr, 80% *ee*
4ag; CO_2Ph, CH_2	89%, >20:1 dr, 83% *ee*
4ah[d]; CN, CH_2	44%, >20:1 dr, 36% *ee*
4ai[d,e]; CO_2Et, O	27%, >20:1 dr, 76% *ee*

Scheme 15. Reaction scope. Isolated yields. Diastereomeric ratio determined by NMR of crude reaction mixture. Enantiomeric excess determined by chiral-stationary phase UPCC. Reaction conditions: **1** (0.15 mmol), **2** (0.1 mmol), **3** (0.02), $CDCl_3$ (400 µL), MS, RT, 20 h. (**a**) Reaction performed at 40 °C. (**b**) Reaction performed with 10 mol% *p*-MeO-BA. (**c**) Reaction performed on 1.0 mmol scale. (**d**) Extensive degradation of **2** observed. (**e**) Indene **1b** applied as limiting reagent with 2 equiv of **2**.

Having demonstrated the stereoselective formation of a range of [10+4]-cycloadducts **4**, the possibility of selectively modifying the tetracyclic products was explored. Specifically, the indene moiety was targeted for application as a nucleophile. Treatment with Michael acceptor **5** in the presence of quinuclidine delivered **6** containing an all-carbon quaternary stereocenter in 40% yield, maintaining the high enantiomeric excess (Scheme 16).

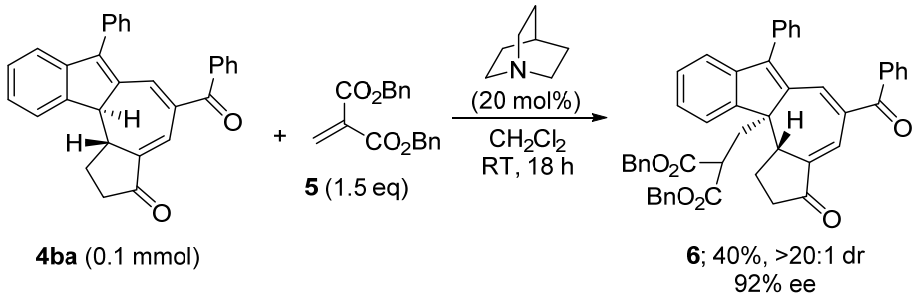

Scheme 16. Functionalization of product **4ba** through a Michael addition strategy.

The reaction of **4ja** with cinnamaldehyde **7** was facilitated by a catalytic amount of pyrrolidine (necessary for reactivity) and quinuclidine. Michael addition onto the iminium-ion activated cinnamaldehyde is proposed, followed by intramolecular [4+2] cycloaddition through an enol/enamine, granting access to the multi-bridged polycyclic compound **8** in 76% yield with maintained enantiomeric excess as a mixture of two diastereoisomers (Scheme 17). This structure is proposed based on NMR analysis and is supported by computational NMR studies.

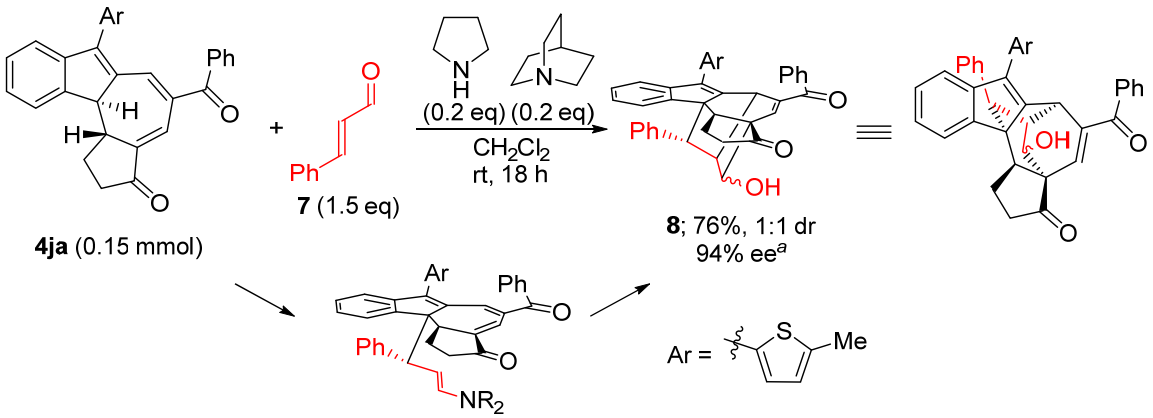

Scheme 17. Functionalization of product **4ja** through Michael addition-intramolecular [4+2] cycloaddition.

6.3.1 Computational investigations

In the [10+4] cycloaddition between 3-substituted 1*H*-indene-2-carbaldehydes **1** through amino isobenzofulvenes and dienes **2**, excellent diastereoselectivity is observed. Products **4** are formed with *anti*-configuration in agreement with the reaction proceeding through an *exo*-transition state. This is expected to be favorable in [6+4] cycloadditions due to unfavorable interactions in the *endo*-approach (Scheme 18).[110]

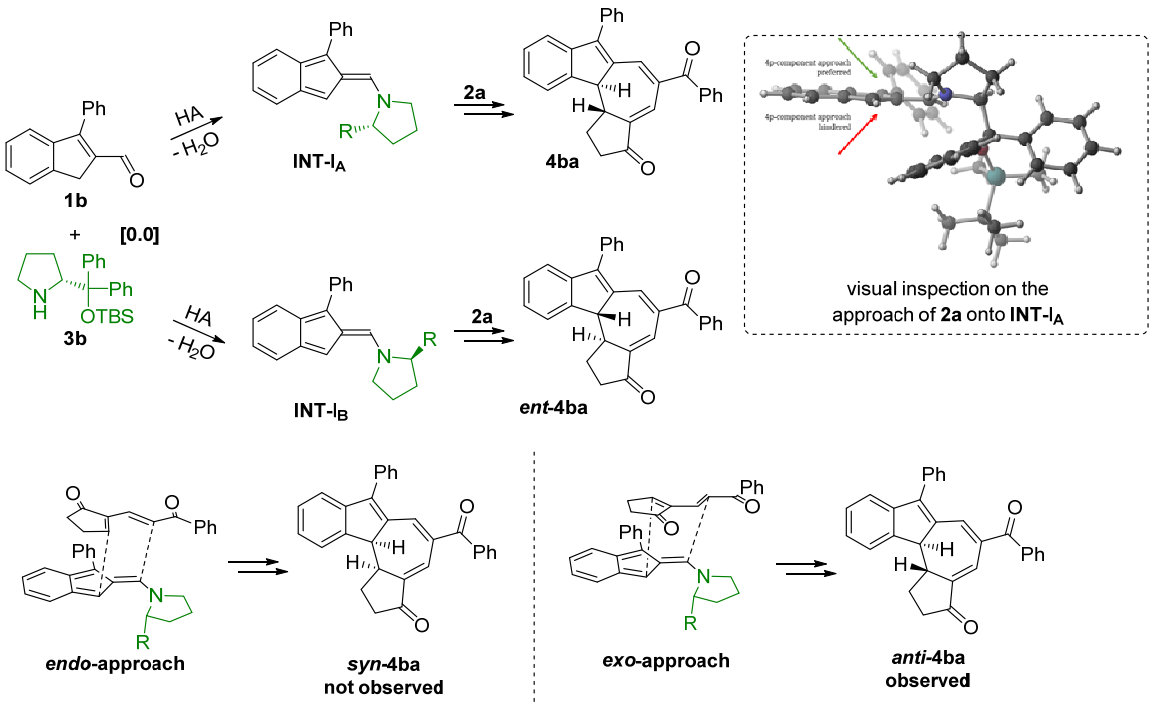

Scheme 18. [10+4] cycloaddition between **1b** and **2a** catalyzed by **3b**: relevant intermediates, visual inspection on the facial selectivity and *endo*/*exo* approach.

A significant effect on enantioselectivity was exerted by acid additives and water in the reaction when catalyst **3b** was employed. Moreover, by visual inspection, it was deemed unlikely that **INT-I$_B$** could lead to **4ba** or **INT-I$_A$** could lead to ***ent*-4ba** with diene **2a** approaching from the sterically hindered face. Based on this experimental observation the following hypothesis was formulated (Scheme 18).

"The enantioselectivity of the present [10+4] cycloaddition arises from a kinetical preference for the formation of isobenzofulvene INT-I$_A$ leading to 4ba over INT-I$_B$ leading to *ent*-4ba". Thus, it should not depend on the conjugate addition of the amino isobenzofulvenes onto **2**. This was stated since the acid additive is postulated to play a fundamental role in the condensation of **3b** and **1** leading to **INT-I$_A$** and **INT-I$_B$**, rather than in other steps. However, since we were not able to observe the intermediates by NMR analysis and computational modelling of such condensations is very difficult, we sought to prove the hypothesis indirectly. At the end of the following session the exact role of the acid in enhancing the enantioselectivity will not be addressed, as it does not stand in our interest. It served indeed as a hint for the formulation of the mechanistic hypothesis.

For the previous statement to be verified and relevant, some experimental and computational features have to be addressed.

1) There is not a thermodynamic preference for **INT-I$_A$** over **INT-I$_B$**, i.e. **INT-I$_A$** is not the only amino isobenzofulvene intermediate that might be formed.

2) There is no equilibration between **INT-I$_A$** and **INT-I$_B$**, either through reversion to **1** and **3b** or through σ-bond rotation. This is very important, otherwise, point 1) being verified, either a balanced mixture of intermediates or a preference for **INT-I$_B$** would be observed.

3) The pathway leading to **4ba** from **INT-I$_A$** should not be strongly favorable with respect to the one leading to ***ent*-4ba** from **INT-I$_B$**. In the latter case the statement of the kinetic preference of one intermediate over the other might be true, but not relevant for the enantioselectivity dictation.

4) In the case of a catalyst for which **INT-I$_A$** and **INT-I$_B$** are the same compound, (i.e. such catalyst possesses *C2* symmetry) no influence of an acid additive should be observed on the enantioselectivity.

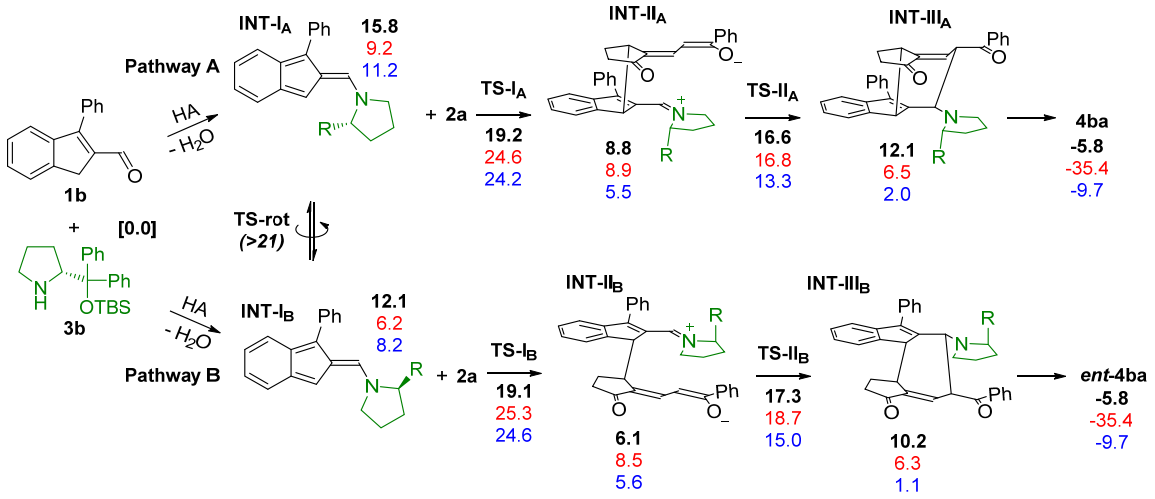

Scheme 19. Computational investigation on the reaction pathway. Relative free energies in kcal/mol (B3LYP-gd3/6-31G(d,p) SMD ($CHCl_3$)) are presented in bold (rotational TS energy in *italics* is an electronic energy relative to INT-I$_B$). Single-point electronic energies were calculated using M062x/6-311+G(d,p) SMD ($CHCl_3$) (red) and wB97x-D/6-311+G(2d,p) SMD ($CHCl_3$) (blue), thermal corrected values are presented.

Through computational and experimental investigations, we were able to verify the following.

1) **INT-I$_B$** was calculated to be 3.7 kcal/mol lower in energy than **INT-I$_A$** (Scheme 19). This suggests that **INT-I$_A$** is kinetically formed under the optimized reaction

conditions, or that it could be a Curtin-Hammett scenario, if equilibration of the structures was possible.

2) The positive effect on enantioselectivity observed upon removal of water under the optimized conditions could owe to a shut-down of reversibility of iminium-ion formation and hence eliminate the potential for equilibration between **INT-I$_A$** and **INT-I$_B$**. To investigate if the rotational barrier between the two is too high to allow for direct interconversion at room temperature, the intermediate was optimized computationally. A scan of the relevant dihedral revealed a barrier of >21 kcal/mol suggesting that **INT-I$_A$** and **INT-I$_B$** are distinct intermediates (Scheme 19).

3) The formation of **4ba** and ***ent*-4ba** from **INT-I$_A$** and **INT-I$_B$**, respectively, was studied computationally by reaction pathway analysis (Scheme 19).[134] The calculations suggest that formation of either **INT-I$_A$** or **INT-I$_B$** is an endergonic process, and that conjugate addition to **2a** proceeds via low barriers and is energetically viable. No concerted pathways for the formation of **INT-III$_A$** or **INT-III$_B$** were found, suggesting a step-wise cycloaddition. Reasonable barriers for the closure of zwitterionic species **INT-II$_A$** and **INT-II$_B$** were located. Pathway **A** leading to **4b** contains higher energy intermediates but lower barriers, while pathway **B** leading to ***ent*-4ba** contains lower energy intermediates but higher barriers. Both pathways contain reasonable barriers for reactivity at room temperature. Thus, if the two intermediates were formed equally in solution, a nearly racemic mixture of **4ba** and ***ent*-4ba** would be expected as both pathways are energetically viable.

4) By employment of the C_2-symmetric catalyst **3c**,[135] for which **INT-I$_A$** and **INT-I$_B$** are equivalent due to the rotational symmetry axis of the catalyst (Scheme 20), the presence of an acid additive and water were found to have no measurable effect on the enantioselectivity. This strongly suggests that those two factors have an effect on the distribution or reactivity of the two rotamers of the amino isobenzofulvene formed from catalyst **3b** and indenes **1**.

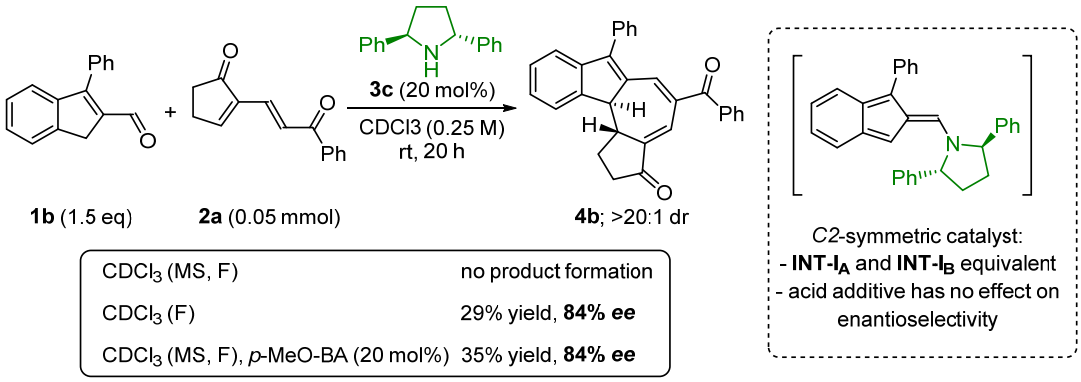

Scheme 20. Additive effects on stereochemistry with C_2-symmetric catalyst. Yield and dr measured by ^{1}H NMR of the crude reaction mixture with $SiEt_4$ as internal standard. Enantiomeric excess determined by chiral-stationary phase UPCC. "F" means that solvent was filtered through a short plug of activated basic alumina prior to reaction set up.

All these features considered it is now clear why, if not exactly how, the removal of water and the presence of an acid additive are important for the enantioselectivity of the reaction, which has been addressed both computationally and experimentally.

6.3.2 Determination of the relative configuration of compound 6.

The following assignments were established on the basis of the gCOSY and HSQC NMR experiments (Table 5, Figure 1and Figure 2):

Table 5. Assignments performed on compound **6**.

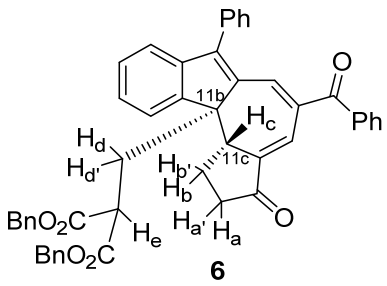

6

Signal ppm	H value	Assignment
3.27	1	H_c
2.87-2.74	3	H_d, $H_{d'}$, H_e
2.64	1	H_a
2.44-2.23	3	H_b, $H_{b'}$, $H_{a'}$

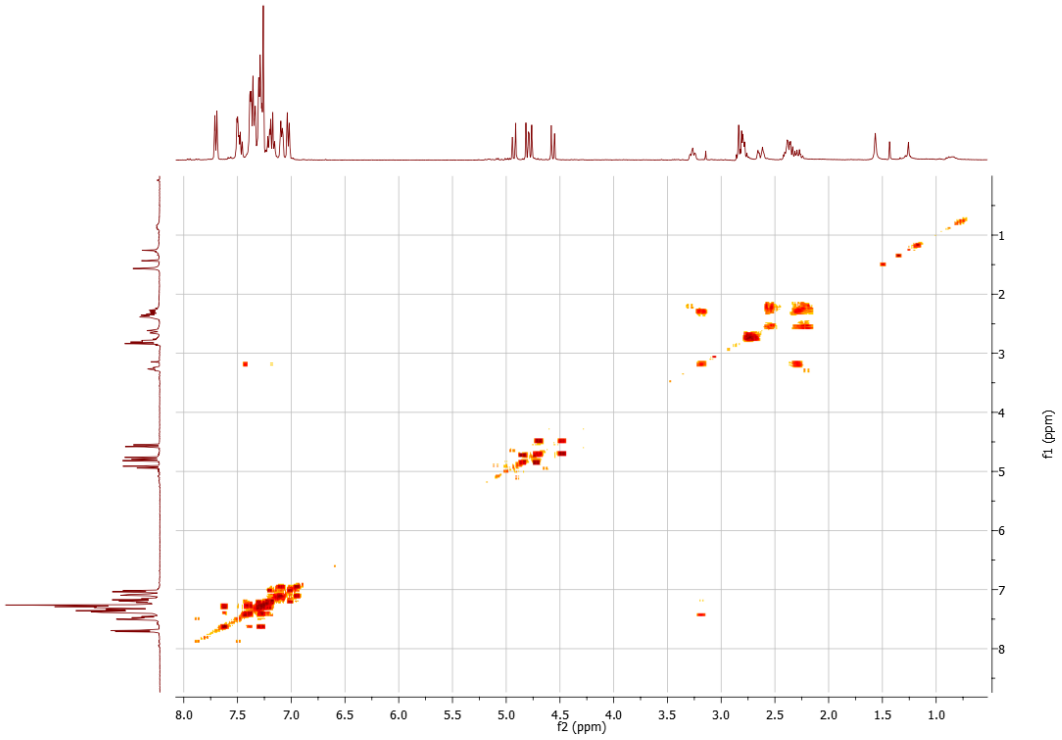

Figure 1. gCOSY NMR spectrum of compound **6**.

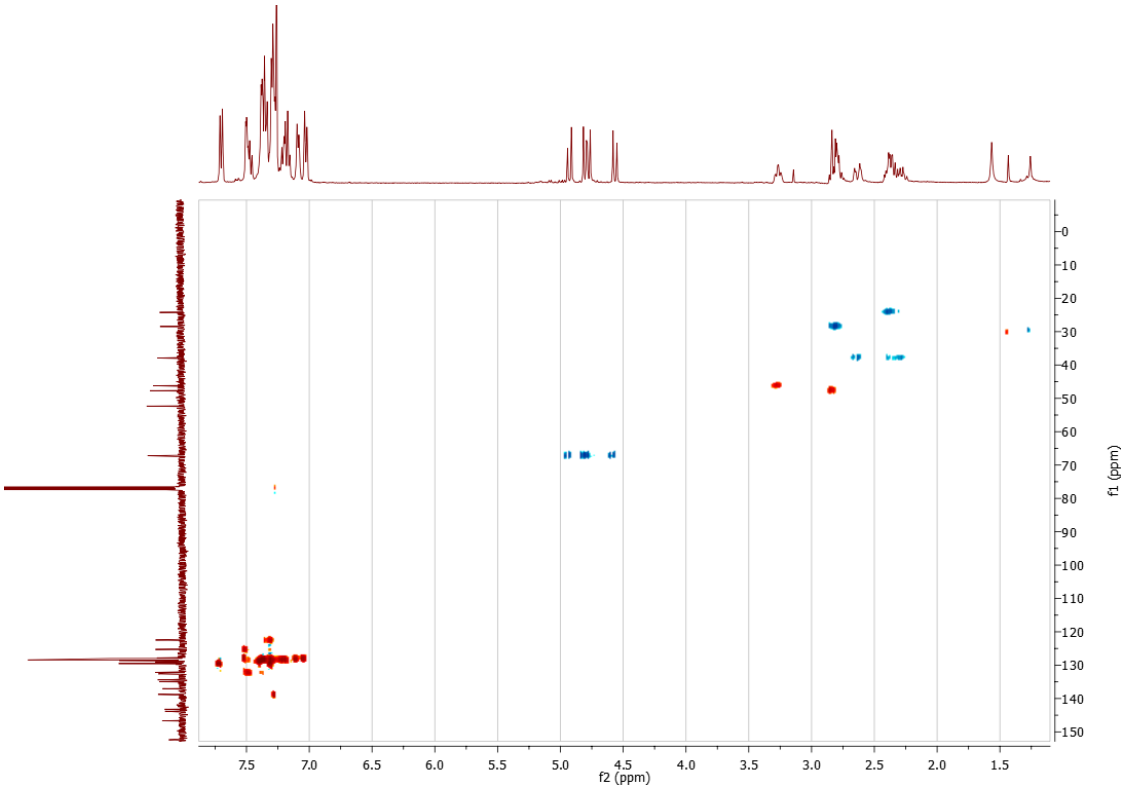

Figure 2. gHSQC NMR spectrum of compound **6**.

The relative stereochemistry at carbons 11b and 11c was assigned on the basis of the closer space proximity in space of H_d/H_d' to H_b/H_b' than to H_c (as shown by the NOESY experiment). The two possible structures **6** and **6'** were optimized computationally and the distances between H_d/H_d' and H_b/H_b' or H_c were deduced from the obtained structures. Indeed, it was observed that H_d/H_d' are closer (2.1 Å) to H_b/H_b' than to H_c only for **6**, and the opposite is observed for **6'** (Figure 3). The NOESY spectrum is thus in accordance to the calculated distances and is distinctive for the relative configuration of compound **6**. The absolute configuration is deduced from the one of **4ba**, since the chirality of carbon 11c is left untouched in the reaction.

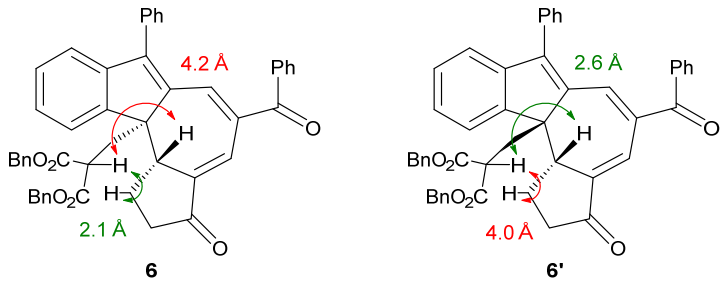

Figure 3. Relevant distances on the optimized structures of **6** and **6'**.

The structure and the relative (and absolute) configuration of compound **8** were proposed on the basis of the whole set of 1D and 2D NMR spectra and confirmed by computational NMR studies. A full explanation on the methods employed is discussed in the Supporting Information of *Angew. Chem. Int. Ed.* **2018**, *57*, 13182 to which the author invites the reader to refer, since they go beyond the scope of this thesis.

6.4 Conclusion

In conclusion, the boundaries of higher-order cycloadditions were pushed as the first catalytic enantioselective [10+4] cycloaddition reaction was developed. This became possible when indene-2-carbaldehydes **1** (10π-components) where reacted with electron-poor dienes **2** (4π-components), in the presence of catalyst **3b**, an acidic co-catalyst and molecular sieves (MS). After E1cB-type catalyst release, complex tetracyclic scaffolds **4** were obtained as single diastereoisomers, in very high yields and enantioselectivities. A careful optimization of the reaction conditions revealed that both the reactivity and the enantioselectivity of the process were heavily related to the removal of water and to the presence of the acidic co-catalyst. Moreover, experimental and computational evidence suggest that the observed stereoselectivities arise from kinetically controlled amino isobenzofulvene formation.

The scope of the reaction was investigated and 21 different cycloadducts **4** were synthesized, varying the nature of the aryl substituent, the decoration of the indene moiety in **1** or of the phenyl ketone in **2**; different EWGs were also tolerated, as well as lactones, instead of cycloalkenones. High yields, coupled with high peri-, diastereo- and enantioselectivity, and a broad substrate scope made this methodology valuable towards the development of complex enantioenriched scaffolds and displayed an unusually robust higher-order cycloaddition. Moreover, the obtained compounds **4** were amenable of interesting functionalizations for the construction of quaternary chiral centres or multi-bridged polycyclic molecules (Scheme 21).

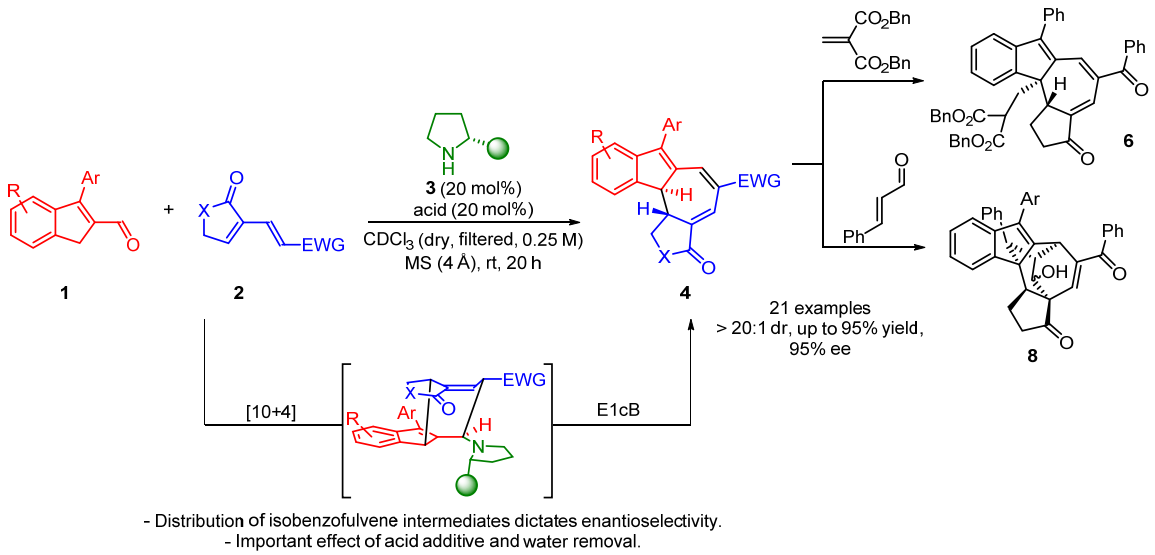

Scheme 21. Organocatalytic [10+4] cycloadditions: project summary.

6.5 Experimental details

6.5.1 General methods and materials

NMR spectra were acquired on a Bruker AVANCE III HD spectrometer running at 400 MHz for ^{1}H, 100 MHz for ^{13}C and 376 MHz for ^{19}F. Chemical shifts (δ) are reported in ppm relative to residual solvent signals ($CDCl_3$, 7.26 ppm for ^{1}H NMR, $CDCl_3$, 77.0 ppm for ^{13}C NMR). Chemical shifts (δ) for ^{19}F NMR are reported in ppm relative to $CFCl_3$ as external reference. The following abbreviations are used to indicate the multiplicity in NMR spectra: s, singlet; d, doublet; t, triplet; q, quartet; m, multiplet. ^{13}C NMR and ^{19}F NMR spectra were acquired in broad band decoupled mode. Mass spectra were recorded on a Bruker Maxis Impact-TOF-MS with electrospray ionization (ESI+) (referenced to the mass of the charged species). Analytical thin layer chromatography (TLC) was performed using pre-coated aluminum-backed plates (Merck Kieselgel 60 F254) and visualized by ultraviolet radiation and/or staining with $KMnO_4$ or vanillin. For flash column chromatography (FC) silica gel (Silica gel 60, 230-400 mesh or Iatrobeads) was used. Optical rotations were measured on a Bellingham+Stanley ADP440+ polarimeter, α values are given in deg·cm^{3}·g^{-1}·dm^{-1}; concentration "c" in g·(100 mL)$^{-1}$.The diastereomeric ratio (dr) of products was evaluated by ^{1}H NMR analysis of the crude mixture. The enantiomeric excess (ee) of the products was determined by Ultra-Performance Convergence Chromatography (ACQUITY UPCC) using Daicel Chiralpak columns (IA, IB, IC and ID) as chiral stationary phases. Unless otherwise noted, gradient runs were performed with 99:1 supercritical CO_2/solvent for 30 sec, then going from 99:1 to 60:40 CO_2/solvent over 4 min, then isocratic 60:40 CO_2/solvent. Reference samples

for UPCC analysis were prepared following the general method using a 1:1 mixture of the (*R*)- and (*S*)-diphenylprolinol *tert*-butyldimethyl silyl ether catalyst unless otherwise noted, analytical grade solvents and commercially available reagents were used without further purification. Below the general procedures, the characterization of the model compound only is reported. For a full description of all the products reported see the Supporting Information of *Angew. Chem. Int. Ed.* **2018**, *57*, 13182.

6.5.2 General procedure for the synthesis of indene 2-carbaldehydes 1

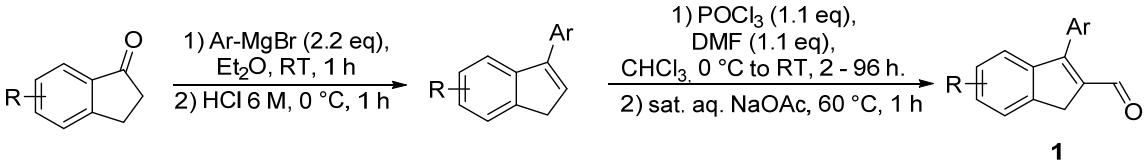

1

Step 1: Addition of Grignard reagents to indanones

In a flame-dried round-bottom flask equipped with a magnetic stirring bar, under inert atmosphere, a solution of 1-indanone (1 eq, 10 mmol) in Et_2O (or 1:1 Et_2O/THF for insoluble indanones) (anh., 20 mL) was added dropwise to a solution of the aryl-Grignard reagent (2.2 eq, 22 mmol) in Et_2O (13 mL) at RT (moderate heat evolution and a formation of a precipitate were usually observed).

A) Commercially available Grignard reagents (1-3 M solutions in Et_2O or THF) were diluted with Et_2O to the indicated volume.

B) For substrates **1e**, **1g**, **1h**, **1j** the Grignard reagents were prepared from commercially available bromides. In a flame-dried round-bottom flask equipped with a magnetic stirring bar and a condenser under an inert atmosphere, an iodine crystal was added to dry Mg turnings (365 mg) and heated while stirring until iodine vapor was observed. After 10 min, Et_2O (anh., 6 mL) was added. A solution of the bromide (2.2 eq, 22 mmol) in Et_2O (anh., 2 mL) was added dropwise, causing the mixture to boil without heating. Finally, an additional 5 mL of anh. Et_2O were added. The mixture was refluxed for 50 min and cooled to RT.

After the addition was completed, the reaction mixture was stirred at rt for 1 h. Then, it was cooled to 0 °C and 6 M HCl (10 mL) was added dropwise. The biphasic mixture was vigorously stirred at 0 °C for 1 h and then transferred to a separatory funnel. The phases were separated, the aq. phase was extracted with Et_2O (2 x 20 mL), the combined organic extracts were washed with sat. aq. Na_2CO_3 (2 x 20mL), dried over anh. Na_2SO_4, filtered and concentrated *in vacuo* to yield the desired 3-arylindene. This could be directly used in the next step or purified by FC on silica gel (pentane or 2% EtOAc in pentane).

Step 2: Vilsmeier formylation of 3-arylindenes

In a flame-dried round-bottom flask containing anh. *N*,*N*-dimethylformamide (1.1 eq, 11 mmol) under an inert atmosphere and cooled to 0 °C, $POCl_3$ (1.1 eq, 11 mmol) was added dropwise. The solution was then stirred at 0 °C until it became a crystalline white solid (within 5 min) and then at RT for an additional 10 min. $CHCl_3$ (anh., 6 mL) was added and the resulting suspension was cooled to 0 °C. To this, a solution of the previously prepared 3-aryl indene (1 eq, 10 mmol) in $CHCl_3$ (anh., 3 mL) was added dropwise. The reaction mixture was stirred at rt for 2–96 h (until full consumption of the starting material was observed by ^{1}H NMR). Sat. aq. NaOAc (20 mL) was added and the biphasic mixture was vigorously stirred at 60 °C for 1 h, cooled to RT, diluted with CH_2Cl_2 (20 mL) and water (10 mL) and transferred to a separatory funnel. The phases were separated, the aq. phase was extracted with CH_2Cl_2 (2 x 10 mL), the combined organic extracts were dried over anh. Na_2SO_4 and concentrated *in vacuo*. The 3-arylindene-2-carbaldehydes were isolated by FC on silica gel.

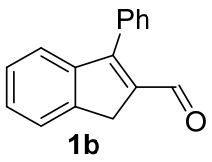

1b

3-Phenyl-1*H*-indene-2-carbaldehyde **1b** was isolated in 83% overall yield over two steps as a pale yellow solid by FC on silica gel (CH_2Cl_2). **^{1}H NMR (400 MHz, $CDCl_3$)** δ 9.92 (s, 1H), 7.62 (d, *J* = 7.2 Hz, 1H), 7.58–7.51 (m, 6H), 7.45 (m, 1H), 7.38 (m, 1H), 3.82 (s, 2H). **^{13}C NMR (100 MHz, $CDCl_3$)** δ 189.4, 159.0, 144.4, 143.7, 140.5, 132.0, 129.6 (2C), 129.3, 129.1, 128.7 (2C), 127.0, 124.9, 123.4, 36.0. **HRMS** (ESI+) *m/z* calcd. for $[C_{16}H_{12}O+H]^+$: 221.0961; found: 221.0963.

6.5.3 Synthesis of 4π-components 2

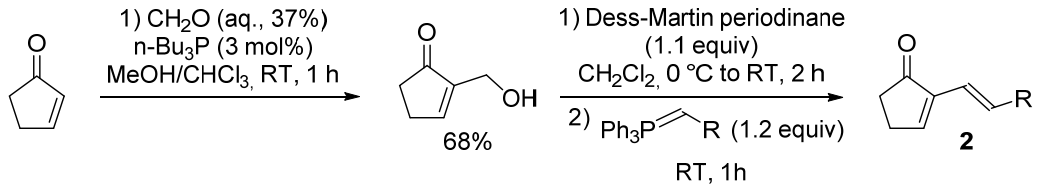

Step 1: Morita-Baylis-Hillman reaction of cycloalkenones and formaldehyde

The allylic alcohol was prepared following a modified literature procedure.[136] In a round-bottom flask equipped with a stirring bar, cyclopentenone (1 eq, 30 mmol) was dissolved in a mixture of MeOH (24 mL) and $CHCl_3$ (36 mL). Aq. formaldehyde (37%, 1.2 eq, 2.68 mL, 36 mmol) and a solution of *n*-Bu_3P (3 mol%, 0.225 mL, 0.9 mmol) in $CHCl_3$ (7.2 mL) were added. The mixture was stirred for 1 h at RT, after which the reaction had reached full conversion according to TLC analysis. The newly formed allylic alcohol was quickly dried *in vacuo* and purified by FC on silica gel (75% EtOAc in pentane) to yield an off-white crystalline solid in 68% yield. Data in accordance with those found in the literature.[136]

Step 2: One-pot oxidation-olefination of allylic alcohols utilizing Dess-Martin periodinane and Wittig reagents.

In a round-bottom flask equipped with a stirring bar, previously prepared allylic alcohol (1 eq) was dissolved in CH_2Cl_2 (concentration of allylic alcohol 0.3 M) and cooled to 0 °C. Dess-Martin periodinane (1.1 eq) was added, and the mixture was stirred for 2 h at rt. After full conversion confirmed by TLC analysis, the stabilized ylide was added at 0 °C and the mixture was stirred for 0.5 h, and then stirred for 0.5 h at rt. Finally, purification by FC on silica gel affords the diene.

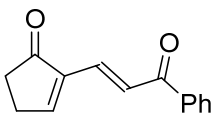

2a

(*E*)-2-(3-Oxo-3-phenylprop-1-en-1-yl)cyclopent-2-en-1-one **2a** was isolated in 40% yield as a pale yellow solid by FC, performed twice, on silica gel (CH_2Cl_2). **^{1}H NMR (400 MHz, $CDCl_3$)** δ 8.19 (d, *J* = 15.6 Hz, 1H), 8.05–8.00 (m, 2H), 7.87 (t, *J* = 3.0 Hz, 1H), 7.60–7.53 (m, 1H), 7.52–7.41 (m, 3H), 2.78–2.71 (m, 2H), 2.61–2.54 (m, 2H). **^{13}C NMR (100 MHz, $CDCl_3$)** δ 207.2, 190.8, 167.1, 139.3, 137.6, 133.1, 133.0, 128.6 (2C), 128.6 (2C), 125.3, 35.9, 27.1. **HRMS** (ESI+) *m/z* calcd. for $[C_{14}H_{12}O_2+H]^+$: 213.0910; found: 213.0912.

6.5.4 General Procedure and Characterization of [10+4]-Cycloadducts 4

In a flame-dried 4 mL vial containing a magnetic stirring bar and 6 spheres of 4Å MS, (*R*)-2-(((*tert*-butyldimethylsilyl)oxy)diphenylmethyl)pyrrolidine **3b** (20 mol%, 7.4 mg, 0.02 mmol) and *p*-methoxybenzoic acid (20 mol%, 3.0 mg, 0.02 mmol) were dissolved in $CDCl_3$ (0.4 mL, filtered through a short plug of activated basic alumina directly before reaction setup). Diene **2** (1 eq, 0.1 mmol) and indene-2-carbaldehyde **1** (1.5 eq, 0.15 mmol) were added. Generation of an intensely red product was visible within short time. The reaction mixture was stirred for 20 h at rt. The [10+4]-cycloadducts were purified directly by FC on silica gel.

Products **4fa**, **4ia**, **4ma**, **4na**, **4ac**, were formed along with isomeric byproducts **4'** (see Table XX) under standard conditions. Two procedure modifications were established to circumvent the byproduct formation from occurring. Products **4fa** and **4ma** were obtained in reactions performed at 40 °C. Products **4ia**, **4na** and **4ac** were obtained in reactions applying 10 mol% of *p*-methoxybenzoic acid.

(11b*S*,11c*R*)-5-Benzoyl-7-phenyl-1,2,11b,11c-tetrahydro-3*H* benzo[*a*]cyclopenta[*h*]azulen-3-one 4ba.

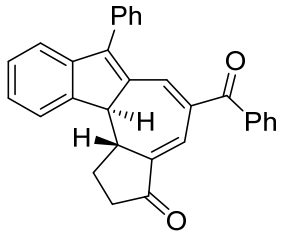

4b

Compound **4ba** was isolated in 85% yield as a red solid by FC on silica gel (2% Et_2O in CH_2Cl_2). $[\alpha]_D^{25}$= -318 (*c* 0.1, CH_2Cl_2) for 92% ee. **^{1}H NMR (400 MHz, $CDCl_3$)** δ 7.89–7.65 (m, 3H), 7.62–7.56 (m, 1H), 7.49 (t, *J* = 7.4 Hz, 1H), 7.46–7.31 (m, 11H), 3.79 (d, *J* = 11.9 Hz, 1H), 3.20–3.08 (m, 1H), 2.78–2.59 (m, 2H), 2.46–2.19 (m, 2H). **^{13}C NMR (100 MHz, $CDCl_3$)** δ 205.6, 196.9, 153.1, 144.3, 143.5, 141.1, 139.9, 137.7, 137.2, 132.8, 132.1, 131.5, 129.6 (2C), 129.4 (2C), 128.9, 128.6 (2C), 128.4, 128.2 (2C), 127.8, 127.5, 125.1, 122.1, 50.7, 42.2, 38.1, 28.4. **HRMS** (ESI+) *m/z* calcd. for $[C_{30}H_{22}O_2+H]^+$: 415.1693; found: 415.1698. **UPCC**: IB, gradient CO_2/*i*PrOH, 3.0 mL·min^{-1} ; t_{major} = 5.96 min; t_{minor} = 6.26 min.

6.5.5 Transformations of [10+4] Cycloadducts

Dibenzyl 2-(((11b*S*,11c*R*)-5-benzoyl-3-oxo-7-phenyl-1,2,3,11c-tetrahydro-11b*H*-benzo[*a*]cyclo-penta[*h*]azulen-11b-yl)-methyl)-malonate

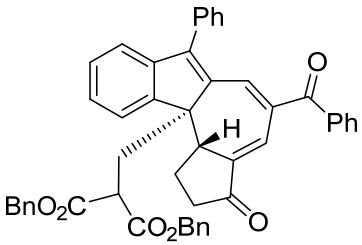

6

In a flame-dried 4 mL vial equipped with a magnetic stirring bar, **4b** (1 eq, 41.5 mg, 0.1 mmol), dibenzyl 2-methylenemalonate (1.2 eq, 35.6 mg, 0.12 mmol) and quinuclidine (20 mol%, 2.2 mg, 0.02 mmol) were dissolved in CH_2Cl_2 (0.4 mL) and the resulting solution was stirred at rt for 18 h. The crude reaction mixture was purified directly by FC on silica gel (1.5% Et_2O in CH_2Cl_2), affording **6** as a red solid in 40% yield. $[\alpha]_D^{25}$ = -284 (*c* 0.1, CH_2Cl_2) for 92% *ee*. **^{1}H NMR (400 MHz, $CDCl_3$)** δ 7.73–7.67 (m, 2H), 7.55–7.43 (m, 3H), 7.43–7.32 (m, 6H), 7.32–7.27 (m, 8H), 7.24–7.13 (m, 3H), 7.13–7.06 (m, 2H), 7.03 (d, *J* = 6.9 Hz, 2H), 4.93 (d, *J* = 12.3 Hz, 1H), 4.84–4.74 (m, 2H), 4.57 (d, *J* = 12.3 Hz, 1H), 3.27 (td, *J* = 10.0, 9.4, 3.2 Hz, 1H), 2.87–2.74 (m, 3H), 2.64 (dt, *J* = 17.0, 3.5 Hz, 1H), 2.44–2.23 (m, 3H). **^{13}C NMR (100 MHz, $CDCl_3$)** δ 205.3, 196.7, 168.9, 168.8, 152.4, 146.7, 143.8, 143.2, 138.8, 137.0, 135.2, 135.0, 134.4, 132.6, 132.4, 132.2, 129.7 (2C), 129.5 (2C), 129.0, 128.6 (3C), 128.4 (4C), 128.4 (2C), 128.3 (2C), 128.2, 128.1 (2C), 128.0 (2C), 127.8, 125.3, 122.5, 67.2, 67.1, 52.3, 47.7, 46.2, 37.9, 28.5, 24.2. **HRMS** (ESI+) *m/z* calcd. for $[C_{48}H_{38}O_6+H]^+$: 711.2741; found: 711.2745. **UPCC**: IA, gradient CO_2/*i*PrOH, 3.0 mL·min^{-1}; t_{major} = 9.23 min; t_{minor} = 13.85 min.

Multi-bridged compound 8.

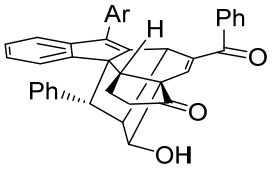

8-I

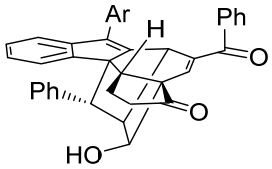

8-II

In a flame-dried 4 mL vial equipped with a magnetic stirring bar, **4j** (1 eq, 65.2 mg, 0.15 mmol), cinnamaldehyde (1.5 eq, 35.4 µL, 0.225 mmol), quinuclidine (20 mol%, 3.34 mg, 0.03 mmol) and pyrrolidine (20 mol%, 2.46 µL, 0.03 mmol) were dissolved in CH_2Cl_2 (0.6 mL, 0.25 M) and the resulting solution was stirred at rt for 18 h. The crude reaction mixture was analyzed by means of ^{1}H NMR revealing a diastereomeric ratio of 1:1. Direct purification by FC on Iatrobeads (25-50% EtOAc in pentane) gave compound **8-I** in 35% yield as the first eluting fraction during FC and **8-II** in 41% yield as the second eluting fraction.

8-II: $[\alpha]_D^{25}$ = +7 (*c* 0.1, CH_2Cl_2) for 94% *ee*. **^{1}H NMR (400 MHz, $CDCl_3$)** δ 7.79 (d, *J* = 8.0 Hz, 2H), 7.61–7.50 (m, 1H), 7.49–7.36 (m, 3H), 7.31–7.24 (m, 1H), 7.17–7.07 (m, 2H), 6.99–6.89 (m, 3H), 6.88–6.80 (m, 2H), 6.69–6.55 (m, 3H), 4.70 (d, *J* = 6.7 Hz, 1H),

4.56 (s, 1H), 3.75 (s, 1H), 3.43 (d, *J* = 6.8 Hz, 1H), 2.90 (dd, *J* = 18.9, 8.6 Hz, 1H), 2.84–2.68 (m, 1H), 2.67–2.56 (m, 1H), 2.56–2.42 (m, 2H), 2.38 (s, 3H). **^{13}C NMR (100 MHz, $CDCl_3$)** δ 216.8, 194.7, 150.6, 146.4, 145.7, 143.4, 139.7, 139.6, 137.4, 137.1, 132.5, 132.0, 129.6 (2C), 128.3 (2C), 128.0 (2C), 127.4, 127.1 (2C), 126.7, 126.3, 126.0, 125.5, 124.4, 124.3, 121.0, 74.7, 68.3, 59.2, 54.9, 50.8, 50.1, 37.3, 37.1, 22.8, 15.2. **HRMS** (ESI+) *m/z* calcd. for $[C_{38}H_{30}O_3S+Na]^+$: 589.1808; found: 589.1813. **UPCC**: ID, gradient CO_2/*i*PrOH, 3.0 mL·min^{-1}; t_{major} = 13.10 min; t_{minor} = 10.62 min.

8-I (not characterized) has been found to slowly lead to **8-II** when standing in solution for prolonged periods of time.

6.5.6 Crystallographic data for compound 4k

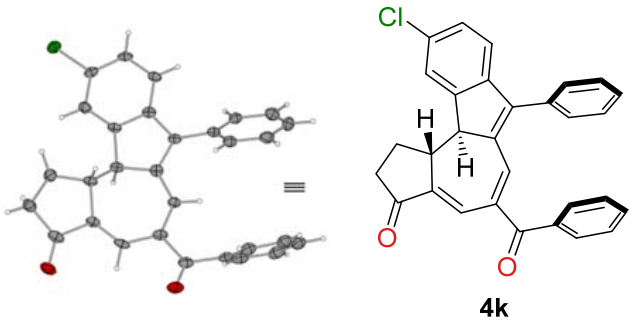

4k

(11b*S*,11c*R*)-5-Benzoyl-10-chloro-7-phenyl-1,2,11b,11c-tetrahydro-3*H*-benzo[*a*] cyclopenta[*h*]azulen-3-one **4k**. CCDC 1852294.

Empirical formula	$C_{30}H_{21}ClO_2$
Formula weight	448.92
Temperature/K	100
Crystal system	orthorhombic
Space group	$P2_12_12$
a/Å	22.6208(16)
b/Å	24.2146(18)
c/Å	7.9435(5)
α/°	90
β/°	90
γ/°	90
Volume/Å^3	4351.1(5)
Z	8
ρ_{calc}g/cm^3	1.371
μ/mm^{-1}	0.113
F(000)	1872.0
Crystal size/mm^3	0.707 × 0.471 × 0.141
Radiation	AgKα (λ = 0.56086)
2Θ range for data collection/°	3.888 to 42.816
Index ranges	-29 ≤ h ≤ 29, -31 ≤ k ≤ 31, -10 ≤ l ≤ 10
Reflections collected	54706
Independent reflections	10042 [R_{int} = 0.1409, R_{sigma} = 0.1058]
Data/restraints/parameters	10042/0/595
Goodness-of-fit on F^2	1.034
Final R indexes [I>=2σ (I)]	R_1 = 0.0565, wR_2 = 0.0897
Final R indexes [all data]	R_1 = 0.1152, wR_2 = 0.1064
Largest diff. peak/hole / e Å^{-3}	0.34/-0.38
Flack parameter	-0.05(6)

7 Organocatalytic Enantioselective Hetero-[6+4] and [6+2] Cycloadditions

The procedures and results here described are part of a manuscript in preparation,

- G. Bertuzzi, M. K. Thøgersen, M. Giardinetti, A. Vidal Albalat, A. Simon, K. Houk, K. A. Jørgensen. "Catalytic Enantioselective Hetero-[6+4] and [6+2] Cycloadditions of Heteroaromatic Compounds" *In preparation*.[a]

This work was carried out at the Department of Chemistry, University of Aarhus, Denmark, supported by "Marco Polo" fellowship of the University of Bologna, Italy. The author of this Doctoral Thesis gratefully acknowledges.

ABSTRACT

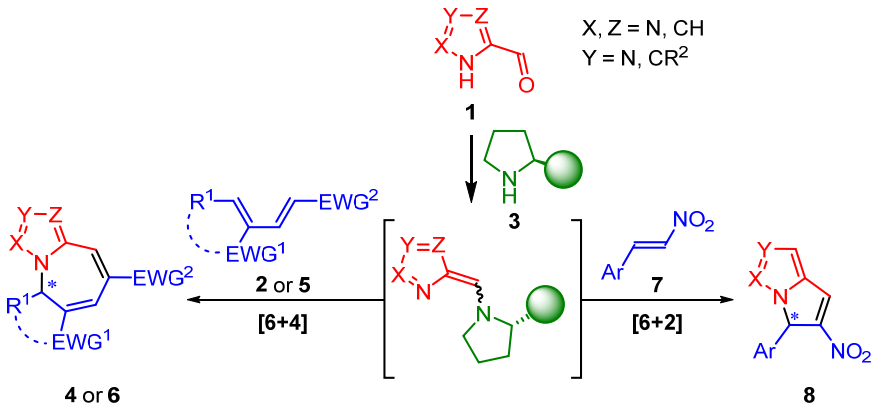

The development of the first chemo-, regio- and stereoselective hetero [6+4] and [6+2] cycloadditions is presented. The concept is based on activation of pyrroles, imidazoles and pyrazoles by an aldehyde handle, which by reaction with an organocatalyst generates an electron-rich hetero-6π-component, which reacts in a chemo-, regio- and stereoselective manner with an electron-deficient diene or olefin. For the hetero [6+4] cycloaddition of the pyrrole system with electron-deficient dienes, a wide variation of both reaction partners is possible, providing attractive pyrrolo-azepine products in high yields and excellent enantioselectivities (up to 99% ee). The hetero [6+4] cycloaddition reaction concepts are extended to include imidazoles and pyrazoles giving imidazolo- and pyrazolo-azepines. The same catalytic concept has successfully been further extended to also include hetero [6+2] cycloadditions of the pyrrole system with

[a] During the subssion and revison of thi thesis the manuscript has been submitted and accepted in *J. Am. Chem. Soc.* with the final title "Catalytic Enantioselective Hetero-[6+4] and –[6+2] Cycloadditions for the Construction of Condesed Polycyclic Pyrroles, Imidazoles and Pyrazoles. DOI:10.1021/jacs.8b13659.

nitroolefins giving important pyrrolizidine alkaloid scaffolds. Several transformations of the hetero [6+4] and [6+2] cycloadducts are presented. Experimental mechanistic studies show that first step of the reaction is rapid formation of an iminium-ion intermediate. Next, the iminium-ion intermediate is converted into the hetero-6π-intermediates. A ratio in favor of the iminium-ion over the enamine intermediate is observed. Addition of the electron-deficient diene to these intermediates leads to formation of the cycloadduct followed by catalyst release.

7.1 Background

In the previous chapter our strategy to involve isobenzofulvenes in organocatalytic enantioselective higher order cycloadditions (HOCs) was presented. Condensation of indene-2-carbaldehydes with chiral secondary amine catalysts enabled the formation of the extended π-system, reacting in [10+4] (and previously [8+2])[130] cycloadditions. We then moved our attention to simple pentafulvenes, exploring the possibility to apply the same strategy for their catalytic generation *in situ*. Indeed, besides the many precedents for productive engagement of 6,6-dialkylfulvenes in HOCs, 6-aminofulvenes were widely employed as 6π-components in [6+2] and [6+4] cycloadditions. Like amino isobenzofulvenes, the amino group stabilizes pentafulvenes as well, enhancing the aromaticity and favoring the preferential reactivity as 6π-components, due to increased polarization. For example, 6-dimethylamino fulvene was reacted with maleimides and maleic anhydrides in [6+2] cycloadditions, enabling the preparation of to pentaleno[1,2-*c*]furans and pentaleno[1,2-*c*]pyrroles, resembling the skeleton of important natural products such as Anislactone and Hirsutane.[137] It is worth remarking that 6,6-dialkylfulvenes react with the same electron deficient systems in [4+2] cycloadditions, enlightening the role of the amino group as a valuable handle for periselectivity switches (Scheme 1).

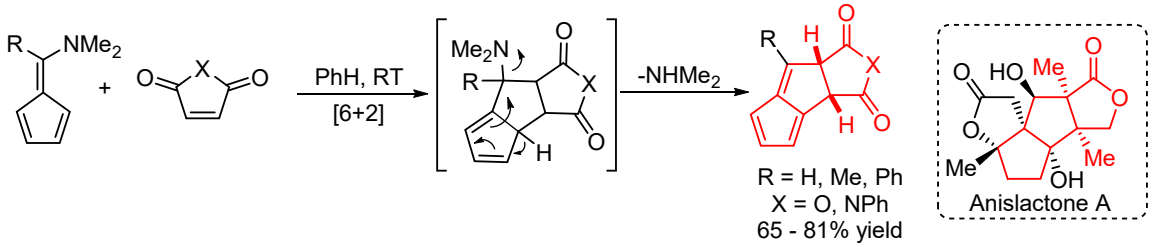

Scheme 1. [6+2] cycloaddition between 6-dimethylamino fulvene and malic anhydrides or maleimides.

Moreover, Hong's group disclosed a [6+4] cycloaddition of 6-dimethylaminofulvenes and α-pyrones, for the preparation of azulene indoles.[138] After the cycloaddition step, decarboxylative elimination of the amino group leads to the aromatization of the whole scaffold, constituting the driving force of the process (Scheme 2).

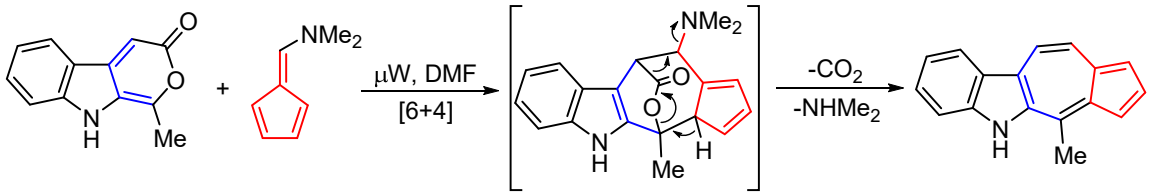

Scheme 2. [6+4] Cycloadditions between indolo-pyrones and 6-dimethylamino fulvene.

All these features considered, an efficient strategy would be the generation of 6-aminofulvenes as catalytic intermediates, by the condensation of aminocatalysts on the corresponding aldehydes. So far, no example of catalytic *in situ* generation of a simple 6-aminofulvene intermediate has been reported, probably due to intrinsic instability of parent cyclopentadiene-2-carbaldehyde. The aromaticity of the benzene ring in indene-2-carbaldehydes ensures stability and prevents spontaneous transformation into the *pseudo* aromatic conjugated enol, as generation of the isobenzofulvene breaks the aromaticity of the benzene ring itself. On the contrary, no stabilization is lost in the enolization of cyclopentadiene-2-carbaldehyde for the formation of the *pseudo* aromatic pentafulvene, which is spontaneously formed and then encounters various decomposition pathways. Indeed, the preparation of 6-dimethylaminofulvene does not rely on the condensation of dimethylamine onto cyclopentadiene-2-carbaldehyde, but on the treatment of the cyclopentadienyl anion with strongly formylating agents, such as the Vilsmeier salt (Scheme 3).[139]

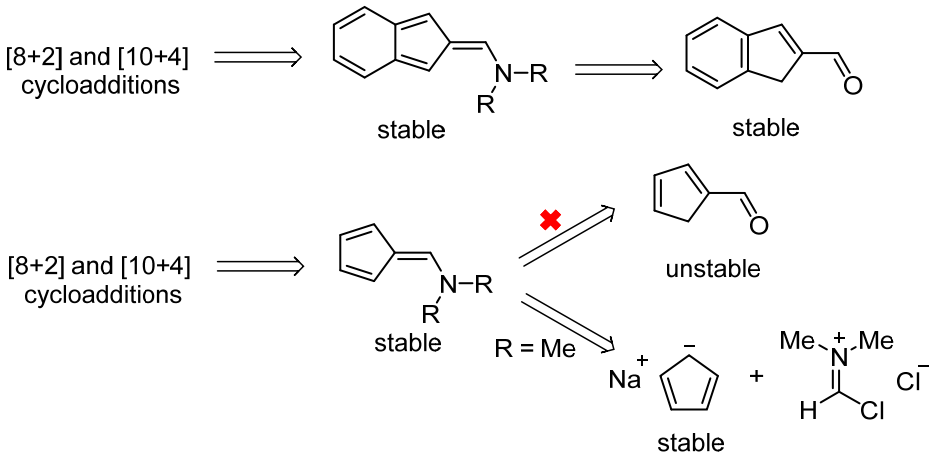

Scheme 3. Differences between 6-amino isobenzofulvenes and 6-amino fulvenes.

On the contrary, azole-2-carbaldehydes, such as pyrrole-2-carbaldehyde, are stable aromatic species which, upon condensation with an aminocatalyst, would render the desired amino azafulvenes, thus allowing the extension of the strategy employed for isobenzofulvenes to 6π-components. The first generation of 6-amino azafulvenes was reported in 1975 by Kanemasa *et al.* employing the condensation of simple amines such as pyrrolidine or morpholine, rendering stable dimers, derived from formal [6+6] cycloaddition.[140] Those compounds were reported to revert back to 6-amino azafulvene monomers upon heating; those latter could be trapped efficiently in [6+2] cycloadditions with cumulenes, such as isocyanates or isothiocyanates (Scheme 4). Although not catalytically, amino azafulvenes were generated *in situ* as transient species, encouraging the applicability of our strategy as well.

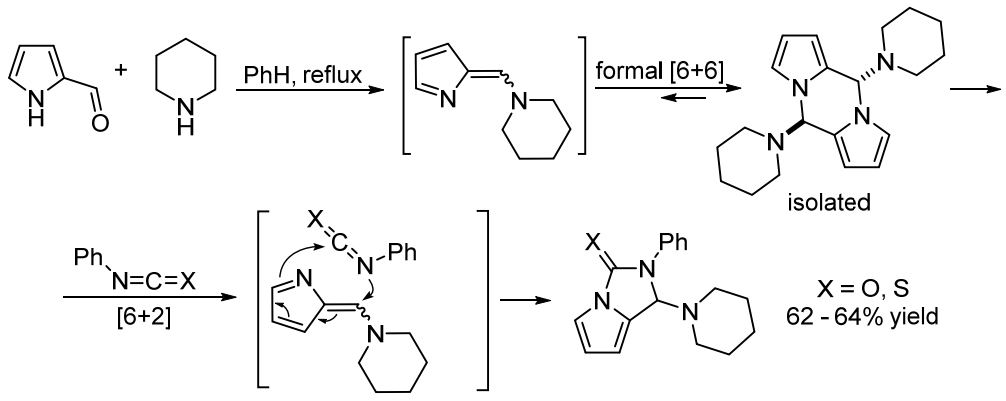

Scheme 4. Generation of 6-amino azafulvene dimers and their [6+2] cycloadditions with cumulenes.

Isolation of stable 6-amino azafulvenes is also possible if mildly electron poor pyrrole-2-carbaldehydes are employed as starting materials. Upon treatment with secondary amines

in strongly acidic media, crystalline iminium ions are obtained, that can be favorably turned into the corresponding 6-amino azafulvenes upon treatment with bases such as sodium hydride. Sonnet was the first to report this strategy, involving the obtained 6π-components, after isolation and characterization, in [6+2] and [6+2+2] cycloadditions with dimethyl acetylenedicarboxylate (Scheme 5).[141]

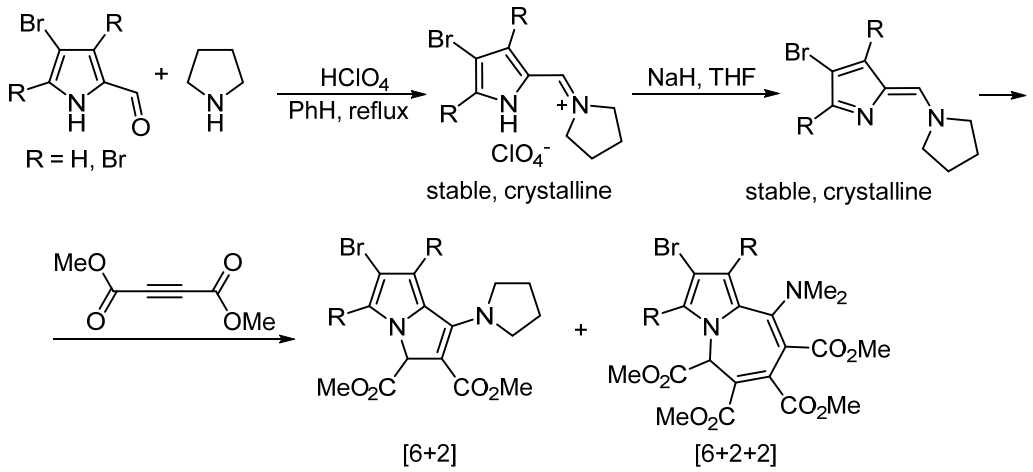

Scheme 5. Generation of stable 6-amino azafulvenes and their [6+2] and [6+2+2] cycloadditions.

Diazafulvenes were also employed as 6π-components in [6+n] cycloadditions. Like 6-amino azafulvenes, 6-amino 1,4-diazafulvenes were found to form homodimers, in equilibrium with the monomer forms. The latter could be trapped with dimethyl acetylenedicarboxylate in [6+2] cycloadditions.[142] In 2006, Barluenga *et al.* reported the [6+2] cycloaddition of 6-dimethylamino 1,4-diazafulvenes with Fischer alkynyl chromium carbene complexes (Scheme 6). A [6+3] cyclization is also described with alkenyl carbenes, although a 1,2-metal shift occurs in order to trigger the ring closure and the whole mechanism cannot be properly defined as a cycloaddition. This served for the preparation of densely functionalized biciclyc scaffolds.[143]

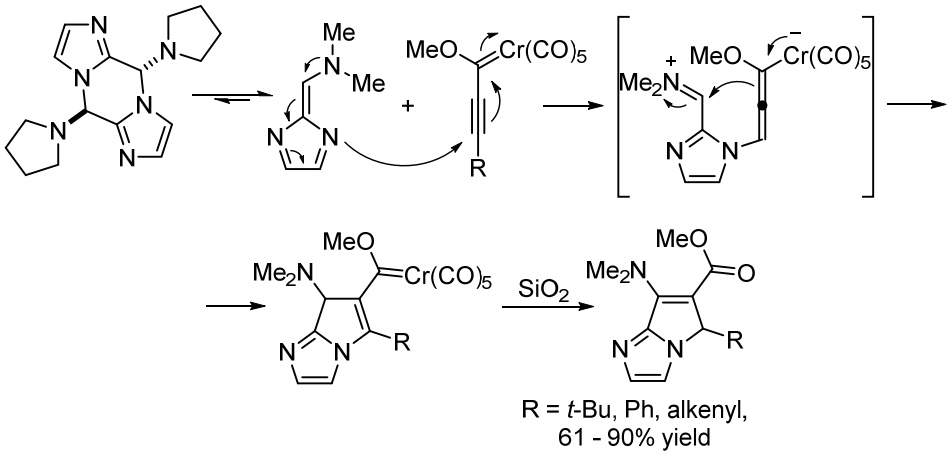

Scheme 6. [6+2] Cycloaddition between alkynyl carbenes and 6-amino diazafulvenes.

From a synthetic point of view, the functionalization of pyrroles and related azoles *via* HOCs involving the whole 6π-system, represents a fruitful way to accomplish *N*-derivatization of such heterocycles. Indeed, the functionalization of pyrroles, imidazoles and pyrazoles has been the center of numerous synthetic efforts, due to their presence in biologically relevant compounds.[144] However, the chemistry around these moieties represents a challenge due to chemo- and regioselectivity issues. The electrophilic C-functionalization of pyrrole is a well-established procedure, whereas its employment as an *N*-centered nucleophile is much less explored, although *N*-fused bicycles are key backbones of many natural products.[145]

An available enantioselective strategy to construct such scaffolds, based on these heterocycles acting as *N*-centered nucleophiles, relies mainly on aza-Michael/aldol cascade reactions, which is highly dependent on the acidity of the NH-moiety and therefore, limited to electron-poor pyrroles. Trifluoro- or trichloroacteyl or pyruvyl dihalopyrroles acted as nucleophile at the *N*-atom towards α,β-unsaturated carbonyls activated *via* chiral iminium ions. After addition, the electrophile turns into a nucleophilic enamine, undergoing aldol condensation on the acetyl group. It is worth stressing that unactivated alkyl ketones, as well as less electron-deficient pyrroles (for instance, displaying no halogens) did not show any reactivity under the optimized conditions (Scheme 7).[146]

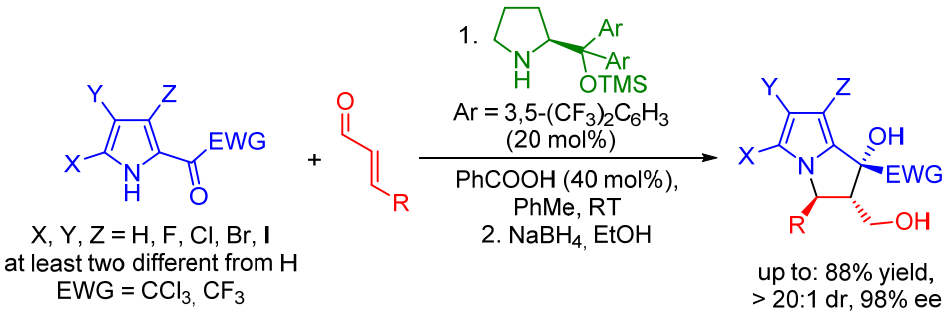

Scheme 7. Organocatalytic asymmetric *aza*-Michael-aldol cascades for the synthesis of annulated pyrroles

In these cases, the acyl group serves as a quencher for the excessive nucleophilicity of simple pyrroles, as well as a useful functionality to complete the cyclization process. In our case, the aldehyde group, retaining these two characteristics, will also serve as the handle to introduce chirality

Moreover, if imidazoles and pyrazoles are used as *N*-centered nucleophiles in aza-Michael reactions,[147] no methodology allowing the construction of bicyclic compounds based on such a strategy has been reported.

The present strategy is a novel concept for the construction of nitrogen-containing fused bicyclic compounds of biological interest. Through the [6+4] cycloaddition reaction, we were able to obtain pyrrolo[1,2-*a*]azepines. This is a common scaffold in the family of cephalotaxine alkaloids **A** (Figure 1)[148] and Stemona alkaloids, like Parvistemonine A[149] (**B**), extracted from the roots of Stemona species, used in Asian medicine as insecticides and for the treatment of pulmonary diseases. Furthermore, Midazolam **C** and related imidazopyrrolobenzodiazepines-based anti-anxiety drugs, present a similar backbone built on a diazole moiety.[150] Employing the [6+2] strategy, pyrrolizine derivatives have been synthesized. The backbone is shared between a large family of recurring natural compounds called pyrrolizidine alkaloids **D**, extracted from over 6000 different plants, exhibiting various ranges of cytotoxicity.[151] In addition, it is the core structure of Ketorolac **E**, a non-steroidal anti-inflammatory drug.[152]

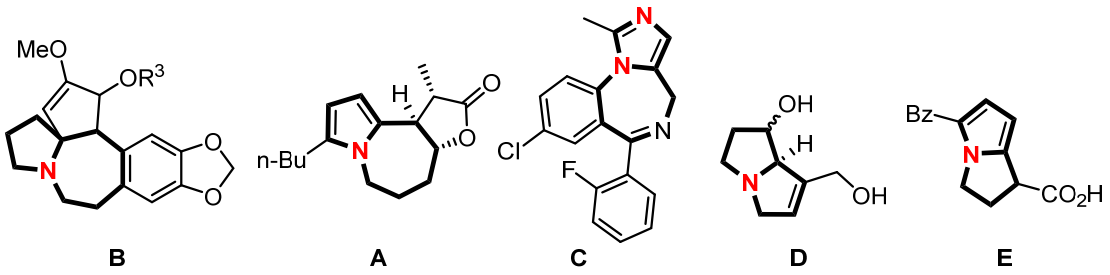

Figure 1. Biologically relevant structures.

7.2 Aim of the work

As stated previously, pyrroled-2-carboxaldehyde **1a** was employed, upon reaction with chiral amine catalysts **3**, as the precursor for the catalytic generation of chiral 6-amino azafulvenes, participating as 6π-components in [6+4] and [6+2] cycloadditions. Dienes **2** were found to react smoothly as 4π-components, rendering, after E1cB catalyst elimination, pyrrolo-azepines **4**. These electron deficient dienes were also employed efficiently in [10+4] cycloadditions (see Section 6), demonstrating the high potential of these scaffolds as electron deficient partners in aminocatalyzed HOCs. Moreover, another class of dienes, based on a completely acyclic motif (**5**), were found to be suitable partners for [6+4] cycloadditions, leading to products **6**. On the other hand, nitroolefins **7** proved to be the most suitable 2π-components for the [6+2] cycloaddition, leading to pyrrolizine-like adducts **8**.

The methodology ([6+4] cycloaddition exclusively) was then extended to 6-amino 1,3-, 1,4- and 1,5-diazafulvenes derived from imidazole-2-carbaldehyde, imidazole-4-carbaldehyde and pyrazole-5-carbaldehyde, respectively. This accomplishment demonstrates the value and the generality of the presented process (Scheme 8).

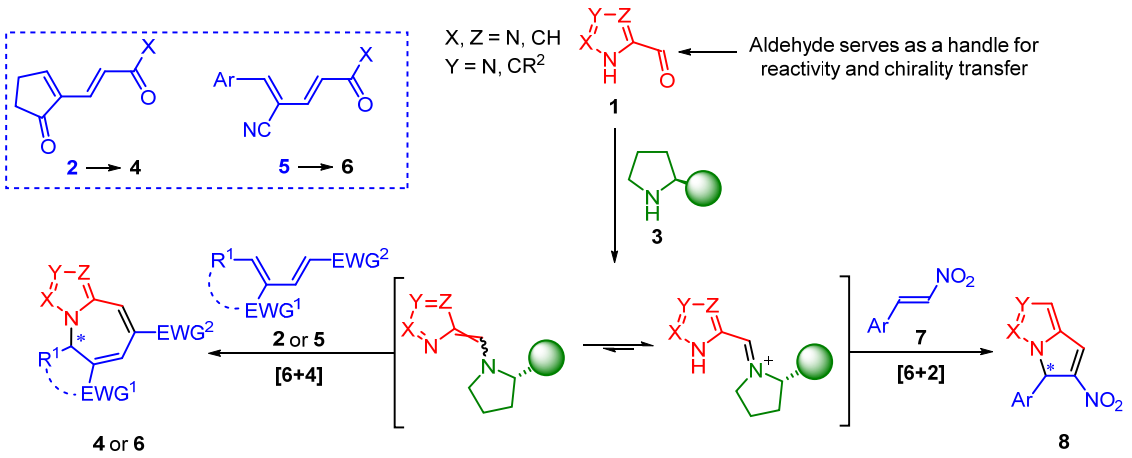

Scheme 8. Project overview.

Various challenges had to be overcome during the course of the optimization of the reaction. First of all the scarce reactivity of pyrrole-2-carbaldehyde **1a**, which, due to the aromaticity and the push-pull stabilization between the electron-rich nucleus of pyrrole and the formyl group, proved to be difficult to transform into the desired reactive species. Secondly, the extension of the methodology to diazoles required some specific optimizations in each case, as the electronic characteristics of pyrrole, imidazole and pyrazole are quite different.

Intrigued by the possibility to obtain stable 6-aminoazafulvenes reported in the literature, we became interested in the observation of some of the reactive intermediates as well. Since amino isobenzofulvenes, derived from the condensation of chiral amine catalysts onto indene-2-carbaldehydes, were never detectable by NMR spectroscopy, observability of some azafulvene intermediates might be important for a better comprehension of chiral fulvenes HOCs in general.

7.3 [6+4] Cycloaddition: Results and Discussions

We started our investigation by treating pyrrole-2-carbaldehyde **1a** with secondary aminocatalysts **3**[71] to provide the desired transient 6-aminoazafulvene, which was captured by diene **2a** in a [6+4] cycloaddition, rendering after E1cB catalyst release, the tricyclic compound **4aa**. Interestingly, it was found that the most commonly employed aminocatalyst **3a**, combined with benzoic acid and Molecular Sieves (MS) as additives in dry $CDCl_3$ at room temperature, delivered the desired compound only in trace amounts

but with an excellent degree of enantioselectivity (99% ee, Table 1, entry 1). Changing for a less bulky fluorine substituted catalyst (**3b**)[153] improved the yield to 40% while maintaining the same enantiomeric excess (entry 2), whereas catalyst **3c**[154] afforded compound **4aa** with improved yield but slightly diminished enantioselectivity (entry 3). We then decided to keep the most stereoselective catalyst and to overcome the poor reactivity by changing other reaction parameters. Notably, to achieve a proper degree of conversion, both benzoic acid and MS had to be applied as additives (entries 4 and 5). Given the low reactivity of the system under conditions specified in entry 2, we tried to raise the reaction temperature to 40 °C. This however caused the yield to drop considerably, probably due to decomposition of **2a** (entry 6). Therefore, all the subsequent reactions were conducted at RT. A small solvent screening was then undertaken, starting with acetonitrile (entry 7), which resulted in the same 40% yield. However, with a complete consumption of **2a**, no room for improving the yield was left. On the other hand, changing the solvent to THF or toluene (entries 8 and 9) did not improve the yield.

Table 1. Initial investigations and catalyst screening in the [6+4] cycloaddition between aldehydes **1a** and dienes **2a**.[a]

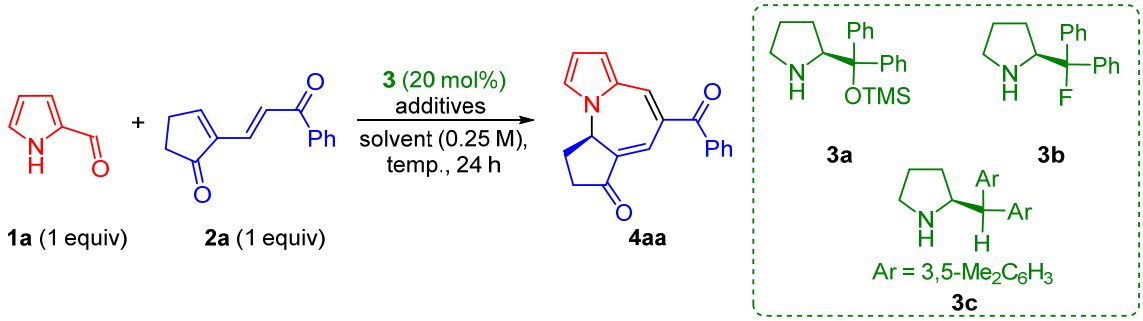

Entry	Catalyst	Additive[b]	Solvent	Consumption[c] **1a**/**2a** (%)	NMR yield[d] (%)	ee[e] (%)
1	**3a**	BA, MS	$CDCl_3$	30/70	5	99
2	**3b**	BA, MS	$CDCl_3$	80/75	40	99
3	**3c**	BA, MS	$CDCl_3$	90/90	65	95
4	**3b**	BA	$CDCl_3$	75	12	n.d.
5	**3b**	MS	$CDCl_3$	44	10	n.d.
6[f]	**3b**	BA, MS	$CDCl_3$	87/94	20	96
7	**3b**	BA, MS	MeCN	71/> 95	40	n.d.
8	**3b**	BA, MS	THF	59/95	23	n.d.
9	**3b**	BA, MS	PhMe	73/88	35	n.d.

(**a**) Reaction conditions: **1a** (0.05 mmol), **2a** (0.05 mmol), **3** (0.01 mmol), $CDCl_3$ (200 μL), RT. (**b**) Benzoic acid (0.01 mmol). (**c**) Amount of **1a** and **2a** present in the reaction mixture divided by initial amount, determined on the crude mixture by ^{1}H NMR in comparison to $SiEt_4$ as internal standard. (**d**) Determined on the crude mixture by ^{1}H NMR in comparison to $SiEt_4$ as internal standard. (**e**) Determined by CSP UPCC on the isolated products **4**. (**f**) Reaction temperature 40 °C.

At this point, since chromatographic separation between **4aa** and **1a** was troublesome, we envisioned that complete consumption of the aldehyde would be advantageous, leading to employ compound **2a** in excess. Even if after one day, the yield was not improved (Table 2, entry 1), less decomposition of the starting material was observed, leading to higher yields after two or three days (entries 2 and 3). We also tried to increase the concentration of the reaction mixture to 0.4 M, affording product **4aa** in an improved yield of 52% (entry 4). Finally, we screened three different acids: while *o*-F-BA and *p*NO_2BzOH showed a drop in reaction efficiency (entries 5 and 6), *p*-MeO-BA improved the yield to 63% after one day (entry 7), which was further increased to 75% after two

days (entry 8). Under these conditions, complete consumption of aldehyde **1a** was achieved, rendering purification of the product easier.

Table 2. Optimization of reaction conditions of [6+4] cycloaddition between aldehydes **1a** and dienes **2a**, fine tuning and acid screening.[a]

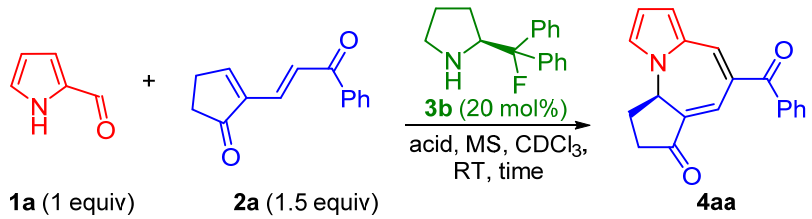

Entry	Acid additive[b]	Concentration (M)	Time (h)	Consumption[c] **1a**/**2a** (%)	NMR yield[d] (%)	ee[e] (%)
1	BA	0.25	24	61/55	38	99
2	BA	0.25	48	75/65	46	99
3	BA	0.25	75	87/79	55	99
4	BA	0.4	24	78/67	52	99
5	*o*-F-BA	0.4	24	56/47	5	n.d.
6	*p*-NO_2-BA	0.4	24	83/67	20	n.d.
7	*p*-MeO-BA	0.4	24	85/74	63	99
8	*p*-MeO-BA	0.4	48	> 95/85	75 (73)[f]	99

(**a**) Reaction conditions: **1a** (0.05 mmol), **2a** (0.075 mmol), **3** (0.01 mmol), $CDCl_3$, RT. (**b**) acid (0.01 mmol). (**c**) Amount of **1a** and **2a** present in the reaction mixture divided by initial amount, determined on the crude mixture by ^{1}H NMR in comparison to $SiEt_4$ as internal standard. (**d**) Determined on the crude mixture by ^{1}H NMR in comparison to $SiEt_4$ as internal standard. (**e**) Determined by CSP UPCC on the isolated products **4**.

With the optimal conditions in hand, the scope between pyrrole-2-carbaldehydes **1a-f** and dienes **2** (Scheme 9). Some variations were thus undertaken on the 4-position of the pyrrole ring, starting from the introduction of some heteroatoms like bromine (**1b**), silicon (4-triisopropyl substituted **1c**) or sulfur (4-thiophenyl substituted **1d**), leading respectively to products **4ba-4da** in 68-90% yield and 99% ee. The absolute configuration of compound **4da** was assigned by single crystal X-ray analysis and extended for analogy to products **4** and **6** (*vide infra*). 4-Phenyl substituted and 4-(*p*-MeO-phenyl) substituted aldehydes **1e** and **1f**) was found to render cycloadducts **4ea** and **4fa** with similarly high yields and stereoselectivities. Modifications on the electron-withdrawing group of **2** were then explored, finding that different aromatic ketones (**2b-**

2d) as well as esters (**2e** and **2f**) allowed the preparation of products **4ab**-**4af** in 54-88% yield and 99% ee. On the contrary, 3-phenyl-, 5-chloro, 3,5-dimethyl and 5-methyl-pyrrole-2-carbaldehydes, turned out to be unreactive under the optimized reaction conditions. Mainly decomposition products were observed when a methyl ketone ore a cyano substituted diene **2** were employed.

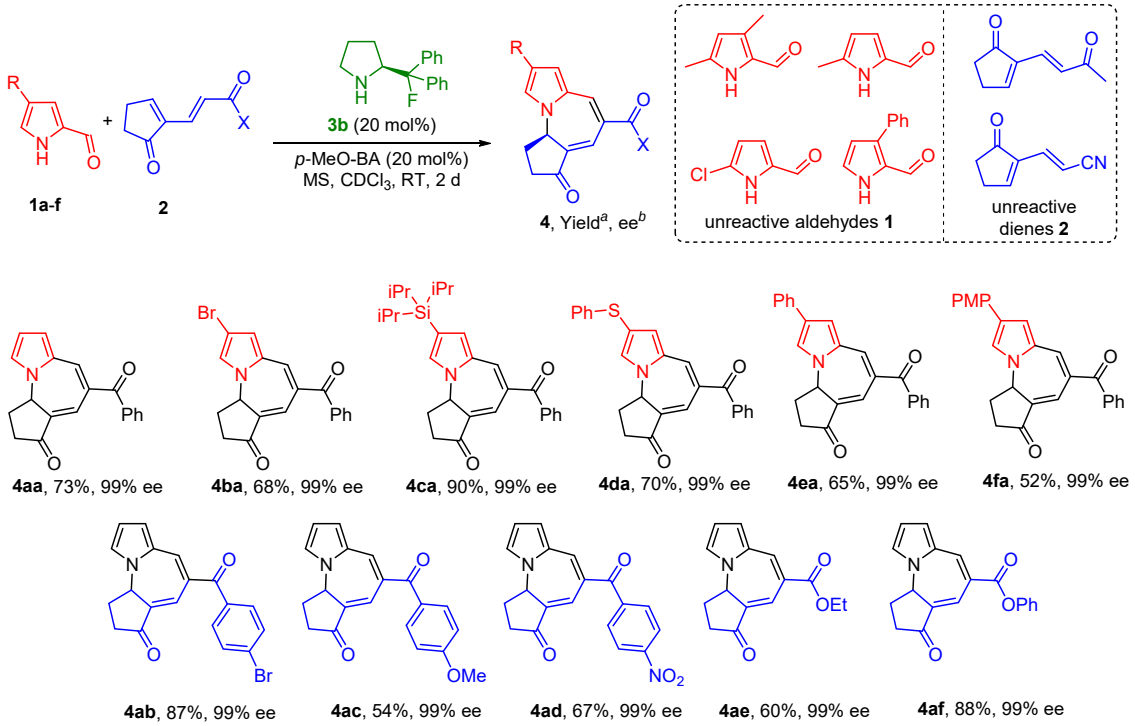

Scheme 9. Scope of the [6+4] cycloaddition between aldehydes **1a-f** and dienes **2**. Reaction conditions: **1** (0.1 mmol), **2a** (0.15 mmol), **3b** (0.02 mmol), *p*-MeO-BA (0.02 mmol), $CDCl_3$ (250 µL), RT, 48 h. (**a**) Isolated yield after flash chromatography. (**b**) Determined by CSP UPCC on the isolated products **4**.

Gratifyingly, the described strategy, requiring some minor modifications, was also applicable to the [6+4] cycloaddition of all possible isomers of 6-aminodiazafulvenes, deriving from diazole-2-carbaldehydes **1g-1i**. This, as stated before, shows the power of this strategy for the functionalization of 5-membered heterocycles. It is indeed very unlikely that the same process, developed for the functionalization of pyrrole derivatives and relying on the intrinsic characteristics of pyrrole itself, can be translated with only a few optimizations to diazoles. These latter possess indeed a pyridine-like *N*-atom, acting as a powerful electron-withdrawing group, quenching the nucleophilicity of the aromatic nucleus. Moreover, differently from pyrrole, imidazole and pyrazole are also basic (i.e. protonation of the pyridine-like *N*-atom is possible). On the other hand, by turning azoles into amino azafulvenes, the electronic characteristics change dramatically and the

reactivity is dictated by the amino group preferentially, rendering the extension of the same concept to different scaffolds possible.

Although the disclosed procedure for the [6+4] cycloaddition of pyrrole-2-carbaldehydes **1a-f** with dienes **2** was generally applicable to diazole-2-carbaldehydes **1g-i**, in order to obtain optimal results, some modifications of the reaction parameters were required. For example, aldehyde **1g** underwent some degree of decomposition under the previously optimized reaction conditions (Table 3, entry 1). It was therefore introduced in excess, resulting in slightly improved yield (entry 2). However, only when the reaction was run under milder conditions, satisfactory yield values were obtained, suggesting also some instability of the product in the reaction mixture (entries 3 and 4). The optimal value of 69% yield and 93% ee was obtained by lowering the catalyst and additive amount to 10 mol% and diluting the reaction medium to 0.1 M (entry 4).

On the other hand, lower yields were obtained when aldehyde **1h** was subjected to the standard conditions, showing in particular both low reactivity and enhanced product instability (entries 5 and 6). Again, lowering the temperature to 0 °C proved to be beneficial (entry 7), as well as lowering the catalyst and additive loading to 10 mol% (entry 8). The optimized value of 34% yield, with excellent 94% ee, was the result of a compromise between aldehyde reactivity and product stability.

Surprisingly, when treated under the optimized conditions for aldehydes **1g** and **1h**, aldehyde **1i** showed almost no reactivity (entry 9). By reapplying the standard conditions, optimized for **1a** (20 mol% catalyst and acid) for a prolonged reaction time of 6 days, it was found to deliver the desired product in 31% yield and 87% ee (entry 10). Unlike products **4ga** and **4ha**, **4ia** didn't show any trace of decomposition during the reaction course. However, given the poor reactivity of substrate **1i**, we decided to employ catalyst **3c,** more reactive towards the [6+4] cycloaddition of **1a** with **2a**. Indeed, compound **4ia** was obtained in 63% yield after 2 days, albeit with an important erosion of the enantiomeric excess (entry 11). Therefore, **3b** was retained as the optimal catalyst, for aldehyde **1i** as well.

Table 3. Optimization of reaction conditions between diazole carbaldehydes **1g-i** and diene **2a**.[a]

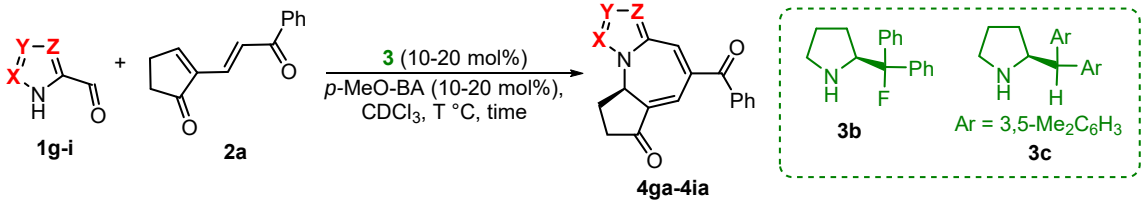

Entry	Aldehyde	Catalyst (mol%)	Temp. (°C) /time (d)	Ratio **1:2a**	Consumption (%, **1/2a**)[b]	Yield (%)[c]	*ee* (%)[d]
1	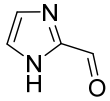 **1g**	**3b** (20)	RT / 1	1:1.5	>99/64	30	92
2		**3b** (20)	RT / 1	2:1	>99/89	38	92
3		**3b** (20)	0 / 1	2:1	>99/85	55	92
4[e]		**3b** (10)	RT / 1	2:1	n.d.	69[f]	93
5	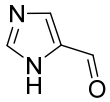 **1h**	**3b** (20)	RT / 1	1:1.5	88/89	18	n.d.
6		**3b** (20)	RT / 2	1:1.5	>99/>99	Traces	n.d.
7		**3b** (20)	0 / 1	2:1	49/61	29	n.d.
8[e]		**3b** (10)	RT / 1	2:1	n.d.	34[f]	94
9[e]	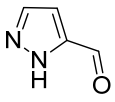 **1i**	**3b** (10)	RT / 1	2:1	n.d.	Traces	n.d.
10		**3b** (20)	RT / 6	2:1	n.d.	31[f]	87
11		**3c** (20)	RT / 2	2:1	n.d.	63[f]	40

(**a**) Reaction conditions: **1** (0.1 or 0.2 mmol), **2a** (0.15 or 0.1 mmol), **3** (0.01 or 0.02 mmol), *p*-MeO-BA (equimolar with **3b**), $CDCl_3$, (0.2 M), RT. (**b**) Amount of **1** and **2a** present in the reaction mixture divided by initial amount, determined on the crude mixture by ^{1}H NMR in comparison to $SiEt_4$ as internal standard. (**c**) Determined on the crude mixture by ^{1}H NMR in comparison to $SiEt_4$ as internal standard. (**d**) Determined by CSP UPCC on the isolated products **4**. (**e**) $CDCl_3$ (0.1 M). (**f**) Isolated yield after flash chromatography.

The scope of diazole-2-carbaldehydes **1g-i** was investigated by reaction with different dienes **2** (Scheme 10). Besides model diene **2a**, which was used for the optimization of the reaction conditions, *p*-bromo substituted phenyl ketone **2b** was reacted with **1h** and **1i**, *p*-nitro-substituted phenyl ketone **2d** was reacted with **1g** and ester **2e** with **1g** and **1h** (reaction with **1i** was unproductive). In general, the reaction was found to be quite independent on the type of diene employed, showing, for each aldehyde, similar results to model compound **2a**.

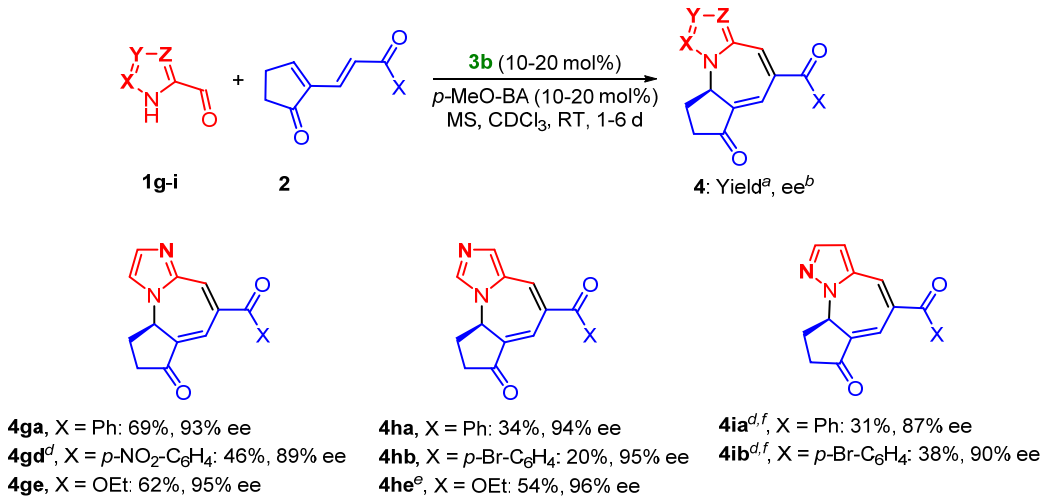

Scheme 10. Scope of diazole carbaldehydes **1g-i** with dienes **2**. Reaction conditions, unless otherwise stated: **1** (0.2 mmol), **2a** (0.1 mmol), **3b** (0.01 mmol), *p*-MeO-BA (0.01 mmol), $CDCl_3$, (0.2 M), RT, 24 h. (**a**) Isolated yields after flash chromatography. (**b**) Determined by CSP UPCC on the isolated products **4**. (**d**) **3b** (0.02 mmol), *p*-MeO-BA (0.02 mmol). (**e**) Reaction time: 2 d. (**f**) Reaction time: 6 d.

We decided to investigate a new class of dienes **5**, not constraining parts of the conjugated moiety in a cycle. This adds some degrees of freedom to the structure that might adopt the reactive *s-cis* conformation more difficultly. We started our optimization with phenyl ketone derivative **5a** and aldehyde **1a**. Under the optimized conditions used for diene **2a**, the desired product **6aa** was obtained in only 23 % yield and 93 % ee (Table 4, entry 1). Since product **6aa** was impossible to separate from diene **5a** by means of column chromatography, the ratio between aldehyde **1a** and **5a** was inverted in favor of the aldehyde. In order to improve the yield, the reaction was conducted over 16 days, resulting however in only a small improvement, probably due to catalyst deactivation or decomposition (entry 2). Catalyst **3c**, especially efficient in promoting the reaction between **1a** and **2a**, was also applied to this system, yielding the desired compound **6aa** in only 26% yield and 81% ee (entry 3). Raising the reaction temperature to 40 or 60 °C was also found to be inefficient (entries 4 and 5). At this point, we chose to increase the catalyst and acid loading to 40 mol% each, resulting in greatly improved 55 % yield after only 4 days, while displaying 96% ee (entry 6).

Table 4. Optimization of reaction conditions for the [6+4] cycloaddition between diene **5a** and aldehyde **1a**.[a]

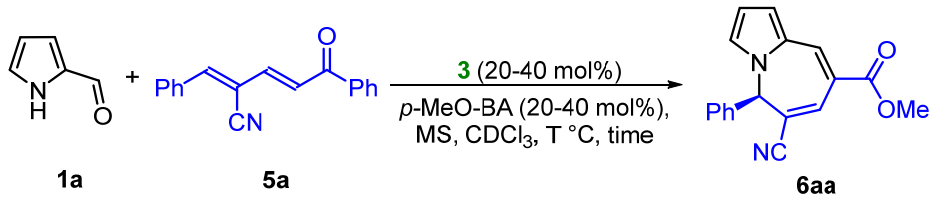

1a **5a** **6aa**

Entry	Catalyst (mol%)	Temp. (°C)	Time (d)	Ratio **1a:5a**	Consumption of **5a** (%)[b]	Yield (%)[c]	*ee* (%)[d]
1	**3b** (20)	RT	2	1:1.5	80/75	23	93
2	**3b** (20)	RT	16	1.5:1	87/94	38	93
3	**3c** (20)	RT	8	1.5:1	71/>99	26	81
4	**3b** (20)	40	14	1.5:1	15	traces	n.d.
5	**3b** (20)	60	8	1.5:1	10	n.d.	n.d.
6	**3b** (40)	RT	4	1.5:1	n.d.	55[e]	96

(**a**) Reaction conditions: **1a** (0.1 or 0.15 mmol), **5a** (0.15 or 0.1 mmol), **3** (0.02 or 0.04 mmol), *p*-MeO-BA (equimolar with **3b**), $CDCl_3$ (0.25 M), RT. (**b**) Amount of **5a** present in the reaction mixture divided by initial amount, determined on the crude mixture by ^{1}H NMR in comparison to $SiEt_4$ as internal standard. (**c**) Determined on the crude mixture by ^{1}H NMR in comparison to $SiEt_4$ as internal standard. (**d**) Determined by CSP UPCC on the isolated products **4**. (**e**) Isolated yield after flash chromatography.

The scope of dienes **5** was investigated briefly by reaction with aldehydes **1a** and **1g** (Scheme 11). Besides electron-neutral aryl substituent **5a**, an electron-poor one (**5b**) was tolerated. Products **6aa** and **6ab**, displaying a different decoration of the seven-membered ring with respect to cycloadducts **4**, were obtained in good yields and excellent enantioselectivities. Imidazole **1g** was also reacted with **5a**, affording **6ga** in moderate yield and slightly diminished enantioselectivity. However, the reaction with ester **5c** was found to give rise to **6gc** in only 10% yield and 51% ee. This demonstrates the broad applicability of the reported methodology for the construction of structurally diverse hetero [6+4] cycloadducts.

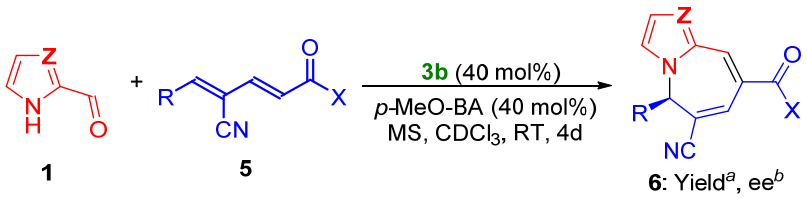

6aa, R = Ph, Z = CH, X = Ph: 55%, 96% ee
6ab, R = *m*-Br-C_6H_4, Z = CH, X = Ph: 60%, 98% ee
6ga, R = Ph, Z = **N**, X = Ph: 47%, 80% ee
6gc, R = Ph, Z = **N**, X = OMe: 10%, 51% ee

Scheme 11. Scope of azole carbaldehydes **1a** and **1g** with dienes **5**. Reaction conditions: **1** (0.2 mmol), **5** (0.1 mmol), **3b** (0.04 mmol), *p*-MeO-BA (0.04 mmol), $CDCl_3$, (0.25 M), RT, 4 d. (**a**) Isolated yields after flash chromatography. (**b**) Determined by CSP UPCC on the isolated products **6**.

7.3.1 Mechanistic investigations on the [6+4] cycloaddition.

As anticipated, the formation of stable 6-amino azafulvenes from 4-bromopyrrole-2-carbaldehyde **1b** was reported in the literature.[141] We therefore tried to apply similar reaction conditions for the observation of intermediates **I** and **II** derived from **1b** and chiral catalyst **3b** and prove that they actively take part to the [6+4] cycloaddition (Scheme 12). The whole investigation can be summarized in three experiments.

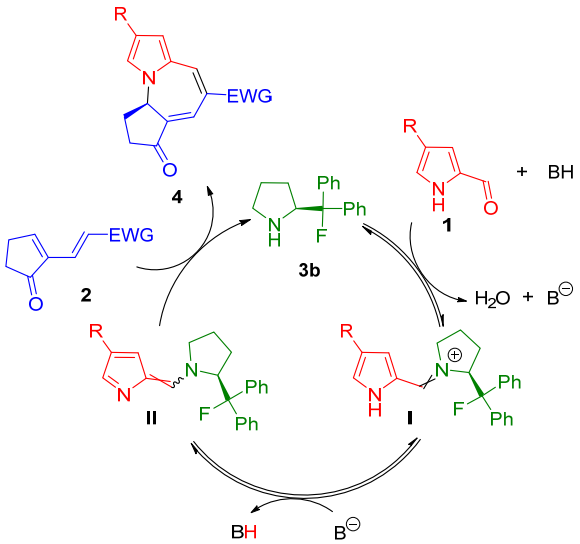

Scheme 12. Proposed catalytic cycle through intermediates **I** and **II**. The crossed double bonds refer to a mixture of *cis*- and *trans* stereoisomers.

Experiment 1, observation of iminium ion I, enamine II and proof of II as a reactive intermediate. The experiment was set up as follows. Aldehyde **1b**, catalyst **3b** and BA (1:1:1 ratio) were mixed overnight in $CDCl_3$ in the presence of molecular sieves. The

presence of iminium ion **I** was confirmed by ^{1}H and ^{19}F NMR. Isolation of this species was not possible due to rapid hydrolysis in air. Indeed, residual traces of water are responsible for partial hydrolysis of the iminium ion, explaining why we could never obtain this intermediate quantitatively. This mixture was then treated with a stoichiometric amount of triethylamine (TEA) for 5 minutes. The disappearance of the iminium ion was checked by ^{1}H and ^{19}F NMR. Moreover, new peaks appeared at the ^{19}F NMR, attributed to two stereoisomers of enamine **II**. This showed very broad signals at the ^{1}H NMR and further characterization was impaired by the tendency of this compound to rapidly hydrolyze. The MS were then removed, diene **2e** was added to the reaction mixture and this was checked at different times[155] by ^{1}H NMR and ^{19}F NMR (Scheme 13)

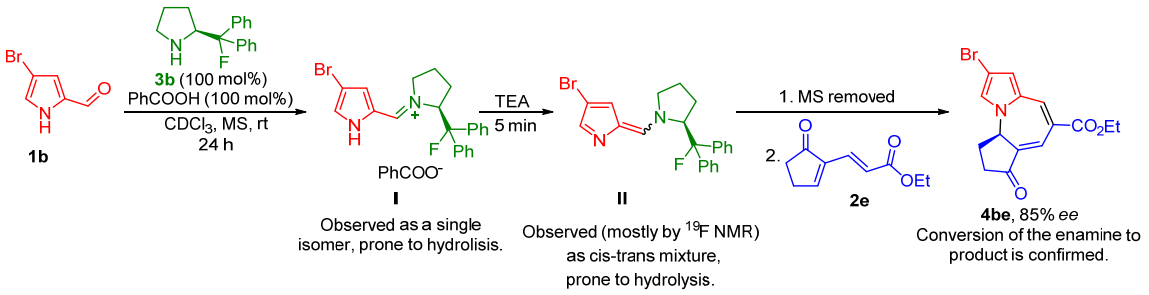

Scheme 13. Description of experiment 1.

Over time, as the formation of product was checked by ^{1}H NMR, the disappearance of enamine **II** and the release of catalyst **3b** were verified by ^{19}F NMR. The ratio of the two signals of the isomers of enamine **II** was difficult to evaluate but it remained qualitatively constant during the whole reaction monitoring. Iminium ion **I** was never observed during the whole process. Since the disappearance of intermediate **II** and the formation of product **4be** were followed with two different sets of spectra, a consistent and thorough plot of the relative quantities vs time was not possible. This should not represent a problem, as the reaction conditions were really different from the actual ones and the specific profile of this particular reaction was not really interesting. Product **4be** was formed in 85% ee, which is not fully consistent with the following experiments. Racemization in the presence of TEA over time was excluded. This might suggest that the formation and equilibration of enamine(s) **II** and iminium ion **I** under the real reaction conditions play a role in the stereoselectivity.

Experiment 2, proof of the iminium I as the reactive intermediate, through enamine II. The reaction was set up as follows. Aldehyde **1b**, catalyst **3b** and BA (1:1:1 ratio) were mixed overnight in $CDCl_3$ in the presence of molecular sieves. The presence of iminium ion **I** was confirmed by ^{1}H and ^{19}F NMR. The MS were then removed, diene **2e** was added to the reaction mixture (Scheme 14) and this was checked at different times[155] by ^{1}H NMR (Figure 2) and ^{19}F NMR (Figure 3).

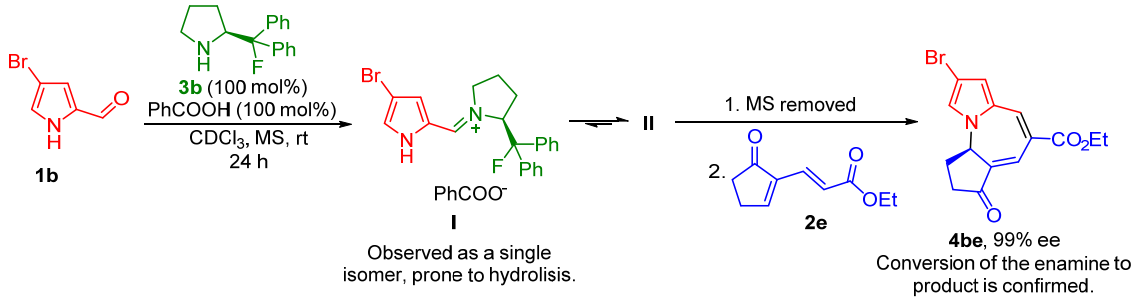

Scheme 14. Description of Experiment 2.

Analyzing the reaction mixture by ^{19}F NMR (and superimposing the spectrum with the one corresponding to the enamine, recorded in experiment 1) it was possible to note that the actual equilibrium iminium **I** –enamine **II** is observable under the real reaction conditions as well (even if the ratio was strongly in favor of iminium **I**). Enamine **II** was detected again as two different signals, presumably associated with the two stereoisomers, and kept being present throughout all the course of the reaction monitoring. The plotting of the various species vs time (Figure 4) clearly shows that disappearance of iminium **I** is proportional to product formation and catalyst release, proving iminium ion **I** being an actual intermediate in the formation of the product (formed this time in 99% ee).

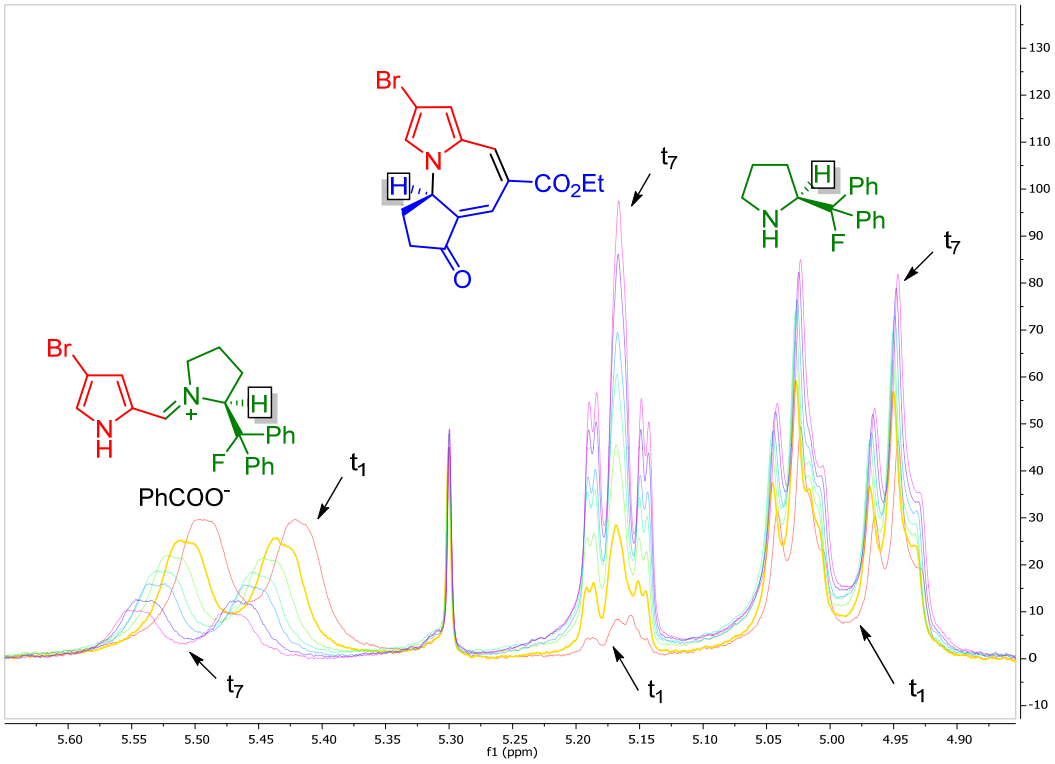

Figure 2. [1]H NMR Spectra recorded at different times (from t_1 in red, to t_7 in purple) on the reaction mixture of Experiment 2, showing intermediate **I** consumption, product **4be** formation and catalyst **3b** release.

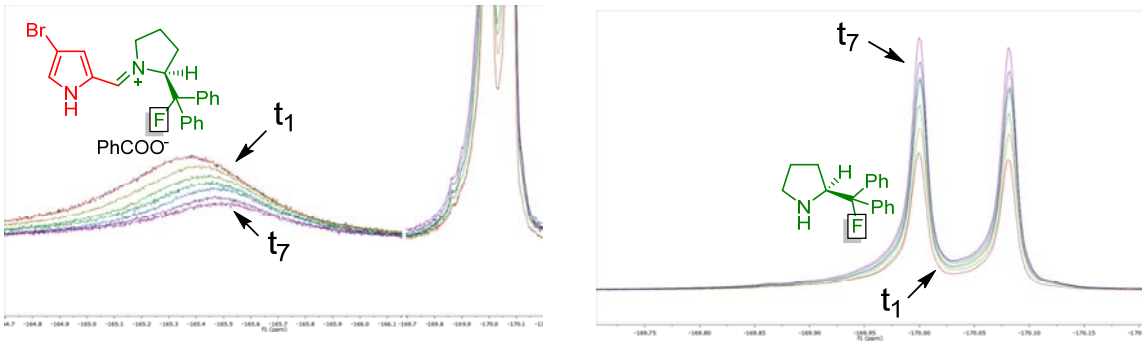

Figure 3. [19]F NMR Spectra recorded at different times (from t_1 in red, to t_7 in purple) on the reaction mixture of Experiment 2, showing intermediate **I** consumption and catalyst **3b** release.

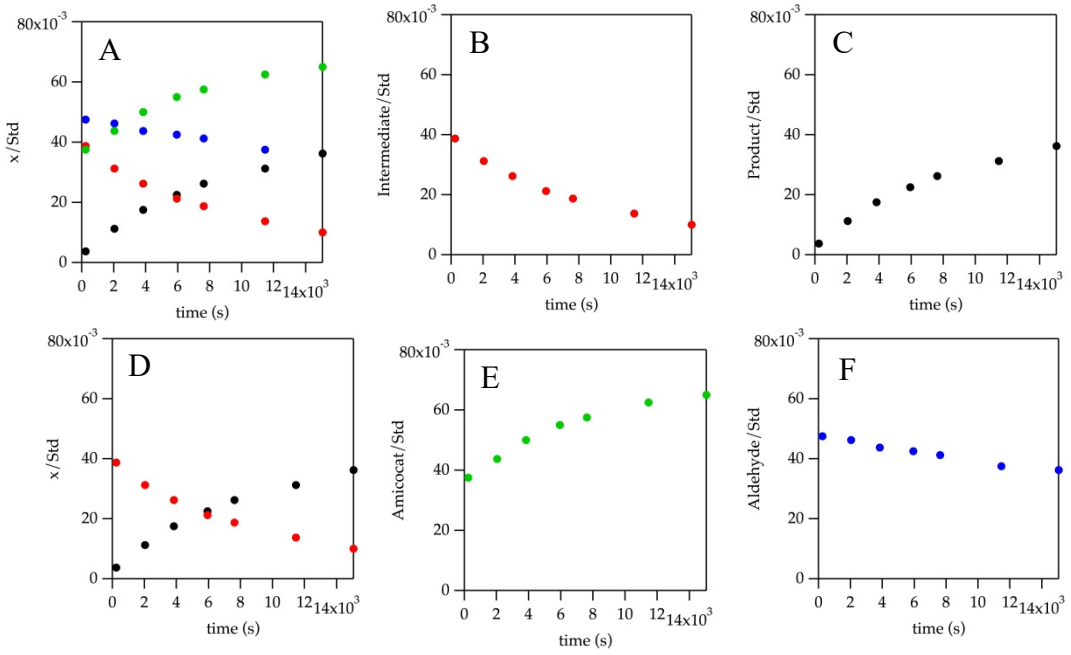

Figure 4. Evolution over time of the relative concentration of: the whole mixture (graph A), **I** (graph B), **4be** (graph C), **I** and **4be** together (graph D), **3b** (graph E) and **1b** (graph F) as calculated from ^{1}H NMR spectra recorded at different times on the reaction mixture of Experiment 2. Et_4Si Was used as internal standard.

Experiment 3, monitoring of the catalytic reaction. The reaction was set up as follows. Aldehyde **1b**, diene **2e**, catalyst **3b** and BA (1:1:0.2:0.2 ratio) were mixed in $CDCl_3$ in the presence of molecular sieves into an NMR tube and the mixture was checked at different times[155] by ^{1}H NMR and ^{19}F NMR (Scheme 15).

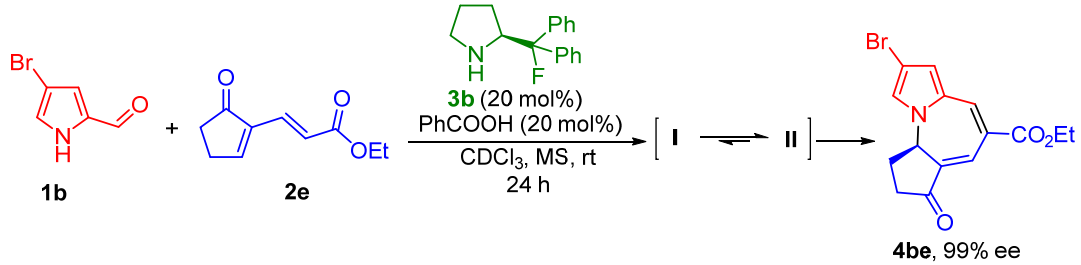

Scheme 15. Description of Experiment 3.

Interestingly, the rapid formation of intermediate **I** (iminium ion) was observed at first and ^{19}F NMR revealed the presence of intermediate **II** (enamine) as well, in about 3:1 ratio in favor of **I**. Intermediates **I** and **II** reached a steady state, and remained constant for several hours, while product **4be** was slowly forming. During these investigations, intermediate **II**, appeared as two distinct signals, confirming the presence of two isomers. The importance of MS was also underlined by this experiment, as they allowed constant replacement of the reacted intermediates by facilitating the condensation of catalyst **3b**

with **1b**. Observability of intermediates **I** and **II** in the experiment under the real optimized reaction conditions (i.e. their formation was not forced), indicates compelling evidence of these species being reactive intermediates in the hetero-[6+4] cycloaddition (Figure 5).

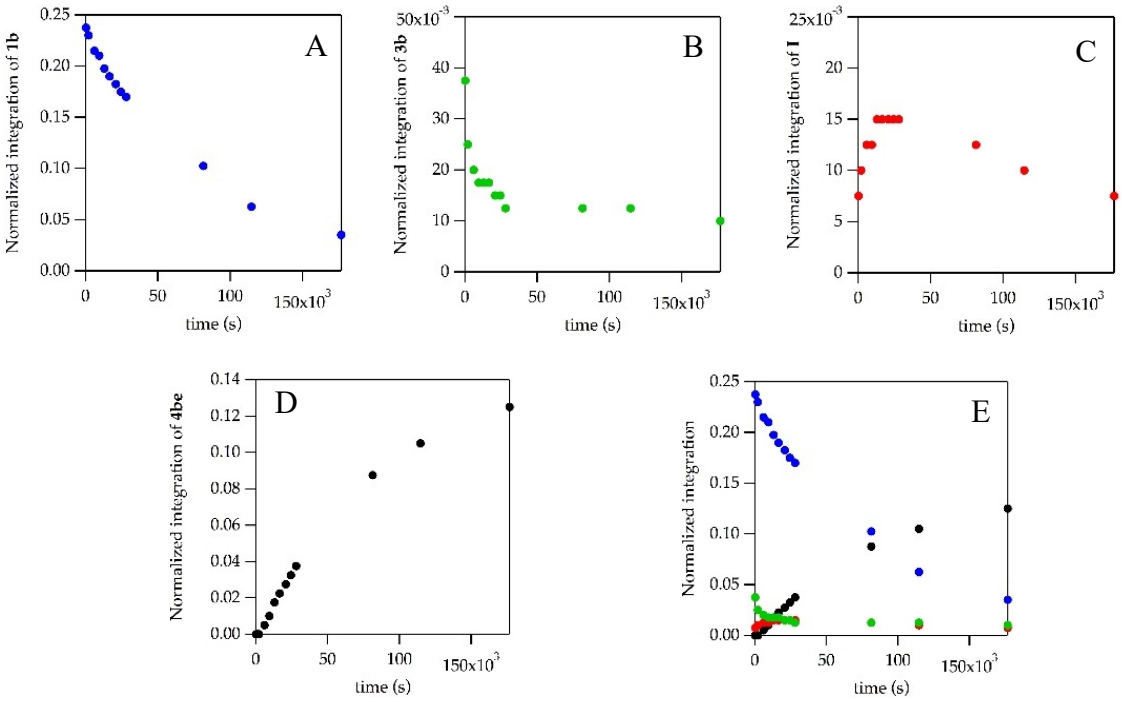

Figure 5. Evolution over time of the relative concentration of: **1b** (graph A), **3b** (graph B), **I** (graph C), **4be** (graph D) and the whole mixture (graph E), as calculated from ^{1}H NMR spectra recorded at different times on the reaction mixture of Experiment 3. Et_4Si Was used as internal standard.

At this point it was clear that enamine **II** was present into the reaction mixture as two distinct isomers that, upon reaction with dienes **2**, are probably going to render opposite enantiomers of the product. Therefore, a question arose on how the reaction displays such a high degree of enantioselectivities. Computational investigations are currently ongoing to address this and other features of the disclosed hetero-[6+2] and [6+4] cycloadditions. The ultimate purpose will be to explain how the catalyst imparts enantioselectivity to the products.

7.4 [6+2] Cycloaddition: Results and Discussions

We then planned to extend this strategy to enantioselective hetero-[6+2] cycloadditions. We initially found that pyrrole-2-carbaldehyde **1a** could be reacted with 1.5 equivalents of *trans*-β-nitrostyrene **7a** in presence of catalyst ***ent*-3a** (20 mol%) in $CDCl_3$ at room

temperature to produce cycloadduct **8aa** in 40% yield and 66% ee after 48 h (Table 5, entry 1). One precedent for this reaction could be found in literature. However, it was not recognized as a [6+2]-cycloaddition and very low enantioselectivity was achieved.[156] The addition of BA (20 mol%) increased the enantioselectivity (entry 2) and performing the reaction in presence of MS allowed to reach the same yield in 24 h (entry 3). Bulkier catalyst **3d** improved the enantioselectivity to 82% ee, without significantly lowering the conversion (entries 4 and 5). Other catalysts, acids and solvents were tested (Table 6, *vide infra*), leading to less satisfactory results. To ease the purification, we inverted the **1a**/**7a** ratio, leading to full consumption of **7a**. During this experiment we noticed that compound **8aa** was prone to double bond shift in the reaction mixture, leading to isomer **8'aa**. We hypothesized that this shift could be acid promoted, and, consequently, its amount was lowered to 10 mol%. Even so, we found that this side reaction still occurred, but only when the nitroolefin was consumed (entries 6 and 7). Therefore, an excess of nitroolefin was reapplied to disfavor the isomerization, thus delivering the optimal conditions (entry 8). Unfortunately, we observed both isomerization and decomposition of **8aa** as isolated compound. At present time we did not elucidate the pathway of this double bond shift. However, we exclude an equilibration between the two isomers, since recovered **8aa** from samples showing extensive isomerized products **8'aa**, showed only slightly diminished enantiomeric excess, instead of displaying complete racemization. Nonetheless, we surmised that exploiting the reactivity of the electrophilic double bond, might circumvent this issue and at the same time bring diversity to the methodology. We therefore conceived a two-step one-pot strategy consisting in the addition of a nucleophile to the reaction mixture at the end of the hetero-[6+2] cycloaddition step.

Table 5. Optimization of the reaction conditions for the [6+2] cycloaddition between aldehyde **1a** and nitroolefin **7a**. Most relevant results.[a]

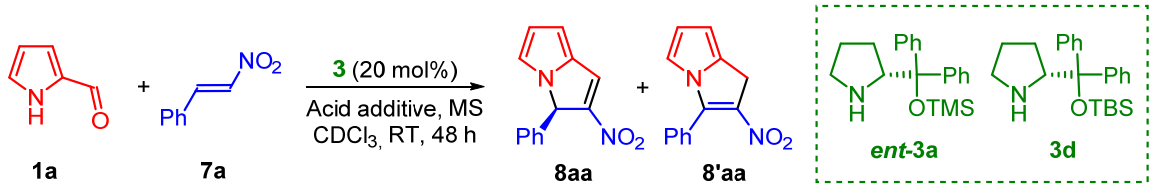

Entry	Catalyst	Time (h)	Additive (mol%)	Ratio **1a**:**7a**	Consumption of **7a** (%)[b]	Ratio **8aa**:**8'aa**[c]	Yield (%)[c]	*ee* (%)[d]
1[e]	***ent*-3a**	48	-	1:1.5	50	> 20:1	40	66
2[e]	***ent*-3a**	48	BA (20)	1:1.5	48	> 20:1	40	76
3	***ent*-3a**	24	BA (20)	1:1.5	52	> 20:1	41	76
4	**3d**	24	BA (20)	1:1.5	30	> 20:1	35	82.
5	**3d**	48	BA (20)	1:1.5	65	18:1	50.	82
6	**3d**	24	BA (10)	1.5:1	80	13:1	40	81
7	**3d**	48	BA (10)	1.5:1	> 95	2.5:1	41	76
8	**3d**	48	BA (10)	1:1.5	65	> 20:1	62	82

(**a**) Reaction conditions: **1a** (0.1 or 0.15 mmol), **7a** (0.15 or 0.1 mmol), **3** (0.02 mmol), $CDCl_3$ (0.25 M), RT. (**b**) Amount of **7a** present in the reaction mixture divided by initial amount, determined on the crude mixture by ^1H NMR in comparison to $SiEt_4$ as internal standard. (**c**) Determined on the crude mixture by ^1H NMR in comparison to $SiEt_4$ as internal standard. (**d**) Determined by CSP UPCC on the isolated products **8**. (**e**) Isolated yield after flash chromatography.

Since the initial enantioselectivity in the [6+2] cycloaddition was observed to be lower than its [6+4] cycloaddition counterpart, a screening of reaction conditions for the [6+2] cycloaddition was performed focusing on achieving higher enantiomeric excess. An attempt was made to lower the temperature, however, this shot down reactivity completely (Table 6, entry 1). Various secondary aminocatalysts were then tested. In particular, since improvement in enantioselectivity was observed moving from OTMS protected ***ent*-3a** to OTBS protected **3d**, we tried bulkier catalysts such as **3e**[157] (entry 2) and **3f** (entry 3), obtaining however lower degrees of enantioenrichment.

Table 6. Optimization of the reaction conditions for the [6+2] cycloaddition between aldehyde **1a** and nitroolefin **7a**. Catalyst and acid screening.[a]

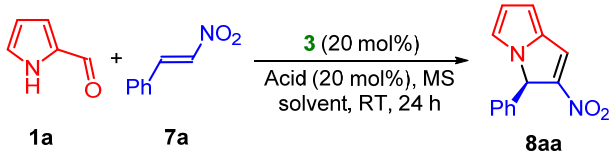

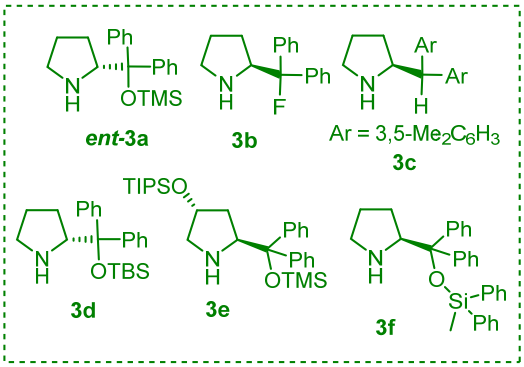

Entry	Catalyst	Temperature (°C)	Additive[b]	Solvent	Yield (%)[c]	*ee* (%)[d]
1	***ent*-3a**	0	BA	$CDCl_3$	traces	-
2	**3e**	RT	BA	$CDCl_3$	5	79
3	**3f**	RT	BA	$CDCl_3$	25	77
4	**3b**	RT	BA	$CDCl_3$	16	76
5	**3c**	RT	BA	$CDCl_3$	58	74
6[e]	**3d**	RT	BA	PhMe	13	80
7	**3d**	RT	BA	Et_2O	12	69
8	**3d**	RT	CSA	$CDCl_3$	traces	-
9	**3d**	RT	*o*-F-BA	$CDCl_3$	13	82
10	**3d**	RT	*m*-Br-BA	$CDCl_3$	20	80
11	**3d**	RT	*p*-NO_2-BA	$CDCl_3$	5	82
12	**3d**	RT	AcOH	$CDCl_3$	11	82
13	**3d**	RT	*p*-MeO-BA	$CDCl_3$	56	80

(**a**) Reaction conditions: **1a** (0.1 or 0.15 mmol), **7a** (0.15 or 0.1 mmol), **3** (0.02 mmol), $CDCl_3$ (0.25 M). (**b**) Equimolar with catalyst **3**. (**c**) Determined on the crude mixture by ^1H NMR in comparison to $SiEt_4$ as internal standard. (**d**) Determined by CSP UPCC on the isolated products **8**.

Indeed, since catalysts **3b** and **3c** performed almost equally to ***ent*-3a** (entries 4 and 5), the enantioselectivity in this case might not be just a matter of bulkiness. Next, a screening of solvents was performed, however, with no improvement of enantioselectivity when compared to chloroform (entries 6 and 7) for representative results). Exploring different acid additives revealed that the strong acid (-)-

camphorsulfonic acid (CSA) did not promote any product formation (entry 8). Finally, variation of the carboxylic acid did not affect the enantioselectivity, giving comparable results to BA (entries 9-12). The screening confirmed that the highest conversion was achieved when BA was employed as acid additive, except for *p*-MeO-BA (entry 13) which ensured slightly higher yields but lower enantioselectivities.

As stated previously, we have conceived a two-step one-pot strategy consisting in the addition of a nucleophile to the reaction mixture at the end of the cycloaddition step (Scheme 16). First of all, we selectively reduced compounds **8** with $NaBH_4$ to prepare dihydropyrrolizines **9**. Under these conditions, model compound **9aa**, derived from pyrrole-2-carbaldehyde **1a** and *trans*-β-nitrostyrene **7a**, was achieved in 45% overall yield and 82% *ee*. This protocol was also successfully applied to the cycloaddition of **1a** with 4-Br and 4-F substituted nitroolefins **7b** and **7c** affording the respective products **9ab** and **9ac** with similar results to **9aa**. 4-Br Substituted aldehyde **1b** underwent the same reaction sequence, displaying slightly diminished efficiency. On the other hand, an aryl group on the pyrrole ring was found to stabilize the [6+2]-adducts; products **8ea** and **8fa**, deriving from aldehydes **1e** and **1f** and nitrostyrene **7a**, were therefore directly isolated after the sole cycloaddition step in good yields and enantioselectivities. 4-MeO and 3-MeO substituted nitroolefins **7d** and **7e** also participated successfully in the [6+2]-cycloaddition with **1a** and the respective products were functionalized by addition of benzyl thiol instead of undergoing the reduction step. This afforded trisubstituted products **10ad** and **10ae** with moderate yields and good enantioselectivities, displaying three contiguous stereocenters, as single diastereoisomers. A neutral nucleophile such as indole was also found to be a competent reaction partner for the one-pot functionalization of the [6+2]-adducts. This protocol was employed to prepare products **11ab** and **11af**, obtained as single diastereoisomers. *ortho*-Substituted or heteroaromatic nitroolefins did not participate successfully in the [6+2]-cycloaddition, as well as 5- or 3-substituted pyrrole-2-carbaldehydes **1** The absolute stereochemistry of compound **8ea** was determined by ECD analysis. For compounds **9**, **10** and **11**, the stereochemistry of the stereocenters created during the transformations, relative to that of the original stereocenter, was assigned by NMR spectroscopy. The disclosed one-pot [6+2] cycloaddition – nucleophilic addition sequence was thus demonstrated to display wide applicability and synthetic utility in the rapid preparation of complex and biologically relevant structures from simple and commercially available starting materials.

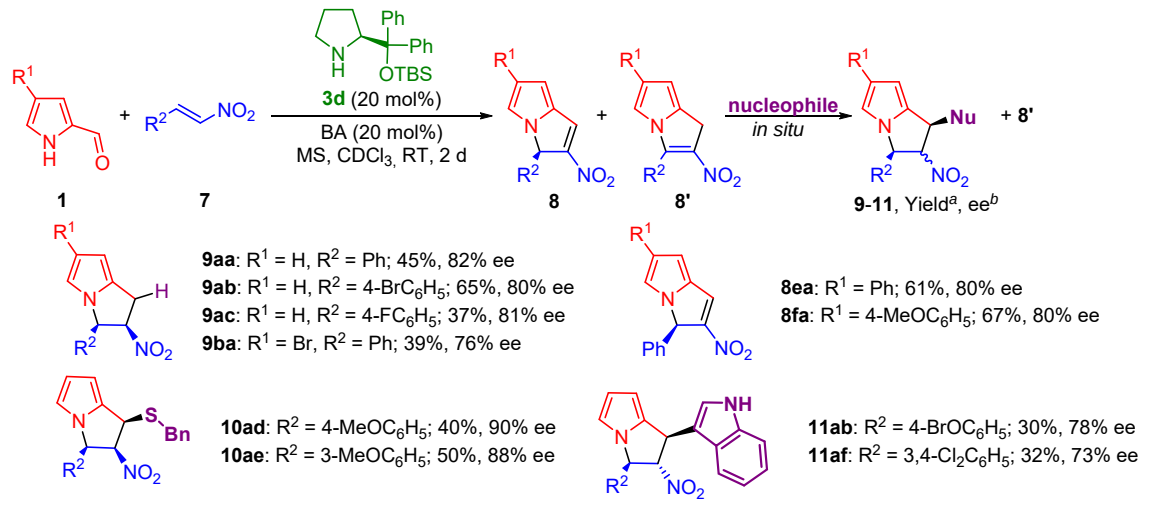

Scheme 16. Scope of the [6+2] cycloaddition – nucleophilic addition between aldehydes **1** and nitroolefins **7**. Reaction conditions: **1** (0.1 mmol), **7** (0.15 mmol), **3d** (0.01 mmol), BA (0.01 mmol), $CDCl_3$, (0.2 M), RT, 24 h then nucleophile (see Section 7.4.3 for specific reaction conditions for this second step). (**a**) Isolated yields after flash chromatography. (**b**) Determined by CSP UPCC on the isolated products **8**-**11**.

7.5 Conclusion

In conclusion, a novel methodology for the functionalizations of pyrroles, imidazoles and pyrazoles has been developed. This relies on organocatalyzed enantioselective hetero-[6+2] and [6+4] cycloadditions. The strategy is centered on the catalytic formation of transient chiral 6-amino (di)azafulvenes from the condensation of azole carbaldehydes **1** and secondary aminocatalysts **3**. The robustness of the method was broadly demonstrated, given the following prominent features (Scheme 17).

i) A broad scope of simple pyrrole-2-carbaldehydes **1a-f** and dienes **2** was investigated, displaying good yields and 99% ee values in every case. The obtained products **4** present the pyrrolo[1,2-*a*]azepine scaffold, core structure of many natural compounds.

ii) The methodology could be extended with very minor adjustment to imidazole- and pyrazole carbaldehydes (**1g-i**), despite the very different electronic properties of these heterocycles compared to pyrrole.

iii) Unconstrained dienes **5** as well, could be employed successfully in the [6+4] cycloaddition, circumventing the necessity to include part of the reactive conjugated system into a cyclic structure.

iv) The [6+2] cycloaddition with nitroolefins **7**, displaying moderate yields and enantioselectivities, allowed the preparation of products capable of undergoing four different functionalizations *in situ* (products **8-12**). This disclosed a powerful methodology for the preparation of highly decorated pyrrolizine scaffolds.

v) Both the postulated iminium **I** and enamine **II** intermediates were observed by NMR spectroscopy, allowing a preliminary comprehension of the whole process.

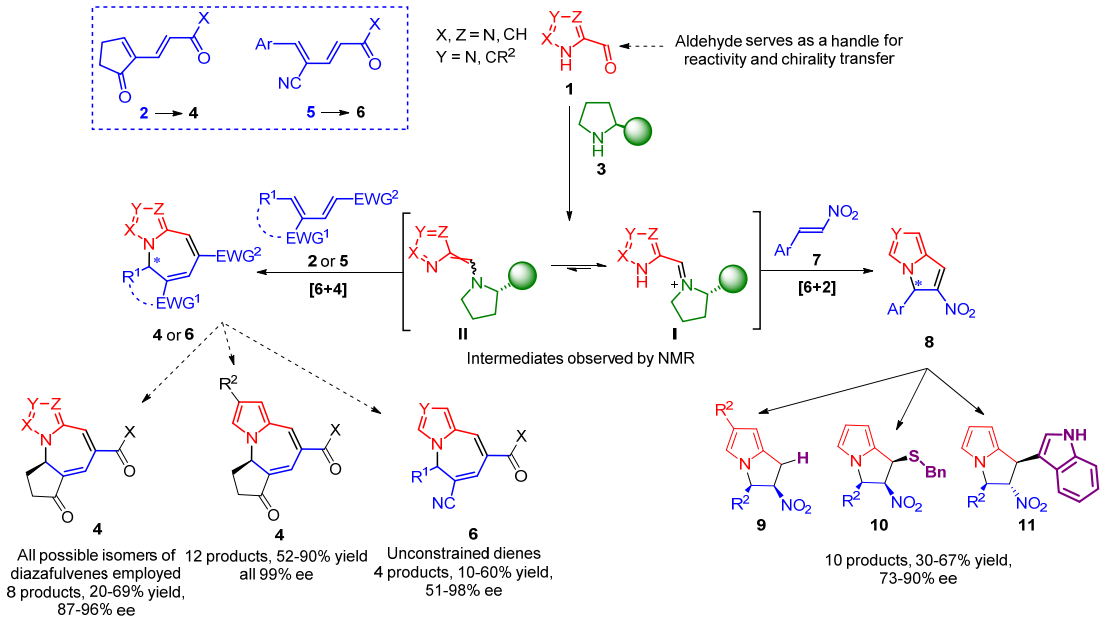

Scheme 17. Project summary.

7.6 Experimental details

7.6.1 General Methods and Materials

Methods. NMR spectra were acquired on a Bruker AVANCE III HD spectrometer running at 400 MHz for ^{1}H, 100 MHz for ^{13}C and 376 MHz for ^{19}F. Chemical shifts (δ) are reported in ppm relative to residual solvent signals ($CDCl_3$, 7.26 ppm for ^{1}H NMR, $CDCl_3$, 77.0 ppm for ^{13}C NMR). Chemical shifts (δ) for ^{19}F NMR are reported in ppm relative to $CFCl_3$ as external reference. The following abbreviations are used to indicate the multiplicity in NMR spectra: s, singlet; d, doublet; t, triplet; q, quartet; m, multiplet. ^{13}C NMR spectra were acquired in broad band decoupled mode. Mass spectra were recorded on a Bruker Maxis Impact-TOF-MS with electrospray ionization (ESI+) (referenced to the mass of the charged species). Analytical thin layer chromatography (TLC) was performed using pre-coated aluminum-backed plates (Merck Kieselgel 60 F254) and visualized by ultraviolet radiation and/or staining with $KMnO_4$ or vanillin. For flash column chromatography (FC) silica gel (Silica gel 60, 230-400 mesh) or Iatrobeads

(IATROBEADS 6RS-82060) were used. Optical rotations were measured on a Bellingham+Stanley ADP440+ polarimeter, α values are given in $deg \cdot cm^3 \cdot g^{-1} \cdot dm^{-1}$; concentration c in $g \cdot (100\ mL)^{-1}$.The diastereomeric ratio (dr) of products was evaluated by ^1H NMR analysis of the crude mixture. The enantiomeric excess (ee) of the products was determined by Ultra-Performance Convergence Chromatography (ACQUITY UPCC) using Daicel Chiralpak columns (IA, IB, IC and ID) as chiral stationary phases. Unless otherwise noted, gradient runs were performed with 99:1 supercritical CO_2/solvent for 30 seconds, then going from 99:1 to 60:40 CO_2/solvent over 4 minutes, then isocratic 60:40 CO_2/solvent. Reference samples for UPCC analysis were prepared following the general method using either proline or a 1:1 mixture of the (*R*)- and (*S*)-diphenylprolinol *tert*-butyldimethyl silyl ether catalyst **3i**. Unless otherwise noted, analytical grade solvents and commercially available reagents were used without further purification. Below the general procedures, the characterization of the model compound only is reported, the characterization of the remaining compounds is under preparation.

Materials. Reference samples for UPCC analysis were prepared following the general method using either pyrrolidine (for the [6+4] cycloaddition leading to products **4** or **6**) or a 1:1 mixture of the (*R*)- and (*S*)-diphenylprolinol *tert*-butyldimethyl silyl ether catalyst **3d** (for the [6+2] cycloaddition leading to products **8**-**11**). Aldehydes **1a**, **1g**, **1h**, and **1i** are commercially available; **1b**,[158] **1c** and **1d**,[159] **1e** and **1f**[158] were prepared according to literature procedures. Dienes **2** were prepared as stated in Section 6. Catalysts **3b**[153c] and **3c**[154] were prepared according to literature procedures. All the experimental data matched with those reported. Analytical grade solvents and commercially available reagents were used without further purification.

7.6.2 Synthesis of linear 4π-components 5

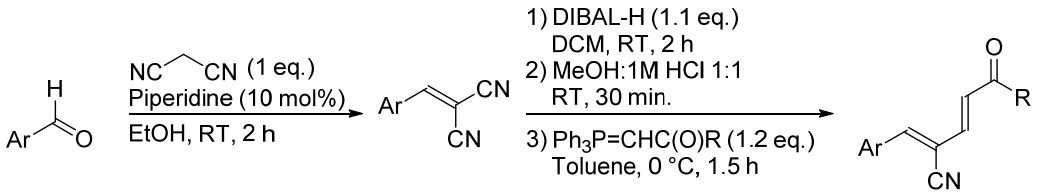

Aryl aldehyde (20 mmol, 1 eq.) was dissolved into EtOH (30 mL). Malononitrile (1.32 g, 20 mmol, 1 eq.) was added, followed by piperidine (0.18 mL, 2 mmol, 10 mol%). The reaction was stirred at RT for 2 hours. Hereafter, 10 mL of a pentane/Et_2O (9:1) mixture were added, the solid was collected by filtration and washed with the same cold mixture (90 mL), affording the pure desired conjugated malononitrile.

Conjugated malononitrile (5 mmol, 1 eq.) was introduced into a dried flask under argon atmosphere. Dry DCM (100 mL) was added. DIBAL-H (1M in heptane, 5.5 mL, 1.1 eq.) was then added dropwise over 20 minutes. The mixture was then stirred for 2 hours at

RT. A 1:1 mixture of MeOH:1M HCl (100 mL) was then added and the resulting mixture was stirred for 30 minutes at RT and diluted with water (50 mL). The layers were separated, and the aqueous layer was extracted with DCM (3x30 mL). The combined organic layers were dried over $MgSO_4$ and solvent was removed under vacuum (without heating). Due to instability of the aldehyde intermediate, the crude mixture was used directly for the next step.

The crude mixture (5 mmol, 1 eq.) was dissolved into dry toluene (10 mL). The solution was cooled down to 0 °C. Phosphonium ylide (6 mmol, 1.2 eq.) was then added portionwise at 0 °C and the resulting mixture was stirred until completion (monitored by TLC, ~2 hours) while being allowed to come back to RT. The crude mixture was directly loaded onto chromatography column on silica gel and eluted with a pentane/EtOAc mixture. The still unclean product was then dissolved into the minimum amount of DCM, and pentane was added slowly until a precipitate appeared. This precipitate was filtered and washed with pentane (30 mL) to afford pure compound **5**.

(E)-2-((Z)-benzylidene)-5-oxo-5-phenylpent-3-enenitrile 5a. Benzaldehyde was used in the first step and 2-(triphenylphosphoranylidene)acetophenone was used as Wittig reagent. Columned using a mixture of pentane/EtOAc 9:1 as eluent. Pale yellow fluffy solid, 15% yield. **^{1}H NMR (400 MHz, $CDCl_3$)** δ 8.08–8.02 (m, 2H), 7.93 (dd, *J* = 6.7, 3.0 Hz, 2H), 7.65–7.43 (m, 9H). **^{13}C NMR (100 MHz, $CDCl_3$)** δ 188.9, 150.8, 141.1, 137.4, 133.4, 132.9, 132.1, 130.0 (2C), 129.2 (2C), 128.8 (2C), 128.6 (2C), 125.4, 115.7, 109.3. **HRMS** (ESI+) *m/z* calcd. for $[C_{18}H_{13}NO+H]^+$: 260.1070; found: 260.1071.

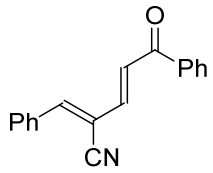

5a

7.6.3 General procedure for the [6+4] cycloadditions.

General procedure for the synthesis of products 4aa-4fa and 4ab-4ae. In a flame-dried screw capped vial equipped with a magnetic stirring bar, 4 Å molecular sieves (MS, 3 spheres), catalyst **3b** (5.1 mg, 0.02 mmol, 20 mol%), *p*-MeO-BA (3.0 mg, 0.02 mmol, 20 mol%), dry $CDCl_3$ (250 μL), diene **2** (0.15 mmol) and aldehyde **1** (0.1 mmol) were added in this order. The resulting solution was stirred for 48 h at room temperature and then directly purified by column chromatography on silica gel (DCM/Et_2O mixtures) to afford the desired compounds **4aa-4fa** and **4ab-4ae** as solids.

(*R*)-5-benzoyl-9,9a-dihydrocyclopenta[*f*]pyrrolo[1,2-*a*]azepin-7(8*H*)-one 4aa. Following the general procedure from pyrrole-2-carbaldehyde **1a** and diene **2a**, product **4aa** was obtained as a red solid in 73% yield after FC on silica gel (2% Et_2O in DCM). $[\alpha]_D^{25}$ = +1095 (*c* 0.1, CH_2Cl_2) for 99% *ee*. **^{1}H NMR (400 MHz, $CDCl_3$)** δ 7.79 (t, *J* = 2.1 Hz, 1H), 7.74–7.69 (m, 2H), 7.56 (t, *J* = 7.4 Hz, 1H), 7.50–7.43 (m, 3H), 7.07 (t, *J* = 2.1 Hz, 1H), 6.66 (dd, *J* = 3.9, 1.5 Hz, 1H), 6.45 (t, *J* = 3.3 Hz, 1H), 5.32 (ddd, *J* =

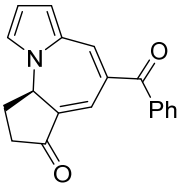

4aa

9.1, 7.0, 2.3 Hz, 1H), 2.91–2.79 (m, 1H), 2.69 (dd, *J* = 17.9, 8.8 Hz, 1H), 2.59–2.33 (m, 2H). **^{13}C NMR (100 MHz, $CDCl_3$)** δ 201.1, 195.8, 137.8, 136.9, 132.0, 131.9, 131.4, 131.0, 129.3 (2C), 128.4 (2C), 126.6, 124.9, 123.9, 113.3, 58.0, 36.3, 26.8. **HRMS** (ESI+) *m/z* calcd. for $[C_{19}H_{15}NO_2+H]^+$: 290.1176; found: 290.1180. **UPC^2**: IB, gradient CO_2/*i*PrOH, 3.0 mL·min^{-1}; t_{major} = 5.373 min; t_{minor} = 5.198 min.

General procedure for the synthesis of products 4, derived from aldehydes 1g, 1h and 1i. In a flame-dried screw capped vial equipped with a magnetic stirring bar, 4 Å molecular sieves (MS, 3 spheres), catalyst **3b** (10 or 20 mol%), *p*-MeO-BA (10 or 20 mol%), dry $CDCl_3$ (1000 μL or 500 μL), diene **2** (0.1 mmol) and aldehyde **1** (0.2 mmol) were added in this order. The resulting solution was stirred for the indicated time at room temperature and then directly purified by column chromatography on Iatrobeads to afford the desired compounds **4** as solids.

(*R*)-5-benzoyl-9,9a-dihydrocyclopenta[*f*]imidazo[1,2-*a*]azepin-7(8*H*)-one 4ga.

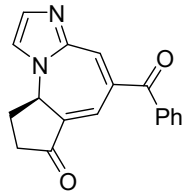

4ga

Following the general procedure (10% **3b**, 10% *p*-MeO-BA, 1000 μL $CDCl_3$, 1 day) from 1*H*-imidazole-2-carbaldehyde **1g** and diene **2a**, product **4gd** was obtained as a brown solid in 69% yield after FC on Iatrobeads (25% EtOAc in DCM). $[\alpha]_D^{25}$ = +617 (*c* 0.1, CH_2Cl_2) for 95% *ee*. **^{1}H NMR (400 MHz, $CDCl_3$)** δ 7.79–7.74 (m, 3H), 7.61–7.56 (m, 2H), 7.51–7.44 (m, 3H), 7.17 (s, 1H), 5.38 (ddd, *J* = 9.2, 7.2, 2.9 Hz, 1H), 2.99–2.83 (m, 1H), 2.79–2.68 (m, 1H), 2.62–2.40 (m, 2H). **^{13}C NMR (100 MHz, $CDCl_3$)** δ 200.3, 195.2, 143.8, 136.5, 135.2, 134.5, 133.3, 132.7, 131.7, 130.7, 129.5 (2C), 128.6 (2C), 120.4, 56.3, 36.3, 26.7. **HRMS** (ESI+) *m/z* calcd. for $[C_{18}H_{14}N_2O_2+H]^+$: 291.1128; found: 291.1134. **UPC^2**: IB, gradient CO_2/MeOH, 3.0 mL·min^{-1}; t_{major} = 4.589 min; t_{minor} = 4.675 min.

(*R*)-5-benzoyl-9,9a-dihydrocyclopenta[*f*]imidazo[1,5-*a*]azepin-7(8*H*)-one 4ha.

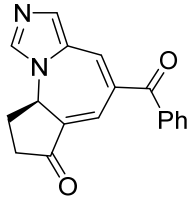

4ha

Following the general procedure (10% **3b**, 10% *p*-MeO-BA, 1000 μL $CDCl_3$, 1 day) from 1*H*-imidazole-4-carbaldehyde **1h** and diene **2a**, product **4ha** was obtained as a bright yellow solid in 34% yield after FC on Iatrobeads (from 1 to 2.5% MeOH in DCM). $[\alpha]_D^{25}$ = +830 (*c* 0.1, CH_2Cl_2) for 97% *ee*. **^{1}H NMR (400 MHz, $CDCl_3$)** δ 7.80–7.70 (m, 4H), 7.63–7.55 (m, 1H), 7.54–7.42 (m, 4H), 5.38 (ddd, *J* = 9.9, 7.4, 2.8 Hz, 1H), 3.02–2.91 (m, 1H), 2.81–2.68 (m, 1H), 2.64–2.38 (m, 2H). **^{13}C NMR (100 MHz, $CDCl_3$)** δ 200.3, 195.1, 140.5, 139.0, 136.9, 133.0, 132.53, 132.45, 131.5, 129.7, 129.4 (2C), 128.6 (2C), 127.7, 56.8, 36.3, 26.3. **HRMS** (ESI+) *m/z* calcd. for $[C_{18}H_{14}N_2O_2+H]^+$: 291.1128; found: 291.1138. **UPC^2**: IB, gradient CO_2/MeOH, 3.0 mL·min^{-1}; t_{major} = 5.231 min; t_{minor} = 5.585 min.

(*R*)-5-benzoyl-9,9a-dihydrocyclopenta[*f*]pyrazolo[1,5-*a*]azepin-7(8*H*)-one 4ia.

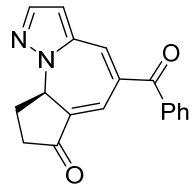

4ia

Following the general procedure (20% **3b**, 20% *p*-MeO-BA, 500 μL $CDCl_3$, 6 days) from 1*H*-pyrazole-5-carbaldehyde **1i** and diene **2a**, product **4ia** was obtained as a pale yellow solid in 31% yield after FC on Iatrobeads (4% Et_2O in DCM). $[\alpha]_D^{25}$ = +110 (*c* 0.1, CH_2Cl_2) for 87% *ee*. **^{1}H NMR (400 MHz, $CDCl_3$)** δ 7.82–7.76 (m, 2H), 7.69 (dd, *J* = 2.5, 1.3 Hz, 1H), 7.65–7.59 (m, 2H), 7.53–7.48 (m, 2H), 7.44 (d, *J* = 1.3 Hz, 1H), 6.59 (d, *J* = 2.0 Hz, 1H), 5.34 (td, *J* = 7.9, 2.6 Hz, 1H), 3.09 (dddd, *J* = 13.7, 10.7, 9.2, 7.6 Hz, 1H), 2.95–2.83 (m, 1H), 2.71 (dddd, *J* = 18.4, 9.2, 4.0, 1.0 Hz, 1H), 2.62–2.50 (m, 1H). **^{13}C NMR (100 MHz, $CDCl_3$)** δ 202.0, 195.0, 140.2, 137.9, 136.5, 134.4, 133.0, 132.9, 131.6, 130.1, 129.6 (2C), 128.6 (2C), 113.4, 60.2, 36.4, 24.4. **HRMS** (ESI+) *m/z* calcd. for $[C_{18}H_{14}N_2O_2+H]^+$: 291.1128; found: 291.1129. **UPC^2**: ID, gradient CO_2/*i*PrOH, 3.0 mL·min^{-1}; t_{major} = 6.416 min; t_{minor} = 5.671 min.

General procedure for the synthesis of products 6aa-6ad. In a flame-dried screw capped vial equipped with a magnetic stirring bar, 4 Å molecular sieves (MS, 3 spheres), catalyst **3b** (10.2 mg, 0.04 mmol, 40 mol%), *p*-MeO-BA (6.1 mg, 0.04 mmol, 40 mol%), dry $CDCl_3$ (250 μL), diene **5** (0.1 mmol) and aldehyde **1a** (0.15 mmol) were added in this order. The resulting solution was stirred for 96 h at room temperature and then directly purified by column chromatography on Iatrobeads to afford the desired compounds **6aa-6ad** as solids.

(*R*)-8-benzoyl-5-phenyl-5*H*-pyrrolo[1,2-*a*]azepine-6-carbonitrile 6aa. Following the general procedure from 1*H*-pyrrole-2-carbaldehyde **1a** and diene **5a**, product **6aa** was obtained as a yellow solid in 55% yield after FC on Iatrobeads (20% pentane in DCM). $[\alpha]_D^{25}$ = -1163 (*c* 0.1, CH_2Cl_2) for 96% ee. **^{1}H NMR (400 MHz, $CDCl_3$)** δ 7.77 (d, *J* = 1.0 Hz, 1H), 7.54–7.48 (m, 1H), 7.39–7.28 (m, 8H), 7.20 (t, *J* = 2.1 Hz, 1H), 6.89–6.84 (m, 2H), 6.72 (dd, *J* = 3.9, 1.6 Hz, 1H), 6.53 (dd, *J* = 4.0, 2.6 Hz, 1H), 6.23 (s, 1H). **^{13}C NMR (100 MHz, $CDCl_3$)** δ 194.4, 142.2, 137.6, 137.5, 136.7, 132.2, 130.0, 129.7, 129.3 (2C), 128.7 (2C), 128.4 (3C), 126.1, 125.4 (2C), 121.7, 120.1, 113.2, 108.2, 62.8. **HRMS** (ESI+) *m/z* calcd. for $[C_{23}H_{16}N_2O+H]^+$: 337.1335; found: 337.1338. **UPC^2**: IB, gradient CO_2/iPrOH, 3.0 mL·min^{-1}; t_{major} = 3.543 min; t_{minor} = 3.448 min.

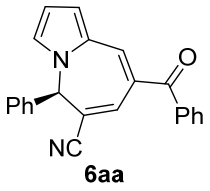

6aa

7.6.4 General procedure for [6+2] cycloaddition and synthetic elaborations.

General procedure for the synthesis of [6+2] cycloadducts 8. In a flame-dried screw capped vial equipped with a magnetic stirring bar, 4 Å molecular sieves (MS, 3 spheres), catalyst **3d** (7.36 mg, 0.02 mmol, 20 mol%), BA (1.2 mg, 0.01 mmol, 10 mol%), dry $CDCl_3$ (500 μL), nitroolefin **7a** (0.15 mmol) and aldehyde **1** (0.1 mmol) were added in this order. The resulting solution was stirred for 24 - 48 h at room temperature and then directly purified by column chromatography on silica gel (Pentane/EtOAc mixtures) to afford the desired compounds **8ea** and **8fa** as solids.

(R)-2-nitro-3,6-diphenyl-3*H*-pyrrolizine 8ea. Following the general procedure from 4-phenyl-1*H*-pyrrole-2-carbaldehyde **1e** and nitroolefin **7a**, product **8ea** was obtained as an orange solid in 61% yield after FC (2% EtOAc in pentane). $[\alpha]_D^{25}$ = -207 (*c* 0.1, CH_2Cl_2) for 80% ee. **^{1}H NMR (400 MHz, $CDCl_3$)** δ 7.83 (d, *J* = 1.6 Hz, 1H), 7.52–7.44 (m, 2H), 7.40–7.30 (m, 5H), 7.25–7.15 (m, 4H), 6.88 (s, 1H), 6.10–6.00 (m, 1H). **^{13}C NMR (100 MHz, $CDCl_3$)** δ 149.9, 136.0, 134.3, 134.2, 132.7, 129.3 (2C), 129.2, 128.8 (2C), 127.8, 127.6 (2C), 126.7, 125.2 (2C), 117.9, 106.7, 64.7. **HRMS** (ESI+) *m/z* calcd. for $[C_{19}H_{14}N_2O_2+H]^+$: 303.1128; found: 303.1132. **UPC^2**: IB, gradient CO_2/*i*PrOH, 3.0 mL·min^{-1}; t_{major} = 4.703 min; t_{minor} = 4.773 min.

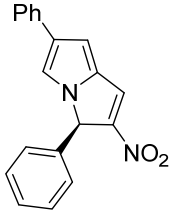

8ea

General procedure for one-pot [6+2] cycloaddition/reduction leading to compounds 9. In a flame-dried screw capped vial equipped with a magnetic stirring bar, 4 Å molecular sieves (MS, 3 spheres), catalyst **3d** (7.36 mg, 0.02 mmol, 20 mol%), BzOH (1.2 mg, 0.01 mmol, 10 mol%), dry $CDCl_3$ (500 μL), nitroolefin **7** (0.15 mmol) and aldehyde **1** (0.1 mmol) were added in this order. The resulting solution was stirred for 24 - 48 h at room temperature. The mixture was then cooled down to 0 °C and $NaBH_4$ (11.3 mg, 0.3 mmol, 3 equiv.) was added. MeOH (250 μL) was then added carefully dropwise. The mixture was stirred for 5 minutes at 0 °C, solvent was removed under reduced pressure and the crude compound was directly purified by column chromatography on Iatrobeads (pentane/EtOAc mixtures) to afford the desired compounds **9aa** - **9ac** and **9ba** as solids.

(2R,3R)-2-nitro-3-phenyl-2,3-dihydro-1H-pyrrolizine 9aa. Following the general procedure from 1*H*-pyrrole-2-carbaldehyde **1a** and nitroolefin **7a**, product **9aa** was obtained as a yellow solid in 45% yield after FC on Iatrobeads (1% EtOAc in pentane). $[\alpha]_D^{25}$ = +10 (*c* 0.1, CH_2Cl_2) for 81% ee. **^{1}H NMR (400 MHz, $CDCl_3$)** δ 7.47–7.28 (m, 3H), 7.10–7.00 (m, 2H), 6.50 (dd, *J* = 2.8, 1.2 Hz, 1H), 6.31 (t, *J* = 3.1 Hz, 1H), 6.01–5.95

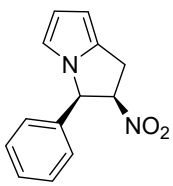

9aa

(m, 1H), 5.89 (d, *J* = 3.4 Hz, 1H), 5.25 (dt, *J* = 7.6, 3.7 Hz, 1H), 3.63 (ddd, *J* = 16.7, 4.0, 1.0 Hz, 1H), 3.52 (ddd, *J* = 16.8, 7.6, 1.1 Hz, 1H). **^{13}C NMR (100 MHz, $CDCl_3$)** δ 137.9, 131.9, 129.3 (2C), 129.1, 126.1 (2C), 114.1 (2C), 100.6, 94.3, 65.9, 29.4. **HRMS** (ESI+) *m/z* calcd. for $[C_{13}H_{12}N_2O_2+H]^+$: 229.0972; found: 229.0975. **UPC^2**: IC, isocratic CO_2/*i*PrOH 95/5, 3.0 mL·min^{-1}; t_{major} = 1.816 min; t_{minor} = 1.712 min. A very small coupling constant displayed by the chiral aliphatic CHs on the five membered ring indicates a *cis* relationship.

General procedure for one-pot [6+2] cycloaddition/thiol addition leading to compounds 10. In a flame-dried screw capped vial equipped with a magnetic stirring bar, 4 Å molecular sieves (MS, 3 spheres), catalyst **3d** (7.36 mg, 0.02 mmol, 20 mol%), BA (1.2 mg, 0.01 mmol, 10 mol%), dry $CDCl_3$ (500 µL), nitroolefin **7** (0.15 mmol) and aldehyde **1** (0.1 mmol) were added in this order. The resulting solution was stirred for 24 - 48 h at room temperature. BnSH (17.6 µL, 0.15 mmol, 1.5 equiv.) Was then added to the mixture and this was stirred for 24 h at RT. The crude compound was directly purified by column chromatography on Iatrobeads (pentane/EtOAc mixtures) to afford the desired compounds **10ad** and **10ae** as solids.

(1S,2S,3R)-1-(benzylthio)-3-(4-methoxyphenyl)-2-nitro-2,3-dihydro-1H-pyrrolizine

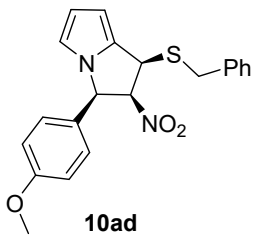

10ad

10ad. Following the general procedure from 1*H*-pyrrole-2-carbaldehyde **1a** and nitroolefin **7e**, product **10ae** was obtained as a yellow solid in 40% yield after FC on Iatrobeads (1% EtOAc in pentane). $[\alpha]_D^{25}$ = +24 (*c* 0.16, CH_2Cl_2) for 90% ee. **^{1}H NMR (400 MHz, $CDCl_3$)** δ 7.36–7.26 (m, 5H), 7.08 (d, *J* = 8.7 Hz, 2H), 6.94–6.89 (m, 2H), 6.44 (dd, *J* = 2.8, 1.2 Hz, 1H), 6.34 (t, *J* = 3.2 Hz, 1H), 6.06 (dd, *J* = 3.5, 1.3 Hz, 1H), 5.67 (d, *J* = 4.6 Hz, 1H), 5.20 (t, *J* = 4.5 Hz, 1H), 4.86 (dd, *J* = 4.3, 1.0 Hz, 1H), 3.91 (d, *J* = 3.5 Hz, 2H), 3.85 (s, 3H). **^{13}C NMR (100 MHz, $CDCl_3$)** δ 160.3, 137.0, 132.2, 129.1, 128.9 (2C), 128.8 (2C), 128.0 (2C), 127.5, 114.7, 114.6, 114.5 (2C), 102.2, 101.2, 65.7, 55.3, 45.7, 36.4. **HRMS** (ESI+) *m/z* calcd. for $[C_{21}H_{20}N_2O_3S+H]^+$: 381.1267; found: 381.1271. **UPC^2**: IC, isocratic CO_2/*i*PrOH 95/5, 3.0 mL·min^{-1}; t_{major} = 3.256 min; t_{minor} = 2.378 min. A very small coupling constant displayed by the three aliphatic CHs on the five membered ring indicates an "all-*cis*" relationship.

General procedure for one-pot [6+2] cycloaddition/indole addition leading to compounds 11. In a flame-dried screw capped vial equipped with a magnetic stirring bar, 4 Å molecular sieves (MS, 3 spheres), catalyst **3d** (7.36 mg, 0.02 mmol, 20 mol%), BA (1.2 mg, 0.01 mmol, 10 mol%), dry $CDCl_3$ (500 µL), nitroolefin **7** (0.15 mmol) and

aldehyde **1** (0.1 mmol) were added in this order. The resulting solution was stirred for 24 h at room temperature. Indole (33 mg, 0.3 mmol, 3.0 equiv.) was then added to the mixture and this was stirred for 48 h at RT. The crude compound was directly purified by column chromatography on Iatrobeads (pentane/EtOAc mixtures) to afford the desired compounds **11ab** and **11af** as solids.

3-((1S,2S,3R)-3-(4-bromophenyl)-2-nitro-2,3-dihydro-1H-pyrrolizin-1-yl)-1H-indole

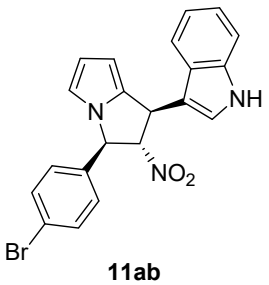

11ab

11ab. Following the general procedure from 1*H*-pyrrole-2-carbaldehyde **1a** and nitroolefin **7b**, product **11ab** was obtained as a brown solid in 30% yield after FC on Iatrobeads (5% EtOAc in pentane). $[\alpha]_D^{25}$ = +32 (*c* 0.1, CH_2Cl_2) for 78% ee. **^{1}H NMR (400 MHz, $CDCl_3$)** δ 8.13 (s, 1H), 7.53–7.44 (m, 2H), 7.40 (d, *J* = 8.2 Hz, 1H), 7.29 (d, *J* = 8.0 Hz, 1H), 7.23 (t, *J* = 7.6 Hz, 1H), 7.15–7.02 (m, 2H), 6.93–6.80 (m, 2H), 6.60–6.49 (m, 1H), 6.40 (t, *J* = 3.1 Hz, 1H), 6.01 (dd, *J* = 3.2, 1.5 Hz, 1H), 5.86 (d, *J* = 7.8 Hz, 1H), 5.79 (dd, *J* = 7.8, 6.3 Hz, 1H), 5.45 (d, *J* = 6.3 Hz, 1H). **^{13}C NMR (100 MHz, $CDCl_3$)** δ 136.7, 134.7, 133.4, 132.1 (2C), 128.6 (2C), 125.6, 123.7, 123.4, 122.7, 120.1, 118.9, 114.4, 113.7, 112.9, 111.5, 102.0, 96.8, 63.1, 38.6. **HRMS** (ESI+) *m/z* calcd. for $[C_{21}H_{16}BrN_3O_2+H]^+$: 422.0499 (^{79}Br), 424.0478 (^{81}Br); found: 422.0495 (^{79}Br), 424.0483 (^{81}Br). **UPC^2**: IC, gradient CO_2/*i*PrOH, 3.0 mL·min^{-1}; t_{major} = 3.720 min; t_{minor} = 3.852 min. A larger coupling constant (with respect to compounds **10**) displayed by three aliphatic CHs on the five membered ring indicates an "all-*trans*" relationship.

7.6.5 Detailed procedures for the NMR observation of I and II

Experiment 1. In a flame-dried screw-capped vial, aldehyde **1a** (17.4 mg, 0.1 mmol), benzoic acid (12.2 mg, 0.1 mmol) and catalyst **3b** (25.5 mg, 0.1 mmol) were dissolved in dry $CDCl_3$ and vigorously stirred in the presence of 6 beads of 4 Å MS for 18 h. This mixture was then carefully transferred in an oven-dried NMR tube under a flow of Argon and analyzed by means of ^{1}H NMR spectroscopy to verify the presence of iminium ion **I**. Hereafter, triethylamine (TEA, 14 μL, 0.1 mmol) was added and the solution was aged for 5 minutes, then analyzed again by means of ^{1}H NMR and ^{19}F NMR to verify the presence of enamine **II**. Finally, diene **2e** (18.0 mg, 0.1 mmol) was added to the tube and the resulting mixture immediately checked by ^{1}H NMR and ^{19}F NMR. Then, additional spectra were taken every 30 minutes for a period of 4 hours, then every hour for a period of 3 hours and a last set of spectra was taken after aging the mixture in the tube overnight.

Experiment 2. In a flame-dried screw-capped vial, aldehyde **1a** (17.4 mg, 0.1 mmol), benzoic acid (12.2 mg, 0.1 mmol) and catalyst **3b** (25.5 mg, 0.1 mmol) were dissolved in dry $CDCl_3$ and vigorously stirred in the presence of 6 beads of 4 Å MS for 18 h. This mixture was then carefully transferred in an oven-dried NMR tube under a flow of Argon and analyzed by means of ^1H NMR spectroscopy to verify the presence of iminium ion **I**. Hereafter, diene **2e** (18.0 mg, 0.1 mmol) was added to the tube and the resulting mixture immediately checked by ^1H NMR and ^{19}F NMR. Then, additional spectra were taken every 30 minutes for a period of 4 hours, then every hour for a period of 3 hours and a last set of spectra was taken after aging the mixture in the tube overnight.

Experiment 3. In an oven-dried NMR tube, aldehyde, **1a** (17.4 mg, 0.1 mmol), benzoic acid (1.2 mg, 0.01 mmol), catalyst **3b** (2.6 mg, 0.01 mmol) and diene **2e** (18.0 mg, 0.1 mmol) were dissolved in dry $CDCl_3$. 3 Beads of 4 Å MS were added to the tube that was manually shaken for 1 minute, after which, the solution was checked by means of ^1H NMR and ^{19}F NMR. Then, 3 magnetic stirrers were added (3 mm diameter, new magnets were employed to make sure that the PTFE coating was intact and no magnetic particles were lost into the tube). The solution was stirred into the tube, positioned over a stirring plate, for 20 minutes. The stirrers were then removed and additional spectra were taken. This operation (adding the stirrers, stirring for 20 minutes, removing the stirrers and taking the spectra) was repeated every 20 minutes for a period of 4 hours, then every hour for a period of 3 hours and a last set of spectra was taken after stirring the mixture into the tube overnight.
Stirring the solution into the tube was important to render the molecular sieves effective (indeed, the reaction failed to proceed if the content of the tube was simply aged instead of being stirred). Avoiding the transfer of the reacting solution was also important to prevent hydrolysis of intermediates **I** and **II**. The presence of 3 beads of MS did not affect the quality of the NMR spectra, as they stayed below the spectral window (on the contrary, powdered molecular sieves caused very poor resolution). A moderate stirring was enough to ensure effectiveness of the MS, a vigorous stirring caused the MS to break and loose some powder, affecting the quality of the spectra.

8 Bibliography

[1] IUPAC, Compendium of Chemical Terminology, 2nd ed., 1997.
[2] J. Gal, *Chirality* **2012**, *24*, 959
[3] R. Noyori, *Adv. Synth. Catal.* **2003**, *345*, 15
[4] D. Seebach, *Angew. Chem. Int. Ed.* **1990**, *29*, 1320.
[5] A. Schmid, J. S. Dordik, B. Hauer, A. Kiener, M. Wubbolts, B. Witholt, *Nature* **2001**, *409*, 258
[6] M. Heitbaum, F. Glorius, I. Escher, *Angew. Chem. Int. Ed.* **2006**, *45*, 4732.
[7] H. U. Blaser, H. J. Federsel, *Asymmetric Catalysis on Industrial Scale*. Wiley VHC, Weinheim, **2011**.
[8] Selected reviews on asymmetric organocatalysis: (a) P. I. Dalko, L. Moisan, *Angew. Chem. Int. Ed.* **2004**, *43*, 5138; (b) B. List, *Asymmetric Organocatalysis.* Wiley VHC, Weinheim, **2005**; (c) B. List, *Chem. Rev.* **2007**, *107*, 5413; (d) H. Pellissier, *Tetrahedron* **2007**, *63*, 926; (e) M. F. Gaunt, C. C. C. Johansson, A. McNally, N. T. Vo, *Drug Discovery Today* **2007**, *12*, 8. (f) D. W. C. MacMillan, *Nature* **2008**, *455*, 304; (g) A. Dondoni, A. Massi, *Angew. Chem. Int. Ed.* **2008**, *47*, 4638.
[9] L. Bernardi, M. Fochi, M. Comes Franchini, A. Ricci, *Org. Biomol. Chem.* **2012**, *10*, 2911.
[10] (a) Z. G. Haios, D. R. Parrish, German patent DE 2102623, **1971**; (b) U. Eder, G. Sauer, R. Wiechert, *Angew. Chem. Int. Ed.* **1971**, *10*, 496; (c) Z. G. Hajos, D. R. Parrish, *J. Org. Chem.* **1974**, *39*, 1615.
[11] Y. Tu, Z. Wang, Y. Shi, *J. Am. Chem. Soc.* **1996**, *118*, 9806.
[12] S. E. Denmark, Z. Wu, C. Crudden, H. Matshuhashi, *J. Org. Chem.* **1997**, *62*, 8288.
[13] D. Yang, *J. Am. Chem. Soc.* **1996**, *118*, 491
[14] M. Sigman, E. N. Jacobsen, *J. Am. Chem. Soc.* **1998**, *120*, 4901
[15] E. J. Corey, M. J. Grogan, *Org. Lett.* **1999**, *1*, 157.
[16] (a) B. List, R. A. Lerner, C. F. III Barbas, *J. Am. Chem. Soc.* **2000**, *120*, 1629; (b) B. List, *J. Am. Chem. Soc.* **2000**, *122*, 9336.
[17] K. A. Ahrendt, C. J. Borths, D. W. C. MacMillan, *J. Am. Chem. Soc.* **2000**, *122*, 4243.
[18] (a) T. Akiyama, J. Itoh, K. Fuchibe, *Adv. Synth. Catal.* **2006**, *348*, 999. (b) M. S. Taylor, E. N. Jacobsen, *Angew. Chem. Int. Ed.* **2006**, *45*, 1520; (c) A. G. Doyle, E. N. Jacobsen, *Chem. Rev.* **2007**, *107*, 5713; (d) Z. Zhang, P. R. Schreiner, *Chem. Soc. Rev.* **2009**, *38*, 1187.
[19] P. Melchiorre, M. Marigo, A. Carlone, G. Bartoli, *Angew. Chem. Int. Ed* **2008**, *47*, 6138.
[20] (a) C. Grondal, M. Jeanty, D. Enders, *Nat. Chem.* **2010**, *2*, 167; (b) C. M. R. Volla, I. Atodiresei, M. Rueping, *Chem. Rev.* **2014**, *114*, 2390.
[21] Z. Du, Z. Shao, *Chem. Soc. Rev.* **2013**, *42*, 1337.
[22] D. Nicewicz, D. W. C. MacMillan, *Science* **2008**, *322*, 77.
[23] A. G. Wenzel, E. N. Jacobsen, *J. Am. Chem. Soc.* **2002**, *124*, 12964.
[24] (a) J. Kacprzak, J. Gawroński, *Synthesis* **2001**, 961; (b) T. Marcelli, H. Hiemstra, *Synthesis* **2010**, 1229.
[25] K. M. Lippert, K. Hof, D. Gerbig, D. Ley, H. Hausmann, S. Guenther, P. R. Schreiner, *Eur. J. Org. Chem.* **2012**, 5919
[26] Y. Okino, Y. Hoashi, Y. Takemoto, *J. Am. Chem. Soc.* **2003**, *125*, 12672.
[27] Y. Okino, Y. Hoashi, X. Xu, Y. Takemoto, *J. Am. Chem. Soc.* **2005**, *127*, 119.
[28] A. Hamza, G. Schubert, T. Soós, I. Pápai, *J. Am. Chem. Soc.* **2006**, *128*, 13151.
[29] Y. Iwabuchi, M. Nakatami, N. Yokoyama, S. Hatakeyama, *J. Am. Chem. Soc.* **1999**, *121*, 10219.
[30] Review on aminocatalysis: (a) S. Bertelsen, K. A. Jørgensen, *Acc. Chem. Res.* **2009**, *38*, 2178; (b) M. Nielsen, D. Worgull, B. Zwifel, S. Bertelsen, K. A. Jørgensen *Chem. Commun.* **2011**, *47*, 632; (c) K. L. Jensen, G. Dickmeiss, H. Jiang, Ł. Albrect, K. A. Jørgensen, *Acc. Chem. Res.* **2012**, *45*, 248. (d) B. S. Donslund, T. K. Johansen, P. H. Poulsen, K. S. Halskov, K. A. Jørgensen, *Angew. Chem. Int. Ed.* **2015**, *54*, 13860.
[31] Earliest reports: (a) S. Bertelsen, M. Marigo, S. Brandes, P. Dinér, K. A. Jørgensen, *J. Am. Chem. Soc.* **2006**, *128*, 12973; (b) Z.-J. Jia, B. Gschwend, Q.-Z. Li, X. Yin. J. Grouleff, Y.-C. Chen, K. A. Jørgensen, *J. Am. Chem. Soc.* **2011**, *135*, 5053.
[32] M. Marigo, T. C. Wabnitz, D. Fielenbach, K. A. Jørgensen, *Angew. Chem. Int. Ed*. **2005**, *44*, 794.
[33] Y. Hayashi, H. Gotoh, T. Hayashi, M. Shoji, *Angew. Chem. Int. Ed.* **2005**, *44*, 4212.

[34] (a) J. Burés, A. Armstrong, D. G. Blackmond, *Acc. Chem. Res.* **2016**, *49*, 214; (b) G. Sahoo, H. Rahaman, Á. Madarász; I. Pápai, M. Melarto, A. Valkonen, P. M. Pihko, *Angew. Chem. Int. Ed.* **2012**, *51*, 13144; (c) K. Patora-Komisarka, M. Benhound, H. Ishikawa, D. Seebach, Y. Hayashi, *Helv. Chim. Acta* **2011**, *94*, 719; (d) T. Földes, Á. Madrasáz, Á. Révész, Z. Dobi, S. Varga, A. Hamza, P. R. Nagi, P. M. Pihko, I. Pápai, *J. Am. Chem. Soc.* **2017**, *139*, 17052; (f) D. Seebach, X. Sun, C. Sparr, M.-O. Ebert, W. B. Schweizer, A. K. Beck, *Helv. Chem. Acta* **2012**, *95*, 1064; (g) J. Burés, A. Armstrong, D. G. Blackmond, *J. Am. Chem. Soc.* **2012**, *134*, 6741, corrigendum: *J. Am. Chem. Soc.* **2012**, *134*, 14264.
[35] J. Bosch, M.-L. Bennasar, *Synlett* **1995**, 587.
[36] J. A. Bull, J. J. Mousseau, G. Pelletier, A. Charette, *Chem Rev*, **2012**, *112*, 2642.
[37] (a) T.-L. Ho, *Tetrahedron* **1985**, *41* 1; (b) R. Yamaguchi, Y. Nakazono, T. Matsuki, E.-I. Yata, M. Kawanisi, *Bull. Chem. Soc. Jpn.* **1987**, *60*, 215.
[38] D.-L. Comins, A. H. Abdullah, *J. Org. Chem.* **1982**, *47*, 4315.
[39] E. Piers, M. Soucy, *Can. J. Chem.* **1974**, *52*, 3563.
[40] K.-Y. Akiba, Y. Nishihara, M. Wada, *Tetrahedron Lett.* **1983**, *24*, 5269.
[41] (a) C. E. Hoesl, J. Pabel, K. Polborn, K. T. Wanner, *Heterocycles* **2002**, *58*, 383; (b) D. L. Comins, R. R. Goehring, S. P. Joseph, S. O'Connor, *J. Org. Chem.* **1990**, *55*, 2574; (c) D. L. Comins, S. P. Joseph, R. R. Goehring, *J. Am. Chem. Soc.* **1994**, *116*, 4719.
[42] K.-Y. Akiba, Y. Iseki, M. Wada, *Tetrahedron Lett.* **1982**, *23*, 429.
[43] (a) A. Hilgeroth, U. Baumeister, *Angew. Chem. Int. Ed.* **2000**, *39*, 576. (b) M.-L. Bennasar, C. Juan, J. Bosch, *Tetrahedron Lett* **1998**, *39*, 9275.
[44] M.-L. Bennasar, C. Juan, J. Bosch, *Tetrahedron Lett.* **2001**, *42*, 585.
[45] M.-L. Bennasar, E. Zulaica, A. Ramìrez, J. Bosch*, Tetrahedron Lett.* **1996**, *37*, 6611.
[46] M.-L. Bennasar, E. Zulaica, C. Juan, L. Llauger, J. Bosch, *Tetrahedron Lett.* **1999**, *40*, 3961.
[47] M. Alvarez, R. Lavilla, J. Bosch, *Heterocycles* **1989**, *29*, 237.
[48] (a) E. Wenkert, G. D. Reynolds, *Synth. Commun.* **1973**, *3*, 241; (b) D. Spitzner, E. Wenkert, *Angew. Chem. Int. Ed.* **1984**, *23*, 984; (c) D. Spitzner, T. Zaubtzer, E. Shi, E. Wenkert, *J. Org. Chem.* **1988**, *53*, 2274.
[49] M.-L. Bennasar, E. Zulaica, J.-M. Jìmenez, J. Bosch, *J. Org. Chem.* **1993**, *58*, 7756.
[50] (a) M. Alvares, R. Lavilla, J. Bosch, *Tetrahedron Lett.* **1987**, *28*, 4457; (b) M.-L. Bennasar, M. Alvares, R. Lavilla, E. Zulaica, J. Bosch, *J. Org. Chem.* **1990**, *55*, 1156.
[51] (a) M.-L. Bennasar, E. Zulaica, M. Lòpez, J. Bosch, *Tetrahedron Lett.* **1988**, *29*, 2361; (b) L. J. Dolby, S. J. Nelson, *J. Org. Chem.* **1973**, *38*, 2882.
[52] S.-G. Wang, Z.-L. Xia, R.-Q. Xu, X.-J. Liu, C. Zheng, S.-L. You, *Angew. Chem. Int. Ed.* **2017**, *56*, 7440.
[53] E. Ichikawa, M. Suzuki, K. Yabu, M. Albert, M. Kanai, M. Shibasaki, *J. Am. Chem. Soc*. **2004**, *126*, 11808.
[54] M. A. Fernandez-Ibàñez, B. Macia, M. G. Pizzuti, A. J. Minnaard, B. L. Feringa, *Angew. Chem. Int. Ed.* **2009**, *48*, 9339.
[55] (a) S. T. Chau, J. P. Lutz, K. Wu, A. G. Doyle, *Angew. Chem. Int. Ed.* **2013**, *52*, 9153; (b) J. P. Lutz, S. T. Chau, A. G. Doyle, *Chem. Sci.* **2016**, *7*, 4105.
[56] N. Christian, S. Aly, K. Belyk, *J. Am. Chem. Soc.* **2011**, *133*, 2878.
[57] O. García Mancheño, S. Asmus, M. Zurro, T. Fischer, *Angew. Chem. Int. Ed.* **2015**, *54*, 8823.
[58] R. J. Phipps, G. L. Hamilton, F. D. Toste, *Nat. Chem.* **2012**, *4*, 603.
[59] (a) K. Brak, E. N. Jacobsen, *Angew. Chem. Int. Ed.* **2013**, *52*, 534; (b) M. S. Taylor, E. N. Jacobsen, *J. Am. Chem. Soc.* **2004**, *126*, 10558; (c) R. S. Klausen, E. N. Jacobsen, *Org. Lett.* **2009**, *11*, 887. (d) D. Lehnherr, D. D. Ford, A. J. Bendelsmith, C. R. Kennedy, E. N. Jacobsen, *Org. Lett.* **2016**, *18*, 3214; (e) D. Ford, D. Lehnherr, C. R. Kennedy, E. N. Jacobsen, *ACS Catal.* **2016**, *6*, 4616; (f) D. Ford, D. Lehnherr, C. R. Kennedy, E. N. Jacobsen, *J. Am. Chem. Soc.* **2016**, *138*, 7860.
[60] R. W. Alder, *Chem. Rev.* **1989**, *89*, 1215.
[61] S. Ingemann, H. Hiemstra, *Comprehensive Enantioselective Organocatalysis: Catalysts, Reactions and Applications,* Vol. 2; Dalko, P. I., Ed.; Wiley −VCH: Weinheim, Germany, **2013**; 119−160.
[62] (a) M. Giese, M. Albrecht, T. Repenko, J. Sackmann, A. Valkonen, K. Rissanen, *Eur. J. Org. Chem.* **2014**, *2014*, 2435; (b) A. Berkessel, S. Das, D. Pekel, J.-M. Neudörfl, *Angew. Chem. Int. Ed.* **2014**, *53*, 11660.
[63] R. Lavilla, O. Coll, R. Kumar, J. Bosch, *J. Org. Chem.* **1998**, *63*, 2728.
[64] M. Baidya, G. Y. Remennikov, P. Mayer, H. Mayr, *Chem. Eur. J.* **2010**, *16*, 1365.
[65] C. S. Yeung, R. E. Ziegler, J. A. Porco Jr., E. N. Jacobsen, *J. Am. Chem. Soc.* **2014**, *136*, 13614.
[66] CCDC No. 1476006 contains the crystallographic data of **4gd**.

[67] J. Kotek, P. Herman, K. Vojtisek, J. Rohovec, I. Lukes, *Collect. Czech. Chem. Commun.* **2000**, *65*, 243.
[68] J. Preindl, S. Chachkrabarty, J. Waser, *Chem. Sci.* **2017**, *8*, 7112.
[69] D. Flanigan, T. Rovis, *Chem. Sci.* **2017**, *8*, 6566.
[70] G. Di Carmine, D. Ragno, O. Bortolini, P. P. Giovannini, A. Mazzanti, A. Massi, M. Fogagnolo, *J. Org. Chem.* **2018**, *83*, 2050.
[71] M. Marigo, T. C. Wabnitz, D. Fielenbach, K. A. Jørgensen, *Angew. Chem. Int. Ed.* **2005**, *44*, 794.
[72] E. Benfatti, E. Benedetto, P. G. Cozzi, *Chem. – Asian J.* **2010**, *5*, 2047.
[73] A. Yin, L. Huang, X. Zhang., F. Ji, H. Jiang, *J. Org. Chem.* **2012**, *77*, 6365.
[74] K. Frisch, A: Landa, S. Saaby, K. A: Jørgensen, *Angew. Chem. Int. Ed.* **2005**, *44*, 6700.
[75] L. Mengozzi, A. Gualandi, P. G. Cozzi, *Chem. Sci.* **2014**, *5*, 3915.
[76] F. Berti, F. Malossi, F. Marchetti, M. Pineschi, *Chem. Commun* **2015***, 51*, 13694.
[77] C. M. R. Volla, E. Fava, I. Atodiresei, M. Rueping, *Chem. Commun.* **2015**, *51*, 15788.
[78] S. Sun, Y. Mao, H. Lou, L. Liu, *Chem. Commun.* **2015**, *51*, 10691.
[79] L. Mengozzi, A. Gualandi, P. G. Cozzi, *Eur. J. Org. Chem.* **2016**, *2016*, 3200.
[80] A. Noole, M. Borissova, M. Lopp, T. Kanger, *J. Org. Chem.* **2011**, *76*, 1538.
[81] (a) L. Huo, A. Ma, Y. Zhang, D. Ma, *Adv. Synth. Catal.* **2012**, *354*, 991; (b) M. Reilly, D. R. Anthony, C. Gallagher, *Tetrahedron Lett.* **2003**, *44*, 2927; (c) X. E. Hu, N. K. Kim, B. Ledoussal, *Org. Lett.* **2002**, *4*, 4499.
[82] X. E. Hu, N. K. Kim, J. L. Gray, J.-I. K. Almstead, W. L. Seibel, B. Ledoussal, *J. Med. Chem.* **2003**, *46*, 3655.
[83] (a) K. Garber, *Nat. Biotechnol.* **2013**, *31*, 3; (b) Y. S. Patil, N. L. Bonde, A. S. Kekan, D. G. Sathe, A. Das, *Org. Process Res. Dev.* **2014**, *18*, 1714.
[84] (a) W.-C. Shieh, G.-P. Chen, S. Xue, J. McKenna, X. Jiang, K. Prasad, O. Repič, *Org. Process Res. Dev.* **2007**, *11*, 711; (b) D. Swinnen, A. Bombrun, WO/2006/008303 A1, **2006**.
[85] J. Burés, A. Armstrong, D. G. Blackmond, *J. Am. Chem. Soc.* **2011**, *133*, 8822.
[86] T. Li, J. Zhu, D. Wu, X. Li, S. Wang, H. Li, J. Li, W. Wang, *Chem. - Eur. J.* **2013**, *19*, 9147. (b) L. Dell'Amico, X. Companyò, T. Naicker, M. Bräuer, K. A. Jørgensen, *Eur. J. Org. Chem.* **2013**, *2013*, 5262.
[87] CCDC No.1522977 contains the crystallographic data of **10**.
[88] J. Stonehouse, P. Adell, J. Keeler, A. J. Shaka, *J. Am. Chem. Soc.* **1994**, *116*, 6037.
[89] D. Seebach, J. Golinski, J. *Helv. Chim. Acta* **1981**, *64*, 1413.
[90] A small aliquot of this crude mixture was evaporated *in vacuo* and the residue analysed by ^{1}H NMR spectroscopy to determine the diastereomeric ratio of the reaction.
[91] J. Clayden, N. Greeves, S. Warren, *Organic Chemistry*; **2012**.
[92] M. Ferrer, F. Sánchez-Baeza, A. Messeguer, *Tetrahedron* **1997**, *53*,15877.
[93] M. Korach, D. R. Nielsen, W. H. Rideout, *Org. Synth.* **1953**, *33*, 79.
[94] S. L. Jain, B. Sain, *Chem. Commun.* **2002**, *10*, 1040.
[95] T. C. Johnson, S. P. Marsden, *Org. Lett.* **2016**, *18*, 5364.
[96] N. Gualo-Soberanes, M. C. Ortega-Alfaro, J. G. Lòpez-Cortés, R. A. Toscano, H. Rudler, C. Álvarez-Toledano, *Tetrahedron Lett.* **2010**, *51*, 3186.
[97] J. Yin, B. Xiang, M. A. Huffman, C. E. Raab, I. W. Davies, *J. Org. Chem.* **2007**, *72*, 4554.
[98] B. Castro, J. Coste, Bromotrispyrrolidinophosphonium hexafluorophosphate. PCT Int. Appl. WO/90/10009, 1990.
[99] A. T. Londregan, S. Jennings, L. Wei, *Org. Lett.* **2010**, *12*, 5254.
[100] (a) A. T. Londregan, S. Jennings, L. Wei, *Org. Lett.* **2011**, *13*, 1840; (b) B. Lecointre, R. Azzouz, L. Bischoff, *Tetrahedron Lett.* **2014**, *55*, 1913.
[101] A. T. Londregan, K. Burford, E. L. Conn, K. D. Hesp, *Org. Lett.* **2014**, *16*, 3336.
[102] Y. Lian, S. B. Coeffy, Q. Li, A. T. Londregan, *Org. Lett.* **2016**, *18*, 1362.
[103] D. Wang, J. Zhao, Y. Wang, J. Hu, L. Li, L. Miao, H. Feng, L. Dsaubry, P. Yu, *Asian. J. Org. Chem.* **2016***, 5*, 1442.
[104] S. Yu, H. Leng Sang, S. Ge, *Angew. Chem. Int. Ed.* **2017**, *56*, 15896.
[105] J. Alemán, S. Cabrera, E. Maerten, J. Overgaard, K. A. Jørgensen, *Angew. Chem. Int. Ed.* **2007**, *46*, 5520.
[106] J. C. Conrad, J. Kong, B. N. Laforteza, D. W. C. MacMillan, *J. Am. Chem. Soc.* **2009**, *131*, 11640; (b) J. M. Um, O. Gutierrez, F. Schoenebeck, K. N. Houk, D. W. C. MacMillan, *J. Am. Chem. Soc.* **2010**, *132*, 6001.
[107] K. C. Nicolaou, R. Reingruber, D. Sarlah, S. Bräse, *J. Am. Chem. Soc.* **2009**, *131*, 2086; correction: *J. Am. Chem. Soc.*, **2009**, *131*, 6640.
[108] A. E. Allen, D. W. C. MacMillan, *J. Am. Chem. Soc.* **2011**, *133*, 4260.

[109] (a) R. Hoffmann, R. B. Woodward, *J. Am. Chem. Soc.* **1965**, *87*, 2046; (b) R. B. Woodward, R. Hoffmann, *J. Am. Chem. Soc.* **1965**, *87*, 395.
[110] R. Hoffmann, R. B. Woodward, *J. Am. Chem. Soc.* **1965**, *87*, 4388.
[111] R. C. Cookson, B. V. Drake, J. Hudec, A. Morrison, *Chem. Commun.* **1966**, *1966*, 15.
[112] K. N. Houk, R. B. Woodward, *J. Am. Chem. Soc.* **1970**, *92*, 4143.
[113] T. A. Palazzo, R. Mose, K. A. Jørgensen, *Angew. Chem. Int. Ed.* **2017**, *56*, 10033.
[114] (a) P. L. Watson, R. N. Warrener, *Aust. J. Chem* **1973**, *26*, 1725; (b) M. N. Paddon-Row, R. Warrener, *Tetrahedron Lett.* **1973**, *43*, 3797.
[115] R. N. Warrener, M. N. Paddon-Row, R. A. Russel, P. L. Watson, *Aust. J. Chem* **1981**, *34*, 397.
[116] K. Hafner, W. Bauer, *Angew. Chem. Int. Ed.* **1968**, *7*, 297.
[117] H. Takeshita, Y. Wada, A. Mori, T. Hatsui, *Chem. Lett.* **1973**, *2*, 335.
[118] K. R. Dahnke, L. A. Paquette, *J. Org. Chem.* **1994**, *59*, 885.
[119] T. Mukai, T. Tezuka, Y. Asaki, *J. Am. Chem. Soc.* **1966**, *88*, 5025.
[120] T. S. Cantrell, *J. Am. Chem. Soc.* **1971**, *93*, 2540.
[121] K. N. Houk, R. B. Woodward, *J. Am. Chem. Soc.* **1970**, *92*, 4145.
[122] P. Li, H. Yamamoto, *J. Am. Chem. Soc.* **2009**, *131*, 16628.
[123] J. H. Rigby, H. S. Ateeq, N. R. Charles, S. V. Cuisiat, M. D. Ferguson, J. A. Henshilwood, A. C. Krueger, C. O. Ogbu, K. M. Short, M. J. Heeg, *J. Am. Chem. Soc.* **1993**, *115*, 1382.
[124] J. H. Rigby, M. Fleming, *Tetrahedron Lett.* **2002**, *43*, 8643.
[125] M. Xie, X. Liu, X. Wu, Y. Cai, L. Lin, X. Feng, *Angew. Chem. Int. Ed.* **2013**, *52*, 5604.
[126] R. Mose, G. Preegel, J. Larsen, S. Jakobsen, E. H. Iversen, K. A. Jørgensen, *Nat. Chem.* **2017**, *9*, 487.
[127] Y. Hayashi, H. Gotoh, M. Honma, K. Sankar, I. Kumar, H. Ishikawa, K. Konno, H. Yui, S: Tsuzuki, T. Uchimaru, *J. Am. Chem. Soc.* **2011**, *133*, 20175.
[128] Z. Zhou, Z.-X. Wang, Y.-C. Zhou, W. Xiao, Q. Ouyang, W. Du, Y.-C. Chen, *Nat. Chem.* **2017**, *9*, 590.
[129] S. Wang, C. Rodrìguez-Escrich, M. A. Pericàs, *Angew. Chem. Int. Ed.* **2018**, *56*, 15608.
[130] B. S. Donslund, A. Monleòn, T. A. Palazzo, M. L. Christensen, A. Dahlgaard, J. D. Erickson, K. A. Jørgensen, *Angew. Chem. Int. Ed.* **2018**, *57*, 1246.
[131] H. Tanida, T. Irie, K. Tori, *Bull. Chem. Soc. Jpn.* **1972**, *46*, 1999.

[132] R. N. Warrener, M. L. A. Hammond, D. N. Butler, *Synth. Commun.* **2001**, *31*, 1167.
[133] Deuterated chloroform was chosen instead of simple chloroform as it does not contain stabilizers and rendered reaction control by ^{1}H NMR analysis easier.
[134] (a) A. V. Marenich, C. J. Cramer, D. G. Truhlar, *J. Phys.Chem. B* **2009**, *113*, 6378; (b) C. Gonzalez, H. B. Schlegel, *J. Phys. Chem.* **1990**, *94*, 5523; (c) A. D. Becke, *J. Chem. Phys.* **1993**, *98*, 5648; (d) A. D. Becke, *J. Chem. Phys.* **1993**, *98*,1372; (e) C. T. Lee, W. T. Yang, R. G. Parr, *Phys.Rev.B* **1988**, *37*, 785; (f) S. Grimme, J. Antony, S. Ehrlich, H. Krieg, J. *Chem. Phys.* **2010**, *132*,154104.
[135] E. K. Kemppainen, G. Sahoo, A. Piisola, A. Hamaza, B. Kltai, I. Pàpai, P. M. Pihko, *Chem. Eur. J.* **2014**, *20*, 5983.
[136] H. Ito, Y. Takenaka, S. Fukunishi, K. Iguchi, *Synthesis* **2005**, 3035.
[137] B.-C. Hong, Y.-J. Shr, J.-L. Wu, A. K. Gupta, K.-J. Lin, *Org. Lett.* **2002**, *13*, 2249.
[138] B.-C. Hong, Y.-F. Jiang, E. S. Kumar, *Bioorg. Med. Chem. Lett.* **2001**, *11*, 1981.
[139] S. Y. Cho, J. Y. Baek, S. S. Han, S. K. Kang, J. D. Ha, J. H. Ahn, J. D. Lee, K. R. Kim, H. G. Cheon, S. D. Rhee, S. D. Yang, G. H. Yon, C. S. Pak, J.-K. Choi, *Bioorg. Med. Chem. Lett.* **2006**, *16*, 499.
[140] M. Watanabe, T. Kobayashi, S. Kajigaeshi, S. Kanemasa, *Chem. Lett.* **1975**, *6*, 607.
[141] P. E. Sonnet, J. L. Flippen, R. D. Gilardi, *J. Het. Chem.* **1974**, *11*, 811.
[142] E. Galeazzi, A. Guzman, G. Rodriguez, J. Muchowski, *J. Org. Chem.* **1993**, *58*, 974.
[143] J. Barluenga, J. Garcìa-Rodrìguez, S. Martìnez, A. L. Suàrez-Sobrino, M. Tomàs, *Chem. Eur. J.* **2006**, *12*, 3201.
[144] V. Bhardwaj, D. Gumber, V. Abbot, S. Dhiman, P. Sharma, *RSC Adv.* **2015**, *5*, 15233.
[145] A. R. Katritzky, C. A. Ramsden, J. A. Joule, V. V. Zhdankin, *Reactivity of Five-Membered Rings with One Heteroatom, Handbook of Heterocyclic Chemistry*, **2010**, 383.
[146] (a) J.-Y. Bae, H.-J. Lee, S.-H. Youn, S.-H. Kwon, C.-W. Cho, *Org. Lett.* **2010**, *12*, 4352; (b) H.-J. Lee, C.-W. Cho, *J. Org. Chem.* **2013**, *78*, 3306; (c) H.-J. Lee, C.-W. Cho, *Eur. J. Org. Chem.* **2014**, *2014*, 387.
[147] (a) P. Li, F. Fang, J. Chen, J. Wang, *Tetrahedron: Asymmetry* **2014**, *25*, 98; (b) N. Fhu, L. Zhang, S. Luo, J. P. Cheng, *Org. Chem. Front* **2014**, *1*, 68; (c) J. Zhang, Y. Zhang, X. Liu, J. Guo, W. Cao, L. Lin, X. Feng, *Adv. Synth. Catal.* **2014**, *356*, 3545.
[148] W. W. Paudler, G. I. Kerley, J. McKay, *J. Org. Chem.* **1963**, *28*, 2194.

[149] S.-Z. Huang, F.-D. Kong, Q.-Y. Ma, Z.-K. Guo, L. M. Zhou, Q. Wang, H.-F. Dai, Y.-X. Zhao, *J. Nat. Prod.* **2016**, *79*, 2599.
[150] A. Walser, R. I. Fryer, *Imidazodiazepines and Processes Therefor.* US4280957 (A), July 28, **1981**.
[151] A.-F. Rizk, *Naturally Occurring Pyrrolizidine Alkaloids*; CRC Press: Boca Raton, FL, USA, **1990**.
[152] P. J. Harrington, H. N. Khatri, G. C. Schloemer, *Preparation of Ketorolac.* US6323344 (B1), November 27, **2001**.
[153] (a) C.-Y. Ho, Y.-C. Chen, M.-K. Wong, D. Yang, *J. Org. Chem.* **2005**, *70*, 898; (b) C. Sparr, W. B. Schweizer, H. M. Senn, R. Gilmour, *Angew. Chem. Int. Ed.* **2009**, *48*, 3065; (c) C. Sparr, E.-M. Tanzer, J. Bachmann, R. Gilmour, *Synthesis*, **2010**, *8*, 1394.
[154] R. Manzano, S. Datta, R. S. Paton, D. Dixon, *Angew. Chem. Int. Ed.* **2017**, *56*, 5834.
[155] At the beginning the reaction was monitored every 30 minutes, then every hour and one last time after 18 hours (overnight). See the experimental section for more details.
[156] G. Yin, R. Zhang, L. Li, J. Tian, L. Chen, *Eur. J. Org. Chem.* **2013**, *24*, 5431.
[157] L. Caruana, F. Kneip, T. K. Johansen, P. H. Poulsen, K. A. Jørgensen, *J. Am. Chem. Soc.* **2014**, *136*, 15929.
[158] V. K. Outlaw, F. B. Dandrea, C. A. Townsend, *Org. Lett.* **2015**, *17*, 1822.
[159] J. M. Muchowski, P. Hess, *Tetrahedron Lett.* **1988**, *29*, 3215.